The Direct Integration Method for Elastic Analysis of Nonhomogeneous Solids

Yuriy Tokovyy
Chien-Ching Ma

The Direct Integration Method for Elastic Analysis of Nonhomogeneous Solids

The Direct Integration Method for Elastic Analysis of Nonhomogeneous Solids

By

Yuriy Tokovyy and Chien-Ching Ma

Cambridge
Scholars
Publishing

The Direct Integration Method for Elastic Analysis
of Nonhomogeneous Solids

By Yuriy Tokovyy and Chien-Ching Ma

This book first published 2021

Cambridge Scholars Publishing

Lady Stephenson Library, Newcastle upon Tyne, NE6 2PA, UK

British Library Cataloguing in Publication Data
A catalogue record for this book is available from the British Library

ISBN (10): 1-5275-6149-6
ISBN (13): 978-1-5275-6149-6

To the brilliant memory of Prof. Vasyl' M. Vihak (Vigak), 1936 – 2003,
and Prof. Viatcheslav (Slava) V. Meleshko, 1951 – 2011,
to whom we are greatly indebted for the contribution
into our scientific endeavors

TABLE OF CONTENTS

PREFACE

The recent progress in computational methods and computer-based simulation models contributed significantly to the efficiency of scientific research in different areas. In the area of thermomechanics, for example, the widespread implementation of the modern computer methods is motivated by the complexity of scientific problems addressing the thermo-mechanical phenomena in material structures, the coupling of processes and physicochemical fields, variety in shape and material properties of the structures or their assemblies, multi-field nature of impacts, time and cost constraints for the computation and analysis, etc. Such a complexity level makes it nearly impossible to derive a solution analytically. This reason tips the scale of interest for students, scholars, and research-engineers towards the "fast and efficient" numerical methods over the analytical ones, which may seem to be "potentially insufficient" and "too sophisticated". This also widens the gap between the "modern" and "pre-computer" scientists in their approach. So maybe it is the time for analytical methods to take their place in the "museum of science" alongside the slide rule and arithmometer?

The authors sincerely believe that the depreciation of analytical methods, in many cases, fails to capture important features of the studied processes and phenomena. In our experience, the implementation solely of even the newest and most efficient numerical methods for the analysis of structures of specific geometries (for example, propellant tanks of launch vehicles) is related to certain complications. One of those is a very large number of equations to solve, which presents a challenge even for modern computational facilities. Therefore, the original boundary value problem on the mechanical analysis of the entire structure is to be segmented into a number of sub-problems formulated for the representative elements of the structure. This, however, imposes a new problem on the adequate evaluation of the boundary conditions for the considered structural element allowing for the simulation of the impact caused by the remaining parts of the structure. The efficiency in solving the latter problem depends on understanding the critical stress behavior which calls for implementing analytical procedures for a clear cause-consequence analysis.

This makes it clear that the progress in the analysis of complex mechanical problems depends, in the final count, on the synergy of analytical and numerical methods. In this regard, we can refer to the motto

of the book [101] by R. W. Hamming: "*The purpose of computing is insight, not numbers*". From this viewpoint, the main demand for the analytical methods is not just constructing a solution (which is now not the final goal of the research but rather an intermediate step), but presenting it in the most convenient form that can be used for further analysis. Such a solution form in mechanics of solids implies the explicit analytical relationship between the loadings and stress-strain fields.

In this book, we present an analytical method for the thermoelastic analysis inhomogeneous solids, the central idea of which is representing the stresses in the form of explicit analytical dependencies on the mechanical and thermal loadings. This method is based on the concept of direct integration of the governing equations of the elasticity and thermoelasticity problems from the "first principles", i.e., by operating with the stresses or displacements without implementation of the potential functions of higher differential order. The method is oriented towards the integrodifferential relationship between the stress-tensor components, which is derived on the basis of equilibrium equations in terms of stresses and thus is irrespective of the material properties. This fact makes this method very attractive for solving thermoelasticity problems in anisotropic and inhomogeneous solids.

The hypotheses and models underlying classical theories of elasticity and thermoelasticity mostly assume the elastic properties of isotropic and anisotropic materials to be constant. However, later, primarily due to a deeper empirical study of the elastic behavior of real-life structures and the needs of engineering practice, it became necessary to take into account the dependence of the material moduli on spatial coordinates. Materials with such properties are known as inhomogeneous materials. The studies of the thermomechanical behavior of inhomogeneous structures under the action of force and thermal loadings attract the attention of specialists in both academia and industry. In particular, this is due to the development of the concept of functional-gradient materials (FGM) and the latest technologies for the formation of inhomogeneous structures with a predetermined distribution profiles of thermophysical and mechanical properties, which are intensively introduced and studied in scientific and industrial centers around the world.

The development of methods for the analysis of the thermomechanical behavior of inhomogeneous or FGM solids is concerned with significant difficulties, caused primarily by the need to solve governing differential equations with variable coefficients within the framework of corresponding problems of thermomechanics. The classical methods, in the vast majority, fail to meet urgent needs in this field, the main of which is to determine the optimal distribution of material characteristics to ensure certain functional

parameters of a structure as a whole, as well as optimal control of their thermostressed state. From this point of view, the determination of the stress-strain state is not the final goal of the research, but only an intermediate stage, which should provide an analytical solution of the direct problem, which satisfies the boundary and initial conditions, fundamental principles and modeling constraints of solids mechanics, and is in the form of an explicit functional dependence on loadings and material properties, which is critical for further application.

This book generalizes the results in solving two-dimensional elasticity and thermoelasticity problems for anisotropic inhomogeneous solids we generated over two decades by developing the direct integration method. We attempted to emphasize the advantages and, what is more important, the disadvantages of the method for solving practical problems.

The book consists of four chapters. The first chapter is devoted to the historical aspects of the research into the thermomechanical performance of inhomogeneous solids along with the review of the dominant analytical methods in this subject area. We intentionally emphasized the earlier studies over the new ones for the reason that, unfortunately, many "new" results published in recent decades reproduce (completely or in some part) the older ones, which we may explain by the lack of knowledge about the studies provided in pioneering research works. The second chapter presents the application of the direct integration method for solving thermoelasticity problems for orthotropic inhomogeneous infinite, semi-infinite, and finite solids in the Cartesian coordinate system. The third chapter presents the analysis of orthotropic inhomogeneous annuli in the polar coordinates. The fourth chapter deals with the construction of solutions to thermoelasticity problems for infinite, semi-infinite, and finite solids in the cylindrical coordinate system. Under the assumption that the material properties are arbitrary functions of the spatial coordinates, besides the construction of solutions in the form of explicit dependencies on the force and thermal loadings, we provided a technique of deriving the necessary existing conditions for the stresses and displacements in terms of the loadings applied, and the one-to-one relationship between the stresses and displacements on the boundary of the considered solids. In every considered coordinate system, we discussed the cases of the material inhomogeneity profiles, which allow for comparatively simple analytical solutions of thermoelasticity problems. We hope, these results may be of interest for scientists and engineers working in the area of thermal stresses with the focus on the effects caused by the material anisotropy and inhomogeneity, as well as for university students with the specialty in mechanical and civil engineering and methods mathematical physics.

We are indebted to many people for this book. First of all, the book is dedicated to the brilliant memory of Professor Vasyl Vihak (Vigak, if the name is transliterated from Russian), who initiated the research into the direct integration of the thermoelasticity equations, and Professor Viatcheslav (Slava) Meleshko, whose valuable comments and suggestions helped us with clarifying a number of critical points in our research. We are also thankful to the researchers of the Departments of Solid Mechanics and Thermomechanics at the Pidstryhach Institute for Applied Problems of Mechanics and Mathematics of the National Academy of Sciences of Ukraine (Lviv, Ukraine) and the Fracture Mechanics Laboratory at the Department of Mechanical Engineering, Colledge of Engineering of the National Taiwan University (Taipei, Taiwan) for the discussions, important critics and valuable comments on different aspects of the presented material. The authors would like to thank the Ministry of Science and Technology of the Republic of China for financially supporting the research projects which provide valuable results in this book.

Lviv – Taipei
Yuriy Tokovyy
Chien-Ching Ma
August 2020

CHAPTER ONE

ELASTIC AND THERMOELASTIC ANALYSIS OF INHOMOGENEOUS SOLIDS

1.1. Introduction

In the first part of the nineteenth century, the classical theory of elasticity broke off into a separate academic discipline within the continua mechanics owing to the fundamental contributions of scientists, such as Claude Louis Marie Henri Navier (1785–1836), Augustin Louis Cauchy (1789–1857), and Siméon Denis Poisson (1781–1840), and others [34, 281, 284]. This theory lays the foundation by which to analyze the elastic response of solids to static and dynamic force loadings, which is crucial to projecting and evaluating the mechanical performance of the structural elements of buildings and mechanisms. The central hypotheses of this theory are based on the assumption that materials are continuous (i.e., each material point of a considered solid can be bijectively represented by a point in three-dimensional Euclidean space) and homogeneous (i.e., mechanical properties are the same at any point in a solid).

By the end of the nineteenth century however, it became obvious that the assumption of material homogeneity is unable to capture several important features pertaining to the mechanical performance of solids. A lack of homogeneity is associated with structural imperfections or microdefects, the consolidation of which within a macrovolume can cause profound disturbances of mechanical and thermal fields. Materials with such properties are known as *inhomogeneous, nonhomogeneous,* or *heterogeneous* [169, 202]. Since that time, there has been considerable research on the analysis of inhomogeneous solids with concern to various aspects and applications [32, 35, 36, 116, 142]. In recent years, this trend has accelerated due to the widespread implementation of modern materials with advanced properties. There has been a particular focus on functionally-graded materials (FGM), the technology of which allows for the intentional modification of material-variation profiles during fabrication [265, 267] in order to meet specific thermo-mechanical

performance requirements. This has led to a proliferation of scientific publications on the various aspects of modeling and analysis of inhomogeneous solids. Sadly, many of these papers reiterate results published in older articles.

Maxwell [170, pp. xiii–xiv] pointed out that "*it is of great advantage to the student of any subject to read the original memoirs on that subject, for science is always most completely assimilated when it is in the nascent state...*". We therefore present in this chapter a brief historical survey of the analysis of inhomogeneous solids, with an emphasis on the dominant methods for elastic materials exhibiting continuously variable properties, as is typical of FGM. Note that this survey is illustrative rather than exhaustive. We direct the interested reader to a number of recent reviews on problems associated with inhomogeneous solids and FGM in particular [63, 121, 268, 269, 279].

According to Maugin [169], "*the most common definition of inhomogeneity*[1] *relates to a whole composed of dissimilar or nonidentical elements or parts*". Such microstructure-dependent elements could be situated within that solid for many reasons [168]. For example, defects in polycrystal material structures, changes in the chemical composition of materials, microcracks, inclusions or dislocations, and sudden or continuous physical and chemical actions can all contribute to inhomogeneity. These elements can induce local disturbances of the mechanical fields, which, when consolidated, affect the macroscopic mechanical performance of the solid [32]. Such consolidation (i.e., material *inhomogeneity*) is caused by various effects, which can be divided into three basic types. The first is environmental effects influenced by specific mechanical, physical, or chemical fields or their superposition, radiation, or diffusion of chemically-active agents, gravity, nonuniform temperature, or humidity, etc. The second is technological effects associated with specific treatments during fabrication and exploitation, such as hot-rolling, forging, pressing, quenching, consolidation, and chemical treatment. The third is design intent, such as the situation where inhomogeneity is an intentional result of engineering aimed at reinforcing a material, such as composite materials, FGM, etc.

It seems that Jasinsky (see a survey of his outstanding contribution into the development of theories of elasticity and strength of materials in [281, pp. 294–297]) was the first to evaluate the effect of macro-inhomogeneity resulting from the consolidation of micro-defects in a solid. According to

[1] Note that Maugin has given preference to the rather mathematical term "*inhomogeneous*" over the terms "*nonhomogeneous*" and "*heterogeneous*", which are more widely used in engineering, material and physical sciences.

his hypothesis [119], the material continua can be considered a homogeneous medium when it meets the following empirical criterion:

$$\frac{\mathcal{L}}{\ell} \geq \mathcal{A}^2 , \tag{1.1.1}$$

where $\mathcal{L}$ is the characteristic length of a solid, ℓ denotes the characteristic length of an element representing certain physical properties, and $\mathcal{A}$ is a large real number $(1/\mathcal{A} \ll 1)$ obtained from stochastic experiments. If this criterion is not met, then the material continua cannot be treated as homogeneous, such that we must account for variations in the material properties within the spatial coordinates. Since the initial publication of this theory, a number of criteria have been formulated for more advanced techniques aimed at estimating material inhomogeneity [203]. However, the Jasinsky formula remains both the simplest and most practical.

It is worth noting that there have been many attempts to systemize the types of inhomogeneity in solids based on their physical nature, mechanical behavior, and geometrical shape. Even the term itself has been given different meanings in different studies. The term *inhomogeneity* was used in [149, 217] to define bodies consisting of a number of homogeneous layers (note that Muskhelishvili [186] referred to such solids as compound or piecewise-homogeneous). Lekhnitskii [154] used the term *nonhomogeneous* to refer to both multilayer solids and bodies with continuous variation in elastic properties. In his book [156], he identifies the latter case as *continuously nonhomogeneous*. In other studies, bodies with macro-defects and macro-inclusions are also regarded as inhomogeneous [169]. Such solids are referred to as *statistically* (*or stochastically*) *inhomogeneous* in cases where the defects are randomly distributed [142, 189] within a solid or its parts.

In cases where the inhomogeneity is associated with certain kinds of impact, the consolidation of defects may induce unidirectional distributions. This is termed *inductive inhomogeneity* [142], and includes three basic types: *i*) multilayer or stratified bodies (material properties are constant in certain layers or blocks of a solid); *ii*) continuously inhomogeneous bodies (the variation profiles of the material properties are continuous but not necessarily smooth); and *iii*) multi-modular bodies (the properties are different under contraction and tension). Often, inductively inhomogeneous solids exhibit anisotropic behavior. More detail on the classifications of inhomogeneities can be found in [103, 142, 202].

An important class of inhomogeneity is concerned with the response of certain materials to non-uniform temperature distributions, which

significantly affect mechanical performance. This effect is usually referred to as *thermosensitivity*, and presents a profound impediment to analysis, due to the fact that heat-conduction and thermoelasticity in thermosensitive materials appear to be nonlinear [107, 195]. Nonlinearity arises not only in the heat-conduction equation (the coefficients of which are dependent on the unknown temperature), but also in the specific types of boundary condition, such as complex heat exchange [151].

One specific type of inhomogeneity is concerned with the effects of time. The material properties of concrete, for example, depend significantly on curing time so that they are non-uniform within the solid (e.g., the surface hardens more quickly). Analogous situations can be observed in the imbibition/drying of porous materials, saturation and material diffusion, and fatigue damage. All of these processes are of the evolutionary type and affect the material properties in a non uniform manner within the solid, such that material inhomogeneity is actually a function of time and/or spatial coordinates.

Inhomogeneity can be also categorized with respect to *i*) the number of variable moduli (whether all or only specific material moduli can be regarded as functions of their spatial coordinates) and *ii*) the direction (whether the inhomogeneity is exhibited in one or more spatial directions). In the case of anisotropic inhomogeneous solids, this type of classification is made more complicated by the large number of independent material moduli and the possibility of changes in anisotropy from point to point.

1.2. History of development

1.2.1. Applications in geomechanics

It appears that most of the pioneering works related to the mechanics of inhomogeneous solids have been related to important problems in the field of geomechanics. Most of those studies were performed at the end of the nineteenth century, and have continued in two main directions: wave propagation in soil deposits (Fig. 1.1), with applications in seismology, and the distribution of forces in massive soil deposits when acted upon by either transient or steady-state localized pressures (Fig. 1.2), i.e., indentation problems with applications in civil engineering.

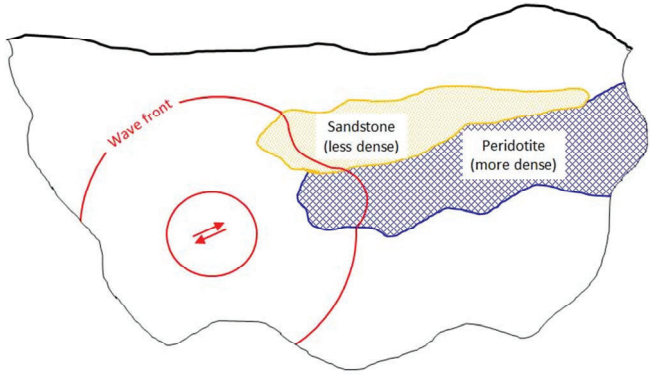

Fig. 1.1 Schematic representation of the soil nonhomogeneity effect in the seismic wave velocity

Due to the stratified nature of soil deposits, most pioneering papers devoted to the analysis of wave propagation have addressed multilayer semi-infinite structures [67, 120, 243]. There are, however, a number of earlier papers that assumed variation in all or certain properties of rocks and soils in a continuous manner with respect to depth coordinate. Specifically, Meissner [172] studied the propagation of surface waves in an inhomogeneous medium, rigidity modulus $G(z)$ and density $\rho(z)$ of which are respectively quadratic and linear functions of depth coordinate z:

$$G(z) = G_0(1+\delta z)^2, \quad \rho(z) = \rho_0(1+\delta z), \quad G_0, \delta = \text{const}. \qquad (1.2.1)$$

Meissner demonstrated that if soil inhomogeneity is taken into account, then the surface waves are purely torsional in character. These waves oscillate horizontally and normally to the direction of propagation, and thus should be regarded as transverse waves. Meissner also demonstrated that these waves exhibit dispersive characteristics, which can be evaluated numerically under the assumption of (1.2.1) using the shear modulus and density given by linear functions of depth. In an attempt to analyze the main features of waves travelling through an inhomogeneous material, Aichi [3] addressed a problem similar to the one considered by Meissner under the assumption that both of the above-mentioned parameters can be represented using exponential functions of depth with dissimilar exponent numbers. Sezawa [248] extended the Meissner–Aichi solution to cases involving two dimensions. The propagation of Rayleigh waves in a continuously-inhomogeneous medium was first considered by Stoneley [263], and later by Pekeris [211]. Further developments were presented in

[40, 47, 51–53, 58, 65, 94, 108–110, 122, 161, 180, 187, 193, 245, 254, 256, 264, 270, 338, 340, 341, 349]. The history of this development is detailed in [67, 188].

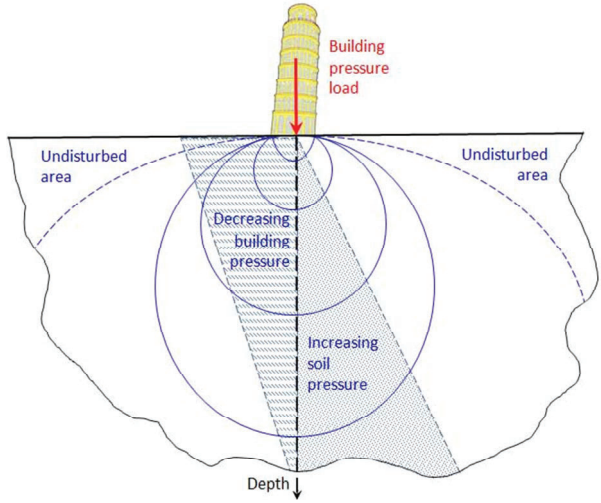

Fig. 1.2 Scheme of pressure distribution in soil due to local pressure

In three papers [42–44], Burmister considered an analogy to the well-known Boussinesq problem to analyze pressure distributions in two- and three-layer soil deposits. Later, Kogan [140] extended this technique to the case of an arbitrary number of layers resting on a homogeneous substrate. A natural development of this technique has been done by Lekhnitskii [155] generalizing the solution for multilayer solids in order to analyze continuous inhomogeneity.

The effect of continuous material inhomogeneity in distribution of pressure in soil deposits due to external force loadings applied to a part of plane boundary or when the boundary suffers a local deflection, has been earlier studied by Fröhlich [74], who has pointed out the importance of encountering the with-the-depth variation of the Young modulus in the evaluation of stress in semi-infinite elastic foundations with a reference to earlier experimental results published by Föppl [72] in 1897. Fröhlich further evaluated the influence of void ratio on variations in the modulus of elasticity in soil deposits modeled by a half-space and attempted thereby the inhomogeneity contribution into the distribution of normal and shearing forces under the plane boundary of a half-space. By making use

of these results, Ohde [201] estimated the depth-variation of the shearing modulus $G(z)$ of an elastic soil foundation as

$$G(z) = g(z + z_0)^w, \tag{1.2.2}$$

with g, w, and z_0 being constants.

Besides the dependence (1.2.2), there were a number of similar estimations for the dependences of elastic moduli on the depth coordinate. For example, Lekhnitskii [155] demonstrated that if the Poisson ratio is assumed to be constant and the Young modulus varies proportionally to the depth, then the radial stress σ_{rr} due to a concentrated force applied to a point on the surface can be expressed as follows:

$$\sigma_{rr} = -\frac{2}{\pi r}(P_x + 2P_y\theta)\cos\theta, \tag{1.2.3}$$

where P_x and P_y are the components of applied force in directions perpendicular and parallel to the surface, respectively, and r and θ are the polar coordinates with the origin at the point where the force is applied. It follows from (1.2.3) that if the applied force is normal to the surface (i.e., $P_y = 0$), then the radial stress distribution within the framework of the plane problem for an incompressible isotropic material is the same as for a homogeneous half-plane. If the Young modulus varies inversely proportional to the depth, formula (1.2.3) takes the form:

$$\sigma_{rr} = -\frac{P_x}{\pi x}, \tag{1.2.4}$$

wher x is the depth coordinate. Furthermore, concentrated force applied parallel to the boundary does not cause any stress in the half-plane.

In [80], Gibson addressed the case of linear depth-variation in the sharing modulus $G(z) = G(0) + mz$ in an incompressible elastic foundation $z \geq 0$. He also pointed out other simple cases of inhomogeneity; i.e., $G(z) = G(0)\exp(\lambda z)$ and

$$G(z) = \frac{\eta G(0)}{\eta + z}, \tag{1.2.5}$$

which allow for the comparatively simple analysis of stresses or displacements in such solids. Here, m, λ, and η are constant parameters and $G(0)$ denotes the value of the shearing modulus on surface $z = 0$. In [83], these results were extended for the case of an inhomogeneous layer. Awojobi [19] was able to solve the dual integral equations of a mixed boundary value problem by studying vertical vibrations in so-called "Gibson soil" (i.e., the kind of inhomogeneity addressed by Gibson). In [20], the same technique was used for the analysis of multilayer coatings resting on a homogeneous substrate. "Gibson soil of second kind" (i.e., soil with the shear modulus given in (1.2.5) with negative η) was analyzed in [21]. Those results were further developed in [22, 38, 39, 82, 84, 86, 253]. Gibson and Sills [85] also analyzed the case where the Poisson ratio varies with depth.

In addition to the distribution of stresses within the depth of soil deposits, another important problem in geomechanics is determining contact pressure on the surface of a half-space (or a half-plane) caused by an indenter applied against the surface or surface deflection resulting from the imposed pressure. In a series of papers, Popov (e.g., [221]) introduced the following simple formula for the calculation of surface deflection $w(x, y)$ due to a force $p(x, y)$ applied to boundary $z = 0$ of half-space $z \geq 0$:

$$w(x,y) = \int_0^\infty f_0(t)dt \iint_{-\infty}^{\infty} J_0\left(\sqrt{(x-\xi)^2 + (y-\eta)^2}\right) p(\xi,\eta)d\xi d\eta, \quad (1.2.6)$$

where $J_0(x)$ is the zero order Bessel function of the first kind. In view of (1.2.6), the problem of determining surface deflection is reduced to determining function $f_0(t)$. Popov demonstrated that if the Young modulus of the half-space varies as a power function of depth (i.e., $E(z) = E_n z^n$, $E_n = \text{const}$, $n = \text{const}$ and $0 < n < 1$), then function $f_0(t)$ can be described in the following form:

$$f_0(t) = \frac{\alpha}{\pi E_n} \frac{\Gamma\left(\frac{1}{2} - \frac{\nu}{2}\right)}{\Gamma\left(\frac{1}{2} + \frac{\nu}{2}\right)} \left(\frac{t}{2}\right)^n . \quad (1.2.7)$$

Here, constant $\alpha = \dfrac{3+n}{2(1+n)(2+n)}$ was contributed by Klein [137], who was the first to derive the following equation for surface deflection in this type of inhomogeneity:

$$w(x,y) = \frac{\alpha}{\pi E_n} \iint_{-\infty}^{\infty} \frac{p(\xi,\eta)d\xi d\eta}{\left((x-\xi)^2 + (y-\eta)^2\right)^{\frac{1+m}{2}}} \quad . \tag{1.2.8}$$

This equation can also be obtained by inserting (1.2.7) into (1.2.6). A similar result was found for the case of exponential variation in the Young modulus (i.e., $E(z) = E_\gamma \exp(\gamma z)$, $E_\gamma = \text{const}$ and $\gamma = \text{const}$ [220]).

The analysis of surface deflections and inner stresses for certain dependences of the Young modulus on depth and various loading profiles $p(x,y)$ have been developed using equations similar to (1.2.8) by Rostovtsev [234, 235], Rostovtsev and Khranevskaia [237], Mossakovskii [185], Chuaprasert and Kassir [56, 131], Kassir [128–130], Carrier and Christian [46], Chuong [57], and many others.

1.2.2. Mechanics of composite materials

The analysis of inhomogeneous materials was developed further in the mid-twentieth century due to advances in materials science and the widespread implementation of composite materials. Composite materials may exhibit anisotropic [55, 154, 156, 277, 310] and/or inhomogeneous [103, 104, 202, 203] mechanical behavior [62, 87, 123, 194], contingent on the methods used to combine constituent phases or reinforcing elements. In the analysis of material inhomogeneity, one important publication of note is a collection of papers [203] presented at *The Warsaw Symposium on Nonhomogeneity in Elasticity and Plasticity (Warsaw, Poland, September 3 – 9, 1958)*. This book reflects the experience of numerous scientists from 14 countries and summarizes the basic methods developed for the analysis of inhomogeneous materials in the fields of elasticity, plasticity, rheology, dynamics, and wave propagation as well as the statistical methods used to characterize micro-non-homogeneity.

It is worth noting that the periodic or semi-periodic material structures found in some composite materials (e.g., fiber composites and reinforced composites) make it possible to nullify the effects of material inhomogeneity through the implementation of various homogenization procedures, such that the focus is shifted solely to the effects of anisotropy

[25]. In many cases however, inhomogeneity must be considered within the context of multilayer structures [217, 258, 259].

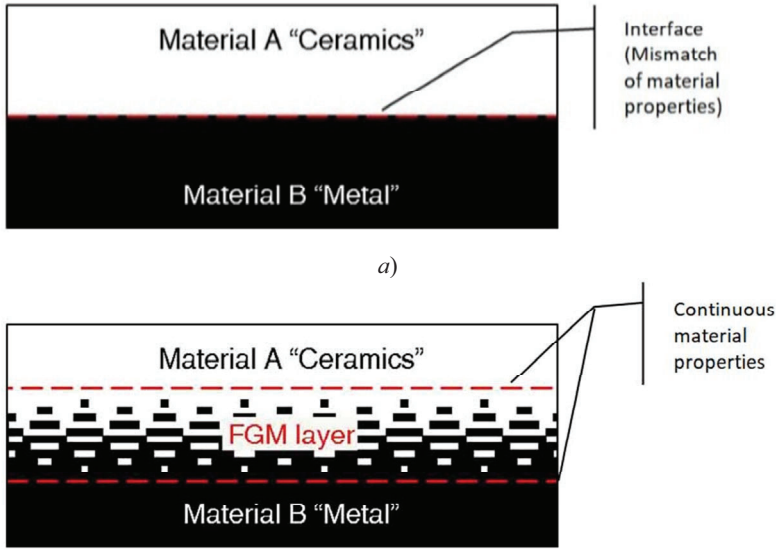

Fig. 1.3. Two-component metal-ceramic composite without (*a*) and with (b) FGM interlayer

1.2.3. Functionally-graded materials

In the 1980s, considerable advances were made in the fabrication of inhomogeneous materials with intentionally-continuous variations in macroscopic material properties based on desired distribution profiles [141, 190, 165]. Much of this work focused on functionally-graded materials (FGM) – a class of multiphase composite combining two or more phase-materials with contrasting properties. According to Rabin and Shiota [231], "*the term FGM, now widely used by the materials community, originated in Japan in the late 1980s as a description of a class of engineering materials exhibiting spatially inhomogeneous microstructure and properties*" (see also [115, 141, 183, 230, 233]). FGM are widely used to improve the operational performance of structural members subjected to mechanical as well as thermal loading [182, 195]. They comprise dissimilar materials that provide high thermal and mechanical resistance (e.g., ceramics and metals) [33, 54, 132, 184, 255,

266, 339]. Residual stresses that develop at the interfaces between the two constituents due to the mismatch in material properties can lead to material degradation (Fig 1.3*a*). This effect can be minimized by continuously (or almost continuously) varying the material properties of FGMs (Fig 1.3*b*) from one constituent material to another [16, 196, 271]. This type of variation is generally presented in the form of arbitrary dependences of the elastic moduli on spatial coordinates. Note that this makes it nearly impossible to solve problems of elasticity and thermoelasticity analytically [272], due to the fact that the governing equations include unknown variable coefficients. Thus, the development of efficient methods applicable to the thermomechanical analysis of inhomogeneous materials (and FGM in particular) is an important problem in modern engineering. The interested reader can find recent reviews of problems related to FGM solids in [63, 121, 268, 269, 279].

1.3. Overview of Solutions

1.3.1. Specific solution methods

Modeling and analysis methods vary according to the type of inhomogeneity. The methods also differ in terms of body shape, coordinate system, the type of solution that is required, techniques used, and loading types. There is really no way therefore to present a comprehensive review of methods used in the analysis of inhomogeneous solids. Thus, in this section, we present a brief description of the methods and solutions that are most relevant to the subject matter dealt with in this book. We are aware that many important results remain beyond the scope of this review, and for this we apologize.

Mikhlin [177] developed a general theory of the hyperbolic equations with variable (piecewise-variable) coefficients used to analyze the dynamic processes in non-homogeneous media with further development, e.g., in [23]. The method of plane waves was presented in [61, 153] aimed at dealing with systems that involve hyperbolic equations with smooth variable coefficients. An extensive review of early work in this area can be found in [24]. This general theory makes it possible to derive important theoretical results, such as the mathematical substantiation of the existence and uniqueness of solutions for certain functional spaces; however, it has not found widespread use in practical engineering applications.

The complex variable method was developed by Mishiku and Teodosiu [181] for the analysis of plane static problems, which were reduced to a set

of conjugation problems to be solved through successive approximations. Gorbachev and Pobedria [92, 93] used the averaging method for differential equations by reducing problems of elasticity in inhomogeneous materials to recurrent problems for homogeneous bodies that approximate but satisfy the boundary conditions. Naumov and Chistyak [191] constructed a formal asymptotic solution to the problem of an arbitrarily inhomogeneous layer. Shevchuk [251] presented a method by which to derive approximate solutions of heat conduction problems in solids with thin multilayer coatings modeled using generalized boundary conditions.

A number of solutions have been constructed using approximate formulations [232] and variational principles [1, 30, 340]. The perturbation method was proposed in [150] to reduce thermoelasticity problems for thermosensitive bodies to a recurrent sequence of boundary-value problems to be solved using differential equations with constant coefficients. The Hamilton variational principle was presented in [102] to develop a hybrid numerical method for the analysis of transient wave propagation in an FGM cylinder. The simplified Gurtin's variational principle was presented in [347] for FGM thermoviscoelastic plates. Variational principles were also used to develop homogenization procedures for micro-inhomogeneous periodic structures [15, 163]. Vasilenko [309] proposed a numerical approach to solving a non-axisymmetric problem for a radially-inhomogeneous anisotropic cylinder. Klimenko [138] reported a numerical solution for a cylinder inhomogeneous in the circumferential direction. Other important methods include the finite element method [91, 171, 276, 307], the boundary element method [95, 97, 113, 350], the method of the displacement potential [127, 212], and the finite difference method [66].

One interesting analytical-numerical technique was developed by Aizikovich et al. [4, 5, 7] for the analysis of contact problems in inhomogeneous materials with arbitrary variations in the properties with respect to depth. This technique is based on the bilateral asymptotic method [8]. The key point is to numerically evaluate the kernels of the obtained integral equations. After the kernel structure is defined, it can be approximated using a special expression, which makes it possible to solve the integral equation analytically. This allows for the calculation of an analytical solution, which is convenient for mechanical analysis of the effects of arbitrary inhomogeneity [147, 148] and FGM material properties using indentation experiments [6, 9]. In the following, we discuss the dominant analytical methods used in the analysis of continuously-inhomogeneous solids.

1.3.2 Dominant methods

1.3.2.1. Material moduli in form of elementary functions of spatial coordinates

The dominant approach to the analysis of continuously-inhomogeneous solids is based on the assumption that the material properties take the form of specific elementary functions (e.g., linear, polynomial, or exponential functions) in a manner that allows for the separation of variables in the governing equations. This yields comparatively simple solutions based on classical techniques. Various issues involved in the separation of variables by means of this approach have been discussed by Kolchin [142], Leknitskii [156], Teodorescu [278], and others.

In illustrating this technique, we consider a plane-stress problem for an elastic element $-a \le x \le a$, $-b \le y \le b$, where x and y are dimensionless Cartesian coordinates and a and b are constant parameters. By introducing the potential Airy function $\varphi(x,y)$ [282], this problem can be reduced to the following equation [288]:

$$\nabla^2\left(\frac{\nabla^2\varphi(x,y)}{E(x,y)}\right) - 2\frac{\partial^2\varphi(x,y)}{\partial x\partial y}\frac{\partial^2}{\partial x\partial y}\left(\frac{1+\nu(x,y)}{E(x,y)}\right)$$

$$-\frac{\partial^2\varphi(x,y)}{\partial y^2}\frac{\partial^2}{\partial x^2}\left(\frac{1+\nu(x,y)}{E(x,y)}\right)$$

$$-\frac{\partial^2\varphi(x,y)}{\partial x^2}\frac{\partial^2}{\partial y^2}\left(\frac{1+\nu(x,y)}{E(x,y)}\right) = 0, \qquad (1.3.1)$$

where ∇^2 stands for the differential Laplace operator. If we assume that the Young modulus is $E = E_0\varsigma(y)$ (where E_0 is a dimensional constant and $\varsigma(y)$ is an arbitrary twice-continuously-differentiable function) and Poisson ratio ν is a constant, then the problem on the elastic equilibrium of the considered element can be reduced to the following equation:

$$\nabla^4\varphi(x,y) - 2\frac{1}{\varsigma(y)}\frac{d\varsigma(y)}{dy}\frac{\partial}{\partial y}\left(\nabla^2\varphi(x,y)\right)$$

$$+\left(\frac{1}{\varsigma(y)}\frac{d^2\varsigma(y)}{dy^2}-2\left(\frac{1}{\varsigma(y)}\frac{d\varsigma(y)}{dy}\right)^2\right)$$

$$\times\left(\nu\frac{\partial^2\varphi(x,y)}{\partial x^2}-\frac{\partial^2\varphi(x,y)}{\partial y^2}\right)=0\,. \qquad (1.3.2)$$

Note that in the plane-strain case, we substitute ν with $\nu/(1-\nu)$ and ς with $\varsigma/(1-\nu^2)$.

Clearly, this equation has constant coefficients under the following condition:

$$\frac{1}{\varsigma(y)}\frac{d\varsigma(y)}{dy}=\kappa=\text{const}\,. \qquad (1.3.3)$$

This means that

$$\varsigma(y)=\varsigma_0\exp(\kappa y)\,, \qquad (1.3.4)$$

where $\varsigma_0>0$ is an arbitrary constant.

If we assume that

$$\frac{1}{\varsigma(y)}\frac{d^2\varsigma(y)}{dy^2}-2\left(\frac{1}{\varsigma(y)}\frac{d\varsigma(y)}{dy}\right)^2=0\,, \qquad (1.3.5)$$

then we obtain the following:

$$\varsigma(y)=\frac{1}{\varsigma_1+\varsigma_2 y}\,, \qquad (1.3.6)$$

where ς_1 and ς_2 are arbitrary constants that ensure the feasibility of the Young modulus; i.e., $\varsigma_1+\varsigma_2 y>0$ for $-b\le y\le b$. This expression does not make the coefficients in (1.3.2) constant; however, it does allow for the representation of (1.3.2) in the following form:

$$(\varsigma_1+\varsigma_2 y)\nabla^4\varphi(x,y)+\varsigma_2\frac{\partial}{\partial y}\left(\nabla^2\varphi(x,y)\right)=0\,, \qquad (1.3.7)$$

which can be integrated (e.g., for the case where φ is a harmonic function), as follows:

$$\nabla^2\varphi(x,y)=0\,. \tag{1.3.8}$$

Note that equation (1.3.7) does not involve the Poisson ratio ν, that is typical for the plane problems of elasticity in homogeneous materials with no body forces or thermal loading [282].

Another type of material-distribution profile that allows for the integration of equation (1.3.2) by making use of the classical methods has the form of a power function

$$\varsigma=\varsigma_3 y^{\kappa_0}\,, \tag{1.3.9}$$

where ς_3 and κ_0 are arbitrary constants.

For obvious reasons, i.e., a comparatively simple solution technique along with the ability to implement classical methods, representations (1.3.4), (1.3.6), and (1.3.8), with some modifications, have remained in the spotlight from the very beginning till nowadays. As mentioned in Section 1.2.1, Gibson [80, 81] presented a simple approach to the analysis of a nonhomogeneous half-space with the shear modulus in the forms given in (1.3.4) and (1.3.6), as well as the linear form for problems in geomechanics. In [21, 46, 253], these types of nonhomogeneity were examined using numerical techniques with different loadings on the half-space boundary. Korenev [143], Mossakovsii [185], Popov [222], and many others have presented solutions to problems involving indentation of a circular punch into an exponentially-nonhomogeneous half-space using the couple-integral equation representation. Mixed and contact problems for a nonhomogeneous half-space with power-law dependences of the elastic moduli on the depth-coordinate were addressed in [155, 234, 236]. Giannakopoulos and Pallot [79] presented an exact solution to the axisymmetric problem of indentation by a circular punch into an elastic half-space, where the Young modulus varies with depth in accordance to the power law and Poisson's ratio is constant. The same material properties were considered in [28] for the analysis of a plane-strain contact problem with an inhomogeneous half-space subjected to the action of a rigid punch within the finite area of its limiting plane. Teodorescu [278, p. 653] generalized the representation (1.3.4) by considering inhomogeneity in the following form:

$$\varsigma=\varsigma_0\exp\big(f(x,y,z)\big)\,, \tag{1.3.10}$$

where $f(x, y, z)$ is a continuous differentiable function of class C^4. An extensive review of studies involving exponential inhomogeneity can be found in [302].

Similar types of inhomogeneity have been analyzed in a wide range of coordinate systems. Zimmerman and Lutz [351] used the Frobenius series method to analyze thermal stresses in an FGM cylinder under uniform heating to characterize the linear dependences of properties on the thickness-coordinate. Horgan and Chan [111, 112] constructed a solution to an isotropic inhomogeneous hollow circular cylinder and disk, where the Young modulus is a power function of the thickness coordinate under constant rotation velocity and uniformly pressurized on inner and outer boundaries. They reduced this problem to the Navier equation for radial displacement to be solved in a closed form. A closed-form solution was also reported by Oral and Anlas [205] for a hollow orthotropic cylinder with analogous variation in the elastic moduli. Jabbari et al. [117] solved plane axi-symmetric elasticity and thermoelasticity problems for hollow cylinders by reducing them to the governing Navier equation. An analytic solution to the latter equation for plane non-axisymmetric elasticity and thermoelasticity problems in a thick hollow cylinder was presented [118] in the form of the complex Fourier series where the material properties are given as power functions of the radial coordinate. The non-axisymmetric temperature has also been derived for cases with a various thermal conduction coefficients. A similar solution was reported by Tarn [274] and Tarn and Chang [275] for a radially-inhomogeneous piezoelectric circular cylinder. Zhang and Hasebe [346] constructed a solution to the plane non-axisymmetric elasticity problem for a radially-inhomogeneous hollow cylinder with an exponential Young's modulus and constant Poisson's ratio.

At this point, the sheer number of studies on this method makes it difficult to present an exhaustive review (numerous references are listed in [63, 121, 269, 279, 335]). The popularity of this approach can be attributed to several advantageous features. First, the assumption that material properties are specific functions of spatial coordinates makes it possible (in many cases) to simplify the governing equations, such that classical methods of mathematical physics are applicable. Second, this approach allows for the modeling and analysis of inhomogeneity implementing the dependence of elastic moduli on more than one spatial coordinate. This makes it possible to obtain closed-form analytical solutions for use as benchmarks in the verification and validation of solutions applicable to problems of greater complexity.

Nonetheless, the solutions obtained using this approach are subject to limitations. First, they are not widely generalizable; therefore, a new

system of fundamental solutions must be constructed for each inhomogeneity profile. Furthermore, the representation of material properties using monotonic functions for infinite or semi-infinite solids often produces unfeasible results, due to the fact that such representations contradict modeling restrictions when the material properties become either zero or infinitely large (see, e.g., [225]). Unfeasible results can be avoided by modeling these solids using combined material properties, e.g., polynomial [224, 273], polynomial-exponential [246], or periodic [247]. Another way to ensure the material properties fall within model restrictions at infinite points is to consider an infinite or a semi-infinite body as an assembly comprising a finite elastic inhomogeneous part perfectly connected to a homogeneous semi-infinite massive (the rest of the original body) [147, 148, 297]. This approach has been used for the analysis of mixed-type boundary-values problems, such as the indentation of semi-infinite inhomogeneous solids. In just such a manner, Choi and Paulino [50] considered thermoelastic contact between a flat punch and a nonhomogeneous assembly consisting of an exponentially-nonhomogeneous layer resting on a homogeneous half-space. Yang et al. [342] considered the thermo-elastic response of a three-layer half-space (with the outer and infinite layers homogeneous and the intermediate layer graded exponentially) to a mixture of Hertz pressure, tangential traction, and frictional heating. Yevtushenko et al. [345] considered transient temperature processes in a composite strip resting on a homogeneous foundation. One solution to the plane problem of thermoelastic contact instability in an FGM layer and homogeneous substrate was recently obtained using the perturbation method [167]. The elastic properties of the layer were assumed to vary exponentially within the thickness coordinate. A similar form of the material properties of a layer resting upon a homogeneous substrate has been addressed in [48] to solve a rigid punch indentation problem with heat generation due to contact friction using an integral transform method.

In most studies based on this method, the Poisson ratio is assumed to be constant because "*Poisson's ratio* ν *has, in general, small variation*" [278, p.653]. However, the effect of variation in Poisson's ratio plays a significant role in the mechanical behavior of inhomogeneous materials [90, 106, 134]. One solution to the problem of elasticity in an inhomogeneous half-plane which is acted upon by a concentrated surface load was obtained in [88, 89] for the case where Poisson's ratio is an exponential function of depth.

The representation of material properties using the specific functions of spatial coordinates provides ample opportunity for the precise analysis of

inhomogeneous solids; however, this approach offers little in terms of characterizing materials with arbitrary material-distribution profiles.

1.3.2.2 Discrete-layer approach

One effective approach to the analysis of solids exhibiting continuous inhomogeneity in one spatial direction (Fig. 1.2*a*) rests upon the representation by assemblies of perfectly-connected homogeneous layers, such that the original dependences of the material properties can be approximated using a piecewise-constant function (Fig. 1.2*b*). Having solved the problem for each homogeneous layer, we can tailor the solutions using interface conditions to obtain a solution for the entire solid, which satisfies the original boundary conditions on its surfaces. This method is known as the discrete-layer approach [229]. Zhang and Hasebe [346] used this approach to approximate an exponentially-graded cylinder with a composite cylinder consisting of a number of perfectly-bounded thin homogeneous cylindrical layers of uniform thickness. They applied the Michell stress function to solve each layer, and provided recommendations for extending this approach to the general case of inhomogeneity. Liew et al. [158] analyzed symmetric and non-symmetric thermal stresses in an FGM hollow cylinder sectioned into a number of sub-cylinders. In [159], a contact between a cylindrical punch and a homogeneous half-space coated with an exponentially-graded layer has been solved. A semi-analytical solution was derived by representing the material using an assembly of homogeneous layers. The same approach was extended in [160] to the case of an arbitrarily-nonhomogeneous layer and in [133] to the case of frictionless contact between indenters and a functionally-graded half-plane with an arbitrarily-varying elastic modulus. This problem was reduced to a Cauchy singular integral equation. By the analogy to a layered media, Green's function has been constructed by Alshits and Kirchner [11] for hollow and solid radially inhomogeneous cylinders. By representing a radially inhomogeneous hollow cylinder as a multilayer solid, Kim and Noda [136] employed the method of Green function in order to solve a thermoelasticity problem in the case of unsteady axisymmetric thermal loading. The same concept has been used in [249] for the analysis of axisymmetric thermal stresses in a cylinder of finite length. A numerical technique for the one-dimensional problem in a thermosensitive FGM cylinder composed of functionally-graded ceramic–metal-based materials was developed in [18]. Different aspects of this method have also been discussed in [135, 192, 204, 215, 250].

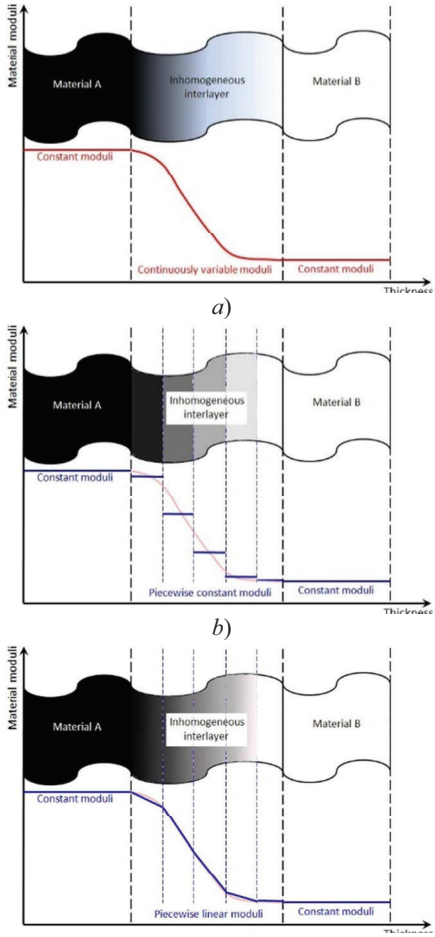

Fig. 1.2. Continuously inhomogeneous solid (*a*) and its discrete-layer models (*b, c*): representation of original material profile using stepwise functions, where the material moduli are constant (*b*) or linear (*c*) within each layer

The discrete-layer method makes it possible to analyze inhomogeneous solids whose moduli have arbitrary variations in a spatial direction. In application however, this approach generates certain complications. Watremetz et al. [336] compared the results of modeling a continuously-inhomogeneous solid with its multi-layer model. This comparison highlighted the weaknesses of the discrete-layer approach, which include

stress discontinuities at layer interfaces, weak convergence of the approximate solution to the exact one when the number of layers is increased, and complex 3D modeling. The effect of discontinuity of the stresses on the interfaces of layers representing a continuously-inhomogeneous solid has also been emphasized in [286].

In order to optimize convergence and avoid discontinuities at layer interfaces, Plevako [213] proposed the formulation of material properties within each layer as linear functions (Fig. 1.2*c*). This allows the approximation of elastic characteristics using continuous polylines instead of piecewise constant functions, thereby improving the approximation toward an exact solution. An analogous approach to the approximation of an inhomogeneous strip using a piecewise-exponential composite was presented by Guo and Noda [98]. It can be seen that this approach combines the discrete-layer method and the representation of material properties in the form of elementary functions.

1.3.3 Direct integration method

An efficient approach to the analysis of inhomogeneous solids can be developed on the basis of a general direct integration concept. The advantages of applying direct integration to elasticity-related problems was clearly delineated by Michell [176] over a hundred years ago: "*In treating the problem of an elastic solid in equilibrium under given volume- and surface-forces, some of the advantages of a direct determination of the stress are so obvious that it is surprising more attention has not been given to this mode of attack*". However, the interpretation of the concept of direct integration requires clarification.

In mathematical physics, the concept of direct methods is concerned, traditionally, with the application of approximate methods for solving certain boundary value problems for differential or integral equations by reducing them to systems of linear algebraic equations [178, 179, 257]. These methods are widely applied to problems in practical engineering as well as theoretical analysis into the existence and correctness of solutions to engineering problems of greater complexity. Direct methods based on variational principles [60, 257] include the energy method (the practical implementation of which deals with the application of the Ritz technique), the Galerkin method, the least-squares method, and the finite-difference method.

In this book, we discuss a direct integration method that differs fundamentally from the above-mentioned methods. Conceptually, the proposed method is based on integration of the governing elasticity and

thermoelasticity equations derived directly from first principles without the use of potential functions of higher differential order. This allows for the construction of correct solutions, particularly for boundary value problems for bounded domains.

With this regard we would refer to a comment made by Gakhov[2] in his foreword to the book [139]: "*In present time, integral transforms can be regarded as the most powerful and widely-used mathematical tool for solving practical problems.*[3]" Potential (harmonic or biharmonic) functions are constructed in the mapping domain an integral transform is used for the separation of variables in boundary value problems of solid mechanics. However, those functions do not necessarily exist in the physical domain unless certain supplementary conditions, such as conditions of general equilibrium of the applied force and thermal loadings, are fulfilled. This can be explained by the divergence of integral representations for potential functions at some points of the physical domain corresponding to the poles of their images in the mapping domain with respect to the transform parameter.

Consider, for example [321], the biharmonic Airy stress function $\varphi_A(x,y)$ for the plane elasticity problem in a half-plane $\{(x,y):|x|<\infty,\ 0\le y<\infty\}$ which is acted upon by normal $-p_0(x)$ and shear $q_0(x)$ force loadings applied to its boundary $y=0$. This function can be represented in the physical domain by the following expression:

$$\varphi_A(x,y)=\frac{1}{2\pi}\int_{-\infty}^{+\infty}\left(\left(\frac{1}{s^2}+\frac{y}{|s|}\right)\bar{p}_0+\frac{iy}{s}\bar{q}_0\right)\exp(-|s|y+isx)\,ds\,, \quad (1.3.11)$$

where $i=\sqrt{-1}$ is an imaginary unit and $\bar{p}_0$ and $\bar{q}_0$ are the images of the force loadings $p_0(x)$ and $q_0(x)$ in the mapping domain of the Fourier integral transform [41]. As shown in (1.3.11), the integrand can be unlimited at the pole $s=0$. This drawback can be removed by subjecting the forces $p_0(x)$ and $q_0(x)$ to the following static conditions of equilibrium:

---

[2] Gakhov, Fyodor Dmitriyevich (1906 – 1980) was a full member of the Academy of Sciences of the Byelorussian SSR. He was recognized as an outstanding Soviet and Belorussian specialist on the theory of boundary value problems in mathematical physics, analytical functions of complex variables, and the theory of integral transforms.

[3] Translated from Russian by the authors.

$$\int_{-\infty}^{+\infty} p_0(x)dx = 0, \quad \int_{-\infty}^{+\infty} xp_0(x)dx = 0, \quad \int_{-\infty}^{+\infty} q_0(x)dx = 0\,, \qquad (1.3.12)$$

where the first and second equations express the self-equilibration of normal loading $p_0(x)$ by its resultant force and moment, and the third condition describes the self-equilibration of the shear loading by its resultant vector. In the mapping domain of the Fourier integral transform, conditions (1.3.12) can be given, respectively, as

$$\overline{p}_0(0) = 0, \quad \overline{p}_0'(0) = 0, \quad \overline{q}_0(0) = 0\,. \qquad (1.3.13)$$

Here, prime stands for a formal derivative by the parameter s. Obviously, in view of conditions (1.3.13), the integrand in formula (1.3.11) is limited for the entire range of variation for transform parameter s.

Conditions (1.3.12) appear obvious if formulating the problem in terms of stresses; however, they are not necessarily captured when formulating this problem in terms of displacement. Thus, when imposing boundary conditions for the displacement vector on the boundary of the half-plane, we must ensure that the displacements induce stress under meeting conditions (1.3.13). This necessity has been shown, e.g., by Muskhelishvili [186]. However, it is usually very difficult to ensure that the boundary displacements are in agreement with the stresses under meeting conditions (1.3.12), albeit with a few exceptions.

If the boundaries of an elastic solid are subjected to mixed-type boundary conditions, the conditions (1.3.12) are even harder to meet during problem formulation. In the formulation of boundary value problems in semi-infinite domains (i.e., contact problems for a half-plane or half-space), infinitely-distant areas are expected to be subjected to infinitesimal force loading. This is meant to equilibrate the non-equilibrated normal and shear stresses at the boundary, in contradiction of conditions (1.3.12). If, for example, shear loading is absent at boundary $y = 0$ of a half-plane, then $q_0(x) = 0$, $x \in (-\infty, \infty)$, and a normal pressure $p_0(x) = p_0^* = \text{const}$ is uniformly distributed over its finite segment $x \in [-x_a, x_a]$, $0 < x_a < \infty$, while $p_0(x) = 0$ for $x \in (-\infty, -x_a) \cup (x_a, \infty)$, such that the resulting force of the applied loading is easily derived as follows:

$$\int_{-\infty}^{+\infty} p_0(x)dx = 2x_a p_0^* . \qquad (1.3.13)$$

This means that *i*) the resultant stresses at the infinitely distant points $y \to \infty$ are to vanish and, at the same time, to be of the resultant force equal to $2x_a p_0^*$ and *ii*) the stress function (1.3.11) is unbounded at point $s = 0$ due to a failure to meet conditions (1.3.13). This failure complicates or makes it impossible to *a*) construct a solution to the formulated problem in the space of bounded and continuous functions, *b*) ensure the elastic strain energy is limited to the considered solid, and *c*) ensure that the conditions for solution correctness are met for the displacements and their integral characteristics (i.e., integral compatibility conditions) [17, 280].

Elucidating the elastic response of solids (particularly inhomogeneous solids) can be viewed as a primary goal in formulating an analytical mode of attack. The previous example makes it clear that this understanding calls for the construction of a solution to a specific boundary value problem and for establishment of fundamental correctness conditions. These conditions are meant to ensure that the fields of stresses and displacements fall within the assumptions of elasticity theory. This guarantees the strain energy accumulated in a solid is a bounded function.

Vihak[4] proposed a direct integration method to deal with this challenge. This was further developed by subsequent researchers [126, 287], resulting in a general approach to optimizing thermal regimes, thermal stresses, and displacements in elastic solids based on the method of inverse thermomechanics [312, 313]. The latter method can be used to determine optimal control function u representing, for example, the density of inner heat sources in an elastic solid $\mathcal{D}^*$. This reduces the problem to minimizing the uniform deflection function of component $S(x,\tau,u)$ of a quasi-static stress-tensor or a displacement vector from a given distribution $\varphi(x,\tau)$, as follows:

$$\mathcal{J}(u) = \max_{(x,\tau)} \left| S(x,\tau,u) - \varphi(x,\tau) \right|, \quad (x,\tau) \in \mathcal{D}^* \times (0,\tau^*] . \qquad (1.3.14)$$

[4] Vihak (or Vigak), Vasyl' Mykhaylovych (1936 – 2003) was a Doctor of Science, leading scientist, and head of the solid mechanics department at the Pidstryhach Institute for Applied Problems of Mechanics and Mathematics of the National Academy of Sciences of Ukraine. He is the author of more than 230 scientific papers (including two fundamental monographs on optimization theory) in the mechanics of solids and optimization theory.

The existence of such a control function (i.e., $u(x,\tau) \in C_{\mathcal{D}^* \times (0,\tau^*]}$) implies the existence of an exact lower limit of the above optimization criterion. This lower limit can be written as follows:

$$S(x,\tau,u) = \varphi(x,\tau), \quad (x,\tau) \in \mathcal{D}^* \times (0,\tau^*]. \tag{1.3.15}$$

Then, heat-conduction and thermoelasticity problems result in the following integral equation of the first kind:

$$\int_0^\tau \int_{\mathcal{D}^*} \mathcal{K}(x,\tilde{x},\tau,\tilde{\tau}) u(\tilde{x},\tilde{\tau}) d\tilde{x} d\tilde{\tau} = \varphi_1(x,\tau), \quad (x,\tau) \in \mathcal{D}^* \times (0,\tau^*], \tag{1.3.16}$$

where $\mathcal{K}(x,\tilde{x},\tau,\tilde{\tau})$ and $\varphi_1(x,\tau)$ are known functions. Solving equation (1.3.16) is generally an ill-posed problem [244]. It was demonstrated by Vihak [312, 313] that an optimal control function $u(x,\tau)$, which meets condition (1.3.15) and, which is the same, satisfies equation (1.3.16), exists only under certain necessary conditions for function $\varphi(x,\tau)$. The conditions include those corresponding to integral conditions of equilibrium and compatibility for the stress-tensor and displacement-vector components.

This "intermediate", at the first glance, result originated an important stage of studies related to the substantiation of a method for the direct integration of differential equilibrium and compatibility equations in terms of stresses. This method makes it possible to reduce a direct elasticity problem to a governing equation for an individual stress-tensor component (or a linear combination of stress-tensor components). This component is referred to as a key function and, in a certain sense, can be regarded as analogous to a control function. The component can be derived using the governing equation by implementing certain integral equilibrium and compatibility conditions in conjunction with relations expressing all quested-for functions in terms of the key function.

The principal strategy underlying the application of this method to problems of elasticity and thermoelasticity in terms of stresses can be represented in a step-wise manner, as follows:

- In the first step, the key functions are selected from the stress-tensor components or their linear combinations (e.g., the first invariant of the stress-tensor) with the aim of achieving the most convenient formulation of the governing equations and the integral conditions. This choice depends strictly on the properties of the differential

operators presenting the original equations of the formulated problem, the boundary conditions, and the material properties. The key functions are usually involved in differential compatibility equations.

- The next step involves deriving the relations expressing all the stress-tensor components through the key functions identically in view of the conditions imposed on the boundary of the solid considered. Such relations can be obtained through the correct integration of the local differential equilibrium equations pertaining to all of the stresses (irrespective of the material properties) within the framework of a static or quasi-static formulation.
- The relations derived in the previous step can then be used to reduce the compatibility equations to the governing equations along with the local and integral conditions for the key functions. This makes it possible to reduce the original problem to a boundary value problem for the key functions. Note that unlike the relations between stresses in the previous step, the governing equations generally involve material properties. This is because they cover strain compatibility in an elastic solid.
- In this step, the key functions are determined from the derived boundary value problem. This can be achieved using an appropriate variable-separation method to construct the key functions in the form of explicit dependences on the given loadings and material properties.
- After the key stresses are determined, the remaining stress-tensor components are restored using the relations obtained in the second step.
- After the stress-tensor components are computed explicitly, the strain-tensor and displacement vector components can be determined through the integration of the strain-displacement equations.

This method was used to construct correct (continuous and integrable) solutions to the plane elasticity and thermoelasticity problems in homogeneous isotropic domains in [314, 319, 329]. For a half-plane, the boundary conditions have been analyzed in detail in terms of stresses, displacements, and mixed-type boundary conditions [283, 299]. In addition to the construction of analytical solutions, this approach allows for derivation of *i*) the integral equilibrium and compatibility conditions for thermal and mechanical loadings along with the quested-for stresses, strains, and displacements, *ii*) expressions for the resultant force and resultant

moment of the normal and sharing stress-tensor components and applied loadings, and *iii*) one-to-one relations between the stress-tensor and displacement-vector components, which remain valid at the boundary of a solid. Similar results have been obtained for the one- and two-dimensional problems of elasticity and thermoelasticity in cylindrical-polar coordinate systems [315].

Note that the advantages of the direct integration method have been demonstrated for problems of elasticity and thermoelasticity in finite domains with corner points (i.e., domains with surface that can be represented by families of dissimilar coordinate surfaces [96]). Obtaining solutions to such problems is complicated by the non-self-conjugated differential operator for domains with such boundaries. This makes it difficult to construct comprehensive orthogonal systems for the separations of variables in the governing equations. Generally, the fundamental functions of such systems are complex, variable, and non-orthogonal, requiring decomposition algorithms of some sophistication [164]. This makes it very difficult to satisfy the boundary conditions throughout the entire surface of the solid (including areas adjacent to corner points). The history of such problems analysis can be traced back to the famous problem on the elastic equilibrium of a cube under arbitrary normal loadings on each side, which has been formulated by Lamé and nominated in 1846 for the "*Grand Prix de Mathématiques"* of the Paris Academy of Sciences [173]. For example, we can mention the method of crosswise superposition [174] and the method of homogeneous solutions [164] as the dominant ones involving biharmonic potential functions and setting the priority in exact satisfaction of the differential equations while the boundary conditions are satisfied approximately. In contrast to these methods, the one suggested by Vihak is aimed in exact satisfaction of the boundary conditions by explicitly expressing the solutions through the functions imposed on the boundary, which is advantageous, e.g., for solving inverse and optimization problems [343, 344]. By making use of this approach, analytical solutions to the plane elasticity and thermoelasticity problems for a rectangular domain $|x| \leq x_0$, $|y| \leq y_0$, where x_0 and y_0 are positive constants, were represented in the form of decompositions by the followings complete and orthogonal systems of functions:

$$\left\{1,\ y,\ \cos\frac{\gamma_n y}{y_0}, \sin\frac{\lambda_n y}{y_0}\right\},$$
$$\left\{1,\ x,\ \cos\frac{\gamma_n x}{x_0}, \sin\frac{\lambda_n x}{x_0}\right\},\quad n=1,2,\ldots, \tag{1.3.17}$$

where $\gamma_n = n\pi$ and λ_n are positive roots of a transcendent equation $\tan\lambda = \lambda$ enumerated in increasing order.

In (1.3.17), subsystems $\left\{\cos\frac{\gamma_n y}{y_0}, \sin\frac{\lambda_n y}{y_0}\right\}$ and $\left\{\cos\frac{\gamma_n x}{x_0}, \sin\frac{\lambda_n x}{x_0}\right\}$ comprise the eigen-functions of the problem and segregate the parts

$$\sigma_{xx}^s = \sum_{n=1}^{\infty}\left(X_n^1(x)\cos\frac{\gamma_n y}{y_0} + X_n^2(x)\sin\frac{\lambda_n y}{y_0}\right),$$
$$\sigma_{yy}^s = \sum_{n=1}^{\infty}\left(Y_n^1(y)\cos\frac{\gamma_n x}{x_0} + Y_n^2(y)\sin\frac{\lambda_n x}{x_0}\right) \tag{1.3.18}$$

of the normal stresses with the resultant force and moment are both zero:

$$\int_{-x_0}^{x_0}\sigma_{yy}^s dx = \int_{-x_0}^{x_0} x\sigma_{yy}^s dx = 0,\quad \int_{-y_0}^{y_0}\sigma_{xx}^s dy = \int_{-y_0}^{y_0} y\sigma_{xx}^s dy = 0. \tag{1.3.19}$$

They correspond to the self-equilibrated parts of the force loadings applied to the sides of the rectangle and the body forces. Here,

$$X_n^1 = \frac{1}{y_0}\int_{-y_0}^{y_0}\sigma_{xx}\cos\frac{\gamma_n y}{y_0}dy,$$
$$X_n^2 = \frac{1}{y_0\sin^2\lambda_n}\int_{-y_0}^{y_0}\sigma_{xx}\sin\frac{\lambda_n y}{y_0}dy,$$
$$Y_n^1 = \frac{1}{x_0}\int_{-x_0}^{x_0}\sigma_{yy}\cos\frac{\gamma_n x}{x_0}dx, \tag{1.3.20}$$

$$Y_n^2 = \frac{1}{x_0 \sin^2 \lambda_n} \int_{-x_0}^{x_0} \sigma_{yy} \sin \frac{\lambda_n x}{x_0} dx.$$

One approach to deriving the above coefficients was developed in [325, 327] for elasticity problems and in [330] for thermoelasticity problems based on an iterative routine that satisfies the governing equations within the required degree of accuracy.

Subsystems $\{1,\ y\}$ and $\{1,\ x\}$ of the system in (1.3.17) comprise the so-called associated functions used to segregate the elementary parts [282]

$$\sigma_{xx}^0 = X_0^1(x) + yX_0^2(x), \quad \sigma_{yy}^0 = Y_0^1(y) + xY_0^2(y) \tag{1.3.21}$$

of normal stresses corresponding to the resultant forces and moments of the applied loadings:

$$2\int_{-y_0}^{y_0} \sigma_{xx}^0 dy = -\int_{-y_0}^{y_0} (p_1 + p_2) dy$$

$$+ \int_{-x_0}^{x_0} \left(q_4(\xi) - q_3(\xi) - \int_{-y_0}^{y_0} F_x(\xi, y) dy \right) \operatorname{sgn}(x - \xi) d\xi,$$

$$2\int_{-y_0}^{y_0} y\sigma_{xx}^0 dy = -\int_{-y_0}^{y_0} (p_1 + p_2) y dy$$

$$+ \int_{-x_0}^{x_0} \left(p_3(\xi) - p_4(\xi) - \int_{-y_0}^{y_0} F_y(\xi, y) dy \right) |x - \xi| d\xi$$

$$+ \int_{-y_0}^{y_0} ((x - x_0)q_1 + (x + x_0)q_2) dy$$

$$- \int_{-x_0}^{x_0} \left(y_0 (q_3(\xi) + q_4(\xi)) + \int_{-y_0}^{y_0} yF_x(\xi, y) dy \right) \operatorname{sgn}(x - \xi) d\xi,$$

$$2\int_{-x_0}^{x_0}\sigma_{yy}^{0}dx=-\int_{-x_0}^{x_0}\left(p_3+p_4\right)dx \tag{1.3.22}$$

$$+\int_{-y_0}^{y_0}\left(q_2(\eta)-q_1(\eta)-\int_{-a}^{a}F_y(x,\eta)dx\right)\operatorname{sgn}(y-\eta)d\eta\,,$$

$$2\int_{-x_0}^{x_0}x\sigma_y dx=-\int_{-x_0}^{x_0}\left(p_3+p_4\right)xdx$$

$$+\int_{-y_0}^{y_0}\left(p_1(\eta)-p_2(\eta)-\int_{-x_0}^{x_0}F_x(x,\eta)dx\right)|y-\eta|\,d\eta$$

$$+\int_{-x_0}^{x_0}\left((y-y_0)q_3+(y+y_0)q_4\right)dx$$

$$-\int_{-y_0}^{y_0}\left(a\left(q_1(\eta)+q_2(\eta)\right)+\int_{-x_0}^{x_0}xF_y(x,\eta)dx\right)\operatorname{sgn}(y-\eta)d\eta\,.$$

Here, $p_j(y)$ and $q_j(y)$ are the normal and shear loadings applied to the sides $x=(-1)^{j+1}x_0$; $p_{j+2}(x)$ and $q_{j+2}(x)$ are the loadings on the sides $y=(-1)^{j+1}y_0$, $j=1,2$; and F_x and F_y are the projections of body forces onto the coordinate axes. The following coefficients were identified and analyzed in [318]:

$$X_0^1=\frac{1}{2y_0}\int_{-y_0}^{y_0}\sigma_{xx}dy,\quad X_0^2=\frac{3}{2y_0^3}\int_{-y_0}^{y_0}y\sigma_{xx}dy,$$
$$Y_0^1=\frac{1}{2x_0}\int_{-x_0}^{x_0}\sigma_{yy}dx,\quad Y_0^2=\frac{3}{2x_0^3}\int_{-x_0}^{x_0}x\sigma_{yy}dx. \tag{1.3.23}$$

In this manner, the following representation of the solution makes it possible to represent the stress state through the superposition of self-equilibrated and non-self-equilibrated parts $\sigma_{\ell\ell}^{0}$ and $\sigma_{\ell\ell}^{s}$, respectively:

$$\sigma_{\ell\ell} = \sigma_{\ell\ell}^{0} + \sigma_{\ell\ell}^{s}, \quad \ell = \{x, y\}. \tag{1.3.24}$$

The self-equilibrated stresses peak (in terms of magnitude) in the vicinity of the loaded zones, and vanish when moving away from these zones. Hence, this representation confirms the Saint-Venant principle of static equivalence [282]. In [323, 326, 328], this approach was extended to plane problems for circular and annular segments and a cylinder of finite length.

The direct integration method also allows us to clear up important theoretical issues in the field of solid mechanics, such as the "overdetermined" system of equations for the three-dimensional formulation of elasticity theory in terms of stresses. Barré de Saint-Venant [281] obtained the following strain-compatibility (or continuity) equations:

$$\frac{\partial^2 \varepsilon_{yy}}{\partial x^2} + \frac{\partial^2 \varepsilon_{xx}}{\partial y^2} = \frac{\partial^2 \varepsilon_{xy}}{\partial x \partial y}, \text{ etc.} \tag{1.3.25}$$

and

$$2\frac{\partial^2 \varepsilon_{zz}}{\partial x \partial y} = \frac{\partial}{\partial z}\left(\frac{\partial \varepsilon_{yz}}{\partial x} + \frac{\partial \varepsilon_{zx}}{\partial y} - \frac{\partial \varepsilon_{xy}}{\partial z}\right), \text{ etc.} \tag{1.3.26}$$

If we eliminate displacements from the Cauchy strain-displacement equations, they can be regarded as classical, and are therefore included into most textbooks on the theory underlying elasticity and thermoelasticity theories. Here, $\varepsilon_{\ell m}$ represents the strain-tensor components, u_{ℓ} represents the displacements, $\ell, m = \{x, y, z\}$, and "etc." indicates two more equations obtained by cyclic permutation of indices and variables of differentiation. Using the constitutive strain-stress equations in conjunction with the equilibrium equations [282], allows us to represent equations (1.3.25) and (1.3.26) in terms of stresses; i.e., the Beltrami-Michell equations [278]. Along with three equilibrium equations, the six Beltrami-Michell equations present a system of nine equations for six stress-tensor components, which is, obviously, overdetermined.

In 1938, Southwell [260] proved that the application of Maxwell potential functions to the solution of a three-dimensional problem using

the Castigliano principle yields only (1.3.25), whereas the application of the Morera functions yields only (1.3.26). In a subsequent paper [261], Southwell noted the following: "*Commenting on these results, Professor G. I. Taylor remarked to me that by them three of the six conditions (11)* [(1.3.25) and (1.3.26) herein] *would seem to be made redundant; for if either the first or the second three of (11) are sufficient to ensure that* U [the total strain energy] *is stationary, then according to Castigliano's principle they should also ensure the existence of single-valued displacements, and no further conditions should be necessary. Once the paradox is revealed its resolution becomes a problem of some urgency...*". In the same paper, he sought to prove that all six of the equations given in (1.3.25) and (1.3.26) are necessary for the identic determination of displacement. His proof, however, was not supported with compelling evidence and the "Southwell paradox" remains an issue of some contention (see, [13, 14, 37, 146, 166, 175, 214, 262, 308, 331–333, 348]). In [337], Washizu used the Bianchi formulae to demonstrate that if equations (1.3.25) are satisfied in the interior points of body $\mathcal{B}$ and equations (1.3.26) are satisfied at its boundary $\partial\mathcal{B}$, then (1.3.26) is necessarily satisfied in the interior points on the body $\mathcal{B}$, and vice versa. Thus, Washizu presumed that while equations (1.3.25) are used as governing equations, equations (1.3.26) serve as a supplementary condition for the determination of displacements.

That hypothesis was confirmed by making use of the direct integration method, when Vihak [320] used three out of six Cauchy strain-displacement equations for an elastic parallelepiped $|x| \le a_x$, $|y| \le a_y$, $|z| \le a_z$ to derive the following expression for displacements:

$$2u_\xi = u_\xi\big|_{\xi=-a_\xi} + u_\xi\big|_{\xi=a_\xi}$$

$$+ \int_{-a_\xi}^{a_\xi} \varepsilon_{\xi\xi}\,\mathrm{sgn}(\xi-\zeta_\xi)\,d\zeta_\xi, \qquad \xi = \{x, y, z\}. \tag{1.3.27}$$

The remaining three Cauchy's equations in view of (1.3.27) yield the following integro-differential compatibility equation:

$$2\varepsilon_{\xi\eta} = \frac{\partial}{\partial\eta}\left(u_\xi\big|_{\xi=-a_\xi} + u_\xi\big|_{\xi=a_\xi} + \int_{-a_\xi}^{a_\xi} \varepsilon_{\xi\xi}\,\mathrm{sgn}(\xi-\zeta_\xi)\,d\zeta_\xi \right)$$

$$+\frac{\partial}{\partial\xi}\left(u_{\eta}\Big|_{\eta=-a_{\eta}}+u_{\eta}\Big|_{\eta=a_{\eta}}+\int_{-a_{\eta}}^{a_{\eta}}\varepsilon_{\eta\eta}\,\mathrm{sgn}(\eta-\zeta_{\eta})d\zeta_{\eta}\right),$$

$$\xi,\eta=\{x,y,z\}. \tag{1.3.28}$$

Differentiating equation (1.3.28), they can be reduced, under certain conditions on the sides of the parallelepiped to (1.3.25). This demonstrated that three out of the six Cauchy equations can be used for the determination of displacements u_{ξ}, $\xi=\{x,y,z\}$, while the remaining three can be used to derive three strain-compatibility equations. In bounded domains, these are generally of the integro-differential type. There are 17 equivalent triads of such equations, which support the results obtained by Ostrosablin [206] almost simultaneously. The advantage of this result has been efficiently used for solution of a number of three-dimensional problems for homogeneous and inhomogeneous solids [301, 302, 304, 316, 317].

The fact that the method of direct integration is oriented primarily toward the use of equilibrium equations and the establishment of relations between stress-tensor components in conjunction with the necessary conditions for stresses, strains, and displacements, irrespective of the material model makes the direct integration method useful for a wide range of applications. It has been combined with the method of conditional plastic strains [216] to develop an experimental-computational technique by which to determine steady-state residual stresses in welded joints modeled using locally-distributed fields of incompatible strains. In experiments, this technique was verified through the analysis of residual stresses in unbounded [324] and rectangular [293] plates with a rectilinear welded joint and a thick-walled elastic cylinder with a circumferential butt-weld [300].

The strategy generally used to apply the direct integration method appears to be an efficient approach to the analysis of elastic and thermoelastic responses of inhomogeneous solids. The efficiency can be explained by the fact that the basic stages of the method deal with the equations of equilibrium in terms of stresses, which are invariant with respect to a model of material properties. When deriving and solving the governing equations for key functions, the variable material properties are involved only in the later stages of the solution process. Thus, the technique used to deal with inhomogeneous solids is similar to that used for homogeneous material. The only difference is the fact that the

governing equations for inhomogeneous solids appear to be of integral or integro-differential type.

Note that the theoretical basis for this type of implementation was established by Lopatynsky [162] and Fichera [69]. The application of the integral equations received further development in papers by Panferov and Leonova [207], Clements and Rogers [58, 59], and Furuhashi [75, 76]. Furuhashi and Kataoka [77, 78], Li et al. [157], and Peng and Li [209, 210] focused on solutions to one-dimensional problems. A systematic implementation of this approach was later presented in [290].

In the following chapters, we systematically illustrate the application of the direct integration method to the solution of some basic boundary value problems related to elasticity, thermoelasticity, and heat-conduction when dealing with inhomogeneous solids.

CHAPTER TWO

PLANE PROBLEMS IN CARTESIAN COORDINATES

2.1. Basic assumptions and governing equations

2.1.1. Thermoelasticity equations for orthotropic inhomogeneous solid

Consider an elastic solid $\mathfrak{S}$ in a dimensionless Cartesian coordinate system (x, y, z). Within the framework of the classical uncoupled theory of thermoelasticity [197, 198], the equilibrium state of the considered solid is governed by the following vector equation

$$\operatorname{div} \hat{\boldsymbol{\sigma}} + \mathbf{B} = 0, \tag{2.1.1}$$

where $\operatorname{div} = (\partial / \partial x, \partial / \partial y, \partial / \partial z)$ is the divergence vector within Cartesian coordinates, $\hat{\boldsymbol{\sigma}} = \left\{ \sigma_{j\ell} \right\}_{\{j,\ell\}=\{x,y,z\}}$ is the symmetric ($\sigma_{j\ell} = \sigma_{\ell j}$) stress tensor, and $\mathbf{B} = (F_x, F_y, F_z)$, F_j is a projection of the resulting body force along the axes $j = \{x, y, z\}$. The above equation can be written in scalar form as follows:

$$\frac{\partial \sigma_{jx}}{\partial x} + \frac{\partial \sigma_{jy}}{\partial y} + \frac{\partial \sigma_{jz}}{\partial z} + F_j = 0, \quad j = \{x, y, z\}. \tag{2.1.2}$$

According to the theory of small deformations [278, 282], every component of the total strain tensor can be represented by a linear combination of stresses along with a thermal strain under the constitutive law as follows:

$$\varepsilon_{jk} = B_{jkxx}\sigma_{xx} + B_{jkxy}\sigma_{xy} + B_{jkxz}\sigma_{xz} + B_{jkyy}\sigma_{yy}$$

$$+B_{jkyz}\sigma_{yz}+B_{jkzz}\sigma_{zz}+\varepsilon_{jk}^{T},\qquad \{j,k\}=\{x,y,z\},\tag{2.1.3}$$

where, $\varepsilon_{jk}^{T}=\alpha_{jk}\delta_{jk}(T-T_0)$ are components of the spherical thermal-strain tensor involving only the diagonal elements expressed through the coefficients of linear thermal expansion $\alpha_{jj}=\alpha_j$ along the Cartesian axes $j=\{x,y,z\}$; δ_{jk} is the Kronecker delta; and T is the steady-state temperature distribution within body $\mathfrak{S}$, where T_0 is the initial temperature corresponding to the thermal-stress-free state, $B_{jk\ell m}$, $\{j,k,\ell,m\}=\{x,y,z\}$, are components of the tensor of material properties (elastic compliance components), which are irrespective of both strains and stresses and are functions of a material point only. In the general case of a linearly elastic solid, there are 21 independent component $B_{jk\ell m}$ out of 36 total. The number of independent components $B_{jk\ell m}$ can be reduced in some specific cases of material anisotropy [199, 240].

For example, if every point of an anisotropic solid can be regarded as an intersection of three mutually perpendicular planes with identical material properties, then, after ensuring that the planes are parallel to the coordinate planes, the number of independent components can be reduced to 9 and the solid referred to as orthotropically anisotropic or orthotropic. The constitutive law given in (2.1.3) in this case takes the following form:

$$\begin{aligned}
\varepsilon_{xx}&=B_{xxxx}\sigma_{xx}+B_{xxyy}\sigma_{yy}+B_{xxzz}\sigma_{zz}+\alpha_x(T-T_0),\\
\varepsilon_{yy}&=B_{xxyy}\sigma_{xx}+B_{yyyy}\sigma_{yy}+B_{yyzz}\sigma_{zz}+\alpha_y(T-T_0),\\
\varepsilon_{zz}&=B_{xxzz}\sigma_{xx}+B_{yyzz}\sigma_{yy}+B_{zzzz}\sigma_{zz}+\alpha_z(T-T_0),\\
\varepsilon_{xy}&=B_{xyxy}\sigma_{xy},\quad \varepsilon_{xz}=B_{xzxz}\sigma_{xz},\quad \varepsilon_{yz}=B_{yzyz}\sigma_{yz}.
\end{aligned}\tag{2.1.4}$$

The elastic compliances in (2.1.4) can also be represented using so-called technical parameters, which gives us another representation of the constitutive law [12, 154, 156]:

$$\varepsilon_{xx} = \frac{1}{E_x}\sigma_{xx} - \frac{\nu_{yx}}{E_y}\sigma_{yy} - \frac{\nu_{zx}}{E_z}\sigma_{zz} + \alpha_x(T - T_0),$$

$$\varepsilon_{yy} = -\frac{\nu_{xy}}{E_x}\sigma_{xx} + \frac{1}{E_y}\sigma_{yy} - \frac{\nu_{zy}}{E_z}\sigma_{zz} + \alpha_y(T - T_0),$$

$$\varepsilon_{zz} = -\frac{\nu_{xz}}{E_x}\sigma_{xx} - \frac{\nu_{yz}}{E_y}\sigma_{yy} + \frac{1}{E_z}\sigma_{zz} + \alpha_z(T - T_0), \tag{2.1.5}$$

$$\varepsilon_{xy} = \frac{1}{G_{xy}}\sigma_{xy}, \quad \varepsilon_{xz} = \frac{1}{G_{xz}}\sigma_{xz}, \quad \varepsilon_{yz} = \frac{1}{G_{yz}}\sigma_{yz}.$$

Here, E_x, E_y, and E_z respectively indicate the Young moduli in the directions of coordinate axes *x*, *y*, and *z*; ν_{jk} denotes the Poisson ratio describing contraction in the *j*-direction at tension in the *k*-direction; and G_{jk} is the shear modulus within the (j,k)-coordinate plane where $\{j,k\} = \{x,y,z\}$, $j \neq k$. Note that the technical parameters must meet the following conditions of symmetry:

$$E_j\nu_{kj} = E_k\nu_{jk}, \quad \{j,k\} = \{x,y,z\}, \quad j \neq k. \tag{2.1.6}$$

If every point in an elastic solid lie along a plane in which all material properties are equal (i.e., the plane of isotropy), then the number of independent elastic compliances is 5 and the body is referred to as transversely isotropic or transtropic. The constitutive law given in (2.1.3) for this type of solid is as follows:

$$\varepsilon_{xx} = B_{xxxx}\sigma_{xx} + B_{xxyy}\sigma_{yy} + B_{xxzz}\sigma_{zz} + \alpha_x(T - T_0),$$

$$\varepsilon_{yy} = B_{xxyy}\sigma_{xx} + B_{xxxx}\sigma_{yy} + B_{xxzz}\sigma_{zz} + \alpha_y(T - T_0),$$

$$\varepsilon_{zz} = B_{xxzz}(\sigma_{xx} + \sigma_{yy}) + B_{zzzz}\sigma_{zz} + \alpha_z(T - T_0), \tag{2.1.7}$$

$$\varepsilon_{xy} = 2(B_{xxxx} - B_{xxyy})\sigma_{xy}, \qquad \varepsilon_{xz} = B_{xzxz}\sigma_{xz}, \quad \varepsilon_{yz} = B_{xzxz}\sigma_{yz}.$$

Then, applying the technical parameters [154], (2.1.7) can be rewritten as follows:

$$\begin{aligned}
\varepsilon_{xx} &= \frac{1}{E}(\sigma_{xx} - \nu\sigma_{yy}) - \frac{\nu'}{E'}\sigma_{zz} + \alpha(T - T_0), \\
\varepsilon_{yy} &= \frac{1}{E}(-\nu\sigma_{xx} + \sigma_{yy}) - \frac{\nu'}{E'}\sigma_{zz} + \alpha(T - T_0), \\
\varepsilon_{zz} &= -\frac{\nu'}{E'}(\sigma_{xx} + \sigma_{yy}) + \frac{\sigma_{zz}}{E'} + \alpha'(T - T_0), \\
\varepsilon_{xy} &= \frac{\sigma_{xy}}{G}, \quad \varepsilon_{xz} = \frac{\sigma_{xz}}{G'}, \quad \varepsilon_{yz} = \frac{\sigma_{yz}}{G'}.
\end{aligned} \tag{2.1.8}$$

Here, E and E' are the Young moduli under tension or compression in the directions respectively lying along the plane of isotropy and in the direction perpendicular to this plane; ν indicates the Poisson ratio characterizing the out-of-plane contraction in response to tension applied in the plane of isotropy; and ν' is the Poisson ratio characterizing the in-plane contraction in response to tension applied in the out-of-plane direction; $G = E/(2+2\nu)$, α and G', α' are the shearing moduli and linear thermal expansion coefficients in the in-plane and out-of-plane directions, respectively.

If an elastic solid is elastically equivalent in all directions (i.e., all of the planes passing through a material point are equivalent), then there are only three independent elastic compliances and the solid can be regarded as isotropic. The constitutive law (2.1.3) for an isotropic solid can be written as follows:

$$\begin{aligned}
E\varepsilon_{xx} &= \sigma_{xx} - \nu(\sigma_{yy} + \sigma_{zz}) + \alpha E(T - T_0), \\
E\varepsilon_{yy} &= \sigma_{yy} - \nu(\sigma_{xx} + \sigma_{zz}) + \alpha E(T - T_0), \\
E\varepsilon_{zz} &= \sigma_{zz} - \nu(\sigma_{xx} + \sigma_{yy}) + \alpha E(T - T_0), \\
G\varepsilon_{xy} &= \sigma_{xy}, \quad G\varepsilon_{xz} = \sigma_{xz}, \quad G\varepsilon_{yz} = \sigma_{yz},
\end{aligned} \tag{2.1.9}$$

where E and G respectively indicate the Young modulus and shearing modulus, ν is the Poisson ratio, and α is the coefficient of linear thermal expansion.

After establishing a connection between the stress- and strain-tensor components in an elastic anisotropic solid, we can use the following Cauchy equations [240, 282] to express strain ε_{jk} and elastic displacement u_j in the direction of the j – coordinate axis, $j,k = x,y,z$:

$$\varepsilon_{xx} = \frac{\partial u_x}{\partial x}, \quad \varepsilon_{yy} = \frac{\partial u_y}{\partial y}, \quad \varepsilon_{zz} = \frac{\partial u_z}{\partial z},$$
$$\varepsilon_{xy} = \frac{\partial u_x}{\partial y} + \frac{\partial u_y}{\partial x}, \quad \varepsilon_{xz} = \frac{\partial u_x}{\partial z} + \frac{\partial u_z}{\partial x}, \quad \varepsilon_{yz} = \frac{\partial u_y}{\partial z} + \frac{\partial u_z}{\partial y}. \tag{2.1.10}$$

Assuming that the initial and current temperature distributions (i.e., T_0 and T) are known, then deriving the solution to a general thermoelasticity problem implies determining the following fifteen unknown functions: six stress-tensor components σ_{jk}, $\{j,k\} = \{x,y,z\}$, six strain-tensor components ε_{jk}, $\{j,k\} = \{x,y,z\}$, and three elastic displacements u_j, $j = \{x,y,z\}$, in elastic body $\mathfrak{S}$ using fifteen equations: the three equilibrium equations (2.1.2), the six constitutive equations (2.1.3) (which can be in the form (2.1.5), (2.1.8), or (2.1.9)), and the six Cauchy strain-displacement equations (2.1.10).

The number of quested-for functions can be reduced by formulating thermoelasticity boundary-value problems in terms of stresses or displacements, which are usually motivated by the boundary conditions imposed on boundary $\partial\mathfrak{S}$ of solid $\mathfrak{S}$.

If, for example, boundary $\partial\mathfrak{S}$ is subjected to external force loadings as follows:

$$\hat{\boldsymbol{\sigma}} \cdot \mathbf{n}\big|_{\partial\mathfrak{S}} = \mathbf{P}, \tag{2.1.11}$$

then it is reasonable to formulate the problems in terms of stresses. Here, $\mathbf{n}$ is the unit vector of outer normal to surface $\partial\mathfrak{S}$ and $\mathbf{P}$ is the vector of external force loadings. In this case, the displacements can be eliminated from the Cauchy equations (2.1.10) in order to derive the following strain-compatibility equations:

$$\frac{\partial^2 \varepsilon_{yy}}{\partial x^2} + \frac{\partial^2 \varepsilon_{xx}}{\partial y^2} = \frac{\partial^2 \varepsilon_{xy}}{\partial x \partial y},$$

$$\frac{\partial^2 \varepsilon_{xx}}{\partial z^2} + \frac{\partial^2 \varepsilon_{zz}}{\partial x^2} = \frac{\partial^2 \varepsilon_{xz}}{\partial x \partial z},$$

$$\frac{\partial^2 \varepsilon_{zz}}{\partial y^2} + \frac{\partial^2 \varepsilon_{yy}}{\partial z^2} = \frac{\partial^2 \varepsilon_{yz}}{\partial y \partial z}, \tag{2.1.12}$$

$$2\frac{\partial^2 \varepsilon_{zz}}{\partial x \partial y} = \frac{\partial}{\partial z}\left(\frac{\partial \varepsilon_{yz}}{\partial x} + \frac{\partial \varepsilon_{zx}}{\partial y} - \frac{\partial \varepsilon_{xy}}{\partial z}\right),$$

$$2\frac{\partial^2 \varepsilon_{xx}}{\partial y \partial z} = \frac{\partial}{\partial x}\left(\frac{\partial \varepsilon_{xz}}{\partial y} + \frac{\partial \varepsilon_{xy}}{\partial z} - \frac{\partial \varepsilon_{yz}}{\partial x}\right),$$

$$2\frac{\partial^2 \varepsilon_{yy}}{\partial x \partial z} = \frac{\partial}{\partial y}\left(\frac{\partial \varepsilon_{xy}}{\partial z} + \frac{\partial \varepsilon_{yz}}{\partial x} - \frac{\partial \varepsilon_{xz}}{\partial y}\right).$$

Substituting the constitutive equations (2.1.3) (or any equivalent such as (2.1.5), (2.1.8), or (2.1.9)), into the compatibility equations (2.1.12) makes it possible to represent the problems in terms of stresses. In the case of homogeneous isotropic solids, these equations are known as the Beltrami-Michell equations [278].

If the components of the displacement vector $\mathbf{u}$ are imposed on surface $\partial\mathfrak{S}$:

$$\mathbf{u}|_{\partial\mathfrak{S}} = \mathbf{u}^*, \tag{2.1.13}$$

where $\mathbf{u}^*$ is a given vector of boundary displacements, the problems can be formulated in terms of displacements by substituting (2.1.3) and (2.1.10) into (2.1.2), which yields three scalar equations for the determination of displacements in solid $\mathfrak{S}$ (in the case of homogeneous isotropic material they are known as the Lamé equations) [145].

The formulation of a boundary-value problem in terms of six stresses or three displacements appears to be simpler than the general formulation; however, it presents a challenge for analytical as well as numerical modes of attack. In some cases, the formulation of the problem can be simplified once the shape of the solids and loading profiles exhibit specific types of symmetry or the loadings show little variation in some spatial directions. One such simplification can be made when implementing the plane-strain

or plane-stress hypotheses, under which problems involving thermoelasticity can be considered using only a plane (two-dimensional) formulation with a smaller number of independent equations and quested-for functions of two spatial variables.

2.1.2. Plane strain

Assume that the length of orthotropic elastic solid $\mathfrak{S}$ in the *z*-direction $|z| < L \gg 1$ far exceeds the dimensions in the x- and *y*-directions. We set the temperature distribution T and external forces $\mathbf{P}$ or boundary displacement $\mathbf{u}^*$ under conditions (2.1.11) and (2.1.13), with body force $\mathbf{B}$ (where $F_z = 0$) independent of coordinate *z*. Then, at a sufficient distance from end-faces $z = \pm L$ of body $\mathfrak{S}$ we assume *i*) the stress- and displacement-fields do not depend on coordinate *z*; i.e., they vary only with coordinates x and y within a planar cross-section $\mathfrak{D} = \{(x, y, z_0), z_0 = \text{const}\}$ of body $\mathfrak{S}$; *ii*) shear strains ε_{xz}, ε_{yz} and stresses σ_{xz}, σ_{yz} are equal to zero; and *iii*) axial strain is constant (i.e., $\varepsilon_{zz} = e_0 = \text{const}$). If both end-faces of body $\mathfrak{S}$ are confined between two smooth rigid planes, then, obviously, $e_0 = 0$. If one or both of the end-faces are free of force loading, then due to (2.1.5), the constant axial strain can be determined as follows:

$$e_0 = \iint\limits_{\mathfrak{D}} \left(-\frac{\nu_{xz}}{E_x}\sigma_{xx} - \frac{\nu_{yz}}{E_y}\sigma_{yy} + \frac{1}{E_z}\sigma_{zz} + \alpha_{zz}(T - T_0) \right) dxdy \,. \quad (2.1.14)$$

In view of the foregoing assumptions, the equilibrium equations (2.1.2) take the following form:

$$\frac{\partial \sigma_{xx}}{\partial x} + \frac{\partial \sigma_{xy}}{\partial y} + F_x = 0, \quad \frac{\partial \sigma_{xy}}{\partial x} + \frac{\partial \sigma_{yy}}{\partial y} + F_y = 0 \,. \quad (2.1.15)$$

In view of the relationship depicted in (2.1.6), the constitutive equation given in (2.1.5) for ε_{zz} becomes

$$\sigma_{zz} = e_0 + \nu_{zx}\sigma_{xx} + \nu_{zy}\sigma_{yy} - \alpha_{zz}E_z(T - T_0) \,. \quad (2.1.16)$$

Substituting (2.1.16) into the first and second equations of (2.1.5) gives yet another form of the constitutive law for the case of plane strain within plane domain $\mathfrak{D}$:

$$\begin{aligned}
\varepsilon_{xx} &= \frac{1-\nu_{zx}\nu_{xz}}{E_x}\sigma_{xx} - \frac{\nu_{yx}+\nu_{zx}\nu_{yz}}{E_y}\sigma_{yy} \\
&\quad -\nu_{zx}e_0 + (\alpha_x + \alpha_z\nu_{zx})(T-T_0), \\
\varepsilon_{yy} &= \frac{\nu_{xy}+\nu_{xz}\nu_{zy}}{E_x}\sigma_{xx} - \frac{1-\nu_{zy}\nu_{yz}}{E_y}\sigma_{yy} \\
&\quad -\nu_{zy}e_0 + (\alpha_y + \alpha_z\nu_{zy})(T-T_0), \\
\varepsilon_{xy} &= \frac{1}{G_{xy}}\sigma_{xy}.
\end{aligned} \tag{2.1.17}$$

In view of the assumptions of the plane-strain hypothesis, the Cauchy equations (2.1.10) can be represented using the following three independent equations:

$$\varepsilon_{xx} = \frac{\partial u_x}{\partial x}, \quad \varepsilon_{yy} = \frac{\partial u_y}{\partial y}, \quad \varepsilon_{xy} = \frac{\partial u_x}{\partial y} + \frac{\partial u_y}{\partial x}. \tag{2.1.18}$$

Furthermore, the Saint-Venant equations (2.1.12) yield only one nontrivial equation:

$$\frac{\partial^2 \varepsilon_{yy}}{\partial x^2} + \frac{\partial^2 \varepsilon_{xx}}{\partial y^2} = \frac{\partial^2 \varepsilon_{xy}}{\partial x \partial y}. \tag{2.1.19}$$

Thus, the problem of determining stresses in solid $\mathfrak{S}$ under the plane strain hypothesis is reduced to determining three stress-tensor components σ_{xx}, σ_{yy}, and σ_{xy}, three strain-tensor components ε_{xx}, ε_{yy}, and ε_{xy}, and two displacements u_x and u_y as functions of x and y. This is achieved using the eight equations (2.1.15), (2.1.17), and (2.1.18) under the conditions represented by (2.1.11) or (2.1.13) imposed on boundary $\partial\mathfrak{D}$ of domain $\mathfrak{D}$. Substituting the constitutive equations in (2.1.17) into the compatibility equation (2.1.19) allows for deriving a compatibility

equation in terms of stresses, which along with two equations of equilibrium (2.1.15) present a closed system of three equations for determination of three stress-tensor components. After the in-plane stresses are computed, out-of-plane stress σ_{zz} can be derived using (2.1.16). Similarly, substituting the Cauchy equations (2.1.18) into the constitutive equations (2.1.17) allows the representation of the equilibrium equations in (2.1.15) in terms of displacement. This creates a closed system in which two Lamé equations are used for the determination of u_x and u_y.

2.1.3. Plane stress

A similar simplified formulation can be found in the case when an elastic body $\mathfrak{S} = \{(x, y, z), |z| < h/2\}$ is a thin plate of constant thickness h, the z-dimension of which is significantly smaller than the in-plane dimensions within domain $\mathfrak{D} = \{(x, y, z_0), \quad z_0 = \text{const}, \quad |z_0| \le h/2\}$. Assume that faces $z = \pm h/2$ are free of force loadings; the circumference of plate $\mathfrak{S}$ is loaded by forces symmetric with respect to its midplane $z = 0$ and parallel to it; the component of body-force vector F_z is absent; and components F_x and F_y along with temperature T are symmetric about the midplane $z = 0$. The assumption of symmetric loadings implies that vertical displacement u_z is zero at the midplane $z = 0$. This, along with small value for h, makes $u_z = 0$ for arbitrary z. Variations in u_x and u_y as a function of z can be regarded as insignificant, which means that they can be substituted with their averaged values

$$\tilde{u}_j = \frac{1}{h} \int_{-h/2}^{h/2} u_j dz, \quad j = \{x, y\}, \tag{2.1.20}$$

which are functions of $(x, y) \in \mathfrak{D}$.

Averaging the stress-tensor components in a fashion similar to (2.1.20), the foregoing assumptions imply that $\tilde{\sigma}_{zz} = \tilde{\sigma}_{xz} = \tilde{\sigma}_{yz} = 0$ and, consequently, $\tilde{\varepsilon}_{xz} = \tilde{\varepsilon}_{yz} = 0$. By omitting the tildes, equations (2.1.15), (2.1.18), and (2.1.19) become valid for the considered case of generalized

plane stress. In this case, the constitutive equations in (2.1.5) take the following form:

$$\varepsilon_{xx} = \frac{1}{E_x}\sigma_{xx} - \frac{\nu_{yx}}{E_y}\sigma_{yy} + \alpha_{xx}(T - T_0), \quad \varepsilon_{xy} = \frac{1}{G_{xy}}\sigma_{xy},$$
$$\varepsilon_{yy} = -\frac{\nu_{xy}}{E_x}\sigma_{xx} + \frac{1}{E_y}\sigma_{yy} + \alpha_{yy}(T - T_0). \tag{2.1.21}$$

The averaged axial strain can then be determined as follows:

$$\varepsilon_{zz} = -\frac{\nu_{xz}}{E_x}\sigma_{xx} - \frac{\nu_{yz}}{E_y}\sigma_{yy} + \alpha_{zz}(T - T_0). \tag{2.1.22}$$

Similar to the case of plane strain, the generalized plane-stress hypothesis makes it possible to reduce the general thermoelasticity problem to three equations for in-plane stresses σ_{xx}, σ_{yy}, and σ_{xy} or two equations for displacements u_x and u_y with the out-of-plane strain ε_{zz} expressed via the in-plane normal stresses using (2.1.22).

2.1.4. Governing thermoelasticity equations in terms of stresses

Despite the fact that the plane-strains and plane-stress hypotheses are applicable to solids of very different shapes (long prismatic bars for plane strain versus thin plates for plane stress), the thermoelasticity problems in both cases imply that in-plane stresses σ_{xx}, σ_{yy}, and σ_{xy} and displacements u_x and u_y must be derived using the same sets of equations (i.e., (2.1.15), (2.1.18), and (2.1.19)) under the constitutive law (in the form of (2.1.17) or (2.1.21)). In order to unify these two cases, the constitutive equations given in (2.1.17) and (2.1.21) can be rewritten as follows:

$$\varepsilon_{xx} = a_{11}\sigma_{xx} + a_{12}\sigma_{yy} - \varepsilon_1 + \alpha_1(T - T_0),$$
$$\varepsilon_{yy} = a_{12}\sigma_{xx} + a_{22}\sigma_{yy} - \varepsilon_2 + \alpha_2(T - T_0), \quad G_{xy}\varepsilon_{xy} = \sigma_{xy}, \tag{2.1.23}$$

where

$$a_{11} = \frac{1}{E_x}\begin{cases}1, \\ 1-\nu_{zx}\nu_{xz},\end{cases} \quad a_{22} = \frac{1}{E_y}\begin{cases}1, \\ 1-\nu_{zy}\nu_{yz},\end{cases}$$

$$a_{12} = -\frac{1}{E_y}\begin{cases}\nu_{yx}, \\ \nu_{yx}+\nu_{zx}\nu_{yz}\end{cases} = -\frac{1}{E_x}\begin{cases}\nu_{xy}, \\ \nu_{xy}+\nu_{xz}\nu_{zy},\end{cases} \tag{2.1.24}$$

$$\alpha_1 = \begin{cases}\alpha_x, \\ \alpha_x+\alpha_z\nu_{zx},\end{cases} \quad \alpha_2 = \begin{cases}\alpha_y, \\ \alpha_y+\alpha_z\nu_{zy},\end{cases} \quad \varepsilon_1 = \begin{cases}0, \\ \nu_{zx}e_0,\end{cases} \quad \varepsilon_2 = \begin{cases}0, \\ \nu_{zy}e_0.\end{cases}$$

The first line under each brace represents a case of plane stress and the second line corresponds to plane strain.

In the case of transversely isotropic materials whose general three-dimensional constitutive equations have the form (2.1.8), the unified plane constitutive law has the form (2.1.23), where

$$a_{11} = a_{22} = \frac{1}{E^*}, \quad a_{12} = -\frac{\nu^*}{E^*}, \quad \alpha_1 = \alpha_2 = \alpha^*,$$
$$\varepsilon_1 = \varepsilon_2 = \varepsilon_0, \quad G_{xy} = G, \tag{2.1.25}$$

and

$$E^* = \begin{cases}E, \\ \dfrac{EE'}{E'-\nu'^2E},\end{cases} \quad \nu^* = \begin{cases}\nu, \\ \dfrac{\nu E'+\nu'^2E}{E'-\nu'^2E},\end{cases}$$
$$\alpha^* = \begin{cases}\alpha, \\ \alpha+\alpha'\nu',\end{cases} \quad \varepsilon_0 = \begin{cases}0, \\ \nu' e_0.\end{cases} \tag{2.1.26}$$

Note that $2G = E^*/(1+\nu^*)$.

In the case of isotropic materials represented by (2.1.9), the unified plane constitutive equations have the form (2.1.23) using the coefficients in (2.1.25), where

$$E^* = \begin{cases}E, \\ \dfrac{E}{1-\nu^2},\end{cases} \quad \nu^* = \begin{cases}\nu, \\ \dfrac{\nu}{1-\nu},\end{cases} \quad \alpha^* = \begin{cases}\alpha, \\ \alpha(1+\nu),\end{cases} \quad \varepsilon_0 = \begin{cases}0, \\ \nu e_0.\end{cases} \tag{2.1.27}$$

Note that due to the fact that $a_{11}a_{22} - a_{12}a_{21} \neq 0$, the constitutive equations (2.1.23) can be inversed to determine the elastic stresses in terms of the strain-tensor components.

Now, by making use of the unified plane constitutive equations (2.1.23), we can represent the compatibility equation (2.1.19) in terms of stresses.

If we assume that the material properties in the unified plane constitutive law (2.1.23) are functions of the in-plane coordinates x and y, then in terms of stresses, the compatibility equation (2.1.19) has variable coefficients. The derived compatibility equation can be simplified using the following formulae:

$$\frac{\partial^2 \sigma_{yy}}{\partial y^2} - \frac{\partial^2 \sigma_{xx}}{\partial x^2} = \frac{\partial F_x}{\partial x} - \frac{\partial F_y}{\partial y},$$
$$2\frac{\partial^2 \sigma_{xy}}{\partial x \partial y} = -\frac{\partial^2 \sigma_{xx}}{\partial x^2} - \frac{\partial^2 \sigma_{yy}}{\partial y^2} - \frac{\partial F_x}{\partial x} - \frac{\partial F_y}{\partial y}. \tag{2.1.28}$$

These formulae follow from the equilibrium equations (2.1.15). In view of equations (2.1.15) and (2.1.28), the third equation of (2.1.23) yields the following:

$$\frac{\partial^2 \varepsilon_{xy}}{\partial x \partial y} = \frac{\partial^2}{\partial x \partial y}\left(\frac{1}{G_{xy}}\right)\sigma_{xy} - \frac{\partial}{\partial x}\left(\frac{1}{G_{xy}}\right)\left(\frac{\partial \sigma_{xx}}{\partial x} + F_x\right)$$
$$-\frac{\partial}{\partial y}\left(\frac{1}{G_{xy}}\right)\left(\frac{\partial \sigma_{yy}}{\partial y} + F_y\right)$$
$$-\frac{1}{2G_{xy}}\left(\frac{\partial^2 \sigma_{xx}}{\partial x^2} + \frac{\partial^2 \sigma_{yy}}{\partial y^2} + \frac{\partial F_x}{\partial x} + \frac{\partial F_y}{\partial y}\right). \tag{2.1.29}$$

Substituting (2.1.29) as well as the first and second equations of (2.1.23) into (2.1.19) yields the following compatibility equation in terms of stresses:

$$\frac{\partial^2}{\partial x^2}\left(a_{12}\sigma_{xx} + a_{22}\sigma_{yy} - \varepsilon_2 + \alpha_2(T - T_0)\right)$$

$$+\frac{\partial^2}{\partial y^2}\left(a_{11}\sigma_{xx}+a_{12}\sigma_{yy}-\varepsilon_1+\alpha_1(T-T_0)\right)$$

$$+\frac{\partial}{\partial x}\left(\frac{1}{G_{xy}}\right)\frac{\partial\sigma_{xx}}{\partial x}+\frac{\partial}{\partial y}\left(\frac{1}{G_{xy}}\right)\frac{\partial\sigma_{yy}}{\partial y}-\frac{1}{2G_{xy}}\left(\frac{\partial^2\sigma_{xx}}{\partial x^2}+\frac{\partial^2\sigma_{yy}}{\partial y^2}\right)$$

$$=\frac{\partial^2}{\partial x\partial y}\left(\frac{1}{G_{xy}}\right)\sigma_{xy}-F_x\frac{\partial}{\partial x}\left(\frac{1}{G_{xy}}\right)$$

$$-F_y\frac{\partial}{\partial y}\left(\frac{1}{G_{xy}}\right)-\frac{1}{G_{xy}}\left(\frac{\partial F_x}{\partial x}+\frac{\partial F_y}{\partial y}\right). \tag{2.1.30}$$

If all of the material properties depend on only one variable, then the compatibility equation can be simplified greatly. If, for example, the material properties are arbitrary functions of y, then equation (2.1.30) takes the following form:

$$\Delta\left(a_{11}\sigma-\alpha_1(T-T_0)\right)=(\alpha_1-\alpha_2)(T-T_0)$$

$$+\frac{\partial}{\partial y}\left(\left(2\beta_1-\frac{1}{G_{xy}}\right)\frac{\partial\sigma_{yy}}{\partial y}\right)$$

$$-\beta_2\frac{\partial^2\sigma_{yy}}{\partial x^2}+\frac{d^2\beta_1}{dy^2}\sigma_{yy}+\frac{d^2\varepsilon_1}{dy^2}$$

$$+\beta_1\left(\frac{\partial F_y}{\partial y}-\frac{\partial F_x}{\partial x}\right)-\frac{\partial}{\partial y}\left(\frac{F_y}{G_{xy}}\right), \tag{2.1.31}$$

where

$$\beta_1=a_{11}-a_{12},\quad \beta_2=a_{22}-a_{11},\quad \Delta=\frac{\partial^2}{\partial x^2}+\frac{\partial^2}{\partial y^2} \tag{2.1.32}$$

and

$$\sigma=\sigma_{xx}+\sigma_{yy} \tag{2.1.33}$$

is the in-plane total stress.

In the case of transversely isotropic or isotropic materials, the compatibility equation (2.1.31) takes the following form:

$$\Delta\left(\frac{1}{E^*}\sigma-\alpha^*(T-T_0)\right)=\frac{\sigma_{yy}}{2}\frac{d^2}{dy^2}\left(\frac{1}{G}\right)+\frac{d^2\varepsilon_0}{dy^2}$$

$$+\frac{1}{G}\left(\frac{\partial F_y}{\partial y}-\frac{\partial F_x}{\partial x}\right)-\frac{\partial}{\partial y}\left(\frac{F_y}{G}\right), \tag{2.1.34}$$

where parameters E^* and α^* are expressed by equations (2.1.26) for transversely isotropic material and by equations (2.1.27) for isotropic material.

The resulting compatibility equations (2.1.31) and (2.1.34) are formulated only for normal stress σ_{yy} and the total stress introduced by (2.1.33). One more equation for these functions can be derived by adding $\partial^2\sigma_{yy}/\partial x^2$ to both sides of the first equation (2.1.28). In view of (2.1.33), this addition yields

$$\Delta\sigma_{yy}=\frac{\partial^2\sigma}{\partial x^2}+\frac{\partial F_x}{\partial x}-\frac{\partial F_y}{\partial y}. \tag{2.1.35}$$

Equations (2.1.35) and (2.1.31) or (2.1.34) present a complete system for the determination of stresses σ_{yy} and σ in an inhomogeneous orthotropic, transversely isotropic, or isotropic solid, whose material properties are arbitrarily differentiable functions of y. Thus, these functions can be regarded as the key function in the realization of the direct integration method procedure (see **Section 1.5**) Calculating these stresses makes it easy to derive the normal stress σ_{xx} using (2.1.33). Shearing stress σ_{xy} can then be determined using the second equation of (2.1.28).

2.1.5. Two-dimensional heat-conduction equation

The governing thermoelasticity equations (2.1.30), (2.1.31), and (2.1.34) involve the temperature field, which can be determined from a relevant heat-conduction problem. If the temperature T varies with z so

little that $dT / dz = 0$, which is the case under the foregoing plane-strain and plane-stress hypotheses, the corresponding steady-state heat-conduction equation is as follows [100, 199]:

$$\frac{\partial}{\partial x}\left(\lambda_x(x,y)\frac{\partial T(x,y)}{\partial x}\right)+\frac{\partial}{\partial y}\left(\lambda_y(x,y)\frac{\partial T(x,y)}{\partial y}\right)=-w(x,y), \quad (2.1.36)$$

where $w(x,y)$ denotes the quantity of heat generated by inner heat sources and $\lambda_x(x,y)$ and $\lambda_y(x,y)$ are the heat transfer coefficients respectively in the directions of the Cartesian axes x and y. For inhomogeneous materials, the heat transfer coefficients can be regarded as arbitrary functions of position (x,y). If we assume that these coefficients are functions of coordinate y only, then equation (2.1.36) can be written in the following form:

$$\lambda_y(y)\Delta T(x,y)+\frac{d\lambda_y(y)}{dy}\frac{\partial T(x,y)}{\partial y}$$

$$+\left(\lambda_x(y)-\lambda_y(y)\right)\frac{\partial^2 T(x,y)}{\partial x^2}=-w(x,y). \quad (2.1.37)$$

For isotropic material and transversely isotropic one for which plane isotropy is parallel to the plane (x,y), the orthotropic coefficients in equation (2.1.36) are $\lambda_x(x,y)=\lambda_y(x,y)=\lambda(x,y)$. For equation (2.1.37), the orthotropic coefficients are $\lambda_x(y)=\lambda_y(y)=\lambda(y)$. If the coefficients are constant, equation (2.1.37) yields the classical heat-conduction coefficient for homogeneous material [197].

To determine the temperature field uniquely, equations (2.1.36) or equation (2.1.37) must be set within relevant boundary conditions. There are three basic types of boundary conditions: *i*) the values of temperature are imposed on the boundary (known as the boundary conditions of the first kind, or Dirichlet boundary conditions), *ii*) the values of heat flux are imposed on the boundary (known as the boundary conditions of the second kind or Neumann boundary conditions), and *iii*) the values of temperature and the heat flux are imposed on the mutually complementary parts of the boundary (mixed-type boundary conditions) or both temperature and heat flux are imposed on the entire boundary (the boundary conditions of the

third kind). The latter is often applied in the modeling of convective heat exchange [200].

Note that many practical cases involve a special type of inhomogeneity, in which the heat conduction coefficients are functions of temperature (e.g., thermosensitive material [195]). In these cases, equation (2.1.36) becomes nonlinear. Moreover, when heat exchange is imposed on the surface of a thermosensitive body, the coefficients can also be dependent on the unknown temperature, which means that the conditions are also nonlinear. This greatly complicates the derivation of solutions for this type of heat-conduction problem and calls for the application of specific linearization techniques to deal with the heat conduction equation and the boundary conditions [151, 223].

2.2. Thermoelasticity solutions for inhomogeneous orthotropic unbounded domain

2.2.1. Formulation and integral conditions

Consider a plane thermoelasticity problem for an inhomogeneous orthotropic unbounded domain $\mathfrak{D}_0 = \{|x| < +\infty, |y| \leq +\infty\}$ related to the dimensionless Cartesian coordinate system (x, y). Assume that all of the material moduli are arbitrary functions of coordinate y and $T_0 = e_0 = 0$. Plane $\mathfrak{D}_0$ is exposed to a steady-state non-uniform distribution of temperature $T(x, y)$ and body forces $F_x(x, y)$ and $F_y(x, y)$.

Under the assumption that the temperature approaches zero, $T(x, y) \to 0$, at infinitely distant points, $x^2 + y^2 \to +\infty$, our intention is to construct a local solution to the equations of equilibrium (2.1.15) and compatibility (2.1.31). This implies that the stress-tensor components also vanish as $x^2 + y^2 \to +\infty$. Before constructing this solution, we must first derive equilibrium conditions for the stress-tensor components and the applied force loadings using the method suggested in [321, 322].

By integrating the first equation in (2.1.15) over x and assuming that the normal stress σ_{xx} tends to zero at $x \to \pm\infty$, we derive the following two expressions:

$$\sigma_{xx} = -\int_{-\infty}^{x} \left(\frac{\partial \sigma_{xy}(\xi, y)}{\partial y} + F_x(\xi, y) \right) d\xi \tag{2.2.1}$$

and

$$\sigma_{xx} = \int_{x}^{+\infty} \left(\frac{\partial \sigma_{xy}(\xi, y)}{\partial y} + F_x(\xi, y) \right) d\xi \,. \tag{2.2.2}$$

Summing these expressions, we obtain the following equality:

$$\sigma_{xx} = -\frac{1}{2} \int_{-\infty}^{+\infty} \left(\frac{\partial \sigma_{xy}(\xi, y)}{\partial y} + F_x(\xi, y) \right) \mathrm{sgn}(x - \xi) d\xi \,. \tag{2.2.3}$$

Equation (2.2.3) expresses normal stress σ_{xx} through shear stress σ_{xy} and body-force component F_x. Here,

$$\mathrm{sgn}(x - \xi) = \begin{cases} 1, & x > \xi, \\ 0, & x = \xi, \\ -1, & x < \xi. \end{cases} \tag{2.2.4}$$

Similarly, the following expression can be obtained by integrating the second equation in (2.1.15) over y:

$$\sigma_{yy} = -\frac{1}{2} \int_{-\infty}^{+\infty} \left(\frac{\partial \sigma_{xy}(x, \eta)}{\partial x} + F_y(x, \eta) \right) \mathrm{sgn}(y - \eta) d\eta \,. \tag{2.2.5}$$

If we let $x \to \pm\infty$ in (2.2.3) and $y \to \pm\infty$ in (2.2.5), while assuming that the stress-tensor components are equal to zero at infinitely distant points, we arrive at the following integral conditions:

$$\begin{aligned} \frac{d}{dy} \int_{-\infty}^{+\infty} \sigma_{xy}(x, y) dx &= -\int_{-\infty}^{+\infty} F_x(x, y) dx, \\ \frac{d}{dx} \int_{-\infty}^{+\infty} \sigma_{xy}(x, y) dy &= -\int_{-\infty}^{+\infty} F_y(x, y) dy. \end{aligned} \tag{2.2.6}$$

Deriving the latter conditions involves switching the integration and differentiation operators. This implies [283] that the involved functions belong to class $\mathbf{L}_{\mathfrak{D}_0}$ of the absolutely integrable functions $f(x, y)$. That is,

$$\iint_{\mathfrak{D}_0} |f(x,y)|\,dx\,dy < \infty . \tag{2.2.7}$$

Because

$$\left|\iint_{\mathfrak{D}_0} f(x,y)\,dx\,dy\right| \le \iint_{\mathfrak{D}_0} |f(x,y)|\,dx\,dy , \tag{2.2.8}$$

then (2.2.7) implies the following:

$$\left|\iint_{\mathfrak{D}_0} f(x,y)\,dx\,dy\right| < \infty . \tag{2.2.9}$$

Equation (2.2.9) means that the absolute values of the stress resultants over the entire domain $\mathfrak{D}_0$ are not allowed to grow infinitely. This can be regarded as a necessary condition of the solution feasibility for the considered plane thermoelasticity problems.

Now, by integrating the first and second equations in (2.2.6) with respect to y and x, respectively, we arrive at the following:

$$\begin{aligned}
&\int_{-\infty}^{+\infty} \sigma_{xy}(x,y)dx = -\frac{1}{2}\iint_{\mathfrak{D}_0} F_x(x,\eta)\,\mathrm{sgn}(y-\eta)dxd\eta, \\
&\int_{-\infty}^{+\infty} \sigma_{xy}(x,y)dy = -\frac{1}{2}\iint_{\mathfrak{D}_0} F_y(\xi,y)\,\mathrm{sgn}(x-\xi)d\xi dy.
\end{aligned} \tag{2.2.10}$$

These express the resultant shearing forces through the integral characteristics of body forces over the entire domain $\mathfrak{D}_0$. If we let $y \to \pm\infty$ and $x \to \pm\infty$ respectively in the equations above, then we can derive the following general equilibrium conditions for the resultants of body forces:

$$\iint_{\mathfrak{D}_0} F_x(x,y)dxdy = 0, \quad \iint_{\mathfrak{D}_0} F_y(x,y)dxdy = 0 . \tag{2.2.11}$$

Note that this implies that the body forces are self-equilibrated by the resultant vector over the entire unbounded domain $\mathfrak{D}_0$. At first glance, this restriction does not appear feasible, as body forces are usually associated with the weight of the body, which is in turn related to its density [282]. However, we have to keep in mind that dealing with unbounded domains is also a kind of modeling generalization which can bring, by itself, a considered problem beyond the feasibility limits for which solutions are not integrable. Thus, it is preferable to use conditions (2.2.11) to understand the local distribution of stresses and displacements in an infinite body. If the body forces for a considered problem do not display this type of local behavior, then the superposition principle can be used to split the stress-strain state into two or more problems. One of these problems is concerned with the local disturbance of forces governed by the conditions given in (2.2.11).

By integrating first and second formulae in (2.2.10) respectively over y and x, we derive the following equilibrium conditions:

$$\iint\limits_{\mathfrak{D}_0} \sigma_{xy}(x,y)dxdy = \iint\limits_{\mathfrak{D}_0} yF_x(x,y)dxdy = \iint\limits_{\mathfrak{D}_0} xF_y(x,y)dxdy\,. \quad (2.2.12)$$

These conditions ensure that the main vector of shear stress within the entire plane $\mathfrak{D}_0$ equals the resultant moments of each body-force component within this plane.

Similar to (2.2.3) and (2.2.5), the following equations can be obtained using (2.1.15):

$$\begin{aligned} \sigma_{xy} &= -\frac{1}{2}\int\limits_{-\infty}^{+\infty}\left(\frac{\partial\sigma_{xx}(x,\eta)}{\partial x} + F_x(x,\eta)\right)\mathrm{sgn}(y-\eta)d\eta, \\ \sigma_{xy} &= -\frac{1}{2}\int\limits_{-\infty}^{+\infty}\left(\frac{\partial\sigma_{yy}(\xi,y)}{\partial y} + F_y(\xi,y)\right)\mathrm{sgn}(x-\xi)d\xi. \end{aligned} \quad (2.2.13)$$

These equations represent shear stress via normal stresses (either σ_{yy} or σ_{xx}). If we let $y \to \pm\infty$ and $x \to \pm\infty$ respectively in the first and second equations of (2.2.13), we derive the following integral conditions:

$$\frac{d}{dx}\int_{-\infty}^{+\infty}\sigma_{xx}(x,y)dy=-\int_{-\infty}^{+\infty}F_x(x,y)dy,$$
$$\frac{d}{dy}\int_{-\infty}^{+\infty}\sigma_{yy}(x,y)dx=-\int_{-\infty}^{+\infty}F_y(x,y)dx. \tag{2.2.14}$$

Then, by integrating these respectively over x and y, we derive the following equilibrium conditions:

$$\int_{-\infty}^{+\infty}\sigma_{xx}(x,y)dy=-\frac{1}{2}\iint_{\mathfrak{D}_0}F_x(\xi,y)\,\mathrm{sgn}(x-\xi)d\xi dy,$$
$$\int_{-\infty}^{+\infty}\sigma_{yy}(x,y)dx=-\frac{1}{2}\iint_{\mathfrak{D}_0}F_y(x,\eta)\,\mathrm{sgn}(y-\eta)dxd\eta. \tag{2.2.15}$$

The latter conditions express the resultant normal stress-tensor components in terms of the given body forces. Note that under $x\to\pm\infty$ and $y\to\pm\infty$, formulae (2.2.15) yield the conditions of general equilibrium for the body forces given in (2.2.11). The integration of the first and second equations in (2.2.15) over x and y, respectively, yields the following conditions:

$$\iint_{\mathfrak{D}_0}\sigma_{xx}(x,y)dxdy=\iint_{\mathfrak{D}_0}xF_x(x,y)dxdy,$$
$$\iint_{\mathfrak{D}_0}\sigma_{yy}(x,y)dxdy=\iint_{\mathfrak{D}_0}yF_y(x,y)dxdy. \tag{2.2.16}$$

Obviously, substituting the first equation of (2.2.13) into (2.2.3) and the second equation of (2.2.13) into (2.2.5) creates identities. However, substituting the second equation of (2.2.13) into (2.2.3) yields the following:

$$\sigma_{xx}=-\frac{1}{2}\int_{-\infty}^{+\infty}\left(F_x(\xi,y)-\frac{1}{2}\int_{-\infty}^{+\infty}\left(\frac{\partial^2\sigma_{yy}(\overline{\xi},y)}{\partial y^2}\right.\right.$$

$$+\frac{\partial F_y(\bar{\xi},y)}{\partial y}\Bigg)\mathrm{sgn}(\xi-\bar{\xi})d\bar{\xi}\Bigg)\mathrm{sgn}(x-\xi)d\xi\,. \qquad (2.2.17)$$

Changing the order of integration, this becomes

$$\sigma_{xx}=\frac{1}{2}\int_{-\infty}^{+\infty}\Bigg(\Bigg(\frac{\partial^2\sigma_{yy}(\xi,y)}{\partial y^2}+\frac{\partial F_y(\xi,y)}{\partial y}\Bigg)|\,x-\xi\,|$$

$$-F_x(\xi,y)\,\mathrm{sgn}(x-\xi)\Bigg)d\xi\,. \qquad (2.2.18)$$

Similarly, the following expression can be derived by substituting the first equation of (2.2.13) into (2.2.5):

$$\sigma_{yy}=\frac{1}{2}\int_{-\infty}^{+\infty}\Bigg(\Bigg(\frac{\partial^2\sigma_{xx}(x,\eta)}{\partial x^2}+\frac{\partial F_x(x,\eta)}{\partial x}\Bigg)|\,y-\eta\,|$$

$$-F_y(x,\eta)\,\mathrm{sgn}(y-\eta)\Bigg)d\eta\,. \qquad (2.2.19)$$

Note that double-differentiating (2.2.18) by x and double-differentiating (2.2.19) by y both yield the first equation of (2.1.28). In view of (2.1.33), this equation makes it possible to derive equation (2.1.35).

If we let $x\to\pm\infty$ in (2.2.18) and $y\to\pm\infty$ in (2.2.19) and assume that the stress-tensor components vanish as x^2+y^2 tends towards infinity, then we can derive the following integral conditions of equilibrium:

$$\begin{aligned}\frac{d^2}{dy^2}\int_{-\infty}^{+\infty}x\sigma_{yy}(x,y)dx&=-\int_{-\infty}^{+\infty}\Bigg(F_x(x,y)+x\frac{\partial F_y(x,y)}{\partial y}\Bigg)dx,\\ \frac{d^2}{dx^2}\int_{-\infty}^{+\infty}y\sigma_{xx}(x,y)dy&=-\int_{-\infty}^{+\infty}\Bigg(F_y(x,y)+y\frac{\partial F_x(x,y)}{\partial x}\Bigg)dy.\end{aligned} \qquad (2.2.20)$$

By respectively integrating the first equation in (2.2.20) twice over y and the second equation in (2.2.20) twice over x, we arrive at the following expressions for the resultant moments of the normal stress-tensor components:

$$\begin{aligned}&\int_{-\infty}^{+\infty} x\sigma_{yy}(x,y)dx\\ &=-\frac{1}{2}\iint_{\mathfrak{D}_0}\Big(F_x(x,\eta)\,|\,y-\eta\,|+xF_y(x,\eta)\operatorname{sgn}(y-\eta)\Big)dxd\eta,\\ &\int_{-\infty}^{+\infty} y\sigma_{xx}(x,y)dx\\ &=-\frac{1}{2}\iint_{\mathfrak{D}_0}\Big(F_y(\xi,y)\,|\,x-\xi\,|+yF_x(\xi,y)\operatorname{sgn}(x-\xi)\Big)d\xi dy.\end{aligned} \tag{2.2.21}$$

If we let $y\to\pm\infty$ in the first equation of (2.2.21) and $x\to\pm\infty$ in the second equation of (2.2.21), then we obtain the following:

$$\iint_{\mathfrak{D}_0} yF_x(x,y)dxdy=\iint_{\mathfrak{D}_0} xF_y(x,y)dxdy\,. \tag{2.2.22}$$

This complies with the conditions given in (2.2.12). By integrating formulae (2.2.21) in view of integral conditions (2.2.11), we obtain the following conditions expressing the resultant moments of the normal stresses within the entire plane $\mathfrak{D}_0$ through the integral characteristics of body forces:

$$\begin{aligned}\iint_{\mathfrak{D}_0} x\sigma_{yy}(x,y)dxdy&=\iint_{\mathfrak{D}_0}\left(xyF_y(x,y)-\frac{y^2}{2}F_x(x,y)\right)dxdy,\\ \iint_{\mathfrak{D}_0} y\sigma_{xx}(x,y)dxdy&=\iint_{\mathfrak{D}_0}\left(xyF_x(x,y)-\frac{x^2}{2}F_y(x,y)\right)dxdy.\end{aligned} \tag{2.2.23}$$

We derived the integral relations between the stress-tensor components (2.2.3), (2.2.5), (2.2.13), (2.2.18), (2.2.19) along with integral equilibrium conditions (2.2.10), (2.2.12), (2.2.15), (2.2.16), (2.2.21), (2.2.23) for the stress-tensor components and necessary integral equilibrium conditions (2.2.11) and (2.2.22) for given components of the body-force vector. Note that these calculations involve integrating the equilibrium equations (2.1.15). Thus, they hold irrespective of material properties and are therefore valid for homogeneous or inhomogeneous materials presenting any form of anisotropy [297, 321, 322].

2.2.2. Solutions of governing equations

In view of the conditions for the body forces (2.2.11) and the assumption that the temperature and stresses vanish at the points of infinity, we hereby introduce the integral Fourier transform [41]:

$$\overline{f}(y) = \overline{f}(y;s) = \int_{-\infty}^{+\infty} f(x,y)\exp(-isx)dx\,, \tag{2.2.24}$$

where s is a parameter of the transform, $i^2 = -1$, and $f(x,y)$ is an arbitrary function, for which the integral (2.2.24) exists.

Applying this transform to (2.1.31) and (2.1.35) and minding the local character of the stress-strain state returns the following boundary value problem for key functions $\overline{\sigma}(y)$ and $\overline{\sigma}_{yy}(y)$ in the mapping domain of transform (2.2.24):

$$\overline{\Delta}\overline{\sigma}_{yy}(y) = -s^2\overline{\sigma}(y) + is\overline{F}_x(y) - \frac{d\overline{F}_y(y)}{dy}, \tag{2.2.25}$$

$$\overline{\Delta}\left(a_{11}(y)\overline{\sigma}(y) + \alpha_1(y)\overline{T}(y)\right) = -s^2\left(\alpha_1(y) - \alpha_2(y)\right)\overline{T}(y)$$

$$+\frac{d}{dy}\left(\left(2\beta_1(y) - \frac{1}{G_{xy}(y)}\right)\frac{d\overline{\sigma}_{yy}(y)}{dy}\right)$$

$$+\left(\frac{d^2\beta_1(y)}{dy^2} + s^2\beta_2(y)\right)\overline{\sigma}_{yy}(y)$$

$$+\beta_1(y)\left(\frac{d\overline{F}_y(y)}{dy}-is\overline{F}_x(y)\right)-\frac{d}{dy}\left(\frac{\overline{F}_y(y)}{G_{xy}(y)}\right), \tag{2.2.26}$$

$$\overline{\sigma}_{yy}\to 0,\quad \overline{\sigma}_{xy}\to 0,\quad y\to\pm\infty. \tag{2.2.27}$$

The boundary value problem (2.2.25) – (2.2.27) can be solved by constructing the following partial solutions to (2.2.25) and (2.2.26):

$$\overline{\sigma}_{yy}(y)=\frac{1}{2|s|}\int_{-\infty}^{+\infty}\left(\frac{d\overline{F}_y(\xi)}{d\xi}-is\overline{F}_x(\xi)\right)\exp\left(-|s||y-\xi|\right)d\xi$$

$$+\frac{|s|}{2}\int_{-\infty}^{+\infty}\overline{\sigma}(\xi)\exp\left(-|s||y-\xi|\right)d\xi \tag{2.2.28}$$

and

$$\overline{\sigma}(y)=\Theta_{\mathrm{PL}}(y)+\frac{1}{a_{11}(y)}\left(\int_{-\infty}^{+\infty}\overline{\sigma}_{yy}(\eta)\gamma_{\mathrm{PL}}(y,\eta)d\eta\right.$$

$$-\frac{1}{2|s|}\int_{-\infty}^{+\infty}\left(\beta_1(\eta)\left(\frac{d\overline{F}_y(\eta)}{d\eta}-is\overline{F}_x(\eta)\right)\right.$$

$$\left.\left.-\frac{d}{d\eta}\left(\frac{\overline{F}_y(\eta)}{G_{xy}(\eta)}\right)\right)\exp\left(-|s||y-\eta|\right)d\eta\right). \tag{2.2.29}$$

Here,

$$\Theta_{\mathrm{PL}}(y)=\frac{1}{a_{11}(y)}\left(-\alpha_1(y)\overline{T}(y)\right.$$

$$\left.+\frac{|s|}{2}\int_{-\infty}^{+\infty}\left(\alpha_1(\eta)-\alpha_2(\eta)\right)\overline{T}(\eta)\exp\left(-|s||y-\eta|\right)d\eta\right), \tag{2.2.30}$$

$$\gamma_{\mathrm{PL}}(y,\eta) = -\frac{1}{2}\left(\left(\frac{d^2\beta_1(\eta)}{d\eta^2} + s^2\beta_2(\eta)\right)\frac{\exp(-|s||y-\eta|)}{|s|}\right.$$

$$\left. + \frac{d}{d\eta}\left(\left(2\beta_1(\eta) - \frac{1}{G_{xy}(\eta)}\right)\exp(-|s||y-\eta|)\operatorname{sgn}(y-\eta)\right)\right). \quad (2.2.31)$$

Substituting (2.2.28) into (2.2.29) and changing the order of integration yields the following integral equation for $\overline{\sigma}(y)$:

$$\overline{\sigma}(y) = \Theta_{\mathrm{PL}}(y) + \Psi_{\mathrm{PL}}(y) + \int_{-\infty}^{+\infty} \overline{\sigma}(\xi)\mathcal{K}_{\mathrm{PL}}(y,\xi)d\xi, \quad (2.2.32)$$

where

$$\Psi_{\mathrm{PL}}(y) = \frac{1}{2|s|a_{11}(y)}\left(\int_{-\infty}^{+\infty}\gamma_{\mathrm{PL}}(y,\eta)\int_{-\infty}^{+\infty}\left(\frac{d\overline{F}_y(\xi)}{d\xi} - is\overline{F}_x(\xi)\right)\right.$$

$$\times\exp(-|s||\eta-\xi|)\,d\xi d\eta$$

$$-\int_{-\infty}^{+\infty}\left(\beta_1(\eta)\left(\frac{d\overline{F}_y(\eta)}{d\eta} - is\overline{F}_x(\eta)\right)\right.$$

$$\left.\left.-\frac{d}{d\eta}\left(\frac{\overline{F}_y(\eta)}{G_{xy}(\eta)}\right)\right)\exp(-|s||y-\eta|)\,d\eta\right),$$

$$\mathcal{K}_{\mathrm{PL}}(y,\xi) = \frac{|s|}{2a_{11}(y)}\int_{-\infty}^{+\infty}\gamma_{\mathrm{PL}}(y,\eta)\exp(-|s||\eta-\xi|)\,d\eta. \quad (2.2.33)$$

The construction of an efficient solution to the second-kind integral equation (2.2.32) presents an interesting problem; however, space limitations limit us to indicating only the dominant approaches that could be employed for its solution: *i*) Picard's process of successive approximations [125, 294, 306], *ii*) the operator series method [27], *iii*) the Bubnov-Galerkin method [68], *iv*) a numerical procedure based on trapezoidal integration and the Newton-Raphson method [73], *v*) iterative-collocation method [99], *vi*) discretization methods, and *vii*) special

kernels and projection-iterative method [64], spline approximations [152], the quadratic-form method [29], and grid methods [209]. Herein we employ the resolvent-kernel algorithm [218, 219] in a manner similar to [295, 296]. This allows us to obtain an explicit-form analytical solution that is convenient for analysis. Using this, the solution to equation (2.2.32) can be obtained as follows:

$$\overline{\sigma}(y) = \Theta_{\mathrm{PL}}(y) + \Psi_{\mathrm{PL}}(y)$$

$$+ \int_{-\infty}^{+\infty} \left(\Theta_{\mathrm{PL}}(\xi) + \Psi_{\mathrm{PL}}(\xi)\right) \mathcal{R}_{\mathrm{PL}}(y,\xi) d\xi, \tag{2.2.34}$$

where the resolvent kernel $\mathcal{R}_{\mathrm{PL}}(y,\xi)$ can be represented in the form of an infinite series

$$\mathcal{R}_{\mathrm{PL}}(y,\xi) = \sum_{n=0}^{\infty} \mathcal{K}_{n+1}^{\mathrm{PL}}(y,\xi) \tag{2.2.35}$$

through the use of recurring kernels

$$\mathcal{K}_1^{\mathrm{PL}}(y,\xi) = \mathcal{K}_{\mathrm{PL}}(y,\xi),$$
$$\mathcal{K}_{n+1}^{\mathrm{PL}}(y,\xi) = \int_{-\infty}^{+\infty} \mathcal{K}_1^{\mathrm{PL}}(y,t) \mathcal{K}_n^{\mathrm{PL}}(t,\xi) dt, \quad n = 1,2,\ldots \tag{2.2.36}$$

Note that this technique follows directly from the solution scheme in the Picard iterative process [311].

It is worth noting that the resolvent kernel (2.2.35) is aggregated using the recurring kernels, which are computed successively from the original kernel (2.2.33) of integral equation (2.2.32) by means of the routine indicated in (2.2.36). Due to the fact that kernel (2.2.33) is expressed solely through material properties and does not involve force or thermal loadings, the resolvent kernel need only be computed once for specific material profiles to be used with a range of loadings.

In many cases of specific dependences of the material properties on coordinates, the series (2.2.35) can be evaluated analytically [227, 311]. However, the practical computation of solution (2.2.34) expressed through the infinite series (2.2.35) generally presents a challenge. Due to the fact that with an increase in the number n, kernels (2.2.36) decrease by both

arguments, the series (2.2.35) can be truncated for practical computation as follows:

$$\mathcal{R}_{\mathrm{PL}}(y,\xi) \approx \mathcal{R}^{N}_{\mathrm{PL}}(y,\xi) = \sum_{n=0}^{N} \mathcal{K}^{\mathrm{PL}}_{n+1}(y,\xi), \tag{2.2.37}$$

where natural digit N can be evaluated either by a succession of numerical experiments [295, 296] or estimated analytically [285] by minimizing the residual term in equation (2.2.32) obtained with expression (2.2.34) and the resolvent-kernel in the form (2.2.37) instead of (2.2.36).

Once we have determined the total stress in the form (2.2.34), normal stress $\overline{\sigma}_{yy}$ can be constructed by substituting (2.2.34) into (2.2.28):

$$\begin{aligned}\overline{\sigma}_{yy}(y) = \frac{1}{2|s|}\int_{-\infty}^{+\infty}\left(\frac{d\overline{F}_y(\eta)}{d\eta} - is\overline{F}_x(\eta)\right)\exp(-|s||y-\eta|)d\eta \\ + \frac{|s|}{2}\int_{-\infty}^{+\infty}\left(\Theta_{\mathrm{PL}}(\xi)+\Psi_{\mathrm{PL}}(\xi)\right)\Bigg(\exp(-|s||y-\xi|) \\ + \int_{-\infty}^{+\infty}\mathcal{R}_{\mathrm{PL}}(\eta,\xi)\exp(-|s||y-\eta|)d\eta\Bigg)d\xi.\end{aligned} \tag{2.2.38}$$

Normal stress $\overline{\sigma}_{xx}$ can then be computed using the equation

$$\overline{\sigma}_{xx} = \overline{\sigma} - \overline{\sigma}_{yy} \tag{2.2.39}$$

that follows from (2.1.33) in the mapping domain of transform (2.2.24). As a result, the stress can be expressed by the following form:

$$\begin{aligned}\overline{\sigma}_{xx}(y) = \Theta_{\mathrm{PL}}(y) + \Psi_{\mathrm{PL}}(y) \\ - \frac{1}{2|s|}\int_{-\infty}^{+\infty}\left(\frac{d\overline{F}_y(\eta)}{d\eta} - is\overline{F}_x(\eta)\right)\exp(-|s||y-\eta|)d\eta \\ + \frac{|s|}{2}\int_{-\infty}^{+\infty}\left(\Theta_{\mathrm{PL}}(\xi)+\Psi_{\mathrm{PL}}(\xi)\right)\Big(\mathcal{R}_{\mathrm{PL}}(y,\xi) - \exp(-|s||y-\xi|)\end{aligned}$$

$$-\int_{-\infty}^{+\infty}\mathcal{R}_{\mathrm{PL}}(\eta,\xi)\exp(-|s||y-\eta|)d\eta\Bigg)d\xi\,. \tag{2.2.40}$$

Shear stress $\overline{\sigma}_{xy}$ can be computed using any of the equations given in (2.2.13) in the mapping domain of the transform (2.2.24). For instance, the second equation of (2.2.13) yields the following:

$$\overline{\sigma}_{xy}(y)=\frac{i}{s}\left(\frac{d\overline{\sigma}_{yy}(y)}{dy}+\overline{F}_{y}(y)\right). \tag{2.2.41}$$

Substituting (2.2.38) into (2.2.41), we arrive at the following:

$$\overline{\sigma}_{xy}(y)=\frac{i}{s}\overline{F}_{y}(y)$$

$$-\frac{i}{2s}\int_{-\infty}^{+\infty}\left(\frac{d\overline{F}_{y}(\eta)}{d\eta}-is\overline{F}_{x}(\eta)\right)\exp(-|s||y-\eta|)\operatorname{sgn}(y-\eta)d\eta$$

$$-\frac{is}{2}\int_{-\infty}^{+\infty}\left(\Theta_{\mathrm{PL}}(\xi)+\Psi_{\mathrm{PL}}(\xi)\right)\Bigg(\exp(-|s||y-\xi|)\operatorname{sgn}(y-\xi)$$

$$+\int_{-\infty}^{+\infty}\mathcal{R}_{\mathrm{PL}}(\eta,\xi)\exp(-|s||y-\eta|)\operatorname{sgn}(y-\eta)d\eta\Bigg)d\xi\,. \tag{2.2.42}$$

The in-plane stresses are found in the form (2.2.34), (2.2.38), (2.2.40), (2.2.42) in the mapping domain of the transform (2.2.24). The corresponding components in the physical domain can then be computed using the following inverse transform, either analytically or numerically [41]:

$$f(x,y)=\frac{1}{2\pi}\int_{-\infty}^{+\infty}\overline{f}(y)\exp(isx)ds\,. \tag{2.2.43}$$

Note that a similar strategy can be employed in cases such as periodic behavior, by implementing an appropriate integral or series transform instead of the direct and inverse integral transforms (2.2.24) and (2.2.43).

2.2.3. Determination of elastic displacements

After finding the stresses as described, we can determine the corresponding elastic displacements using the correct integration of the Cauchy equations (2.1.18). Assuming that plane $\mathfrak{D}_0$ is fixed at an infinitely distant periphery, the first and second equations of (2.1.18) yield the following:

$$u_x(x,y) = \frac{1}{2}\int_{-\infty}^{+\infty} \varepsilon_{xx}(\xi,y)\,\mathrm{sgn}(x-\xi)d\xi,$$
$$u_y(x,y) = \frac{1}{2}\int_{-\infty}^{+\infty} \varepsilon_{yy}(x,\eta)\,\mathrm{sgn}(y-\eta)d\eta. \tag{2.2.44}$$

Putting expressions (2.2.44) into the third equation (2.1.18) yields the following equation

$$2\varepsilon_{xy}(x,y) = \int_{-\infty}^{+\infty} \frac{\partial \varepsilon_{xx}(\xi,y)}{\partial y}\,\mathrm{sgn}(x-\xi)d\xi$$
$$+\int_{-\infty}^{+\infty} \frac{\partial \varepsilon_{yy}(x,\eta)}{\partial x}\,\mathrm{sgn}(y-\eta)d\eta, \tag{2.2.45}$$

which represents the actual strain compatibility equation for the considered problem formulation. Note that after the application of differential operator $\partial^2 / \partial x \partial y$, equation (2.2.45) can be reduced to the classical equation of strain compatibility (2.1.19). Under the assumption that the stress, strain, and displacement fields are local and vanish at the points of infinity, it is not difficult to prove that equation (2.1.19) is equivalent to (2.2.45). It is necessary only to successively integrate (2.1.19) by x and y and then compare the result to (2.2.45). Therefore, if strains $\varepsilon_{xx}(x,y)$, $\varepsilon_{yy}(x,y)$, and $\varepsilon_{xy}(x,y)$ are determined in the form (2.1.23) using the stress-tensor component found in the form (2.2.38), (2.2.40), and (2.2.42) in the physical domain of transform (2.2.43), then we can use any two equations out of three ones of (2.1.18) to determine displacements $u_x(x,y)$ and $u_y(x,y)$. Thus, after determination of the

displacements in the form (2.2.44), the third equation (2.1.18) is fulfilled automatically.

In the mapping domain of transform (2.2.24), expressions (2.2.44) take the following form:

$$\overline{u}_x(y) = -\frac{i}{s}\overline{\varepsilon}_{xx}(y), \quad \overline{u}_y(y) = \frac{1}{2}\int_{-\infty}^{+\infty}\overline{\varepsilon}_{yy}(\eta)\,\mathrm{sgn}(y-\eta)d\eta\,. \quad (2.2.46)$$

Making use of the strain representations (2.1.23) in the mapping domain of transform (2.2.24) along with the expressions (2.2.34), (2.2.38), and (2.2.40), the elastic displacements (2.2.46) can be written as follows:

$$\overline{u}_x(y) = i\frac{a_{11}(y)-a_{12}(y)}{2s\,|\,s\,|}$$

$$\times\int_{-\infty}^{+\infty}\left(\frac{d\overline{F}_y(\eta)}{d\eta} - is\overline{F}_x(\eta)\right)\exp(-|\,s\,||\,y-\eta\,|)d\eta$$

$$-\frac{i}{s}\left(a_{11}(y)\left(\Theta_{\mathrm{PL}}(y)+\Psi_{\mathrm{PL}}(y)\right)+\alpha_1(y)\overline{T}(y)\right)$$

$$+\frac{i}{s}\int_{-\infty}^{+\infty}\left(\Theta_{\mathrm{PL}}(\xi)+\Psi_{\mathrm{PL}}(\xi)\right)\left(|\,s\,|\frac{a_{11}(y)-a_{12}(y)}{2}\right.$$

$$\times\left(\exp(-|\,s\,||\,y-\xi\,|)+\int_{-\infty}^{+\infty}\mathcal{R}_{\mathrm{PL}}(\eta,\xi)\exp(-|\,s\,||\,y-\eta)d\eta\right)$$

$$\left.-a_{11}(y)\mathcal{R}_{\mathrm{PL}}(y,\xi)\right)d\xi\,, \quad (2.2.47)$$

$$\overline{u}_y(y) = \int_{-\infty}^{+\infty}\left(\frac{d\overline{F}_y(\eta)}{d\eta} - is\overline{F}_x(\eta)\right)$$

$$\times\int_{-\infty}^{+\infty}\frac{a_{22}(\xi)-a_{12}(\xi)}{4\,|\,s\,|}\exp(-|\,s\,||\,\xi-\eta\,|)\,\mathrm{sgn}(y-\xi)d\xi d\eta$$

$$+\frac{1}{2}\int_{-\infty}^{+\infty}\left(\Theta_{\mathrm{PL}}(\xi)+\Psi_{\mathrm{PL}}(\xi)\right)\Bigg(a_{12}(\xi)\operatorname{sgn}(y-\xi)$$

$$+\frac{|s|}{2}\int_{-\infty}^{+\infty}\left(a_{22}(\eta)-a_{12}(\eta)\right)\exp\left(-|s||\eta-\xi|\right)\operatorname{sgn}(y-\xi)d\eta$$

$$+\int_{-\infty}^{+\infty}\mathcal{R}_{\mathrm{PL}}(\eta,\xi)\Bigg(a_{12}(\eta)\operatorname{sgn}(y-\eta)$$

$$+\frac{|s|}{2}\int_{-\infty}^{+\infty}\left(a_{22}(\zeta)-a_{12}(\zeta)\right)\exp\left(-|s||\zeta-\eta|\right)\operatorname{sgn}(y-\zeta)d\zeta\Bigg)d\eta\Bigg)d\xi$$

$$+\frac{1}{2}\int_{-\infty}^{+\infty}\alpha_2(\xi)\bar{T}(\xi)\operatorname{sgn}(y-\xi)d\xi. \qquad (2.2.48)$$

After the elastic displacements are found using (2.2.47) and (2.2.48) in the mapping domain of transform (2.2.24), they can be restored in the physical domain using the inverse transform (2.2.43).

2.2.4. Steady-state temperature determination

In the previous sections, we constructed stresses (2.2.38), (2.2.40), and (2.2.42) and displacements (2.2.47) and (2.2.48) as functions of body forces and temperature $T(x,y)$. The temperature field $T(x,y)$ in plane $\mathfrak{D}_0$ can be found by correct solving a boundary value problem for the heat-conduction equation (2.1.37). In order to do so, let us first derive integral conditions of thermal balance in inhomogeneous orthotropic plane $\mathfrak{D}_0$. Introduce the heat flux components by the following expressions:

$$\Phi_x(x,y)=\lambda_x(y)\frac{\partial T(x,y)}{\partial x},$$
$$\Phi_y(x,y)=\lambda_y(y)\frac{\partial T(x,y)}{\partial y}. \qquad (2.2.49)$$

In the context of the latter formulae, the heat-conduction equation (2.1.37) can be given as follows:

$$\frac{\partial \Phi_x(x,y)}{\partial x} + \frac{\partial \Phi_y(x,y)}{\partial y} = -w(x,y). \tag{2.2.50}$$

Assume that components of heat flux have local distribution profiles that vanish for infinitely distant points as follows:

$$\lim_{x^2 \to +\infty} \Phi_x(x,y) = \lim_{y^2 \to +\infty} \Phi_y(x,y) = 0\,. \tag{2.2.51}$$

By integrating (2.2.50) in view of conditions (2.2.51), we can obtain the following equation:

$$\frac{d}{dy} \int_{-\infty}^{+\infty} \Phi_y(x,y)dx = -\int_{-\infty}^{+\infty} w(x,y)dx\,. \tag{2.2.52}$$

Integration of the latter equation by y yields

$$\int_{-\infty}^{+\infty} \Phi_y(x,y)dx = -\iint_{\mathfrak{D}_0} w(x,\eta)\,\mathrm{sgn}(y-\eta)dxd\eta$$

$$+\frac{1}{2}\lim_{y\to+\infty}\int_{-\infty}^{+\infty}\Phi_y(x,y)dx + \frac{1}{2}\lim_{y\to-\infty}\int_{-\infty}^{+\infty}\Phi_y(x,y)dx\,. \tag{2.2.53}$$

Letting $y \to \pm\infty$ in (2.2.53) allows for deriving the following condition

$$\iint_{\mathfrak{D}_0} w(x,y)dxdy = \lim_{y\to-\infty}\int_{-\infty}^{+\infty}\Phi_y(x,y)dx$$

$$-\lim_{y\to+\infty}\int_{-\infty}^{+\infty}\Phi_y(x,y)dx\,. \tag{2.2.54}$$

Now, integrating (2.2.53) over y from L_1 to L_2, where L_1 and L_2 are large real numbers and $L_1 < L_2$, yields

$$\int_{L_1}^{L_2}\int_{-\infty}^{+\infty}\Phi_y(x,y)dxdy$$

$$=\frac{L_2-L_1}{2}\left(\lim_{y\to+\infty}\int_{-\infty}^{+\infty}\Phi_y(x,y)dx+\lim_{y\to-\infty}\int_{-\infty}^{+\infty}\Phi_y(x,y)dx\right)$$

$$-\frac{L_1+L_2}{2}\iint_{\mathfrak{D}_0}w(x,y)dxdy+\iint_{\mathfrak{D}_0}yw(x,y)dxdy. \tag{2.2.55}$$

Due to the fact that L_1 and L_2 can tend independently towards $-\infty$ and $+\infty$, while the resultant of heat flux $\Phi_y(x,y)$ over the entire domain remains finite, i.e.,

$$\left|\iint_{\mathfrak{D}_0}\Phi_y(x,y)dxdy\right|<+\infty, \tag{2.2.56}$$

equation (2.2.55) implies the following conditions:

$$\iint_{\mathfrak{D}_0}w(x,y)dxdy=0, \tag{2.2.57}$$

$$\lim_{y\to\pm\infty}\int_{-\infty}^{+\infty}\Phi_y(x,y)dx=0, \tag{2.2.58}$$

and

$$\iint_{\mathfrak{D}_0}\Phi_y(x,y)dxdy=\iint_{\mathfrak{D}_0}yw(x,y)dxdy. \tag{2.2.59}$$

It can be shown in a similar fashion that

$$\lim_{x\to\pm\infty}\int_{-\infty}^{+\infty}\Phi_x(x,y)dx=0, \tag{2.2.60}$$

and

$$\iint\limits_{\mathfrak{D}_0} \Phi_x(x,y)dxdy = \iint\limits_{\mathfrak{D}_0} xw(x,y)dxdy\,. \tag{2.2.61}$$

Conditions (2.2.58) and (2.2.60) imply that the local distribution (2.2.51) of the heat fluxes in the in-plane directions necessarily leads to local distributions of their resultants. Due to conditions (2.2.59) and (2.2.61), the average heat fluxes over the entire domain $\mathfrak{D}_0$ are equal to the thermal "moments" generated by the internal heat sources. Equation (2.2.57) imposes the necessary condition for the density of inner heat sources to ensure the correct solution of the steady-state heat-transfer problem in plane $\mathfrak{D}_0$.

Under the assumption that the heat conduction coefficients are functions of y and $T_0 = 0$, equation (2.1.37) the following form in the mapping domain of transform (2.2.24):

$$\frac{d^2\overline{T}(y)}{dy^2} - s^2\overline{T}(y) = s^2\frac{\lambda_x(y)-\lambda_y(y)}{\lambda_y(y)}\overline{T}(y)$$

$$-\frac{d\ln\lambda_y(y)}{dy}\frac{d\overline{T}(y)}{dy} - \frac{\overline{w}(y)}{\lambda_y(y)}\,. \tag{2.2.62}$$

If the density of heat sources and consequently the temperature vanish at $y \to \pm\infty$, then the solution to equation (2.2.62) with respect to its left-hand side is as follows:

$$\overline{T}(y) = w_{\mathrm{PL}}(y) + \int\limits_{-\infty}^{+\infty} \overline{T}(\eta)\mathcal{L}_{\mathrm{PL}}(y,\eta)d\eta\,, \tag{2.2.63}$$

where

$$w_{\mathrm{PL}}(y) = \frac{1}{2|s|}\int\limits_{-\infty}^{+\infty}\frac{\overline{w}(\eta)}{\lambda_y(\eta)}\exp(-|s||y-\eta|)d\eta\,, \tag{2.2.64}$$

$$\mathcal{L}_{\mathrm{PL}}(y,\eta) = \frac{1}{2|s|}\left(s^2\frac{\lambda_y(\eta)-\lambda_x(\eta)}{\lambda_y(\eta)}\right.$$

$$-|s|\frac{d\ln\lambda_y(\eta)}{d\eta}\operatorname{sgn}(y-\eta)$$

$$-\frac{d^2\ln\lambda_y(\eta)}{d\eta^2}\Bigg)\exp\left(-|s||y-\eta|\right). \tag{2.2.65}$$

Equation (2.2.63) is similar to (2.2.32). Thus, we can apply the resolvent-kernel technique to obtain the following solution to (2.2.63):

$$\overline{T}(y)=w_{\mathrm{PL}}(y)+\int_{-\infty}^{+\infty}w_{\mathrm{PL}}(\eta)\mathcal{T}_{\mathrm{PL}}(y,\eta)d\eta, \tag{2.2.66}$$

where the resolvent kernel $\mathcal{T}_{\mathrm{PL}}(y,\eta)$ can either be evaluated analytically or computed using an infinite series

$$\mathcal{T}_{\mathrm{PL}}(y,\eta)=\sum_{n=0}^{\infty}\mathcal{T}_{n+1}^{\mathrm{PL}}(y,\eta) \tag{2.2.67}$$

of recurring kernels

$$\begin{aligned}\mathcal{T}_1^{\mathrm{PL}}(y,\eta)&=\mathcal{L}_{\mathrm{PL}}(y,\eta),\\ \mathcal{T}_{n+1}^{\mathrm{PL}}(y,\eta)&=\int_{-\infty}^{+\infty}\mathcal{T}_1^{\mathrm{PL}}(y,t)\mathcal{T}_n^{\mathrm{PL}}(t,\eta)dt.\end{aligned} \tag{2.2.68}$$

It should be possible to sum up the resolvent kernel (2.2.67) analytically; however, if that poses a challenge, then the following approximate formula can be applied:

$$\mathcal{T}_{\mathrm{PL}}(y,\eta)\approx\mathcal{T}_{\mathrm{PL}}^{M}(y,\eta)=\sum_{n=0}^{M}\mathcal{T}_{n+1}^{\mathrm{PL}}(y,\eta), \tag{2.2.69}$$

where M is a positive integer evaluated numerically or based on the minimization of the residual term, which occurs after the substitution of solution (2.2.66) with approximated resolvent-kernel (2.2.69) into equation (2.2.63).

After temperature is constructed in the form (2.2.66) in the mapping domain of the transform (2.2.24), it can be restored in the physical domain

via analytical or numerical implementation of the inverse transform (2.2.43).

2.3. Thermoelasticity solutions for inhomogeneous orthotropic half-plane

2.3.1. Formulation, integral conditions, and governing equations

Consider applying the direct integration method to the plane thermoelasticity problem for an inhomogeneous orthotropic half-plane $\mathfrak{D}_1 = \{|\, x \,| < +\infty,\ y \geq 0\}$. We assume that all of the material properties are arbitrary functions of coordinate y and $T_0 = e_0 = 0$. The elastic equilibrium of domain $\mathfrak{D}_1$ is governed by equations (2.1.15) and (2.1.19) in view of the constitutive equations (2.1.23). Boundary $y = 0$ of half-plane $\mathfrak{D}_1$ is exposed to static force loadings

$$\sigma_{yy}(x,0) = -p_0(x), \quad \sigma_{xy}(x,0) = q_0(x), \qquad |\, x \,| < +\infty, \qquad (2.3.1)$$

where $p_0(x)$ and $q_0(x)$ are given functions. The interior of half-plane $\mathfrak{D}_1$ is subject to body forces $F_x(x,y)$ and $F_y(x,y)$ and a steady-state temperature distribution $T(x,y)$, which can be determined using a relevant heat-conduction problem.

By following a strategy similar to the one presented in Section 2.2.1, we can conclude that the functions presenting the force loadings satisfy the following integral conditions:

$$\iint_{\mathfrak{D}_1} F_x(x,y)\,dx\,dy = \int_{-\infty}^{+\infty} q_0(x)\,dx,$$

$$\iint_{\mathfrak{D}_1} F_y(x,y)\,dx\,dy = -\int_{-\infty}^{+\infty} p_0(x)\,dx, \qquad (2.3.2)$$

$$\iint_{\mathfrak{D}_1} \left(yF_x(x,y) - xF_y(x,y)\right)dx\,dy = \int_{-\infty}^{+\infty} xp_0(x)\,dx.$$

Similarly, the relations between the stress-tensor components can be derived in the following form:

$$2\sigma_{xy}(x,y) = -\int_{-\infty}^{+\infty}\left(\frac{\partial\sigma_{yy}(\xi,y)}{\partial y} + F_y(\xi,y)\right)\mathrm{sgn}(x-\xi)d\xi$$

$$= q_0(x) - \int_0^{+\infty}\left(\frac{\partial\sigma_{xx}(x,\eta)}{\partial x} + F_x(x,\eta)\right)\mathrm{sgn}(y-\eta)d\eta,$$

$$2\sigma_{xx}(x,y) = -\int_{-\infty}^{+\infty}\left(\frac{\partial\sigma_{xy}(\xi,y)}{\partial y} + F_x(\xi,y)\right)\mathrm{sgn}(x-\xi)d\xi$$

$$= \int_{-\infty}^{+\infty}\left(\left(\frac{\partial^2\sigma_{yy}(\xi,y)}{\partial y^2} + \frac{\partial F_y(\xi,y)}{\partial y}\right)|x-\xi|\right.$$

$$\left. - F_x(\xi,y)\mathrm{sgn}(x-\xi)\right)d\xi, \qquad (2.3.3)$$

$$2\sigma_{yy}(x,y) = -p_0(x)$$

$$-\int_0^{+\infty}\left(\frac{\partial\sigma_{xy}(x,\eta)}{\partial x} + F_y(x,\eta)\right)\mathrm{sgn}(y-\eta)d\eta$$

$$= -p_0(x) - y\frac{dq_0(x)}{dx}$$

$$+\int_0^{+\infty}\left(\left(\frac{\partial^2\sigma_{xx}(x,\eta)}{\partial x^2} + \frac{\partial F_x(x,\eta)}{\partial x}\right)|y-\eta|\right.$$

$$\left. - F_y(x,\eta)\mathrm{sgn}(y-\eta)\right)d\eta\,.$$

We can also derive equations for the resultant forces and moments, as follows:

$$2\int_0^{+\infty}\sigma_{xx}(x,y)dy=\int_{-\infty}^{+\infty}\left(q_0(\xi)-\int_0^{+\infty}F_x(\xi,y)dy\right)\operatorname{sgn}(x-\xi)d\xi,$$

$$2\int_{-\infty}^{+\infty}\sigma_{yy}(x,y)dx=-\int_{-\infty}^{+\infty}\left(p_0(x)+\int_0^{+\infty}F_y(x,\eta)\operatorname{sgn}(y-\eta)d\eta\right)dx,$$

$$2\int_{-\infty}^{+\infty}\sigma_{xy}(x,y)dx=\int_{-\infty}^{+\infty}\left(q_0(x)-\int_0^{+\infty}F_x(x,\eta)\operatorname{sgn}(y-\eta)d\eta\right)dx$$

$$=-\int_{-\infty}^{+\infty}\left(p_0(\xi)+\int_0^{+\infty}F_y(\xi,y)dy\right)\operatorname{sgn}(x-\xi)d\xi,$$

$$2\int_0^{+\infty}y\sigma_{xx}(x,y)dy=-\int_{-\infty}^{+\infty}\left(\left(p_0(\xi)+\int_0^{+\infty}F_y(\xi,y)dy\right)|x-\xi|\right. \tag{2.3.4}$$

$$\left.=-\int_0^{+\infty}yF_x(\xi,y)\operatorname{sgn}(x-\xi)dy\right)d\xi,$$

$$2\int_{-\infty}^{+\infty}x\sigma_{yy}(x,y)dx=\int_{-\infty}^{+\infty}\left(yq_0(x)-xp_0(x)\right.$$

$$\left.-\int_0^{+\infty}\left(F_x(x,\eta)|y-\eta|+xF_y(x,\eta)\operatorname{sgn}(y-\eta)\right)d\eta\right)dx\,.$$

The integral equilibrium conditions can be established in the following form:

$$\iint_{\mathfrak{D}_1}\sigma_{xx}(x,y)dxdy=\int_{-\infty}^{+\infty}x\left(\int_0^{+\infty}F_x(x,y)dy-q_0(x)\right)dx,$$

$$\iint_{\mathfrak{D}_1}\sigma_{yy}(x,y)dxdy=\iint_{\mathfrak{D}_1}yF_y(x,y)dxdy,$$

$$\iint_{\mathfrak{D}_1} \sigma_{xy}(x,y)dxdy = \iint_{\mathfrak{D}_1} yF_x(x,y)dxdy$$

$$= \int_{-\infty}^{+\infty} x\left(p_0(x) + \int_0^{+\infty} F_y(x,y)dy \right) dx, \tag{2.3.5}$$

$$\iint_{\mathfrak{D}_1} y\sigma_{xx}(x,y)dxdy$$

$$= \int_{-\infty}^{+\infty} \left(\int_0^{+\infty} xyF_x(x,y)dy - \frac{x^2}{2}\left(p_0(x) + \int_0^{+\infty} F_y(x,y)dy \right) \right) dx,$$

$$\iint_{\mathfrak{D}_1} x\sigma_{yy}(x,y)dxdy$$

$$= \iint_{\mathfrak{D}_1} \left(xyF_y(x,y) - \frac{y^2}{2}F_x(x,y) \right) dxdy.$$

Note that the formulae in (2.3.2) – (2.3.5) are based on the equilibrium equations (2.1.15) in view of boundary conditions (2.3.1). They are irrespective of the material properties and thus they are the same as for the case of isotropic homogeneous [321, 322] and inhomogeneous [297] half-planes.

2.3.2. Stress determination

Applying the second equation in (2.1.15) allows us to transform the condition for shear stress given in (2.3.1) to obtain the derivative of normal stress as follows:

$$\left. \frac{\partial \sigma_{yy}(x,y)}{\partial y} \right|_{y=0} = -\frac{dq_0(x)}{dx} - F_y(x,0)\,. \tag{2.3.6}$$

In the mapping domain of the transform (2.2.24), the first boundary conditions in (2.3.1) and (2.3.6) take the form:

$$\overline{\sigma}_{yy}(0) = -\overline{p}_0, \quad \left.\frac{d\overline{\sigma}_{yy}(y)}{dy}\right|_{y=0} = -is\overline{q}_0 - \overline{F}_y(0). \tag{2.3.7}$$

The governing equations used to determine key stresses $\overline{\sigma}$ and $\overline{\sigma}_{yy}$ are given by (2.2.25) and (2.2.26).

One solution to equation (2.2.25) for half-plane $\mathfrak{D}_1$ in view of the first condition (2.3.7) can be derived as follows:

$$\overline{\sigma}_{yy}(y) = -\overline{p}_0 \exp(-|s|y)$$

$$+\frac{1}{2|s|}\int_0^{+\infty}\left(is\overline{F}_x(\xi) - \frac{d\overline{F}_y(\xi)}{d\xi} - s^2\overline{\sigma}(\xi)\right)$$

$$\times\left(\exp(-|s|(y+\xi)) - \exp(-|s||y-\xi|)\right)d\xi. \tag{2.3.8}$$

Substituting (2.3.8) into the second condition of (2.3.7) yields, after some algebra, the following integral condition for the total stress in the mapping domain:

$$s^2\int_0^{+\infty}\overline{\sigma}(y)\exp(-|s|y)dy = -|s|\,\overline{p}_0 - is\overline{q}_0 - \overline{F}_y(0)$$

$$+\int_0^{+\infty}\left(is\overline{F}_x(y) - \frac{d\overline{F}_y(y)}{dy}\right)\exp(-|s|y)dy. \tag{2.3.9}$$

In view of condition (2.3.9), formula (2.3.8) can be expressed as follows:

$$\overline{\sigma}_{yy}(y) = \left(\frac{is\overline{q}_0 + \overline{F}_y(0)}{|s|} - \overline{p}_0\right)\frac{\exp(-|s|y)}{2}$$

$$-\frac{s}{2|s|}\int_0^{+\infty}\left(i\overline{F}_x(\xi) - \frac{d\overline{F}_y(\xi)}{sd\xi}\right)\exp(-|s||y-\xi|)\,d\xi$$

$$+\frac{|s|}{2}\int_0^{+\infty}\overline{\sigma}(\xi)\exp(-|s||y-\xi|)d\xi. \tag{2.3.10}$$

One solution to equation (2.2.26) for half-plane $\mathfrak{D}_1$ can be constructed as follows:

$$a_{11}(y)\overline{\sigma}(y)+\alpha_1(y)\overline{T}(y)=A_0\exp(-|s|y)$$

$$+\frac{|s|}{2}\int_0^{+\infty}(\alpha_1(\eta)-\alpha_2(\eta))\overline{T}(\eta)\exp(-|s||y-\eta|)d\xi$$

$$-\frac{1}{2|s|}\int_0^{+\infty}\left(\beta_1(\eta)\left(\frac{d\overline{F}_y(\eta)}{d\eta}-is\overline{F}_x(\eta)\right)\right.$$

$$\left.-\frac{d}{d\eta}\left(\frac{\overline{F}_y(\eta)}{G_{xy}(\eta)}\right)\right)\exp(-|s||y-\eta|)d\eta$$

$$-\frac{1}{2|s|}\int_0^{+\infty}\exp(-|s||y-\eta|)$$

$$\times\frac{d}{d\eta}\left(\left(2\beta_1(\eta)-\frac{1}{G_{xy}(\eta)}\right)\frac{d\overline{\sigma}_{yy}(\eta)}{d\eta}\right)d\eta$$

$$-\frac{1}{2|s|}\int_0^{+\infty}\left(\frac{d^2\beta_1(\eta)}{d\eta^2}+s^2\beta_2(\eta)\right)$$

$$\times\overline{\sigma}_{yy}(\eta)\exp(-|s||y-\eta|)d\eta\,. \qquad (2.3.11)$$

Substituting (2.3.10) into (2.3.11), after some algebra, yields the following integral equation:

$$\overline{\sigma}(y)=A_0\frac{\exp(-|s|y)}{a_{11}(y)}+F_0(y)+\int_0^{+\infty}\overline{\sigma}(\xi)\mathcal{K}_{\mathrm{HP}}(y,\xi)d\xi\,, \qquad (2.3.12)$$

where

$$F_0(y)=P_0(y)+Q_0(y)+\Theta_0(y)+\Psi_0(y),$$

$$P_0(y)=\frac{\chi(y)}{2a_{11}(y)}\,\overline{p}_0,\qquad Q_0(y)=-\frac{\chi(y)}{2\,|\,s\,|\,a_{11}(y)}\,is\overline{q}_0,$$

$$\Theta_0(y)=\frac{1}{a_{11}(y)}\Bigg[-\alpha_1(y)\overline{T}(y)$$

$$+\frac{|\,s\,|}{2}\int_0^{+\infty}\left(\alpha_1(\eta)-\alpha_2(\eta)\right)\overline{T}(\eta)\exp(-|\,s\,||\,y-\eta\,|)d\eta\Bigg],$$

$$\Psi_0(y)=-\frac{1}{2\,|\,s\,|\,a_{11}(y)}\Bigg[\int_0^{+\infty}\Bigg(\beta_1(\eta)\left(\frac{d\overline{F}_y(\eta)}{d\eta}-is\overline{F}_x(\eta)\right)$$

$$-\frac{d}{d\eta}\left(\frac{\overline{F}_y(\eta)}{G_{xy}(\eta)}\right)\Bigg)\exp(-|\,s\,||\,y-\eta\,|)d\eta \qquad (2.3.13)$$

$$+\int_0^{+\infty}\gamma_{\mathrm{PL}}(y,\eta)\int_0^{+\infty}\left(is\overline{F}_x(\xi)-\frac{d\overline{F}_y(\xi)}{d\xi}\right)$$

$$\times\exp(-|\,s\,||\,\eta-\xi\,|)d\xi d\eta+\chi(y)\overline{F}_y(0)\Bigg],$$

$$\chi(y)=\left(2\beta_1(0)-\frac{1}{G_{xy}(0)}\right)\exp(-|\,s\,|\,y)$$

$$-\int_0^{+\infty}\gamma_{\mathrm{PL}}(y,\eta)\exp(-|\,s\,|\,\eta)d\eta\,,$$

$$\mathcal{K}_{\mathrm{HP}}(y,\xi)=\frac{|\,s\,|}{2a_{11}(y)}\int_0^{+\infty}\gamma_{\mathrm{PL}}(y,\eta)\exp(-|\,s\,||\,\eta-\xi\,|)d\eta\,,$$

where $\gamma_{\mathrm{PL}}(y,\eta)$ is given in (2.2.31).

Note that kernel in (2.3.13) is similar to that in (2.2.33) obtained for the analogous problem pertaining to plane $\mathfrak{D}_0$. The only difference is the lower limit of integration.

By solving equation (2.3.12) in a manner similar to (2.2.32) and eliminating the constant of integration A_0 by making use of condition (2.3.9), the total stress can be derived as follows:

$$\overline{\sigma}(y) = \overline{p}_0 P_{\mathrm{HP}}(y) + is\overline{q}_0 Q_{\mathrm{HP}}(y) + \Theta_{\mathrm{HP}}(y) + \Psi_{\mathrm{HP}}(y). \qquad (2.3.14)$$

Here,

$$P_{\mathrm{HP}}(y) = \chi_0(y) - \frac{h_0^+}{c_0} f_{\mathrm{HP}}(y),$$

$$Q_{\mathrm{HP}}(y) = -\frac{1}{|s|}\left(\chi_0(y) + \frac{h_0^-}{c_0} f_{\mathrm{HP}}(y)\right), \qquad (2.3.15)$$

$$\Theta_{\mathrm{HP}}(y) = \Theta_0(y)$$

$$+\int_0^{+\infty} \Theta_0(\xi)\left(\mathcal{R}_{\mathrm{HP}}(y,\xi) - \frac{f_{\mathrm{HP}}(y)}{c_0} g_{\mathrm{HP}}(\xi)\right) d\xi, \qquad (2.3.16)$$

$$\Psi_{\mathrm{HP}}(y) = \Psi_0(y)$$

$$+\int_0^{+\infty} \Psi_0(\xi)\left(\mathcal{R}_{\mathrm{HP}}(y,\xi) - \frac{f_{\mathrm{HP}}(y)}{c_0} g_{\mathrm{HP}}(\xi)\right) d\xi$$

$$-\frac{f_{\mathrm{HP}}(y)}{s^2 c_0}\left(\overline{F}_y(0) + \int_0^{+\infty}\left(\frac{d\overline{F}_y(y)}{dy} - is\overline{F}_x(y)\right)\exp(-|s|y)dy\right), \qquad (2.3.17)$$

$$\chi_0(y) = \frac{\chi(y)}{2a_{11}(y)} + \frac{1}{2}\int_0^{+\infty} \frac{\chi(\xi)}{a_{11}(\xi)} \mathcal{R}_{\mathrm{HP}}(y,\xi) d\xi,$$

$$h_0^{\pm} = \frac{1}{|s|} \pm \int_0^{+\infty} \frac{\chi(\xi) g_{\mathrm{HP}}(\xi)}{a_{11}(\xi)} d\xi, \qquad (2.3.18)$$

$$g_{\mathrm{HP}}(\xi)=\exp(-|s|\xi)+\int_0^{+\infty}\exp(-|s|y)\mathcal{R}_{\mathrm{HP}}(y,\xi)dy\,, \qquad (2.3.19)$$

$$c_0=\int_0^{+\infty}\frac{\exp(-2|s|y)}{a_{11}(y)}dy$$

$$+\int_0^{+\infty}\frac{\exp(-|s|\xi)}{a_{11}(\xi)}\int_0^{+\infty}\exp(-|s|y)\mathcal{R}_{\mathrm{HP}}(y,\xi)dyd\xi\,, \qquad (2.3.20)$$

$$f_{\mathrm{HP}}(y)=\frac{\exp(-|s|y)}{a_{11}(y)}+\int_0^{+\infty}\frac{\mathcal{R}_{\mathrm{HP}}(y,\xi)\exp(-|s|\xi)}{a_{11}(\xi)}d\xi, \qquad (2.3.21)$$

and

$$\mathcal{R}_{\mathrm{HP}}(y,\xi)=\sum_{n=0}^{\infty}\mathcal{K}_{n+1}^{\mathrm{HP}}(y,\xi) \qquad (2.3.22)$$

is the resolvent kernel, which can be computed as a series of recurring kernels, as follows:

$$\begin{gathered}\mathcal{K}_1^{\mathrm{HP}}(y,\xi)=\mathcal{K}_{\mathrm{HP}}(y,\xi),\\ \mathcal{K}_{n+1}^{\mathrm{HP}}(y,\xi)=\int_0^{+\infty}\mathcal{K}_1^{\mathrm{HP}}(y,t)\mathcal{K}_n^{\mathrm{HP}}(t,\xi)dt,\quad n=1,2,\ldots\end{gathered} \qquad (2.3.23)$$

In practical computations, the resolvent can be evaluated analytically; however, if this presents a challenge, the series (2.3.22) can be truncated, such that the resolvent kernel is approximated using the following finite sum:

$$\mathcal{R}_{\mathrm{HP}}(y,\xi)\approx\mathcal{R}_{\mathrm{HP}}^{N}(y,\xi)=\sum_{n=0}^{N}\mathcal{K}_{n+1}^{\mathrm{HP}}(y,\xi)\,, \qquad (2.3.24)$$

where N is a natural digit allowing for satisfaction of equation (2.3.12) using (2.3.14) with the resolvent kernel (2.3.24) instead of (2.3.22).

Once we have determined the total stress in the form (2.3.14), we can construct normal stress $\overline{\sigma}_{yy}$ by substituting (2.3.14) into (2.3.10) to yield the following:

$$\overline{\sigma}_{yy}(y) = \overline{p}_0 P^y_{\mathrm{HP}}(y) + is\overline{q}_0 Q^y_{\mathrm{HP}}(y) + \Theta^y_{\mathrm{HP}}(y) + \Psi^y_{\mathrm{HP}}(y)\,. \quad (2.3.25)$$

Here,

$$P^y_{\mathrm{HP}}(y) = \frac{1}{2}\left(|s| \int_0^{+\infty} P_{\mathrm{HP}}(\eta)\exp(-|s||y-\eta|)d\eta - \exp(-|s|y) \right),$$

$$Q^y_{\mathrm{HP}}(y) = \frac{1}{2|s|}\left(s^2 \int_0^{+\infty} Q_{\mathrm{HP}}(\eta)\exp(-|s||y-\eta|)d\eta + \exp(-|s|y) \right),$$

$$\Theta^y_{\mathrm{HP}}(y) = \frac{|s|}{2}\int_0^{+\infty} \Theta_{\mathrm{HP}}(\eta)\exp(-|s||y-\eta|)d\eta\,,$$

$$\Psi^y_{\mathrm{HP}}(y) = \frac{|s|}{2}\int_0^{+\infty} \Psi_{\mathrm{HP}}(\eta)\exp(-|s||y-\eta|)d\eta$$

$$+\frac{\overline{F}_y(0)}{2|s|}\exp(-|s|y)$$

$$+\frac{1}{2|s|}\int_0^{+\infty}\left(\frac{d\overline{F}_y(\eta)}{d\eta} - is\overline{F}_x(\eta) \right)\exp(-|s||y-\eta|)d\eta\,. \quad (2.3.26)$$

Normal stress $\overline{\sigma}_{xx}$ and shear stress $\overline{\sigma}_{xy}$ can be computed using the total and normal stresses $\overline{\sigma}$ and $\overline{\sigma}_{yy}$ via (2.2.39) and (2.2.41), as follows:

$$\overline{\sigma}_{xx}(y) = \overline{p}_0 P^x_{\mathrm{HP}}(y) + is\overline{q}_0 Q^x_{\mathrm{HP}}(y) + \Theta^x_{\mathrm{HP}}(y) + \Psi^x_{\mathrm{HP}}(y)\,, \quad (2.3.27)$$

$$\overline{\sigma}_{xy}(y) = \overline{p}_0 P^{xy}_{\mathrm{HP}}(y) + is\overline{q}_0 Q^{xy}_{\mathrm{HP}}(y) + \Theta^{xy}_{\mathrm{HP}}(y) + \Psi^{xy}_{\mathrm{HP}}(y)\,. \quad (2.3.28)$$

Here,

$$P_{\mathrm{HP}}^{x}(y)=\frac{\exp(-|s|y)}{2}+\chi_0(y)-\frac{h_0^{+}}{c_0}f_{\mathrm{HP}}(y)$$

$$-\frac{|s|}{2}\int_0^{+\infty}P_{\mathrm{HP}}(\eta)\exp(-|s||y-\eta|)d\eta, \qquad (2.3.29)$$

$$Q_{\mathrm{HP}}^{x}(y)=-\frac{1}{|s|}\left(\frac{\exp(-|s|y)}{2}+\chi_0(y)+\frac{h_0^{-}}{c_0}f_{\mathrm{HP}}(y)\right.$$

$$\left.+\frac{s^2}{2}\int_0^{+\infty}Q_{\mathrm{HP}}(\eta)\exp(-|s||y-\eta|)d\eta\right), \qquad (2.3.40)$$

$$\Theta_{\mathrm{HP}}^{x}(y)=\Theta_{\mathrm{HP}}(y)-\frac{|s|}{2}\int_0^{+\infty}\Theta_{\mathrm{HP}}(\eta)\exp(-|s||y-\eta|)d\eta, \qquad (2.3.41)$$

$$\Psi_{\mathrm{HP}}^{x}(y)=\Psi_{\mathrm{HP}}(y)-\frac{|s|}{2}\int_0^{+\infty}\Psi_{\mathrm{HP}}(\eta)\exp(-|s||y-\eta|)d\eta$$

$$-\frac{\overline{F}_y(0)}{2|s|}\exp(-|s|y)$$

$$-\frac{1}{2|s|}\int_0^{+\infty}\left(\frac{d\overline{F}_y(\eta)}{d\eta}-is\overline{F}_x(\eta)\right)\exp(-|s||y-\eta|)d\eta, \qquad (2.3.42)$$

$$P_{\mathrm{HP}}^{xy}(y)=\frac{i}{2}\frac{|s|}{s}\exp(-|s|y)$$

$$-\frac{is}{2}\int_0^{+\infty}P_{\mathrm{HP}}(\eta)\exp(-|s||y-\eta|)\operatorname{sgn}(y-\eta)d\eta,$$

$$Q_{\mathrm{HP}}^{xy}(y)=-\frac{is}{2}\int_0^{+\infty}Q_{\mathrm{HP}}(\eta)\exp(-|s||y-\eta|)\operatorname{sgn}(y-\eta)d\eta$$

$$-\frac{i}{2s}\exp(-|s|y),$$

$$\Theta_{\mathrm{HP}}^{xy}(y) = -\frac{is}{2}\int_0^{+\infty}\Theta_{\mathrm{HP}}(\eta)\exp(-|s||y-\eta|)\operatorname{sgn}(y-\eta)d\eta,$$

$$\Psi_{\mathrm{HP}}^{xy}(y) = \frac{i}{s}\left(\bar{F}_y(y) - \frac{\bar{F}_y(0)}{2}\exp(-|s|y)\right)$$

$$-\frac{is}{2}\int_0^{+\infty}\Psi_{\mathrm{HP}}(\eta)\exp(-|s||y-\eta|)\operatorname{sgn}(y-\eta)d\eta$$

$$-\frac{i}{2s}\int_0^{+\infty}\left(\frac{d\bar{F}_y(\eta)}{d\eta} - is\bar{F}_x(\eta)\right)\exp(-|s||y-\eta|)\operatorname{sgn}(y-\eta)d\eta. \qquad (2.3.43)$$

After finding the in-plane stresses in the mapping domain of the transform (2.2.24), we can compute the corresponding components in the physical domain using the inverse transform (2.2.43).

2.3.3. Determination of thermo-elastic displacements

Consider the thermoelasticity problem for an inhomogeneous orthotropic half-plane $\mathfrak{D}_1$, where the boundary conditions (2.3.1) are substituted using the following conditions for in-plane displacements:

$$u_x(x,0) = u_0(x), \quad u_y(x,0) = v_0(x). \qquad (2.3.44)$$

where $u_0(x)$ and $v_0(x)$ are given functions of a local distribution profile; i.e., they vanish as $|x| \to +\infty$.

In view of conditions (2.3.44), integration of the first and second Cauchy equations of (2.1.18) yields the following:

$$u_x(x,y)=\frac{1}{2}\int_{-\infty}^{+\infty}\varepsilon_{xx}(\xi,y)\,\mathrm{sgn}(x-\xi)d\xi,$$
$$u_y(x,y)=\frac{v_0(x)}{2}+\frac{1}{2}\int_{0}^{+\infty}\varepsilon_{yy}(x,\eta)\,\mathrm{sgn}(y-\eta)d\eta. \tag{2.3.45}$$

If we let $|x|\to\infty$ in the first equation of (2.3.45) and take the local distribution of the displacement field into consideration, we can then obtain the following integral compatibility condition for strain-tensor component $\varepsilon_{xx}(x,y)$:

$$\int_{-\infty}^{+\infty}\varepsilon_{xx}(x,y)dx=0\,. \tag{2.3.46}$$

Similarly, by substituting $y=0$ in the second equation of (2.3.45), we arrive at the following integral compatibility condition for strain-tensor component $\varepsilon_{yy}(x,y)$:

$$\int_{0}^{+\infty}\varepsilon_{yy}(x,y)dy=-v_0(x)\,. \tag{2.3.47}$$

Substituting (2.3.45) into the third Cauchy equation of (2.1.18) yields the following compatibility equation:

$$2\varepsilon_{xy}(x,y)-\frac{dv_0(x)}{dx}=\int_{-\infty}^{+\infty}\frac{\partial\varepsilon_{xx}(\xi,y)}{\partial y}\mathrm{sgn}(x-\xi)d\xi$$
$$+\int_{0}^{+\infty}\frac{\partial\varepsilon_{yy}(x,\eta)}{\partial x}\mathrm{sgn}(y-\eta)d\eta\,. \tag{2.3.48}$$

Clearly, the application of the mixed derivative $\partial^2/\partial x\partial y$ to equation (2.3.48) reduces it to the classical strain compatibility equation (2.1.19). It is important to mention, however, that deriving (2.3.48) from (2.1.19) requires that the following necessary condition be fulfilled:

$$\frac{dv_0(x)}{dx} = \varepsilon_{xy}(x,0) - \frac{1}{2}\int\limits_{-\infty}^{+\infty} \frac{\partial \varepsilon_{xx}(\xi,0)}{\partial y} \operatorname{sgn}(x-\xi)d\xi\,. \qquad (2.3.49)$$

Condition (2.3.49) was derived by integrating equation (2.1.19) by x and y and comparing the result with (2.3.48). It can also be obtained from the fulfillment of equation (2.3.48) on the boundary $y = 0$ of half-plane $\mathfrak{D}_1$ by taking into account boundary conditions (2.3.44).

Now, applying the Fourier transform (2.2.24) to expressions (2.3.45) in view of formula (2.3.47), we obtain the following expressions for displacements in the mapping domain:

$$\begin{gathered} \overline{u}_x(y) = -\frac{i}{s}\overline{\varepsilon}_{xx}(y), \\ \overline{u}_y(y) = \frac{1}{2}\int\limits_0^{+\infty} \overline{\varepsilon}_{yy}(\eta)\big(\operatorname{sgn}(y-\eta)-1\big)d\eta. \end{gathered} \qquad (2.3.50)$$

Using formulae (2.3.50) in conjunction with equations for strain-tensor components (2.1.23) expressed through stresses (2.3.14) and (2.3.25), we obtain the following expressions for displacements:

$$\overline{u}_x(y) = \overline{p}_0 P_{\mathrm{HP}}^{[x]}(y) + is\overline{q}_0 Q_{\mathrm{HP}}^{[x]}(y) + \Theta_{\mathrm{HP}}^{[x]}(y) + \Psi_{\mathrm{HP}}^{[x]}(y)\,, \qquad (2.3.51)$$

$$\overline{u}_y(y) = \overline{p}_0 P_{\mathrm{HP}}^{[y]}(y) + is\overline{q}_0 Q_{\mathrm{HP}}^{[y]}(y) + \Theta_{\mathrm{HP}}^{[y]}(y) + \Psi_{\mathrm{HP}}^{[y]}(y)\,. \qquad (2.3.52)$$

Here,

$$P_{\mathrm{HP}}^{[x]}(y) = \frac{i}{s}\Big(\big(a_{11}(y) - a_{12}(y)\big)P_{\mathrm{HP}}^{y}(y) - a_{11}(y)P_{\mathrm{HP}}(y)\Big)\,,$$

$$Q_{\mathrm{HP}}^{[x]}(y) = \frac{i}{s}\Big(\big(a_{11}(y) - a_{12}(y)\big)Q_{\mathrm{HP}}^{y}(y) - a_{11}(y)Q_{\mathrm{HP}}(y)\Big)\,,$$

$$\Theta_{\mathrm{HP}}^{[x]}(y) = \frac{i}{s}\Big(\big(a_{11}(y) - a_{12}(y)\big)\Theta_{\mathrm{HP}}^{y}(y) - a_{11}(y)\Theta_{\mathrm{HP}}(y) - \alpha_1(y)\overline{T}(y)\Big)\,,$$

$$\Psi_{\mathrm{HP}}^{[x]}(y) = \frac{i}{s}\Big(\big(a_{11}(y) - a_{12}(y)\big)\Psi_{\mathrm{HP}}^{y}(y) - a_{11}(y)\Psi_{\mathrm{HP}}(y)\Big)\,,$$

$$P_{\mathrm{HP}}^{[y]}(y)=\frac{1}{2}\int_0^{+\infty}\left(a_{12}(\eta)P_{\mathrm{HP}}(\eta)+\left(a_{22}(\eta)-a_{12}(\eta)\right)P_{\mathrm{HP}}^{y}(\eta)\right)$$

$$\times\left(\operatorname{sgn}(y-\eta)-1\right)d\eta,$$

$$Q_{\mathrm{HP}}^{[y]}(y)=\frac{1}{2}\int_0^{+\infty}\left(a_{12}(\eta)Q_{\mathrm{HP}}(\eta)+\left(a_{22}(\eta)-a_{12}(\eta)\right)Q_{\mathrm{HP}}^{y}(\eta)\right)$$

$$\times\left(\operatorname{sgn}(y-\eta)-1\right)d\eta,$$

$$\Theta_{\mathrm{HP}}^{[y]}(y)=\frac{1}{2}\int_0^{+\infty}\left(\alpha_2(\eta)\overline{T}(\eta)+a_{12}(\eta)\Theta_{\mathrm{HP}}(\eta)\right.$$

$$\left.+\left(a_{22}(\eta)-a_{12}(\eta)\right)\Theta_{\mathrm{HP}}^{y}(\eta)\right)\left(\operatorname{sgn}(y-\eta)-1\right)d\eta,$$

$$\Psi_{\mathrm{HP}}^{[y]}(y)=\frac{1}{2}\int_0^{+\infty}\left(a_{12}(\eta)\Psi_{\mathrm{HP}}(\eta)+\left(a_{22}(\eta)-a_{12}(\eta)\right)\Psi_{\mathrm{HP}}^{y}(\eta)\right)$$

$$\times\left(\operatorname{sgn}(y-\eta)-1\right)d\eta. \qquad (2.3.53)$$

Equations (2.3.51) and (2.3.52) represent the elastic displacements in half-plane $\mathfrak{D}_1$ due to the force loadings (2.3.1), body forces, F_x and F_y, and temperature field $T(x,y)$ in the mapping domain of transform (2.2.44). Note that these displacements are also to satisfy the boundary conditions (2.3.44). This necessitates a one-to-one relationship between the stresses (2.3.1) and displacements (2.3.44) at boundary $y=0$ of half-plane $\mathfrak{D}_1$.

2.3.4. One-to-one relationship between stresses and displacements on boundary of inhomogeneous orthotropic half-plane

The method of direct integration makes it possible to express stresses (2.3.25), (2.3.27), and (2.3.28) and displacements (2.3.51) and (2.3.52) in terms of applied loadings explicitly. This opens up opportunities for

solving thermoelasticity problems related to inhomogeneous orthotropic half-plane $\mathfrak{D}_1$ using boundary conditions given in terms of displacements or mixed-type boundary conditions. Obviously, substituting $y = 0$ into expressions (2.3.51) and (2.3.52) allows for the derivation of a one-to-one relationship between the boundary displacements and the boundary tractions:

$$\overline{u}_0 = \overline{p}_0 P_{\mathrm{HP}}^{[x]}(0) + is\overline{q}_0 Q_{\mathrm{HP}}^{[x]}(0) + \Theta_{\mathrm{HP}}^{[x]}(0) + \Psi_{\mathrm{HP}}^{[x]}(0)\,, \qquad (2.3.54)$$

$$\overline{v}_0 = \overline{p}_0 P_{\mathrm{HP}}^{[y]}(0) + is\overline{q}_0 Q_{\mathrm{HP}}^{[y]}(0) + \Theta_{\mathrm{HP}}^{[y]}(0) + \Psi_{\mathrm{HP}}^{[y]}(0)\,, \qquad (2.3.55)$$

where $\overline{u}_0$ and $\overline{v}_0$ are mappings of the boundary displacements introduced in conditions (2.3.44), and $\overline{p}_0$ and $\overline{q}_0$ are the boundary tractions involved in conditions (2.3.7). Note that equation (2.3.55) can be replaced by a simpler one obtained from condition (2.3.49) in the mapping domain of transform (2.2.44), as follows:

$$\overline{v}_0 = \frac{1}{s^2}\frac{d\overline{\varepsilon}_{xx}(0)}{dy} - \frac{i}{s}\overline{\varepsilon}_{xy}(0)\ . \qquad (2.3.56)$$

In view of expressions

$$\overline{\varepsilon}_{xy}(0) = \frac{\overline{q}_0}{G_{xy}(0)},$$

$$\left.\frac{d\overline{\varepsilon}_{xx}(y)}{dy}\right|_{y=0} = -\overline{p}_0 \left.\frac{d(a_{12}(y) - a_{11}(y))}{dy}\right|_{y=0}$$

$$+(a_{11}(0) - a_{12}(0))\left(is\overline{q}_0 + \overline{F}_y(0)\right)$$

$$+\frac{d}{dy}(a_{11}(y)\overline{\sigma}(y) + \alpha_1(y)\overline{T}(y))\Big|_{y=0}\,, \qquad (2.3.57)$$

which follow from constitutive equations (2.1.23) and boundary conditions (2.3.7), formula (2.3.56) can be rewritten as follows:

$$\overline{v}_0 = \overline{p}_0 \frac{1}{s^2}\frac{d}{dy}\left((1 + P_{\mathrm{HP}}(y))a_{11}(y) - a_{12}(y)\right)\Big|_{y=0}$$

$$+\frac{i}{s}\overline{q}_0\left(\frac{d}{dy}\left(a_{11}(y)Q_{\mathrm{HP}}(y)\right)-\frac{1}{sG_{xy}(y)}-a_{12}(y)+a_{11}(y)\right)\Bigg|_{y=0}$$

$$+\frac{1}{s^2}\frac{d}{dy}\left(a_{11}(y)\Theta_{\mathrm{HP}}(y)+\alpha_1(y)\overline{T}(y)\right)\Big|_{y=0}$$

$$+\frac{1}{s^2}\left(\frac{d}{dy}\left(a_{11}(y)\Psi_{\mathrm{HP}}(y)\right)+\left(a_{11}(y)-a_{12}(y)\right)\overline{F}_y(y)\right)\Bigg|_{y=0} \qquad (2.3.58)$$

with expression (2.3.14) in mind.

Equations (2.3.54) and (2.3.58) yield the following:

$$\begin{pmatrix}\overline{u}_0\\ \overline{v}_0\end{pmatrix}=\begin{pmatrix}\mu_{11} & \mu_{12}\\ \mu_{21} & \mu_{22}\end{pmatrix}\begin{pmatrix}\overline{p}_0\\ \overline{q}_0\end{pmatrix}+\begin{pmatrix}\theta_1+\psi_1\\ \theta_2+\psi_2\end{pmatrix}, \qquad (2.3.59)$$

where

$$\mu_{11}=P_{\mathrm{HP}}^{[x]}(0),\quad \mu_{12}=isQ_{\mathrm{HP}}^{[x]}(0),$$

$$\theta_1=\Theta_{\mathrm{HP}}^{[x]}(0),\quad \psi_1=\Psi_{\mathrm{HP}}^{[x]}(0),$$

$$\mu_{21}=\frac{1}{s^2}\frac{d}{dy}\left((1+P_{\mathrm{HP}}(y))a_{11}(y)-a_{12}(y)\right)\Big|_{y=0},$$

$$\mu_{22}=\frac{i}{s}\left(\frac{d}{dy}\left(a_{11}(y)Q_{\mathrm{HP}}(y)\right)-\frac{1}{sG_{xy}(y)}-a_{12}(y)+a_{11}(y)\right)\Bigg|_{y=0},$$

$$\theta_2=\frac{1}{s^2}\frac{d}{dy}\left(a_{11}(y)\Theta_{\mathrm{HP}}(y)+\alpha_1(y)\overline{T}(y)\right)\Big|_{y=0},$$

$$\psi_2=\frac{1}{s^2}\left(\frac{d}{dy}\left(a_{11}(y)\Psi_{\mathrm{HP}}(y)\right)+\left(a_{11}(y)-a_{12}(y)\right)\overline{F}_y(y)\right)\Bigg|_{y=0}. \qquad (2.3.60)$$

Due to the fact that system of equations (2.3.59) always has a unique solution, it can be inverted to express the boundary tractions in terms of boundary displacements, as follows:

$$\begin{pmatrix} \overline{p}_0 \\ \overline{q}_0 \end{pmatrix} = \begin{pmatrix} \mu_{11}^* & \mu_{12}^* \\ \mu_{21}^* & \mu_{22}^* \end{pmatrix} \begin{pmatrix} \overline{u}_0 \\ \overline{v}_0 \end{pmatrix} + \begin{pmatrix} \theta_1^* + \psi_1^* \\ \theta_2^* + \psi_2^* \end{pmatrix}, \tag{2.3.61}$$

where

$$\mu_{11}^* = \frac{\mu_{22}}{\mu}, \quad \mu_{12}^* = -\frac{\mu_{12}}{\mu},$$

$$\theta_1^* = \frac{\theta_2\mu_{12} - \theta_1\mu_{22}}{\mu}, \quad \psi_1^* = \frac{\psi_2\mu_{12} - \psi_1\mu_{22}}{\mu},$$

$$\mu_{21}^* = -\frac{\mu_{21}}{\mu}, \quad \mu_{22}^* = \frac{\mu_{11}}{\mu}, \quad \theta_2^* = \frac{\theta_1\mu_{21} - \theta_2\mu_{11}}{\mu},$$

$$\psi_2^* = \frac{\psi_1\mu_{21} - \psi_2\mu_{11}}{\mu}, \ \mu = \mu_{11}\mu_{22} - \mu_{12}\mu_{21}. \tag{2.3.62}$$

Thus, when solving a thermoelasticity problem for inhomogeneous orthotropic half-plane $\mathfrak{D}_1$ with the boundary conditions given in terms of stresses (2.3.1), the solution for stresses can be obtained directly using (2.3.25), (2.3.27), and (2.3.28). The solution for displacements can be found using (2.3.51) and (2.3.52). For a thermoelasticity problem with boundary conditions given in terms of displacements (2.3.44), we first use (2.3.61) to determine unknown boundary tractions through the given boundary displacements. We can then combine these with (2.3.25), (2.3.27), (2.3.28), (2.3.51), and (2.3.52) to determine stresses and displacements in domain $\mathfrak{D}_1$. A similar strategy can be used if the boundary of inhomogeneous orthotropic half-plane $\mathfrak{D}_1$ is exposed to one of the boundary tractions (either p_0 or q_0) with one of the boundary displacements (either u_0 or v_0) imposing mixed-type boundary conditions [149].

If, for example, the limiting surface $y = 0$ of half-plane $\mathfrak{D}_1$ is under conditions of sliding support, i.e. it is constrained to move vertically and induces no friction; then traction $p_0(x)$ in conditions (2.3.1) remains unknown while

$$q_0(x) = 0. \tag{2.3.63}$$

and $v_0(x) = 0$ in conditions (2.3.44). Then, making use of (2.3.61) allows for determining the unknown traction in the mapping domain of transform (2.2.44) in the form as follows:

$$\overline{p}_0 = \frac{\mu_{12}^* \theta_2 + \theta_1^*}{1 - \mu_{12}^* \mu_{21}} + \frac{\psi_1^* - \mu_{12}^* \psi_2}{1 - \mu_{12}^* \mu_{21}}. \tag{2.3.64}$$

Now, tractions (2.3.63) and (2.3.64) can be used in conditions (2.3.1) to determine the stress-tensor and displacement-vector components in inhomogeneous orthotropic half-plane $\mathfrak{D}_1$.

2.3.5. Steady-state temperature field in inhomogeneous half-plane

In the following, we consider the problem of steady-state temperature $T = T(x, y)$ in half-plane $\mathfrak{D}_1$ due to the action of inner heat sources with density $w(x, y)$ and the following generalized thermal conditions at boundary $y = 0$:

$$\ell_0 T(x, 0) + \ell_1 \left. \frac{\partial T(x, y)}{\partial y} \right|_{y=0} = T_0(x). \tag{2.3.65}$$

where $T_0(x)$ is given and constants ℓ_0 and ℓ_1 define the type of boundary condition. If, for example, $\ell_1 = 0$ and $\ell_0 \neq 0$, then (2.3.65) is the Dirichlet boundary condition, which imposes temperature on the boundary. If, on the other hand, $\ell_0 = 0$ and $\ell_1 = \lambda_y(0)$, then (2.3.65) is the Neumann boundary condition, which imposes heat flux through the boundary as follows:

$$\lambda_y(0) \left. \frac{\partial T(x, y)}{\partial y} \right|_{y=0} = \Phi(x), \tag{2.3.66}$$

where $\Phi(x) = T_0(x)$. If both $\ell_0 \neq 0$ and $\ell_1 \neq 0$, then (2.3.65) imposes heat exchange between half-plane $\mathfrak{D}_1$ and its surroundings via boundary $y = 0$.

Before we determine the temperature due to (2.3.65) and the inner heat sources of density $w(x, y)$, we derive the conditions of thermal balance to ensure that the temperature has a finite value within half-plane $\mathfrak{D}_1$. In [239], the following integral condition of thermal balance is derived for the case of a homogeneous isotropic half-plane, where $\Phi(x)$ is the heat flux imposed through the boundary by (2.3.66):

$$\iint_{\mathfrak{D}_1} w(x, y)dxdy = \int_{-\infty}^{+\infty} \Phi(x)dx . \tag{2.3.67}$$

A similar condition has been derived in [299] for an isotropic inhomogeneous half-plane. In the following, we prove that (2.3.67) holds for the case of inhomogeneous orthotropic half-plane $\mathfrak{D}_1$.

Following the strategy used in [239, 299], we introduce the heat flux components (2.2.49) and refer to the heat conduction equation in the form (2.2.50). We assume that the components of heat flux vanish for infinitely distant points:

$$\lim_{|x|\to+\infty} \Phi_x(x, y) = \lim_{y\to+\infty} \Phi_y(x, y) = 0 . \tag{2.3.68}$$

In view of (2.3.68), integrating (2.2.50) by x from $-\infty$ to $+\infty$ yields

$$\frac{d}{dy}\int_{-\infty}^{+\infty} \Phi_y(x, y)dx = -\int_{-\infty}^{+\infty} w(x, y)dx . \tag{2.3.69}$$

Now, we integrate (2.3.69) over y to obtain the following:

$$\int_{-\infty}^{+\infty} \Phi_y(x, y)dx = A_0 - \frac{1}{2}\iint_{\mathfrak{D}_1} w(x, \eta)\,\mathrm{sgn}(y - \eta)dxd\eta . \tag{2.3.70}$$

where $A_0 = \mathrm{const}$. By setting $y = 0$ and letting $y \to +\infty$ in (2.3.70), we obtain the following:

$$A_0 = \frac{1}{2}\int_{-\infty}^{+\infty} \Phi_y(x,0)dx + \frac{1}{2}\lim_{y\to+\infty}\int_{-\infty}^{+\infty} \Phi_y(x,y)dx,$$
$$\iint_{\mathfrak{D}_1} w(x,y)dxdy = \int_{-\infty}^{+\infty} \Phi_y(x,0)dx - \lim_{y\to+\infty}\int_{-\infty}^{+\infty} \Phi_y(x,y)dx. \tag{2.3.71}$$

Integrating (2.3.70) over y from 0 to L, where L is a large real number, we derive the following:

$$\int_{-\infty}^{+\infty}\int_{0}^{L} \Phi_y(x,y)dxdy = \left(A_0 - \frac{1}{2}\iint_{\mathfrak{D}_1} w(x,y)dxdy\right)L$$
$$+\iint_{\mathfrak{D}_1} yw(x,y)dxdy\,. \tag{2.3.72}$$

We account for the fact that L can grow infinitely while the resultant heat flux within the half-plane is finite:

$$\left|\iint_{\mathfrak{D}_1} \Phi_y(x,y)dxdy\right| < +\infty\,. \tag{2.3.73}$$

Then, (2.3.72) implies that

$$A_0 = \frac{1}{2}\iint_{\mathfrak{D}_1} w(x,y)dxdy \tag{2.3.74}$$

and

$$\iint_{\mathfrak{D}_1} \Phi_y(x,y)dxdy = \iint_{\mathfrak{D}_1} yw(x,y)dxdy\,. \tag{2.3.75}$$

Combining (2.3.74) with (2.3.71) yields the following:

$$A_0 = \frac{1}{2}\int_{-\infty}^{+\infty} \Phi_y(x,0)dx, \quad \lim_{y\to+\infty}\int_{-\infty}^{+\infty} \Phi_y(x,y)dx = 0 \tag{2.3.76}$$

and

$$\iint_{\mathfrak{D}_1} w(x,y)dxdy = \int_{-\infty}^{+\infty} \Phi_y(x,0)dx\,. \tag{2.3.77}$$

The second equation in (2.3.76) stipulates that the resultant of the heat-flux $\Phi_y(x,y)$ vanishes as $y \to \infty$. The condition given in (2.3.77) relates to thermal balance and, in view of (2.3.66), it coincides with the condition given in (2.3.67).

Similarly, in view of (2.3.68), by integrating (2.2.50) over y from 0 to $+\infty$, we obtain the following:

$$\frac{d}{dx}\int_0^{+\infty} \Phi_x(x,y)dy = \Phi_y(x,0) - \int_0^{+\infty} w(x,y)dy\,. \tag{2.3.78}$$

Integrating this over x, we obtain the following:

$$\int_0^{+\infty} \Phi_x(x,y)dy = B_0$$

$$+\frac{1}{2}\int_{-\infty}^{+\infty}\left(\Phi_y(\xi,0) - \int_0^{+\infty} w(\xi,y)dy\right)\operatorname{sgn}(x-\xi)d\xi\,, \tag{2.3.79}$$

where $B_0 = \text{const}$. If we let $|x| \to +\infty$ in (2.3.79), we derive the following:

$$B_0 = \frac{1}{2}\lim_{x\to+\infty}\int_0^{+\infty} \Phi_x(x,y)dy + \frac{1}{2}\lim_{x\to-\infty}\int_0^{+\infty} \Phi_x(x,y)dy,$$

$$\int_{-\infty}^{+\infty}\left(\Phi_y(x,0) - \int_0^{+\infty} w(x,y)dy\right)dx$$

$$= \lim_{x\to+\infty}\int_0^{+\infty} \Phi_x(x,y)dy - \lim_{x\to-\infty}\int_0^{+\infty} \Phi_x(x,y)dy\,. \tag{2.3.80}$$

Integrating (2.3.79) over x from L_1 to $L_2 > L_1$ yields

$$\int_0^{+\infty}\int_{L_1}^{L_2}\Phi_x(x,y)dxdy = B_0(L_2 - L_1)$$

$$+\frac{L_1+L_2}{2}\int_{-\infty}^{+\infty}\left(\Phi_y(x,0) - \int_0^{+\infty} w(x,y)dy\right)dx$$

$$-\int_{-\infty}^{+\infty} x\Phi_y(x,0)dx + \iint_{\mathfrak{D}_1} xw(x,y)dxdy\,. \qquad (2.3.81)$$

The fact that constants L_1 and L_2 respectively tend toward $-\infty$ and $+\infty$ leads us to condition (2.3.77) and $B_0 = 0$. The conditions in (2.3.80) thereby yield

$$\lim_{x\to-\infty}\int_0^{+\infty}\Phi_x(x,y)dy = \lim_{x\to+\infty}\int_0^{+\infty}\Phi_x(x,y)dy = 0\,. \qquad (2.3.82)$$

This implies that the resultant of heat flux $\Phi_x(x,y)$ vanishes as $|x|\to+\infty,$ and the following thermal balance condition holds:

$$\int_{-\infty}^{+\infty} x\Phi_y(x,y)dy = \iint_{\mathfrak{D}_1}\left(xw(x,y) - \Phi_x(x,y)\right)dxdy. \qquad (2.3.83)$$

Condition (2.3.83) verbalizes the balance between the thermal "moment" of the heat flux through the surface $y = 0$ and the longitudinal heat flux and heat generated by thermal sources. This means that the thermal loadings cannot be imposed arbitrarily; i.e., they must support the derived integral conditions of thermal balance.

After the thermal balance conditions are derived, we can obtain an analytic solution to equation (2.2.62) with respect to its left-hand side, which vanishes as $y\to+\infty$ and possess a degree of freedom in order to meet condition (2.3.65), as follows:

$$\overline{T}(y) = C\exp(-|s|y) + \frac{1}{2|s|}\int_0^{+\infty} \frac{\overline{w}(\eta)}{\lambda_y(\eta)}\exp(-|s||y-\eta|)d\eta$$

$$+\frac{1}{2}\int_0^{+\infty} \overline{T}(\eta)\left(|s|\frac{\lambda_y(\eta)-\lambda_x(\eta)}{\lambda_y(\eta)} - \frac{d\ln\lambda_y(\eta)}{d\eta}\operatorname{sgn}(y-\eta)\right.$$

$$\left. -\frac{1}{|s|}\frac{d^2\ln\lambda_y(\eta)}{d\eta^2}\right)\exp(-|s||y-\eta|)d\eta\,. \qquad (2.3.84)$$

where C is the constant of integration. We first determine this constant from the following condition, which is obtained by applying integral transform (2.2.24) to (2.3.65):

$$\ell_0\overline{T}(0) + \ell_1\left.\frac{d\overline{T}(y)}{dy}\right|_{y=0} = \overline{T}_0\,. \qquad (2.3.85)$$

Within the context of the latter condition, equation (2.3.84) can be transformed into the following integral equation:

$$\overline{T}(y) = \overline{T}_0\frac{\exp(-|s|y)}{æ^-} + W_{\mathrm{HP}}(y) + \int_0^{+\infty}\overline{T}(\eta)\mathcal{L}_{\mathrm{HP}}(y,\eta)d\eta\,, \quad (2.3.86)$$

where

$$W_{\mathrm{HP}}(y) = \frac{1}{2|s|}\int_0^{+\infty}\frac{\overline{w}(\eta)}{\lambda_y(\eta)}$$

$$\times\left(\exp(-|s||y-\eta|) - \frac{æ^+}{æ^-}\exp(-|s|(y+\eta))\right)d\eta\,,$$

$$\mathcal{L}_{\mathrm{HP}}(y,\eta) = \frac{1}{2}\left(|s|\frac{\lambda_y(\eta)-\lambda_x(\eta)}{\lambda_y(\eta)} - \frac{1}{|s|}\frac{d^2\ln\lambda_y(\eta)}{d\eta^2}\right)$$

$$\times\left(\exp(-|s||y-\eta|) - \frac{æ^+}{æ^-}\exp(-|s|(y+\eta))\right)\Bigg) \qquad (2.3.87)$$

$$-\frac{1}{2}\frac{d\ln\lambda_y(\eta)}{d\eta}\Bigg(\exp(-|s||y-\eta|)\operatorname{sgn}(y-\eta)$$

$$+\frac{æ^+}{æ^-}\exp(-|s|(y+\eta))\Bigg),$$

$$æ^{\pm}=\ell_0\pm\ell_1\left(|s|\mp æ_0\right),\quad æ_0=\frac{1}{\lambda_y(0)}\frac{d\lambda_y(y)}{dy}\bigg|_{y=0}.$$

The resolvent-kernel technique can then be used to solve the integral equation (2.3.86) in the form as follows:

$$\overline{T}(y)=\overline{T}_0 t_{\mathrm{HP}}(y)+w_{\mathrm{HP}}(y), \tag{2.3.88}$$

where resolvent kernel $\mathcal{T}_{\mathrm{HP}}(y,\eta)$ can be computed using an infinite series

$$\mathcal{T}_{\mathrm{HP}}(y,\eta)=\sum_{n=0}^{\infty}\mathcal{T}_{n+1}^{\mathrm{HP}}(y,\eta) \tag{2.3.89}$$

of the recurring kernels

$$\begin{gathered}\mathcal{T}_1^{\mathrm{HP}}(y,\eta)=\mathcal{L}_{\mathrm{HP}}(y,\eta),\\ \mathcal{T}_{n+1}^{\mathrm{HP}}(y,\eta)=\int_0^{+\infty}\mathcal{T}_1^{\mathrm{HP}}(y,t)\mathcal{T}_n^{\mathrm{HP}}(t,\eta)dt,\ \ n=1,2,...,\end{gathered} \tag{2.3.90}$$

and

$$\begin{gathered}t_{\mathrm{HP}}(y)=\frac{1}{æ^-}\left(\exp(-|s|y)+\int_0^{+\infty}\exp(-|s|\eta)\mathcal{T}_{\mathrm{HP}}(y,\eta)d\eta\right),\\ w_{\mathrm{HP}}(y)=W_{\mathrm{HP}}(y)+\int_0^{+\infty}W_{\mathrm{HP}}(\eta)\mathcal{T}_{\mathrm{HP}}(y,\eta)d\eta.\end{gathered} \tag{2.3.91}$$

In practical computations, resolvent kernel (2.3.89) can be substituted with the following approximate expression:

$$\mathcal{T}_{\mathrm{HP}}(y,\eta) \approx \mathcal{T}_{\mathrm{HP}}^{M}(y,\eta) = \sum_{n=0}^{M} \mathcal{T}_{n+1}^{\mathrm{HP}}(y,\eta), \tag{2.3.92}$$

where M is a positive integer evaluated either analytically or on the basis of numerical experiments.

After we construct the temperature using (2.3.88) in the mapping domain of transform (2.2.24), it can be restored in the physical domain using either analytical or numerical implementation of the inverse transform (2.2.43).

2.4. Thermoelastic analysis of inhomogeneous orthotropic strip

2.4.1. Formulation, integral conditions, and solutions in terms of stresses

Consider the problem on the determination of thermoelastic stresses and displacements in an inhomogeneous orthotropic strip $\mathfrak{D}_2 = \{(x,y) \in (-\infty,+\infty)\times[-1,1]\}$, where all of the material properties are arbitrary functions of coordinate y and $T_0 = e_0 = 0$. The stress state is governed by equations (2.1.15) and (2.1.31). Strip $\mathfrak{D}_2$ is exposed to the following static force loadings on sides $y = \pm 1$:

$$\begin{aligned} &\sigma_{yy}(x,1) = -p_1(x), \quad \sigma_{xy}(x,1) = q_1(x), \qquad |x| < +\infty, \\ &\sigma_{yy}(x,-1) = -p_2(x), \quad \sigma_{xy}(x,-1) = q_2(x), \qquad |x| < +\infty. \end{aligned} \tag{2.4.1}$$

The interior of the strip is exposed to temperature field distribution $T(x,y)$, which can be determined from a relevant problem of heat-conduction, and body forces $F_x(x,y)$ and $F_y(x,y)$.

Following a similar strategy to that presented in Section 2.3.1, we can establish the necessary conditions for the force loadings applied to the interior and periphery of domain $\mathfrak{D}_2$:

$$\begin{aligned}
&\int_{-\infty}^{+\infty}\big(q_2(x)-q_1(x)\big)dx=\iint_{\mathfrak{D}_2}F_x(x,y)dxdy,\\
&\int_{-\infty}^{+\infty}\big(p_1(x)-p_2(x)\big)dx=\iint_{\mathfrak{D}_2}F_y(x,y)dxdy,\\
&\int_{-\infty}^{+\infty}\big(x\big(p_2(x)-p_1(x)\big)-q_1(x)-q_2(x)\big)dx\\
&\qquad=\iint_{\mathfrak{D}_2}\big(yF_x(x)-xF_y(x)\big)dxdy.
\end{aligned}\tag{2.4.2}$$

The integral expressions for stress-tensor components can be derived as follows:

$$\begin{aligned}
2\sigma_{xy}(x,y)&=-\int_{-\infty}^{+\infty}\left(\frac{\partial\sigma_{yy}(\xi,y)}{\partial y}+F_y(\xi,y)\right)\operatorname{sgn}(x-\xi)d\xi\\
&=q_1(x)+q_2(x)-\int_{-1}^{1}\left(\frac{\partial\sigma_{xx}(x,\eta)}{\partial x}+F_x(x,\eta)\right)\operatorname{sgn}(y-\eta)d\eta,\\
2\sigma_{xx}(x,y)&=-\int_{-\infty}^{+\infty}\left(\frac{\partial\sigma_{xy}(\xi,y)}{\partial y}+F_x(\xi,y)\right)\operatorname{sgn}(x-\xi)d\xi\\
&=\int_{-\infty}^{+\infty}\left(\frac{\partial^2\sigma_{yy}(\xi,y)}{\partial y^2}+\frac{\partial F_y(\xi,y)}{\partial y}\right)|x-\xi|\,d\xi\\
&\quad-\int_{-\infty}^{+\infty}F_x(\xi,y)\operatorname{sgn}(x-\xi)d\xi,\\
2\sigma_{yy}(x,y)&=-p_1(x)-p_2(x)\\
&\quad-\int_{-1}^{1}\left(\frac{\partial\sigma_{xy}(x,\eta)}{\partial x}+F_y(x,\eta)\right)\operatorname{sgn}(y-\eta)d\eta
\end{aligned}\tag{2.4.3}$$

$$= -p_1(x) - p_2(x) + \frac{d}{dx}\big(q_1(x) - q_2(x)\big)$$

$$-y\frac{d}{dx}\big(q_1(x) + q_2(x)\big)$$

$$+\int_{-1}^{1}\left(\frac{\partial^2 \sigma_{xx}(x,\eta)}{\partial x^2} + \frac{\partial F_x(x,\eta)}{\partial x}\right)|\, y-\eta\,|\, d\eta$$

$$-\int_{-1}^{1} F_y(x,\eta)\,\mathrm{sgn}(y-\eta)d\eta\,.$$

We can also derive equations for the resultant forces and moments as follows:

$$2\int_{-1}^{1}\sigma_{xx}(x,y)dy = \int_{-\infty}^{+\infty}\big(q_2(\xi) - q_1(\xi)\big)\,\mathrm{sgn}(x-\xi)d\xi$$

$$-\iint_{\mathfrak{D}_2} F_x(\xi,y)\,\mathrm{sgn}(x-\xi)d\xi dy,$$

$$2\int_{-\infty}^{+\infty}\sigma_{yy}(x,y)dx = -\int_{-\infty}^{+\infty}\big(p_1(x) + p_2(x)\big)dx$$

$$-\iint_{\mathfrak{D}_2} F_y(x,\eta)\,\mathrm{sgn}(y-\eta)dxd\eta\,,$$

$$2\int_{-\infty}^{+\infty}\sigma_{xy}(x,y)dx = -\int_{-\infty}^{+\infty}\big(q_1(x) + q_2(x)\big)dx$$

$$-\iint_{\mathfrak{D}_2} F_x(x,\eta)\,\mathrm{sgn}(y-\eta)dxd\eta$$

$$= \int_{-\infty}^{+\infty}\big(p_1(\xi) - p_2(\xi)\big)\,\mathrm{sgn}(x-\xi)d\xi \qquad (2.4.4)$$

$$-\iint_{\mathfrak{D}_2} F_y(\xi, y)\operatorname{sgn}(x-\xi)d\xi dy,$$

$$2\int_{-1}^{1} y\sigma_{xx}(x,y)dy = \int_{-\infty}^{+\infty}\left(p_1(\xi)-p_2(\xi)\right)|x-\xi|d\xi$$

$$-\iint_{\mathfrak{D}_2} F_y(\xi, y)|x-\xi|d\xi$$

$$-\int_{-\infty}^{+\infty}\left(q_1(\xi)+q_2(\xi)\right)\operatorname{sgn}(x-\xi)d\xi$$

$$-\iint_{\mathfrak{D}_2} yF_x(\xi, y)\operatorname{sgn}(x-\xi)d\xi,$$

$$2\int_{-\infty}^{+\infty} x\sigma_{yy}(x,y)dx = -\int_{-\infty}^{+\infty} x\left(p_1(x)+p_2(x)\right)dx$$

$$+\int_{-\infty}^{+\infty}\left(q_1(x)+q_2(x)\right)dx + y\int_{-\infty}^{+\infty}\left(q_1(x)+q_2(x)\right)dx$$

$$-\iint_{\mathfrak{D}_2}\left(F_x(x,\eta)|y-\eta| - xF_y(x,\eta)\operatorname{sgn}(y-\eta)\right)dxd\eta\,.$$

The integral equilibrium conditions can also be derived as follows:

$$\iint_{\mathfrak{D}_2}\sigma_{xx}(x,y)dxdy = \int_{-\infty}^{+\infty} x\left(q_1(x)-q_2(x)\right)dx$$

$$+\iint_{\mathfrak{D}_2} xF_x(x,y)dxdy,$$

$$\iint_{\mathfrak{D}_2}\sigma_{yy}(x,y)dxdy = -\int_{-\infty}^{+\infty}\left(p_1(x)+p_2(x)\right)dx$$

$$+\iint_{\mathfrak{D}_2} yF_y(x,y)dxdy,$$

$$\iint_{\mathfrak{D}_2} \sigma_{xy}(x,y)dxdy = \int_{-\infty}^{+\infty} \big(q_1(x)+q_2(x)\big)dx$$

$$+\iint_{\mathfrak{D}_2} yF_x(x,y)dxdy$$

$$= \int_{-\infty}^{+\infty} x\big(p_2(x)-p_1(x)\big)dx + \iint_{\mathfrak{D}_2} xF_y(x,y)dxdy, \qquad (2.4.5)$$

$$\iint_{\mathfrak{D}_2} y\sigma_{xx}(x,y)dxdy = \int_{-\infty}^{+\infty} x\big(q_1(x)+q_2(x)\big)dx$$

$$+\frac{1}{2}\int_{-\infty}^{+\infty} x^2\big(p_1(x)-p_2(x)\big)dx$$

$$+\iint_{\mathfrak{D}_2} xyF_x(x,y)dxdy - \frac{1}{2}\iint_{\mathfrak{D}_2} x^2F_y(x,y)dxdy,$$

$$\iint_{\mathfrak{D}_2} x\sigma_{yy}(x,y)dxdy = \frac{1}{2}\int_{-\infty}^{+\infty} \big(q_2(x)-q_1(x)\big)dx$$

$$-\int_{-\infty}^{+\infty} x\big(p_1(x)+p_2(x)\big)dx$$

$$+\iint_{\mathfrak{D}_2} xyF_y(x,y)dxdy - \frac{1}{2}\iint_{\mathfrak{D}_2} y^2F_x(x,y)dxdy.$$

Note that formulae (2.4.2) – (2.4.5) are derived on the basis of the equilibrium equations (2.1.15), and are irrespective of the material properties. Thus, they hold for the cases of isotropic homogeneous [321, 322] and inhomogeneous [297] half-planes.

Using the second equation of (2.1.15), conditions (2.4.1) for shear stress can be transformed into conditions for the derivatives of normal stress:

$$\left.\frac{\partial \sigma_{yy}(x,y)}{\partial y}\right|_{y=1} = -\frac{dq_1(x)}{dx} - F_y(x,1),$$
$$\left.\frac{\partial \sigma_{yy}(x,y)}{\partial y}\right|_{y=-1} = -\frac{dq_2(x)}{dx} - F_y(x,-1). \tag{2.4.6}$$

In the mapping domain of the transform (2.2.24), the boundary conditions (2.4.6) along with (2.4.1) for normal stress take the following form:

$$\overline{\sigma}_{yy}(1) = -\overline{p}_1, \quad \overline{\sigma}_{yy}(-1) = -\overline{p}_2, \tag{2.4.7}$$

$$\left.\frac{d\overline{\sigma}_{yy}(y)}{dy}\right|_{y=1} = -is\overline{q}_1 - \overline{\overline{F}}_y(1),$$
$$\left.\frac{d\overline{\sigma}_{yy}(y)}{dy}\right|_{y=-1} = -is\overline{q}_2 - \overline{\overline{F}}_y(-1). \tag{2.4.8}$$

The system of governing equations used to determine the key functions $\overline{\sigma}(y)$ and $\overline{\sigma}_{yy}(y)$ in domain $\mathfrak{D}_2$ is presented by equations (2.2.25) and (2.2.26).

In view of conditions (2.4.7), a solution to equation (2.2.25) can be derived as follows:

$$\overline{\sigma}_{yy}(y) = -\overline{p}_2 \frac{\sinh s(1-y)}{\sinh 2s}$$
$$-\left(\overline{p}_1 + \frac{1}{s}\int_{-1}^{1}\left(is\overline{F}_x(y) - \frac{d\overline{F}_y(y)}{dy} - s^2\overline{\sigma}(y)\right)\sinh s(1-y)dy\right)$$
$$\times\frac{\sinh s(1+y)}{\sinh 2s}$$

$$+\frac{1}{s}\int_{-1}^{y}\left(is\overline{F}_x(\xi)-\frac{d\overline{F}_y(\xi)}{d\xi}-s^2\overline{\sigma}(\xi)\right)\sinh s(y-\xi)d\xi\,. \tag{2.4.9}$$

Substituting expression (2.4.9) into conditions (2.4.8) yields, after some algebra, the following integral conditions for total stress $\overline{\sigma}(y)$ in the mapping domain:

$$\int_{-1}^{1}\overline{\sigma}(y)\sinh sydy=Z_1,\quad \int_{-1}^{1}\overline{\sigma}(y)\cosh sydy=Z_2\ . \tag{2.4.10}$$

Here,

$$\begin{aligned}
Z_1=&-\frac{1}{s}\left(\overline{p}_1-\overline{p}_2\right)\cosh s+\frac{i}{s}\left(\overline{q}_1+\overline{q}_2\right)\sinh s\\
&+\frac{1}{s^2}\left(\overline{F}_y(1)+\overline{F}_y(-1)\right)\sinh s\\
&+\frac{1}{s^2}\int_{-1}^{1}\left(is\overline{F}_x(y)-\frac{d\overline{F}_y(y)}{dy}\right)\sinh sydy,
\end{aligned} \tag{2.4.11}$$

$$\begin{aligned}
Z_2=&-\frac{1}{s}\left(\overline{p}_1+\overline{p}_2\right)\sinh s+\frac{i}{s}\left(\overline{q}_1-\overline{q}_2\right)\cosh s\\
&+\frac{1}{s^2}\left(\overline{F}_y(1)-\overline{F}_y(-1)\right)\cosh s\\
&+\frac{1}{s^2}\int_{-1}^{1}\left(is\overline{F}_x(y)-\frac{d\overline{F}_y(y)}{dy}\right)\cosh sydy.
\end{aligned}$$

Using (2.4.10) and (2.4.11) yields the following equality:

$$\begin{aligned}
&\frac{1}{s}\int_{-1}^{1}\left(is\overline{F}_x(y)-\frac{d\overline{F}_y(y)}{dy}-s^2\overline{\sigma}(y)\right)\sinh s(1-y)dy\\
&=-\overline{p}_1+\overline{p}_2\cosh 2s+\left(i\overline{q}_2+\frac{\overline{F}_y(-1)}{s}\right)\sinh 2s\,.
\end{aligned} \tag{2.4.12}$$

In view of this, expression (2.4.9) can be simplified as follows:

$$\overline{\sigma}_{yy}(y) = -\overline{p}_2 \cosh s(1+y) - \left(i\overline{q}_2 + \frac{\overline{F}_y(-1)}{s} \right) \sinh s(1+y)$$

$$+\frac{1}{s}\int_{-1}^{y} \left(is\overline{F}_x(\xi) - \frac{d\overline{F}_y(\xi)}{d\xi} - s^2\overline{\sigma}(\xi) \right) \sinh s(y-\xi)d\xi. \qquad (2.4.13)$$

A solution to equation (2.2.26) for strip $\mathfrak{D}_2$ can be derived as follows:

$$\overline{\sigma}(y) = \frac{1}{a_{11}(y)} \Bigg[A\cosh sy + B\sinh sy - \alpha_1(y)\overline{T}(y)$$

$$-s\int_{-1}^{y} \left(\alpha_1(\xi) - \alpha_2(\xi)\right)\overline{T}(\xi)\sinh s(y-\xi)d\xi$$

$$+\left(2\beta_1(-1) - \frac{1}{G_{xy}(-1)} \right)$$

$$\times \left(\overline{p}_2 \cosh s(1+y) + \left(i\overline{q}_2 + \frac{\overline{F}_y(-1)}{s} \right) \sinh s(1+y) \right)$$

$$+\frac{1}{s}\int_{-1}^{y} \left(\beta_1(\xi) \left(\frac{d\overline{F}_y(\xi)}{d\xi} - is\overline{F}_x(\xi) \right) \right.$$

$$\left. - \frac{d}{d\xi}\left(\frac{\overline{F}_y(\xi)}{G_{xy}(\xi)} \right) \right) \sinh s(y-\xi)d\xi$$

$$+\left(2\beta_1(y) - \frac{1}{G_{xy}(y)} \right)\overline{\sigma}_{yy}(y)$$

$$+\int_{-1}^{y} \overline{\sigma}_{yy}(\xi) \left(\left(\frac{d^2\beta_1(\xi)}{d\xi^2} + s^2\beta_2(\xi) \right) \frac{\sinh s(y-\xi)}{s} \right.$$

$$-\frac{d}{d\xi}\left(\left(2\beta_1(\xi)-\frac{1}{G_{xy}(\xi)}\right)\cosh s(y-\xi)\right)\Bigg)d\xi\Bigg]. \qquad (2.4.14)$$

Here, A and B are arbitrary constants of integration. Substituting (2.4.13) into (2.4.14) yields the following integral equation:

$$\bar{\sigma}(y)=A\frac{\cosh sy}{a_{11}(y)}+B\frac{\sinh sy}{a_{11}(y)}+\bar{p}_2P(y)+is\bar{q}_2Q(y)$$

$$+\Theta(y)+\Psi(y)+\int_{-1}^{y}\bar{\sigma}(\xi)\mathcal{K}_{ST}(y,\xi)d\xi, \qquad (2.4.15)$$

where

$$\Theta(y)=-\frac{1}{a_{11}(y)}\Bigg(\alpha_1(y)\bar{T}(y)$$

$$+s\int_{-1}^{y}\left(\alpha_1(\xi)-\alpha_2(\xi)\right)\bar{T}(\xi)\sinh s(y-\xi)d\xi\Bigg),$$

$$P(y)=-\frac{1}{sa_{11}(y)}\int_{-1}^{y}\Bigg(\left(\frac{d^2\beta_1(\eta)}{d\eta^2}+s^2\beta_2(\eta)\right)$$

$$\times\sinh s(y-\eta)\cosh s(1+\eta)+s^2\left(2\beta_1(\eta)-\frac{1}{G_{xy}(\eta)}\right)$$

$$\times\cosh s(y-\eta)\sinh s(1+\eta)\Bigg)d\eta,$$

$$Q(y)=\frac{\bar{q}_2}{s^2a_{11}(y)}\Bigg(\left(2\beta_1(-1)-\frac{1}{G_{xy}(-1)}\right)s\sinh s(1+y)$$

$$-\int_{-1}^{y}\Bigg(\left(\frac{d^2\beta_1(\eta)}{d\eta^2}+s^2\beta_2(\eta)\right)\sinh s(y-\eta)\sinh s(1+\eta)$$

$$+\left(2\beta_1(\eta)-\frac{1}{G_{xy}(\eta)}\right)s^2\cosh s(y-\eta)\cosh s(y+1)\Bigg)d\eta\Bigg),$$

$$\Psi(y)=\frac{1}{sa_{11}(y)}\Bigg(sa_{11}(y)Q(y)\overline{F}_y(-1) \tag{2.4.16}$$

$$+\int_{-1}^{y}\left(\beta_1(\xi)\left(\frac{d\overline{F}_y(\xi)}{d\xi}-is\overline{F}_x(\xi)\right)-\frac{d}{d\xi}\left(\frac{\overline{F}_y(\xi)}{G_{xy}(\xi)}\right)\right)\sinh s(y-\xi)d\xi$$

$$+\left(2\beta_1(y)-\frac{1}{G_{xy}(y)}\right)\int_{-1}^{y}\left(is\overline{F}_x(\xi)-\frac{d\overline{F}_y(\xi)}{d\xi}\right)\sinh s(y-\xi)d\xi$$

$$+\int_{-1}^{y}\int_{-1}^{\eta}\left(is\overline{F}_x(\xi)-\frac{d\overline{F}_y(\xi)}{d\xi}\right)\sinh s(\eta-\xi)d\xi\varphi(y,\eta)d\eta\Bigg),$$

$$\mathcal{K}_{\mathrm{ST}}(y,\xi)=-\frac{s}{a_{11}(y)}\Bigg(\left(2\beta_1(y)-\frac{1}{G_{xy}(y)}\right)\sinh s(y-\xi)$$

$$+\int_{\xi}^{y}\varphi(y,\eta)\sinh s(\eta-\xi)d\eta\Bigg), \tag{2.4.17}$$

$$\varphi(y,\eta)=\left(\frac{d^2\beta_1(\eta)}{d\eta^2}+s^2\beta_2(\eta)\right)\frac{\sinh s(y-\eta)}{s}$$

$$-\frac{d}{d\eta}\left(\left(2\beta_1(\eta)-\frac{1}{G_{xy}(\eta)}\right)\cosh s(y-\eta)\right).$$

Note that the expression for $\varphi(y,\eta)$ resembles the expression for $\gamma_{\mathrm{PL}}(y,\eta)$ given in (2.2.31) for the orthotropic inhomogeneous plane $\mathfrak{D}_1$, which was also used for the half-plane in (2.3.13). A resolvent-kernel solution to integral equation (2.4.15) is as follows:

$$\overline{\sigma}(y)=Af_A(y)+Bf_B(y)+\Phi(y)\,. \tag{2.4.18}$$

Here,

$$f_A(y)=\frac{\cosh sy}{a_{11}(y)}+\int_{-1}^{y}\frac{\cosh s\xi}{a_{11}(\xi)}\mathcal{R}_{\mathrm{ST}}(y,\xi)d\xi,$$

$$f_B(y)=\frac{\sinh sy}{a_{11}(y)}+\int_{-1}^{y}\frac{\sinh s\xi}{a_{11}(\xi)}\mathcal{R}_{\mathrm{ST}}(y,\xi)d\xi, \tag{2.4.19}$$

$$\Phi(y)=\overline{p}_2\left(P(y)+\int_{-1}^{y}P(\xi)\mathcal{R}_{\mathrm{ST}}(y,\xi)d\xi\right)$$

$$+is\overline{q}_2\left(Q(y)+\int_{-1}^{y}Q(\xi)\mathcal{R}_{\mathrm{ST}}(y,\xi)d\xi\right)$$

$$+\Theta(y)+\Psi(y)+\int_{-1}^{y}(\Theta(\xi)+\Psi(\xi))\mathcal{R}_{\mathrm{ST}}(y,\xi)d\xi, \tag{2.4.20}$$

$$A=\frac{F_1I_{22}-F_2I_{12}}{I_{11}I_{22}-I_{12}I_{21}},\qquad B=\frac{F_2I_{11}-F_1I_{21}}{I_{11}I_{22}-I_{12}I_{21}},$$

$$F_1=Z_1-\int_{-1}^{1}\Phi(y)\sinh sydy,\qquad F_2=Z_2-\int_{-1}^{1}\Phi(y)\cosh sydy,$$

$$I_{11}=\int_{-1}^{1}f_A(y)\sinh sydy,\quad I_{21}=\int_{-1}^{1}f_A(y)\cosh sydy,$$

$$I_{12}=\int_{-1}^{1}f_B(y)\sinh sydy,\quad I_{22}=\int_{-1}^{1}f_B(y)\cosh sydy, \tag{2.4.21}$$

and

$$\mathcal{R}_{\mathrm{ST}}(y,\xi)=\sum_{n=0}^{\infty}\mathcal{K}_{n+1}^{\mathrm{ST}}(y,\xi) \tag{2.4.22}$$

is the resolvent kernel, which can be computed as a series of the recurring kernels

$$\mathcal{K}_1^{\mathrm{ST}}(y,\xi)=\mathcal{K}_{\mathrm{ST}}(y,\xi),$$
$$\mathcal{K}_{n+1}^{\mathrm{ST}}(y,\xi)=\int_{\xi}^{y}\mathcal{K}_1^{\mathrm{ST}}(y,t)\mathcal{K}_n^{\mathrm{ST}}(t,\xi)dt,\quad n=1,2,... \tag{2.4.23}$$

For practical computations, the series (2.4.22) can be truncated so that the resolvent-kernel can be approximated with the following finite sum:

$$\mathcal{R}_{\mathrm{ST}}(y,\xi)\approx\mathcal{R}_{\mathrm{ST}}^{N}(y,\xi)=\sum_{n=0}^{N}\mathcal{K}_{n+1}^{\mathrm{ST}}(y,\xi), \tag{2.4.24}$$

where N is a natural digit allowing for the satisfaction of equation (2.4.15) with expression (2.4.18), where resolvent kernel (2.4.22) is substituted with the approximate formula (2.4.24).

In view of the formulae (2.4.19) – (2.4.21), the solution (2.4.18) can be rewritten as follows:

$$\overline{\sigma}(y)=\overline{p}_1P_1(y)+\overline{p}_2P_2(y)$$
$$+is\left(\overline{q}_1Q_1(y)+\overline{q}_2Q_2(y)\right)+\Theta_{\mathrm{ST}}(y)+\Psi_{\mathrm{ST}}(y). \tag{2.4.25}$$

Here,

$$P_1(y)=\frac{1}{s}\chi_{11}(y,1),$$

$$P_2(y)=\frac{1}{s}\chi_{12}(y,1)+P^*(y)-\int_{-1}^{1}P^*(\xi)\chi_{21}(y,\xi)d\xi,$$

$$Q_1(y)=\frac{1}{s^2}\chi_{21}(y,1),$$

$$Q_2(y)=\frac{1}{s^2}\chi_{22}(y,1)+Q^*(y)-\int_{-1}^{1}Q^*(\xi)\chi_{21}(y,\xi)d\xi,$$

$$\Theta_{\mathrm{ST}}(y)=\Theta^{*}(y)-\int_{-1}^{1}\Theta^{*}(\xi)\chi_{21}(y,\xi)d\xi,$$

$$\Psi_{\mathrm{ST}}(y)=\frac{1}{s^{2}}\left(\overline{F}_{y}(1)\chi_{21}(y,1)+\overline{F}_{y}(-1)\chi_{22}(y,1)\right)+\Psi^{*}(y)$$

$$+\int_{-1}^{1}\left(\frac{1}{s}\overline{F}_{x}(\xi)-\frac{1}{s^{2}}\frac{d\overline{F}_{y}(\xi)}{d\xi}-\Psi^{*}(\xi)\right)\chi_{21}(y,\xi)d\xi,$$

$$P^{*}(y)=P(y)+\int_{-1}^{y}P(\xi)\,\mathcal{R}_{\mathrm{ST}}(y,\xi)d\xi,$$

$$Q^{*}(y)=Q(y)+\int_{-1}^{y}Q(\xi)\,\mathcal{R}_{\mathrm{ST}}(y,\xi)d\xi,$$

$$\Theta^{*}(y)=\Theta(y)+\int_{-1}^{y}\Theta(\xi)\,\mathcal{R}_{\mathrm{ST}}(y,\xi)d\xi,$$

$$\Psi^{*}(y)=\Psi(y)+\int_{-1}^{y}\Psi(\xi)\,\mathcal{R}_{\mathrm{ST}}(y,\xi)d\xi,$$

$$\chi_{1n}(y,\xi)=\left(\mu_{12}f_{A}(y)-\mu_{11}f_{B}(y)\right)\sinh s\xi$$

$$+(-1)^{n}\left(\mu_{22}f_{A}(y)-\mu_{21}f_{B}(y)\right)\cosh s\xi,$$

$$\chi_{2n}(y,\xi)=\left(\mu_{22}f_{A}(y)-\mu_{21}f_{B}(y)\right)\sinh s\xi$$

$$+(-1)^{n}\left(\mu_{12}f_{A}(y)-\mu_{11}f_{B}(y)\right)\cosh s\xi,$$

$$\mu_{nm}=\frac{I_{nm}}{I_{11}I_{22}-I_{21}I_{12}},\quad n,m=1,2. \tag{2.4.26}$$

Solution (2.4.25) explicitly expresses the total stress in terms of the force and thermal loadings. Substituting it into (2.4.13) yields the following expression for the mapping of normal stress $\overline{\sigma}_{yy}(y)$:

$$\overline{\sigma}_{yy}(y) = \overline{p}_1 P_1^y(y) + \overline{p}_2 P_2^y(y)$$

$$+is\left(\overline{q}_1 Q_1^y(y) + \overline{q}_2 Q_2^y(y)\right) + \Theta_{\mathrm{ST}}^y(y) + \Psi_{\mathrm{ST}}^y(y). \qquad (2.4.27)$$

Here,

$$P_1^y(y) = -s\int_{-1}^{y} P_1(\xi)\sinh s(y-\xi)d\xi,$$

$$P_2^y(y) = -\cosh s(1+y) - s\int_{-1}^{y} P_2(\xi)\sinh s(y-\xi)d\xi,$$

$$Q_1^y(y) = -s\int_{-1}^{y} Q_1(\xi)\sinh s(y-\xi)d\xi,$$

$$Q_2^y(y) = -\frac{\sinh s(1+y)}{s} - s\int_{-1}^{y} Q_2(\xi)\sinh s(y-\xi)d\xi,$$

$$\Theta_{\mathrm{ST}}^y(y) = -s\int_{-1}^{y} \Theta_{\mathrm{ST}}(\xi)\sinh s(y-\xi)d\xi,$$

$$\Psi_{\mathrm{ST}}^y(y) = -\overline{F}_y(-1)\frac{\sinh s(1+y)}{s}$$

$$+\frac{1}{s}\int_{-1}^{y}\left(is\overline{F}_x(\xi) - \frac{d\overline{F}_y(\xi)}{d\xi} - s^2\Psi_{\mathrm{ST}}(\xi)\right)\sinh s(y-\xi)d\xi. \qquad (2.4.28)$$

Using (2.2.39) and (2.2.41) in view of (2.4.25) and (2.4.27) yields equations for $\overline{\sigma}_{xx}$ and $\overline{\sigma}_{xy}$:

$$\overline{\sigma}_{xx}(y) = \overline{p}_1 P_1^x(y) + \overline{p}_2 P_2^x(y)$$

$$+is\left(\overline{q}_1 Q_1^x(y) + \overline{q}_2 Q_2^x(y)\right) + \Theta_{\mathrm{ST}}^x(y) + \Psi_{\mathrm{ST}}^x(y), \qquad (2.4.29)$$

$$\overline{\sigma}_{xy}(y) = \overline{p}_1 P_1^{xy}(y) + \overline{p}_2 P_2^{xy}(y)$$

$$+is\left(\overline{q}_1 Q_1^{xy}(y) + \overline{q}_2 Q_2^{xy}(y)\right) + \Theta_{\mathrm{ST}}^{xy}(y) + \Psi_{\mathrm{ST}}^{xy}(y)\,. \qquad (2.4.30)$$

where

$$P_1^x(y) = P_1(y) + s\int_{-1}^{y} P_1(\xi)\sinh s(y-\xi)d\xi,$$

$$P_2^x(y) = P_2(y) + \cosh s(1+y) + s\int_{-1}^{y} P_2(\xi)\sinh s(y-\xi)d\xi,$$

$$Q_1^x(y) = Q_1(y) + s\int_{-1}^{y} Q_1(\xi)\sinh s(y-\xi)d\xi,$$

$$Q_2^y(y) = Q_2(y) + \frac{\sinh s(1+y)}{s} + s\int_{-1}^{y} Q_2(\xi)\sinh s(y-\xi)d\xi,$$

$$\Theta_{\mathrm{ST}}^x(y) = \Theta_{\mathrm{ST}}(y) + s\int_{-1}^{y} \Theta_{\mathrm{ST}}(\xi)\sinh s(y-\xi)d\xi,$$

$$\Psi_{\mathrm{ST}}^x(y) = \Psi_{\mathrm{ST}}(y) + \overline{F}_y(-1)\frac{\sinh s(1+y)}{s}$$

$$-\frac{1}{s}\int_{-1}^{y}\left(is\overline{F}_x(\xi) - \frac{d\overline{F}_y(\xi)}{d\xi} - s^2\Psi_{\mathrm{ST}}(\xi)\right)\sinh s(y-\xi)d\xi\,,$$

$$P_1^{xy}(y) = -is\int_{-1}^{y} P_1(\xi)\cosh s(y-\xi)d\xi,$$

$$P_2^{xy}(y) = -i\sinh s(1+y) - is\int_{-1}^{y} P_2(\xi)\cosh s(y-\xi)d\xi, \qquad (2.4.31)$$

$$Q_1^{xy}(y) = -is\int_{-1}^{y} Q_1(\xi)\cosh s(y-\xi)d\xi,$$

$$Q_2^{xy}(y) = -\frac{i}{s}\cosh s(1+y) - is\int_{-1}^{y} Q_2(\xi)\cosh s(y-\xi)d\xi,$$

$$\Theta_{\mathrm{ST}}^{xy}(y) = -is\int_{-1}^{y} \Theta_{\mathrm{ST}}(\xi)\cosh s(y-\xi)d\xi,$$

$$\Psi_{\mathrm{ST}}^{xy}(y) = \frac{i}{s}\overline{F}_y(y) - \frac{i}{s}\overline{F}_y(-1)\cosh s(1+y)$$

$$-\int_{-1}^{y}\left(\overline{F}_x(\xi) + \frac{i}{s}\frac{d\overline{F}_y(\xi)}{d\xi} + is\Psi_{\mathrm{ST}}(\xi)\right)\cosh s(y-\xi)d\xi.$$

After deriving the stresses in the mapping domain of transform (2.2.24), they can be restored in the physical domain by applying the inverse transform (2.2.43) to the expressions (2.4.27), (2.4.29), and (2.4.30).

2.4.2. Determination of elastic displacements under displacement- and mixed-type boundary conditions

Consider the situation where the following displacements

$$\begin{aligned} &u_x(x,1) = u_1(x), \quad u_x(x,-1) = u_2(x), \\ &u_y(x,1) = v_1(x), \quad u_y(x,-1) = v_2(x) \end{aligned} \tag{2.4.32}$$

pertain to the boundary of inhomogeneous orthotropic strip $\mathfrak{D}_2$, where $u_n(x)$ and $v_n(x)$ are given and vanish as $|x| \to +\infty$, $n = 1,2$.

With conditions (2.4.32) in mind, the first and second Cauchy equations (2.1.18) yield the following expressions for components of the displacement vector:

$$u_x(x,y)=\frac{1}{2}\int_{-\infty}^{+\infty}\varepsilon_{xx}(\xi,y)\,\mathrm{sgn}(x-\xi)d\xi,$$

$$u_y(x,y)=\frac{1}{2}\big(v_1(x)+v_2(x)\big) \tag{2.4.33}$$

$$+\frac{1}{2}\int_{-1}^{1}\varepsilon_{yy}(x,\eta)\,\mathrm{sgn}(y-\eta)d\eta.$$

Under the assumption that the boundary displacements vanish as $|x|\to+\infty$, the first equation of (2.4.33) as $|x|\to\infty$ yields the following integral condition

$$\int_{-\infty}^{+\infty}\varepsilon_{xx}(x,y)dx=0 \tag{2.4.34}$$

of self-balancing normal strain $\varepsilon_{xx}(x,y)$. Putting $y=\pm1$ into the second equation of (2.4.33) in view of (2.4.32) makes it possible to derive the following condition, which implies that the resulting strain is equal the difference between vertical boundary displacements:

$$\int_{-1}^{1}\varepsilon_{yy}(x,y)dy=v_1(x)-v_2(x)\,. \tag{2.4.35}$$

Substituting expressions (2.4.33) into the third Cauchy equation of (2.1.18), we obtain the following compatibility equation:

$$2\varepsilon_{xy}(x,y)-\frac{d}{dx}\big(v_1(x)+v_2(x)\big)$$

$$=\int_{-\infty}^{+\infty}\frac{\partial\varepsilon_{xx}(\xi,y)}{\partial y}\,\mathrm{sgn}(x-\xi)d\xi$$

$$+\int_{-1}^{1}\frac{\partial\varepsilon_{yy}(x,\eta)}{\partial x}\,\mathrm{sgn}(y-\eta)d\eta\,. \tag{2.4.36}$$

Applying derivative $\partial^2 / \partial x \partial y$ to equation (2.4.36) reduces it to the classical strain compatibility equation (2.1.19). Conversely, deriving equation (2.4.36) from (2.1.19) requires that the following necessary condition be fulfilled:

$$\varepsilon_{xy}(x,1) + \varepsilon_{xy}(x,-1) - \frac{d}{dx}\big(v_1(x) + v_2(x)\big)$$

$$= \frac{1}{2}\int_{-\infty}^{+\infty}\left(\frac{\partial \varepsilon_{xx}(\xi,1)}{\partial y} + \frac{\partial \varepsilon_{xx}(\xi,-1)}{\partial y}\right)\operatorname{sgn}(x-\xi)d\xi\,. \qquad (2.4.37)$$

Condition (2.4.37) was derived by integrating equation (2.1.19) over x and y, and comparing the result with (2.4.36). The same condition can also be obtained by fulfilling (2.4.36) for the boundaries $y = \pm 1$ of half-plane $\mathfrak{D}_2$ under the conditions (2.4.32) and (2.4.35) in mind:

$$\varepsilon_{xy}(x,1) - \frac{dv_1(x)}{dx} = \frac{1}{2}\int_{-\infty}^{+\infty}\frac{\partial \varepsilon_{xx}(\xi,1)}{\partial y}\operatorname{sgn}(x-\xi)d\xi,$$

$$\varepsilon_{xy}(x,-1) - \frac{dv_2(x)}{dx} = \frac{1}{2}\int_{-\infty}^{+\infty}\frac{\partial \varepsilon_{xx}(\xi,-1)}{\partial y}\operatorname{sgn}(x-\xi)d\xi. \qquad (2.4.38)$$

In the mapping domain of the Fourier transform (2.2.24), the expressions in (2.4.33) take the following form:

$$\overline{u}_x(y) = -\frac{i}{s}\overline{\varepsilon}_{xx}(y),$$

$$\overline{u}_y(y) = \frac{1}{2}\big(\overline{v}_1 + \overline{v}_2\big) + \frac{1}{2}\int_{-1}^{1}\overline{\varepsilon}_{yy}(\eta)\operatorname{sgn}(y-\eta)d\eta. \qquad (2.4.39)$$

Note that implementing the condition (2.4.35) means that the second equation of (2.4.39) can be represented in two alternative forms:

$$\overline{u}_y(y) = \overline{v}_1 + \frac{1}{2}\int_{-1}^{1}\overline{\varepsilon}_{yy}(\eta)\big(\operatorname{sgn}(y-\eta) - 1\big)d\eta \qquad (2.4.40)$$

or

$$\overline{u}_y(y) = \overline{v}_2 + \frac{1}{2}\int_{-1}^{1} \overline{\varepsilon}_{yy}(\eta)\big(\operatorname{sgn}(y-\eta)+1\big)\,d\eta\,. \qquad (2.4.41)$$

Using the first equation in (2.4.39) in conjunction with the equation (2.1.23) for the strain-tensor component $\overline{\varepsilon}_{xx}$ represented in terms of the stresses (2.4.25) and (2.4.27), we obtain the following equation for displacement $\overline{u}_x(y)$:

$$\overline{u}_x(y) = \overline{p}_1 P_1^{[x]}(y) + \overline{p}_2 P_2^{[x]}(y)$$

$$+is\Big(\overline{q}_1 Q_1^{[x]}(y) + \overline{q}_2 Q_2^{[x]}(y)\Big) + \Theta_{\mathrm{ST}}^{[x]}(y) + \Psi_{\mathrm{ST}}^{[x]}(y)\,, \qquad (2.4.42)$$

where

$$P_n^{[x]}(y) = \frac{i}{s}\Big(\big(a_{11}(y)-a_{12}(y)\big)P_n^y(y) - a_{11}(y)P_n(y)\Big),$$

$$Q_n^{[x]}(y) = \frac{i}{s}\Big(\big(a_{11}(y)-a_{12}(y)\big)Q_n^y(y)$$

$$-a_{11}(y)Q_n(y)\Big), \quad n=1,2\,,$$

$$\Theta_{\mathrm{ST}}^{[x]}(y) = \frac{i}{s}\Big(\big(a_{11}(y)-a_{12}(y)\big)\Theta_{\mathrm{ST}}^y(y)$$

$$-a_{11}(y)\Theta_{\mathrm{ST}}(y) - \alpha_1(y)\overline{T}(y)\Big),$$

$$\Psi_{\mathrm{ST}}^{[x]}(y) = \frac{i}{s}\Big(\big(a_{11}(y)-a_{12}(y)\big)\Psi_{\mathrm{ST}}^y(y) - a_{11}(y)\Psi_{\mathrm{ST}}(y)\Big). \qquad (2.4.43)$$

Horizontal (in parallel to the sides $y=\pm 1$) displacement $\overline{u}_x(y)$ is represented by (2.4.42) in terms of the applied force loadings (2.4.1), body forces, and the temperature field in the mapping domain of the transform (2.2.24). In deriving a similar expression for vertical displacement $\overline{u}_y(y)$, it is important to eliminate boundary displacements $\overline{v}_1$ and $\overline{v}_2$ from the second equation of (2.4.39).

To determine the boundary displacements in terms of the force and thermal loadings, we can employ the necessary conditions (2.4.38), which take the following form in the mapping domain of the transform given in (2.2.24):

$$\begin{aligned}\overline{v}_1 &= \frac{1}{s^2}\frac{d\overline{\varepsilon}_{xx}(y)}{dy}\bigg|_{y=1} - \frac{i}{s}\overline{\varepsilon}_{xy}(1),\\ \overline{v}_2 &= \frac{1}{s^2}\frac{d\overline{\varepsilon}_{xx}(y)}{dy}\bigg|_{y=-1} - \frac{i}{s}\overline{\varepsilon}_{xy}(-1).\end{aligned} \tag{2.4.44}$$

In view of the constitutive equations (2.1.23) and conditions (2.4.7) and (2.4.8), we derive the following:

$$\begin{aligned}&\overline{\varepsilon}_{xy}(1) = \frac{\overline{q}_1}{G_{xy}(1)}, \quad \overline{\varepsilon}_{xy}(-1) = \frac{\overline{q}_2}{G_{xy}(-1)},\\ &\frac{d\overline{\varepsilon}_{xx}(y)}{dy}\bigg|_{y=1} = \frac{d}{dy}\left(a_{11}(y)\overline{\sigma}(y) + \alpha_1(y)\overline{T}(y)\right)\Big|_{y=1}\\ &\qquad + \overline{p}_1\frac{d}{dy}\left(a_{11}(y) - a_{12}(y)\right)\Big|_{y=1}\\ &\qquad + \left(a_{11}(1) - a_{12}(1)\right)\left(is\overline{q}_1 + \overline{F}_y(1)\right),\\ &\frac{d\overline{\varepsilon}_{xx}(y)}{dy}\bigg|_{y=-1} = \frac{d}{dy}\left(a_{11}(y)\overline{\sigma}(y) + \alpha_1(y)\overline{T}(y)\right)\Big|_{y=-1}\\ &\qquad + \overline{p}_2\frac{d}{dy}\left(a_{11}(y) - a_{12}(y)\right)\Big|_{y=-1}\\ &\qquad + \left(a_{11}(-1) - a_{12}(-1)\right)\left(is\overline{q}_2 + \overline{F}_y(-1)\right).\end{aligned} \tag{2.4.45}$$

In view of expressions (2.4.45), the boundary displacements can be derived from (2.4.44) in the following form:

$$\overline{v}_n = c_{n1}\overline{p}_1 + c_{n2}\overline{p}_2 + is\left(d_{n1}\overline{q}_1 + d_{n2}\overline{q}_2\right)$$

$$+t_n+\varphi_n,\quad n=1,2, \tag{2.4.46}$$

where

$$c_{11}=\frac{1}{s^2}\frac{d}{dy}\left(\left(1+P_1(y)\right)a_{11}(y)-a_{12}(y)\right)\Big|_{y=1},$$

$$c_{12}=\frac{1}{s^2}\frac{d}{dy}\left(a_{11}(y)P_2(y)\right)\Big|_{y=1},$$

$$c_{21}=\frac{1}{s^2}\frac{d}{dy}\left(a_{11}(y)P_1(y)\right)\Big|_{y=-1},$$

$$c_{22}=\frac{1}{s^2}\frac{d}{dy}\left(\left(1+P_2(y)\right)a_{11}(y)-a_{12}(y)\right)\Big|_{y=-1},$$

$$d_{11}=\frac{1}{s^2}\left(\frac{d}{dy}\left(a_{11}(y)Q_1(y)\right)\right.$$

$$\left.-\frac{1}{G_{xy}(y)}-a_{12}(y)+a_{11}(y)\right)\Big|_{y=1},$$

$$d_{22}=\frac{1}{s^2}\left(\frac{d}{dy}\left(a_{11}(y)Q_2(y)\right)\right.$$

$$\left.-\frac{1}{G_{xy}(y)}-a_{12}(y)+a_{11}(y)\right)\Big|_{y=-1},$$

$$d_{12}=\frac{1}{s^2}\frac{d}{dy}\left(a_{11}(y)Q_2(y)\right)\Big|_{y=1},$$

$$d_{21}=\frac{1}{s^2}\frac{d}{dy}\left(a_{11}(y)Q_1(y)\right)\Big|_{y=-1},$$

$$t_n=\frac{1}{s^2}\frac{d}{dy}\left(a_{11}(y)\Theta_{\mathrm{ST}}(y)+\alpha_1(y)\overline{T}(y)\right)\Big|_{y=(-1)^{n+1}},$$

$$\varphi_n = \frac{1}{s^2}\left(\frac{d}{dy}\left(a_{11}(y)\Psi_{\mathrm{ST}}(y)\right) \right.$$

$$\left. + \left(a_{11}(y) - a_{12}(y)\right)\overline{F}_y(y) \right)\Big|_{y=(-1)^{n+1}}. \qquad (2.4.47)$$

Now, using expressions (2.4.46) in conjunction with the second equation of (2.4.39) yields the following expression for displacement $\overline{u}_y(y)$:

$$\overline{u}_y(y) = \overline{p}_1 P_1^{[y]}(y) + \overline{p}_2 P_2^{[y]}(y)$$

$$+is\left(\overline{q}_1 Q_1^{[y]}(y) + \overline{q}_2 Q_2^{[y]}(y)\right) + \Theta_{\mathrm{ST}}^{[y]}(y) + \Psi_{\mathrm{ST}}^{[y]}(y). \qquad (2.4.48)$$

Here,

$$P_n^{[y]}(y) = \frac{1}{2}\left(c_{1n} + c_{2n} \right.$$

$$\left. + \int_{-1}^{1} \left(a_{21}(\eta)P_n(\eta) + \left(a_{22}(\eta) - a_{21}(\eta)\right)P_n^y(\eta)\right)\mathrm{sgn}(y-\eta)d\eta \right),$$

$$Q_n^{[y]}(y) = \frac{1}{2}\left(d_{1n} + d_{2n} \right.$$

$$\left. + \int_{-1}^{1} \left(a_{21}(\eta)Q_n(\eta) + \left(a_{22}(\eta) - a_{21}(\eta)\right)Q_n^y(\eta)\right)\mathrm{sgn}(y-\eta)d\eta \right),$$

$$\Theta_{\mathrm{ST}}^{[y]}(y) = \frac{1}{2}\left(t_1 + t_2 + \int_{-1}^{1} \left(a_{21}(\eta)\Theta_{\mathrm{ST}}(\eta) \right.\right.$$

$$\left.\left. + \left(a_{22}(\eta) - a_{21}(\eta)\right)\Theta_{\mathrm{ST}}^y(\eta) + \alpha_2(\eta)\overline{T}(\eta) \right)\mathrm{sgn}(y-\eta)d\eta \right),$$

$$\Psi_{\mathrm{ST}}^{[y]}(y)=\frac{1}{2}\Bigg(\varphi_1+\varphi_2+\int_{-1}^{1}\big(a_{21}(\eta)\Psi_{\mathrm{ST}}(\eta)$$

$$+\big(a_{22}(\eta)-a_{21}(\eta)\big)\Psi_{\mathrm{ST}}^{y}(\eta)\Bigg)\operatorname{sgn}(y-\eta)d\eta\Bigg). \qquad (2.4.49)$$

Using formula (2.4.48), we can determine vertical displacement $\overline{u}_y(y)$ via the force loading applied to the sides of strip $\mathfrak{D}_2$, as well as the body forces and temperature field within the interior of the strip. If the boundary of the strip is exposed to the boundary conditions in terms of displacements (2.4.32), then formula (2.4.46) can be used with the following equation:

$$\overline{u}_n=c_{n1}^{*}\overline{p}_1+c_{n2}^{*}\overline{p}_2+is\left(d_{n1}^{*}\overline{q}_1+d_{n2}^{*}\overline{q}_2\right)+t_n^{*}+\varphi_n^{*},\ n=1,2 \quad (2.4.50)$$

to determine the unknown boundary tractions $\overline{p}_n$ and $\overline{q}_n$, $n=1,2$, using the given boundary displacements $\overline{u}_n$ and $\overline{v}_n$. Formula (2.4.50) follows from (2.4.42) at $y=\pm1$, where

$$c_{nm}^{*}=P_m^{[x]}(-(-1)^n),\quad d_{nm}^{*}=Q_m^{[x]}(-(-1)^n),$$

$$t_n^{*}=\Theta_{\mathrm{ST}}^{[x]}(-(-1)^n),\qquad \varphi_n^{*}=\Psi_{\mathrm{ST}}^{[x]}(-(-1)^n),\quad n,m=1,2. \quad (2.4.51)$$

A similar strategy can be used for the case of mixed boundary conditions on sides $y=\pm1$ of strip $\mathfrak{D}_2$. If, for example, the sides $y=\pm1$ of the strip are under conditions of sliding support, then the following conditions hold:

$$\overline{q}_1=\overline{q}_2=\overline{v}_1=\overline{v}_2=0, \qquad (2.4.52)$$

while $\overline{p}_1$, $\overline{p}_2$ and $\overline{u}_1$, $\overline{u}_2$ remain unknown. In order to use formulae (2.4.27), (2.4.29), and (2.4.30) for the stress determination and (2.4.42) and (2.4.48) for displacements, one needs to evaluate the boundary tractions $\overline{p}_1$ and $\overline{p}_2$ in view of conditions (2.4.52). Making use of equation (2.4.42) along with (2.4.52) yield

$$\overline{p}_1 = \frac{(t_2 + \varphi_2)c_{12} - (t_1 + \varphi_1)c_{22}}{c_{11}c_{22} - c_{12}c_{21}},$$
$$\overline{p}_2 = \frac{(t_1 + \varphi_1)c_{21} - (t_2 + \varphi_2)c_{11}}{c_{11}c_{22} - c_{12}c_{21}}. \tag{2.4.53}$$

Now, the normal boundary tractions (2.4.53) can be used together with the shear ones given in (2.4.52) to evaluate the stresses and displacements in orthotropic inhomogeneous strip $\mathfrak{D}_2$.

2.4.3. Steady-state temperature field

Consider the problem on the determination of steady-state temperature $T = T(x, y)$ in strip $\mathfrak{D}_2$ due to inner heat sources of density $w(x, y)$ and the following generalized thermal conditions on sides $y = \pm 1$:

$$\ell_{11}T(x,1) + \ell_{12}\left.\frac{\partial T(x,y)}{\partial y}\right|_{y=1} = T_1(x),$$
$$\ell_{21}T(x,-1) + \ell_{22}\left.\frac{\partial T(x,y)}{\partial y}\right|_{y=-1} = T_2(x), \tag{2.4.54}$$

where $T_n(x)$ is given and constants ℓ_{nm}, $n, m = 1, 2$, define the type of boundary condition (similar to (2.3.65) in Section 2.3.5).

To derive the integral balance conditions, we introduce the heat fluxes (2.2.49) and represent the heat conduction equation in the form (2.2.50). Let us assume that

$$\lim_{x^2 \to +\infty} \Phi_x(x, y) = 0. \tag{2.4.55}$$

We integrate (2.2.50) over x from $-\infty$ to $+\infty$, which brings us to formula (2.3.69). Integrating (2.3.69) over y yields

$$\int_{-\infty}^{+\infty} \Phi_y(x, y)dx = \frac{1}{2}\int_{-\infty}^{+\infty} \left(\Phi_y(x,1) + \Phi_y(x,-1)\right)dx$$

$$-\frac{1}{2}\iint\limits_{\mathfrak{D}_2} w(x,\eta)\,\mathrm{sgn}(y-\eta)\,dx\,d\eta\,. \tag{2.4.56}$$

At $y=\pm 1$, the following integral condition can be derived from (2.4.56):

$$\iint\limits_{\mathfrak{D}_2} w(x,y)\,dx\,dy = -\int\limits_{-\infty}^{+\infty}\Big(\Phi_y(x,1)-\Phi_y(x,-1)\Big)\,dx\,. \tag{2.4.57}$$

This condition implies the action resulting from the inner heat sources within domain $\mathfrak{D}_2$ is equal to the difference between the resulting heat fluxes through sides $y=\pm 1$.

Integrating (2.3.56) over y from -1 to 1 allows us to derive the following condition for the resultant of the vertical heat flux over the entire domain $\mathfrak{D}_2$:

$$\iint\limits_{\mathfrak{D}_2}\Phi_y(x,y)\,dx\,dy = \int\limits_{-\infty}^{+\infty}\Big(\Phi_y(x,1)+\Phi_y(x,-1)\Big)\,dx + \iint\limits_{\mathfrak{D}_2} y\,w(x,y)\,dx\,dy\,. \tag{2.4.58}$$

Combining formulae (2.4.57) and (2.4.58) yields the following:

$$\begin{aligned}\int\limits_{-\infty}^{+\infty}\Phi_y(x,1)\,dx &= \frac{1}{2}\iint\limits_{\mathfrak{D}_2}\Big(\Phi_y(x,y)-w(x,y)(1+y)\Big)\,dx\,dy,\\ \int\limits_{-\infty}^{+\infty}\Phi_y(x,-1)\,dx &= \frac{1}{2}\iint\limits_{\mathfrak{D}_2}\Big(\Phi_y(x,y)+w(x,y)(1-y)\Big)\,dx\,dy.\end{aligned} \tag{2.4.59}$$

Similarly, integrating (2.2.50) over y from -1 to 1 yields the following:

$$\frac{d}{dx}\int\limits_{-1}^{1}\Phi_x(x,y)\,dy+\Phi_y(x,1)-\Phi_y(x,-1) = -\int\limits_{-1}^{1} w(x,y)\,dy\,. \tag{2.4.60}$$

After integrating this over x, we obtain the following formula:

$$\int_{-1}^{1} \Phi_x(x,y)dy = A$$

$$-\frac{1}{2}\int_{-\infty}^{+\infty} \Big(\Phi_y(\xi,1) - \Phi_y(\xi,-1)\Big)\operatorname{sgn}(x-\xi)d\xi$$

$$-\frac{1}{2}\iint_{\mathfrak{D}_2} w(\xi,y)\operatorname{sgn}(x-\xi)d\xi dy\,, \tag{2.4.61}$$

where A is a constant of integration. If we let $x \to \pm\infty$ in (2.4.61), we derive the following conditions:

$$A = \frac{1}{2}\lim_{x\to+\infty}\int_{-1}^{1} \Phi_x(x,y)dy + \frac{1}{2}\lim_{x\to-\infty}\int_{-1}^{1} \Phi_x(x,y)dy\,, \tag{2.4.62}$$

$$\int_{-\infty}^{+\infty} \Big(\Phi_y(x,-1) - \Phi_y(x,1)\Big)dx - \iint_{\mathfrak{D}_2} w(x,y)dxdy$$

$$= \lim_{x\to+\infty}\int_{-1}^{1} \Phi_x(x,y)dy - \lim_{x\to-\infty}\int_{-1}^{1} \Phi_x(x,y)dy\,. \tag{2.4.63}$$

Integrating (2.4.61) over x from L_1 to $L_2 \gg L_1$ yields

$$\int_{-1}^{1}\int_{L_1}^{L_2} \Phi_x(x,y)dxdy = (L_2 - L_1)A$$

$$+\int_{-\infty}^{\infty} x\Big(\Phi_y(x,1) - \Phi_y(x,-1)\Big)dx + \iint_{\mathfrak{D}_2} xw(x,y)dxdy$$

$$+\frac{L_1+L_2}{2}\int_{-\infty}^{\infty}\left(\Phi_y(x,-1) - \Phi_y(x,1) - \int_{-1}^{1} w(x,y)dy\right)dx\,. \tag{2.4.64}$$

Since L_1 and L_2 respectively tend toward $-\infty$ and $+\infty$ independently, formula (2.4.64) implies that $A = 0$ and formula (2.4.57) holds. Under the conditions (2.4.60) and (2.4.61), we can conclude that

$$\lim_{x \to \pm\infty} \int_{-1}^{1} \Phi_x(x, y)dy = 0 . \tag{2.4.65}$$

Then (2.4.64) yields the following thermal balance condition:

$$\int_{-\infty}^{\infty} x\Big(\Phi_y(x,1) - \Phi_y(x,-1)\Big)dx$$

$$+\iint_{\mathfrak{D}_2} \big(xw(x, y) - \Phi_x(x, y)\big)dxdy = 0 . \tag{2.4.66}$$

In such manner, we derived thermal balance conditions (2.4.57), (2.4.58), and (2.4.66) ensuring the average temperature field within orthotropic inhomogeneous strip $\mathfrak{D}_2$ not to grow infinitely.

Now, an analytical solution to equation (2.2.62) that has two degrees of freedom to meet conditions (2.4.54) can be given as follows:

$$\overline{T}(y) = A\cosh sy + B\sinh sy$$

$$+\frac{1}{2s}\int_{-1}^{1} \overline{T}(\eta)\Bigg(\Bigg(s^2\,\frac{\lambda_x(\eta) - \lambda_y(\eta)}{\lambda_y(\eta)}$$

$$+\frac{d^2 \ln \lambda_y(\eta)}{d\eta^2}\Bigg)\sinh s\,|\,y - \eta\,|$$

$$-\frac{1}{2s}\int_{-1}^{1} \frac{\overline{w}(\eta)}{\lambda_y(\eta)}\sinh s\,|\,y - \eta\,|\,d\eta$$

$$-s\frac{d \ln \lambda_y(\eta)}{d\eta}\cosh s(y - \eta)\,\mathrm{sgn}(y - \eta)\Bigg)d\eta . \tag{2.4.67}$$

We first eliminate the constants of integration A and B by substituting (2.4.67) into conditions (2.4.54) in the mapping domain of transform (2.2.24). We then obtain the following expression for temperature:

$$\overline{T}(y) = \frac{\gamma_{22}\cosh sy - \gamma_{21}\sinh sy}{\gamma}\overline{T}_1$$

$$+\frac{\gamma_{11}\sinh sy - \gamma_{12}\cosh sy}{\gamma}\overline{T}_2$$

$$+w^*(y) + \int_{-1}^{1}\overline{T}(\eta)\mathcal{L}_{\mathrm{ST}}(y,\eta)d\eta\,, \tag{2.4.68}$$

where

$$\mathcal{L}_{\mathrm{ST}}(y,\eta) = \frac{1}{2s}\left\{\left(s^2\frac{\lambda_x(\eta)-\lambda_y(\eta)}{\lambda_y(\eta)} + \frac{d^2\ln\lambda_y(\eta)}{d\eta^2}\right)\right.$$

$$\times\left[\sinh s\,|\,y-\eta\,| - \left[\gamma_{22}\ell_{11}\sinh s(1-\eta)\right.\right.$$

$$+\gamma_{22}\ell_{12}\left(s\cosh s(1-\eta) - \left.\frac{d\ln\lambda_y(y)}{dy}\right|_{y=1}\sinh s(1-\eta)\right)$$

$$-\gamma_{12}\ell_{21}\sinh s(1+\eta)$$

$$\left.\left.+\gamma_{12}\ell_{22}\left(s\cosh s(1+\eta) + \left.\frac{d\ln\lambda_y(y)}{dy}\right|_{y=-1}\sinh s(1+\eta)\right)\right]\frac{\cosh sy}{\gamma}\right.$$

$$\left.-\left[\gamma_{11}\ell_{21}\sinh s(1+\eta)\right.\right.$$

$$\left.\left.-\gamma_{11}\ell_{22}\left(s\cosh s(1+\eta) + \left.\frac{d\ln\lambda_y(y)}{dy}\right|_{y=-1}\sinh s(1+\eta)\right)\right.\right.$$

$$-\gamma_{21}\ell_{11}\sinh s(1-\eta)$$

$$-\gamma_{21}\ell_{12}\left(s\cosh s(1-\eta)-\left.\frac{d\ln\lambda_y(y)}{dy}\right|_{y=1}\sinh s(1-\eta)\right)\Bigg]\frac{\sinh sy}{\gamma}\Bigg]$$

$$+s\frac{d\ln\lambda_y(\eta)}{d\eta}\Bigg[-\cosh s(y-\eta)\operatorname{sgn}(y-\eta)$$

$$+\Bigg[\gamma_{22}\ell_{11}\cosh s(1-\eta)$$

$$+\gamma_{22}\ell_{12}\left(s\sinh s(1-\eta)-\left.\frac{d\ln\lambda_y(y)}{dy}\right|_{y=1}\cosh s(1-\eta)\right)$$

$$+\gamma_{12}\ell_{21}\cosh s(1+\eta)-\gamma_{12}\ell_{22}\Bigg(s\sinh s(1+\eta)$$

$$+\left.\frac{d\ln\lambda_y(y)}{dy}\right|_{y=-1}\cosh s(1+\eta)\Bigg)\Bigg]\frac{\cosh sy}{\gamma}$$

$$+\Bigg[\gamma_{11}\ell_{22}\left(s\sinh s(1+\eta)+\left.\frac{d\ln\lambda_y(y)}{dy}\right|_{y=-1}\cosh s(1+\eta)\right)$$

$$-\gamma_{21}\ell_{11}\cosh s(1-\eta)-\gamma_{11}\ell_{21}\cosh s(1+\eta)$$

$$-\gamma_{21}\ell_{12}\Bigg(s\sinh s(1-\eta)$$

$$-\left.\frac{d\ln\lambda_y(y)}{dy}\right|_{y=1}\cosh s(1-\eta)\Bigg)\Bigg]\frac{\sinh sy}{\gamma}\Bigg]\Bigg\}, \qquad (2.4.69)$$

$$w^*(y)=\frac{1}{2s}\int_{-1}^{1}\frac{\overline{w}(\eta)}{\lambda_y(\eta)}\Bigg[-\sinh s\,|\,y-\eta\,|$$

$$+\Bigg[\gamma_{22}\ell_{11}\sinh s(1-\eta)$$

$$+\gamma_{22}\ell_{12}\left(s\cosh s(1-\eta)-\left.\frac{d\ln\lambda_y(y)}{dy}\right|_{y=1}\sinh s(1-\eta)\right)$$

$$-\gamma_{12}\ell_{21}\sinh s(1+\eta)$$

$$+\gamma_{12}\ell_{22}\left(s\cosh s(1+\eta)+\left.\frac{d\ln\lambda_y(y)}{dy}\right|_{y=-1}\sinh s(1+\eta)\right)\Bigg]\frac{\cosh sy}{\gamma}$$

$$+\Bigg[\gamma_{11}\ell_{21}\sinh s(1+\eta)-\gamma_{21}\ell_{11}\sinh s(1-\eta)$$

$$-\gamma_{11}\ell_{22}\left(s\cosh s(1+\eta)+\left.\frac{d\ln\lambda_y(y)}{dy}\right|_{y=-1}\sinh s(1+\eta)\right)$$

$$-\gamma_{21}\ell_{12}\Bigg(s\cosh s(1-\eta)$$

$$-\left.\frac{d\ln\lambda_y(y)}{dy}\right|_{y=1}\sinh s(1-\eta)\Bigg)\Bigg]\frac{\sinh sy}{\gamma}\Bigg]d\eta\,, \qquad (2.4.70)$$

$$\gamma_{11}=\left(\ell_{11}-\ell_{12}\left.\frac{d\ln\lambda_y(y)}{dy}\right|_{y=1}\right)\cosh s+\ell_{12}s\sinh s,$$

$$\gamma_{12}=\left(\ell_{11}-\ell_{12}\left.\frac{d\ln\lambda_y(y)}{dy}\right|_{y=1}\right)\sinh s+\ell_{12}s\cosh s,$$

$$\gamma_{21} = \left(\ell_{21} - \ell_{22} \left. \frac{d \ln \lambda_y(y)}{dy} \right|_{y=-1} \right) \cosh s - \ell_{22} s \sinh s,$$

$$\gamma_{22} = -\left(\ell_{21} - \ell_{22} \left. \frac{d \ln \lambda_y(y)}{dy} \right|_{y=-1} \right) \sinh s + \ell_{22} s \cosh s,$$

$$\gamma = \gamma_{11}\gamma_{22} - \gamma_{12}\gamma_{21}. \tag{2.4.71}$$

Using the resolvent-kernel method, a solution to equation (2.4.68) can be derived explicitly as

$$\overline{T}(y) = \overline{T}_1 \tau_1(y) + \overline{T}_2 \tau_2(y) + w_{\mathrm{ST}}(y). \tag{2.4.72}$$

Here,

$$\tau_1(y) = \frac{\gamma_{22}\tau_{\mathrm{c}}(y) - \gamma_{21}\tau_{\mathrm{s}}(y)}{\gamma}, \qquad \tau_2(y) = \frac{\gamma_{11}\tau_{\mathrm{s}}(y) - \gamma_{12}\tau_{\mathrm{c}}(y)}{\gamma},$$

$$\tau_{\mathrm{c}}(y) = \cosh sy + \int_{-1}^{1} \cosh s\eta \mathcal{T}_{\mathrm{ST}}(y,\eta) d\eta,$$

$$\tau_{\mathrm{s}}(y) = \sinh sy + \int_{-1}^{1} \sinh s\eta \mathcal{T}_{\mathrm{ST}}(y,\eta) d\eta,$$

$$w_{\mathrm{ST}}(y) = w^*(y) + \int_{-1}^{1} w^*(\eta) \mathcal{T}_{\mathrm{ST}}(y,\eta) d\eta, \tag{2.4.73}$$

and the resolvent-kernel has the form of an infinite series

$$\mathcal{T}_{\mathrm{ST}}(y,\eta) = \sum_{n=0}^{\infty} \mathcal{L}_{n+1}^{\mathrm{ST}}(y,\eta) \tag{2.4.74}$$

using the following recurring kernels:

$$\mathcal{L}_1^{\mathrm{ST}}(y,\eta)=\mathcal{L}_{\mathrm{ST}}(y,\eta),$$
$$\mathcal{L}_{n+1}^{\mathrm{ST}}(y,\eta)=\int_{-1}^{1}\mathcal{L}_1^{\mathrm{ST}}(y,t)\mathcal{L}_n^{\mathrm{ST}}(t,\eta)dt,\quad n=1,2,\ldots \tag{2.4.75}$$

If the analytical evaluation of the series given in (2.4.74) presents a challenge, it can be substituted with the following approximation:

$$\mathcal{T}_{\mathrm{ST}}(y,\eta)\approx\mathcal{T}_{\mathrm{ST}}^{N}(y,\eta)=\sum_{n=0}^{N}\mathcal{L}_{n+1}^{\mathrm{ST}}(y,\eta), \tag{2.4.76}$$

where N is a natural digit allowing for the satisfying of equation (2.4.68) with solution (2.4.72) together with the approximate resolvent kernel (2.4.76) within an appropriate level of accuracy.

2.5. Special cases of anisotropy and inhomogeneity

As it can be concluded from the foregoing **Sections 2.2.2**, **2.3.2**, and **2.4.1**, the key point of the solution construction to the formulated thermoelasticity problems is to solve the governing integral equations for total stress; i.e., (2.2.32) for plane $\mathfrak{D}_0$, (2.3.12) for half-plane $\mathfrak{D}_1$, and (2.4.15) for strip $\mathfrak{D}_2$. Obtaining explicit solutions to these equations requires construction of the resolvent kernels (2.2.35), (2.3.22), and (2.4.22), respectively. The resolvent kernels are constructed by successions of recurring kernels originated by kernels (2.2.33), (2.3.13), and (2.4.17) of the integral equations (2.2.32), (2.3.12), and (2.4.15), respectively. Thus, they do not depend on the force or thermal loadings; they depend directly on the material properties and indirectly on the geometry of the domains via integral limits in their expressions. From this perspective, specific cases of orthotropic material inhomogeneity permit relatively simple analysis of the thermoelasticity solutions to the problems being considered.

The simplest situation seems to be the one when solutions (2.2.34), (2.3.14), and (2.4.25) can be computed without evaluation of the corresponding resolvent kernels; i.e.: *i*) $\mathcal{R}_{\mathrm{PL}}(y,\eta)=0$ for $(y,\eta)\in(-\infty,+\infty)^2$; *ii*) $\mathcal{R}_{\mathrm{HP}}(y,\eta)=0$ for $(y,\eta)\in[0,+\infty)^2$; and *iii*) $\mathcal{R}_{\mathrm{ST}}(y,\eta)=0$ for $(y,\eta)\in[-1,1]\times[-1,y]$. In view of formulae (2.2.36), (2.3.23), and (2.4.23) within the context of (2.2.33), (2.3.13), and (2.4.17),

this case manifests when the material properties meet the following conditions:

$$\frac{d^2\beta_1(y)}{dy^2} + s^2\beta_2(y) = 0, \quad \beta_1(y) = \frac{1}{2G_{xy}(y)}. \tag{2.5.1}$$

In (2.5.1), variable y falls within the corresponding range, i.e., $y \in (-\infty, +\infty)$ for plane $\mathfrak{D}_0$, $y \in [0, +\infty)$ for half-plane $\mathfrak{D}_1$, and $y \in [-1,1]$ for strip $\mathfrak{D}_2$. Due to the fact that the material properties do not depend on transform parameter s, the first equation of (2.5.1) yields the following conditions:

$$\beta_2(y) = 0, \qquad \frac{d^2\beta_1(y)}{dy^2} = 0. \tag{2.5.2}$$

The second equation of (2.5.1) together with the second one in (2.5.2) imply that

$$\frac{d^2}{dy^2}\left(\frac{1}{G_{xy}(y)}\right) = 0. \tag{2.5.3}$$

In view of expressions (2.1.32), the first condition in (2.5.2) means that

$$a_{11}(y) = a_{22}(y). \tag{2.5.4}$$

Taking into account (2.1.24), equation (2.5.4) presents the following condition of equality for the orthotropic Young moduli in the case of plane stress:

$$E_x(y) = E_y(y). \tag{2.5.5}$$

Then, in view of the symmetry condition (2.1.6),

$$\nu_{xy}(y) = \nu_{yx}(y). \tag{2.5.6}$$

In the case of plane strain, conditions (2.5.4) and (2.1.24) mean that

$$E_x(y)\big(1 - \nu_{zy}(y)\nu_{yz}(y)\big) = E_y(y)\big(1 - \nu_{zx}(y)\nu_{xz}(y)\big). \tag{2.5.7}$$

By implementing the symmetry condition (2.1.6), formula (2.5.4) can be expressed in many alternative forms, for example:

$$\frac{E_x^2(y)}{E_y^2(y)} = \frac{E_x(y) - \nu_{xz}^2(y)E_z(y)}{E_y(y) - \nu_{yz}^2(y)E_z(y)}, \tag{2.5.8}$$

$$\frac{E_x(y)}{E_y(y)} = \frac{E_z(y) - \nu_{zx}^2(y)E_x(y)}{E_z(y) - \nu_{zy}^2(y)E_y(y)}, \tag{2.5.9}$$

or

$$\nu_{zy}^2(y) - \nu_{zx}^2(y) = \frac{E_x(y) - E_y(y)}{E_x(y)E_y(y)}E_z(y). \tag{2.5.10}$$

Similarly, the orthotropic Young moduli can be eliminated from formula (2.5.7) to obtain the following relationship between the Poisson ratios:

$$\frac{E_x(y)}{E_y(y)} = \frac{1 - \nu_{zx}(y)\nu_{xz}(y)}{1 - \nu_{zy}(y)\nu_{yz}(y)}. \tag{2.5.11}$$

In view of (2.1.32), the second equation of (2.5.1) can be written as follows:

$$2a_{11}(y) - 2a_{12}(y) = \frac{1}{G_{xy}(y)}. \tag{2.5.12}$$

This, along with (2.1.24) and (2.5.4) – (2.5.6), yields the following expression for the case of plane stress:

$$G_{xy}(y) = \frac{E^*(y)}{2\left(1 + \nu^*(y)\right)}, \tag{2.5.13}$$

where $E^*(y) = E_x(y) = E_y(y)$ and $\nu^*(y) = \nu_{xy}(y) = \nu_{yx}(y)$.

For the case of plane strain, we can similarly obtain the following:

$$G_{xy}(y) = \frac{E_x(y)}{2\left(1 + \nu_{xy}(y) + \left(\nu_{zy}(y) - \nu_{zx}(y)\right)\nu_{xz}(y)\right)}$$

$$= \frac{E_y(y)}{2\left(1+\nu_{yx}(y)+\left(\nu_{zx}(y)-\nu_{zy}(y)\right)\nu_{yz}(y)\right)}, \qquad (2.5.14)$$

which is to be considered within the context of equalities (2.5.7) –(2.5.11).

Under the hypotheses of both plane stress and plane strain, equation (2.5.3) implies that

$$G_{xy}(y) = \frac{G_0}{a_0 y + b_0}, \qquad (2.5.15)$$

where G_0 is an arbitrary constant in dimension of stresses, and a_0 and b_0 are dimensionless constants.

Under the physical constraint $0 < G_{xy}(y) < +\infty$ for the shear modulus [154], expression (2.5.15) is valid for

$$G_0 > 0, \quad a_0 y + b_0 > 0 \qquad (2.5.16)$$

or

$$G_0 < 0, \quad a_0 y + b_0 < 0 \qquad (2.5.17)$$

for the entire range of variation associated with variable y. Thus, for the case of inhomogeneous orthotropic plane $\mathfrak{D}_0$ where $-\infty < y < +\infty$, conditions (2.5.16) and (2.5.17) necessitate that $a_0 = 0$ and

$$G_{xy}(y) = \frac{G_0}{b_0} = \text{const} > 0. \qquad (2.5.18)$$

In view of this, formula (2.5.13) for plane stress yields the following:

$$E^*(y) = 2\frac{G_0}{b_0}(1+\nu^*(y)). \qquad (2.5.19)$$

Similarly, adopting (2.5.18) and (2.5.14) for the case of plane strain allows us to obtain, e.g., the following equality:

$$E_x(y) = 2\frac{G_0}{b_0}\left(1+\nu_{xy}(y)+\nu_{xz}(y)\left(\nu_{zy}(y)-\nu_{zx}(y)\right)\right). \qquad (2.5.20)$$

Note that formula (2.5.19) implies functional variation of Poisson's ratio $\nu^*(y)$ with the coordinate y in the following form in the case of plane stress:

$$\nu^*(y) = \frac{b_0}{2G_0} E^*(y) - 1. \tag{2.5.21}$$

In the case of plane strain, this dependence is more complex, as follows from (2.5.20).

In the case of plane stress, formulae (2.5.6), (2.5.13) and (2.5.19) cover the variations of material properties occurring within an orthotropic inhomogeneous plane $\mathfrak{D}_0$ for which resolvent kernel (2.2.35) equals zero. Similarly, formulae (2.5.7) – (2.5.11), (2.5.14), and (2.5.20) cover the material properties ensuring resolvent kernel (2.2.35) to be zero in the case of plane strain. For both the plane strain and plane stress, solution (2.2.34) of the governing integral equation (2.2.33) can be written explicitly as follows:

$$\overline{\sigma}(y) = \Theta_{\mathrm{PL}}(y) + \Psi^0_{\mathrm{PL}}(y), \tag{2.5.22}$$

where $\Theta_{\mathrm{PL}}(y)$ is given by (2.2.30),

$$\Psi^0_{\mathrm{PL}}(y) = \frac{1}{2|s|a_{11}(y)} \int_{-\infty}^{+\infty} \varpi(\eta) \exp\left(-|s||y-\eta|\right) d\eta, \tag{2.5.23}$$

and

$$\varpi(\eta) = \beta_1(\eta)\left(\frac{d\overline{F}_y(\eta)}{d\eta} + is\overline{F}_x(\eta)\right) + 2\overline{F}_y(\eta)\frac{d\beta_1(\eta)}{d\eta}. \tag{2.5.24}$$

Thus, stress-tensor components (2.2.38), (2.2.40), and (2.2.42) take the following form:

$$\overline{\sigma}_{yy}(y) = \frac{1}{2|s|} \int_{-\infty}^{+\infty} \Xi_{\mathrm{PL}}(\eta) \exp(-|s||y-\eta|) d\eta,$$

$$\overline{\sigma}_{xx}(y) = \Theta_{\mathrm{PL}}(y) + \Psi^0_{\mathrm{PL}}(y)$$

$$-\frac{1}{2|s|}\int_{-\infty}^{+\infty}\Xi_{\mathrm{PL}}(\eta)\exp(-|s||y-\eta|)d\eta, \tag{2.5.25}$$

$$\overline{\sigma}_{xy}(y)=\frac{i}{s}\left(\overline{F}_{y}(y)\right.$$

$$\left.-\frac{1}{2}\int_{-\infty}^{+\infty}\Xi_{\mathrm{PL}}(\eta)\exp(-|s||y-\eta|)\operatorname{sgn}(y-\eta)d\eta\right).$$

Here,

$$\Xi_{\mathrm{PL}}(\eta)=\frac{d\overline{F}_{y}(\eta)}{d\eta}-is\overline{F}_{x}(\eta)+s^{2}\left(\Theta_{\mathrm{PL}}(\eta)+\Psi^{0}_{\mathrm{PL}}(\eta)\right). \tag{2.5.26}$$

Similar simplifications can be made for the displacements (2.2.47) and (2.2.48).

For the case of inhomogeneous orthotropic half-plane $\mathfrak{D}_1$ where $0\le y<+\infty$, conditions (2.5.16) and (2.5.17) imply that

$$G_0>0,\quad a_0\ge 0,\quad b_0>0 \tag{2.5.27}$$

or

$$G_0<0,\quad a_0\le 0,\quad b_0<0. \tag{2.5.28}$$

Taken together, (2.5.13) and (2.5.15) in view of (2.5.27) and (2.5.28) yield the following condition for the case of plane stress:

$$E^{*}(y)=2G_0\frac{1+\nu^{*}(y)}{a_0y+b_0}. \tag{2.5.29}$$

For the case of plane strain, formulae (2.5.13) and (2.5.15) yield, e.g., the following equality

$$E_x(y)=2G_0\frac{1+\nu_{xy}(y)+\nu_{xz}(y)\left(\nu_{zy}(y)-\nu_{zx}(y)\right)}{a_0y+b_0}. \tag{2.5.30}$$

Formulae (2.5.5), (2.5.6), (2.5.13), and (2.5.29), in the case of plane stress, and formulae (2.5.7) – (2.5.11), (2.5.14), and (2.5.30), in the case of plane strain, cover the material properties variation within an orthotropic inhomogeneous half-plane $\mathfrak{D}_1$ for which resolvent kernel (2.3.22) equals zero. Thus, the solution to the governing integral equation (2.3.12) can be given in explicit analytical form (2.3.14), where

$$P_{\mathrm{HP}}(y) = -\frac{\exp(-|s|y)}{|s|c_0 a_{11}(y)}, \quad Q_{\mathrm{HP}}(y) = -\frac{\exp(-|s|y)}{s^2 c_0 a_{11}(y)},$$

$$\Theta_{\mathrm{HP}}(y) = \Theta_0(y) - \frac{1}{c_0 a_{11}(y)} \int_0^{+\infty} \Theta_0(\xi) \exp(-|s|(y+\xi)) d\xi,$$

$$\Psi_{\mathrm{HP}}(y) = \Psi_0(y) - \frac{\exp(-|s|y)}{s^2 c_0 a_{11}(y)} \overline{F}_y(0)$$

$$-\frac{1}{s^2 c_0 a_{11}(y)} \int_0^{+\infty} \left(\Psi_0(\xi) + \frac{1}{s^2} \frac{d\overline{F}_y(\xi)}{d\xi} - \frac{i}{s} \overline{F}_x(\xi) \right) \exp(-|s|(y+\xi)) d\xi,$$

$$\Psi_0(y) = \frac{1}{2|s| a_{11}(y)} \int_0^{+\infty} \varpi(\eta) \exp(-|s||y-\eta|) d\eta,$$

$$c_0 = \int_0^{+\infty} \frac{\exp(-2|s|y)}{a_{11}(y)} dy, \tag{2.5.31}$$

and $\Theta_0(y)$ is given by (2.3.13) and $\varpi(\eta)$ has the form (2.5.24). Thus, coefficients (2.3.26), (2.3.29) – (2.3.43) for stress-tensor components (2.3.25), (2.3.27), and (2.3.28), as well as the coefficients (2.3.53) for the displacements (2.3.51) and (2.3.52) can be expressed through coefficients (2.5.31).

In the case of inhomogeneous orthotropic strip $\mathfrak{D}_2$ where $|y| \le 1$, conditions (2.5.16) and (2.5.17) imply that

$$b_0 > 0, \qquad |a_0| < b_0 \ \text{ for } \ G_0 > 0 \tag{2.5.32}$$

or

$$b_0 < 0, \qquad |a_0| < -b_0 \ \text{ for } \ G_0 < 0\,. \tag{2.5.33}$$

Then, formulae (2.5.5), (2.5.6), (2.5.13), and (2.5.29) for the plane stress, and (2.5.7) – (2.5.11), (2.5.14), and (2.5.30) for the plane strain, in view of the parameter constrains (2.5.32) or (2.5.33), cover the material properties variation in orthotropic inhomogeneous strip $\mathfrak{D}_2$ when the resolvent kernel (2.4.22) equals to zero. Thus, solution (2.4.25) for the governing integral equation (2.4.15) can be expressed using the following coefficients:

$$P_1(y) = \frac{I_2 \sinh(s(1+y))}{sIa_{11}(y)}$$

$$-\frac{I_0 \sinh(s(1-y)) + I_1 \cosh(s(1+y))}{sIa_{11}(y)},$$

$$P_2(y) = \frac{I_2 \sinh(s(1-y))}{sIa_{11}(y)}$$

$$-\frac{I_0 \sinh(s(1+y)) - I_1 \cosh(s(1+y))}{sIa_{11}(y)},$$

$$Q_1(y) = \frac{\chi_1(y,1)}{s^2}, \qquad Q_2(y) = \frac{\chi_2(y,1)}{s^2},$$

$$\Theta_{\mathrm{ST}}(y) = \Theta(y) - \int_{-1}^{1} \Theta(\xi)\chi_1(y,\xi)d\xi\,,$$

$$\Psi_{\mathrm{ST}}(y) = \frac{1}{s^2}\left(\overline{F}_y(1)\chi_1(y,1) + \overline{F}_y(-1)\chi_2(y,1)\right)$$

$$-\frac{1}{sa_{11}(y)}\int_{-1}^{y} \varpi(\eta)d\eta$$

$$+\int_{-1}^{1}\left(\frac{1}{s}\overline{F}_x(\xi) - \frac{1}{s^2}\frac{d\overline{F}_y(\xi)}{d\xi} + \frac{1}{sa_{11}(\xi)}\int_{-1}^{\xi} \varpi(\eta)d\eta,\right)\chi_1(y,\xi)d\xi\,, \tag{2.5.34}$$

$$\chi_1(y,\xi)=\frac{I_0\cosh(s(y-\xi))}{Ia_{11}(y)}$$

$$\frac{I_1\sinh(s(y+\xi))-I_2\cosh(s(y+\xi))}{Ia_{11}(y)},$$

$$\chi_2(y,\xi)=-\frac{I_0\cosh(s(y+\xi))}{Ia_{11}(y)}$$

$$-\frac{I_1\sinh(s(y-\xi))-I_2\cosh(s(y-\xi))}{Ia_{11}(y)},$$

$$I_1=\frac{1}{2}\int_{-1}^{1}\frac{\sinh 2sy}{a_{11}(y)}dy,\quad I_2=\frac{1}{2}\int_{-1}^{1}\frac{\cosh 2sy}{a_{11}(y)}dy,$$

$$I_0=\frac{1}{2}\int_{-1}^{1}\frac{dy}{a_{11}(y)},\quad I=I_0^2+I_1^2-I_2^3,$$

where $\Theta(y)$ is given by (2.4.16) and $\varpi(\eta)$ is presented in (2.5.24). Coefficients (2.4.28) and (2.4.31) for the stress-tensor components (2.4.27), (2.4.29), and (2.4.30), as well as coefficients (2.4.43) and (2.4.49) for displacements (2.4.42) and (2.4.48) can be expressed through the coefficients (2.5.34).

In view of expressions (2.1.25) – (2.1.27), it is easy to conclude that relations (2.5.1) are always valid for the case of inhomogeneous isotropic or transversely isotropic material properties. Thus, to eliminate the resolvent kernel from the corresponding thermoelasticity solutions, it is enough to ensure that condition (2.5.3) holds. This yields an expression similar to (2.5.15):

$$G(y)=\frac{G_0}{a_0y+b_0}. \tag{2.5.35}$$

Note that this representation of the shear modulus corresponds to the well-known model of "Gibson soil" for the problem in an isotropic inhomogeneous half-plane (see equation (1.2.5) in **Section 1.2.1**). In this case, key stresses (2.4.25) and (2.4.27) for an inhomogeneous isotropic

strip $\mathfrak{D}_2$, for example, can be given in the mapping domain of transform (2.2.24) as follows:

$$\overline{\sigma}(y)=\frac{2G(y)}{1-\nu(y)}\big(A\cosh sy+B\sinh sy$$

$$+H(y)-\alpha(y)(1+\nu(y))\overline{T}(y)\big),$$

$$\overline{\sigma}_{yy}=-\overline{p}_2\cosh s(1+y)-\left(i\overline{q}_2+\frac{1}{s}\overline{F}_y(-1)\right)\sinh s(1+y) \qquad (2.5.36)$$

$$-2s\int_{-1}^{y}\frac{G(\xi)\big(A\cosh s\xi-B\sinh s\xi\big)\sinh s(y-\xi)}{1-\nu(\xi)}d\xi$$

$$+s\int_{-1}^{y}\frac{\alpha(\xi)E(\xi)\overline{T}(\xi)-2G(\xi)H(\xi)}{1-\nu(\xi)}\sinh s(y-\xi)d\xi,$$

where

$$A=\frac{I_2}{I_2I_3-I_1^2}\Psi_1-\frac{I_1}{I_2I_3-I_1^2}\Psi_2,$$

$$B=\frac{I_3}{I_2I_3-I_1^2}\Psi_2-\frac{I_1}{I_2I_3-I_1^2}\Psi_1,$$

$$I_1=\frac{1}{2}\int_{-1}^{1}\frac{G(\xi)}{1-\nu(\xi)}\sinh 2s\xi d\xi,$$

$$I_2=\int_{-1}^{1}\frac{G(\xi)}{1-\nu(\xi)}\sinh^2 s\xi d\xi,$$

$$I_3=\int_{-1}^{1}\frac{G(\xi)}{1-\nu(\xi)}\cosh^2 s\xi d\xi,$$

$$\Psi_1=Z_2-H_c+\frac{1}{2}\Theta_c,\quad \Psi_2=Z_1-H_s+\frac{1}{2}\Theta_s,$$

$$H_c = \int_{-1}^{1} \frac{G(\xi)H(\xi)}{1-\nu(\xi)} \cosh s\xi d\xi, \tag{2.5.37}$$

$$\Theta_c = \int_{-1}^{1} \frac{\alpha(\xi)E(\xi)\overline{T}(\xi)}{1-\nu(\xi)} \cosh s\xi d\xi,$$

$$H_s = \int_{-1}^{1} \frac{G(\xi)H(\xi)}{1-\nu(\xi)} \sinh s\xi d\xi,$$

$$\Theta_s = \int_{-1}^{1} \frac{\alpha(\xi)E(\xi)\overline{T}(\xi)}{1-\nu(\xi)} \sinh s\xi d\xi;$$

$$H(y) = -\frac{1}{s}\int_{-1}^{y} \left(\overline{F}_y(\xi) \frac{d}{d\xi}\left(\frac{1}{G(\xi)}\right) \right.$$

$$\left. + \frac{1}{2G(\xi)}\left(is\overline{F}_x(\xi) + \frac{d\overline{F}_y(\xi)}{d\xi} \right) \right) \sinh s(y-\xi) d\xi$$

and Z_1 and Z_2 are given by (2.4.11).

Note that (2.5.37) can be regarded as a benchmark solution for the verification of various methods. Its usefulness in verification is associated with its functional flexibility, which is greater than that of approaches in which material properties are formulated as specific elementary dependences on the coordinates (see **Section 1.2.1**). For example, it can be used to analyze the effect of variations in the Poisson ratio associated with the distribution of thermal stress within inhomogeneous domains.

Consider, for example, the case of inhomogeneous isotropic strip $\mathfrak{D}_2$ subject to external normal loadings (2.4.1), where

$$\begin{gathered} p_1(x) = p_2(x) = p\varsigma(x), \\ q_1(x) = q_2(x) = F_x(x,y) = F_y(x,y) = T(x,y) = 0, \end{gathered} \tag{2.5.38}$$

$\varsigma(x) = \exp(-a_p x^2)$, $0 < a_p = \text{const}$, and p is a constant in dimension of stresses.

Assume that the material properties of the strip are as follows:

$$G = G_0 = \text{const}, \quad \nu(y) = 1 - \frac{1}{a_\nu - b_\nu y}, \qquad (2.5.39)$$

$$a_\nu = \text{const}, \ b_\nu = \text{const}.$$

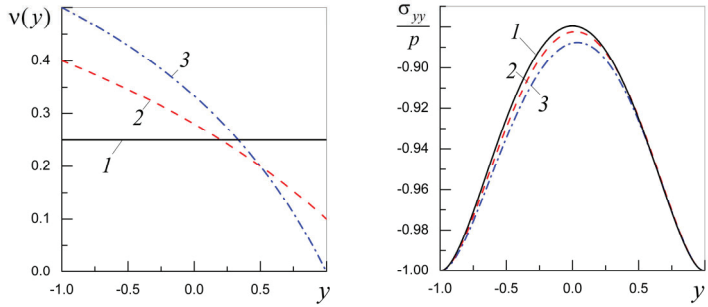

a) *b*)

Figure 2.1. Effect of the variable Poisson ratio (2.5.39) under constant shear modulus in the transversal stress for inhomogeneous isotropic strip subjected to loadings (2.4.1) and (2.5.38): *a*) distributions of Poisson's ratio versus strip width for cases of $a_\nu = 1.33, b_\nu = 0.00$ (homogeneous material – curve *1*); $a_\nu = 1.39, b_\nu = 0.28$ (curve *2*); and $a_\nu = 1.50, b_\nu = 0.50$ (curve *3*); *b*) distribution of transversal stress (2.5.36) due to loading (2.5.38) for cases of $a_p = 1$ at $x = 0$; the curve numbers correspond to the material parameters in plot *a*

Then,

$$E(y) = \frac{4(a_\nu - b_\nu y) - 2}{a_\nu - b_\nu y} G_0 . \qquad (2.5.40)$$

and the material properties (2.5.39) and (2.5.40) are within the constraints (2.5.2) and (2.5.3), such that the key stresses can be expressed using formulae (2.5.36).

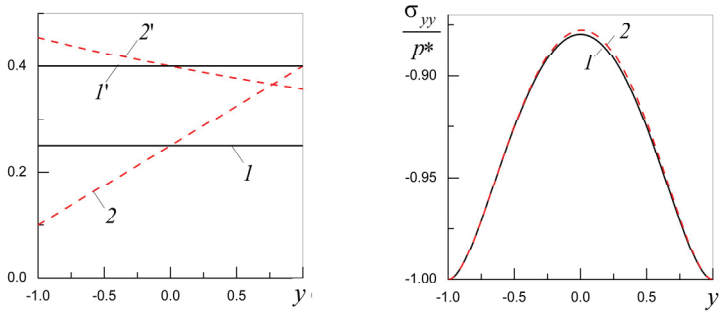

a) *b*)

Figure 2.2. Effect of material properties (2.5.41) and (2.5.42) under constant Young's modulus in the transversal stress (2.5.36) for an inhomogeneous isotropic strip subjected to loadings (2.4.1) and (2.5.38): *a*) distributions of Poisson's ratio (2.5.41) – curves *1* and *2* corresponding to $a_\nu = 3/20, b_\nu = 1/4$ and $a_\nu = 0$, $b_\nu = 1/4$; distributions of shear modulus (2.5.42) – curves *1'* and *2'* corresponding to the same values versus strip width; *b*) distribution of the transversal stress due to loading (2.5.38) for cases of $a_p = 1$ at $x = 0$; the curve numbers correspond to the material parameters in plot *a.*

The effect of variable Poisson's ratio and Young's modulus under the constant shear modulus is illustrated in Fig 2.1. In the case of homogeneous material (curves *1* in plots *a* and *b*), the transversal stress is symmetric about $y = 0$, due to the symmetry of loading (2.5.38). As Poisson's ratio is varied, the symmetry in the stress values is no longer observed. In cases where the variation in Poisson ratio's (2.5.39) presents a steeper gradients, there is a corresponding drop in the magnitude of stress.

The effect of linear variation of Poisson's ratio

$$\nu(y) = a_\nu y + b_\nu, \quad a_\nu = \text{const}, \ b_\nu = \text{const}, \tag{2.5.41}$$

is illustrated in Fig. 2.2 in the case of constant Young's modulus, $E(y) = E_0 = \text{const}$, allowing the shear modulus

$$G(y) = \frac{E_0}{2(1 + b_\nu + a_\nu y)} \tag{2.5.42}$$

to meet the condition (2.5.3). As shown in Fig. 2.3 in comparison to Fig. 2.2, allowing Poisson's ratio (2.5.41) to drop into negative values (when the one side of the strip exhibits auxetic material properties [238]) has a critical effect on the stress field.

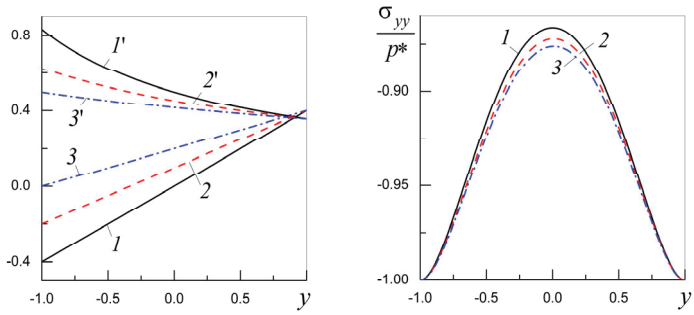

a) *b*)

Figure 2.3. Effect of material properties (2.5.41) and (2.5.42) under constant Young's modulus in the transversal stress in the case of inhomogeneous isotropic strip subject to loadings (2.4.1) and (2.5.38) when Poisson's ratio of the material moves into negative values: *a*) distributions of Poisson's ratio (2.5.41) – curves *1, 2,* and *3* respectively correspond to $a_\nu = 2/5, b_\nu = 0$, $a_\nu = 3/10, b_\nu = 1/10$ and $a_\nu = 1/5, b_\nu = 1/5$; distributions of shear modulus (2.5.42) – curves *1', 2',* and *3'* correspond to the same values versus strip width; *b*) distribution of the transversal stress due to loading (2.5.38) for cases of $a_p = 1$ at $x = 0$; the curve numbers correspond to the material parameters in plot *a.*

Note that in the case of homogeneous isotropic or transversely isotropic materials (all elastic material moduli are constants), the conditions (2.5.2) and (2.5.3) are fulfilled automatically for any possible interrelations between the elastic moduli. This, however is not the case for homogeneous orthotropic materials, for which condition $\beta_2(y) = 0$ is not always satisfied. This means that the resolvent kernel is to be computed for the case of homogeneous orthotropic material, when $a_{11} \neq a_{22}$.

In the case of homogeneous orthotropic material, an exact solution can be constructed by making use of equations (2.1.35) and (2.1.31). The latter one takes the following form:

$$\Delta\left(a_{11}\sigma - \alpha_1(T - T_0)\right) = (\alpha_1 - \alpha_2)(T - T_0)$$

$$+\left(2\beta_1-\frac{1}{G_{xy}}\right)\frac{\partial^2\sigma_{yy}}{\partial y^2}$$

$$-\beta_2\frac{\partial^2\sigma_{yy}}{\partial x^2}+\beta_1\left(\frac{\partial F_y}{\partial y}-\frac{\partial F_x}{\partial x}\right)-\frac{1}{G_{xy}}\frac{\partial F_y}{\partial y}. \tag{2.5.43}$$

By eliminating the total stress from the system of equations (2.1.35) and (2.5.43) in view of (2.1.32), the following fourth-order partial-differential equation can be obtained:

$$\frac{\partial^4\sigma_{yy}}{\partial y^4}+2a_1\frac{\partial^4\sigma_{yy}}{\partial x^2\partial y^2}+a_2\frac{\partial^4\sigma_{yy}}{\partial x^2}$$

$$=\frac{1}{a_{11}}\frac{\partial^2}{\partial x^2}\left(\alpha_1\Delta\left(T-T_0\right)+\left(\alpha_1-\alpha_2\right)\left(T-T_0\right)\right)$$

$$+\frac{\partial^3F_x}{\partial x\partial y^2}-\frac{\partial^3F_y}{\partial y^3}-\frac{a_{12}G_{xy}+1}{a_{11}G_{xy}}\frac{\partial^3F_y}{\partial x^2\partial y}+\frac{a_{12}}{a_{11}}\frac{\partial^3F_x}{\partial x^3}, \tag{2.5.44}$$

where

$$a_1=\frac{2a_{12}G_{xy}+1}{2a_{11}G_{xy}},\quad a_2=\frac{a_{22}}{a_{11}}. \tag{2.5.45}$$

The characteristic equation

$$\mu^4-2a_1s^2\mu^2+a_2s^4=0 \tag{2.5.46}$$

makes it possible to determine the eigenvalues for equation (2.5.44) as follows:

$$\mu_{1,2}=\pm\lambda_1 s,\quad \mu_{3,4}=\pm\lambda_2 s, \tag{2.5.47}$$

where

$$\lambda_1 = \sqrt{a_1 - \sqrt{a_1^2 - a_2}} = \alpha_1 + i\beta_1,$$
$$\lambda_2 = \sqrt{a_1 + \sqrt{a_1^2 - a_2}} = \alpha_2 + i\beta_2, \tag{2.5.48}$$

s is the transform parameter and $i^2 = -1$. By taking into consideration the constrains [49, 154]

$$E_j > 0, \quad G_{xy} > 0, \quad j = x, y, z,$$
$$|\nu_{zx} + \nu_{yx}\nu_{zy}| < \frac{1}{\sqrt{E_y E_z}} \sqrt{E_x - E_y \nu_{yx}} \sqrt{E_y - E_z \nu_{zy}},$$
$$|\nu_{yx}| < \sqrt{\frac{E_x}{E_y}}, \quad |\nu_{xy}| < \sqrt{\frac{E_y}{E_x}}, \tag{2.5.49}$$
$$|\nu_{zy}| < \sqrt{\frac{E_y}{E_z}}, \quad |\nu_{yz}| < \sqrt{\frac{E_z}{E_y}}$$

for material properties, it can be concluded that the form of an analytical solution to equation (2.5.44) depends on the interrelation between the coefficients (2.5.45), which are expressed through material properties falling within the constrains (2.5.49). The behavior of the real and imaginary parts of the eigenvalues (2.5.48) is shown in Fig. 2.4. This fact complicates the construction of general solutions to equation (2.5.44) for infinite or semi-infinite domains satisfying the condition of solution boundedness. In this case, the developed resolvent-kernel solution presents an efficient alternative to the construction of solutions in a unique way for any possible interrelations between material properties.

In order to verify our solution for various material properties, consider the case of a general orthotropic inhomogeneous material with the following material properties variation profiles:

$$E_x = E_x^0 \omega(y), \qquad E_y = E_y^0 \omega(y),$$
$$G_{xy} = G_{xy}^0 \omega(y), \qquad \omega(y) = \exp(ky), \tag{2.5.50}$$

where $k = \text{const}$ and $E_x^0, E_y^0,$ and G_{xy}^0 are constant values of Young's and shear moduli E_x, E_y, and G_{xy} on the line $y = 0$. Assume that $G_{xy}^0 = E_x^0 / (2 + 2\nu_{xy})$ and the Poisson ratio $\nu_{xy} = 0.2$. We introduce the following orthotropic parameter to characterize the relationship between the elastic moduli:

$$\varepsilon = \frac{E_x^0}{E_y^0}. \tag{2.5.51}$$

In view of the symmetry condition (2.1.6) and expression (2.5.50), it can be shown that $\nu_{xy} = \varepsilon \nu_{yx}$ and $G_{xy}^0 = \varepsilon E_y^0 / (2 + 2\nu_{xy})$. Obviously, $\varepsilon = 1$ for isotropic materials.

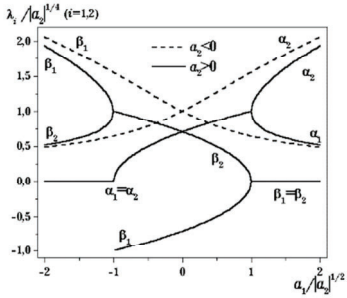

Figure 2.4. Behavior of real and imaginary parts of eigenvalues (2.5.48)

The distribution of transversal stress is shown in Fig. 2.5 for different values of orthotropic parameter (2.5.51) and inhomogeneity value k in (2.5.50) due to loading (2.5.38). In the case of $k = 0$, this stress reaches extreme values at midline $y = 0$. In the inhomogeneous case of $k = -1$, the extreme values shift in the direction of increased inhomogeneity. Under the parameters considered in this example, the effect of orthotropy is more pronounced in the distribution of stress than in the effects of inhomogeneity.

A similar effect is observed in Fig. 2.6 for the material properties given by

$$E_x = E_x^0 w(y), \qquad E_y = E_y^0 w(y),$$
$$G_{xy} = G_{xy}^0 w(y), \quad w(y) = (c_1 + c_2 y)^k. \tag{2.5.52}$$

Interested readers can find detailed analysis of the thermoelastic response of orthotropic inhomogeneous solids under specific material properties profiles in our previous works [296, 297, 299, 301, 302].

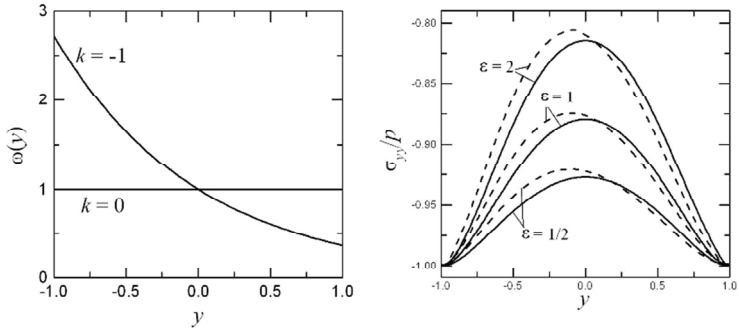

a) *b*)

Figure 2.5. *a*) Distribution of function $\omega(y) = \exp(ky)$ presenting variation profiles of orthotropic material properties (2.5.50) for $k = 0;\ -1$; *b*) Distribution of the transversal stress at $x = 0$ under various orthotropic parameter values $\varepsilon = 1/2; 1; 2$ in cases of homogeneous material $k = 0$ (solid lines) and inhomogeneous material $k = -1$ (dashed lines), due to loading (2.5.38), where $a_p = 1$ (adapted from our paper [296])

Consider the computation of thermal stresses in an isotropic inhomogeneous half-plane $\mathfrak{D}_1$ due to thermal loading (2.3.55) of its boundary $y = 0$, where $\ell_0 = 1$, $\ell_1 = 0$, and

$$T_0(x) = \tau_0 \left(x^2 - x_0^2\right) \exp\left(-x^2\right), \qquad x_0 = \text{const} \tag{2.5.53}$$

and τ_0 is a constant parameter in dimension of temperature. Assume the internal heat sources, as well as all the force loadings to be absent. As shown in [239], thermal loading (2.5.53) meets the conditions of thermal balance derived in Section 2.3.5, if $x_0 = 1/\sqrt{2}$. By assuming the heat-conduction coefficient of the considered isotropic half-plane to be

constant, the temperature field (2.3.88) in the mapping domain of transform (2.2.44) takes the following form:

$$\overline{T} = -\frac{\tau_0 \sqrt{\pi}}{4} s^2 \exp\left(-|s| \left(y + \frac{|s|}{4} \right) \right). \qquad (2.5.54)$$

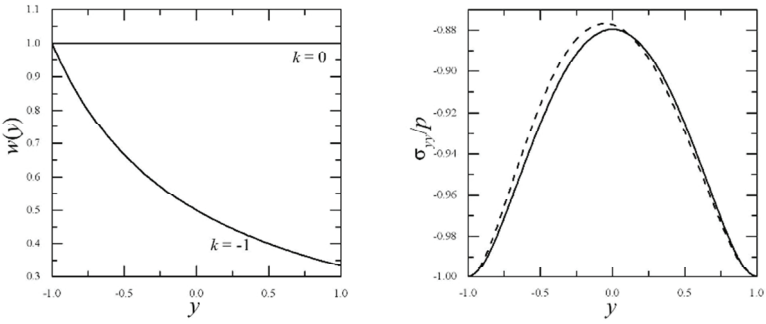

a) *b*)

Figure 2.6. *a*) Distributions of function $w(y)$ in cases of $c_1 = 2$, $c_2 = 1$, $k = 0, -1$; *b*) Transversal stress σ_{yy} / p at $x = 0$ in the strip with properties (2.5.52) for cases of $\varepsilon = 1$, $c_1 = 2$, $c_2 = 1$, $k = 0$ (solid lines) and $k = -1$ (dashed lines) due to loading (2.5.38), where $a_p = 1$ (adapted from our paper [296])

Its distribution in the physical domain is shown in Fig. 2.7.

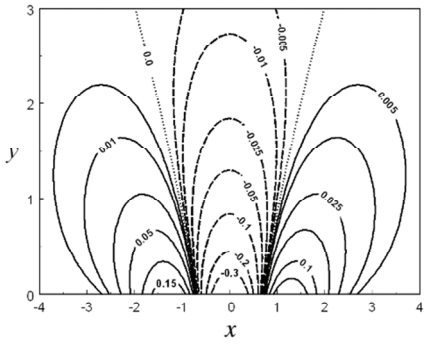

Figure 2.7. Distribution of the static temperature $T(x, y) / \tau_0$, which corresponds to the Fourier mapping function (2.5.54) (adapted from our paper [239]).

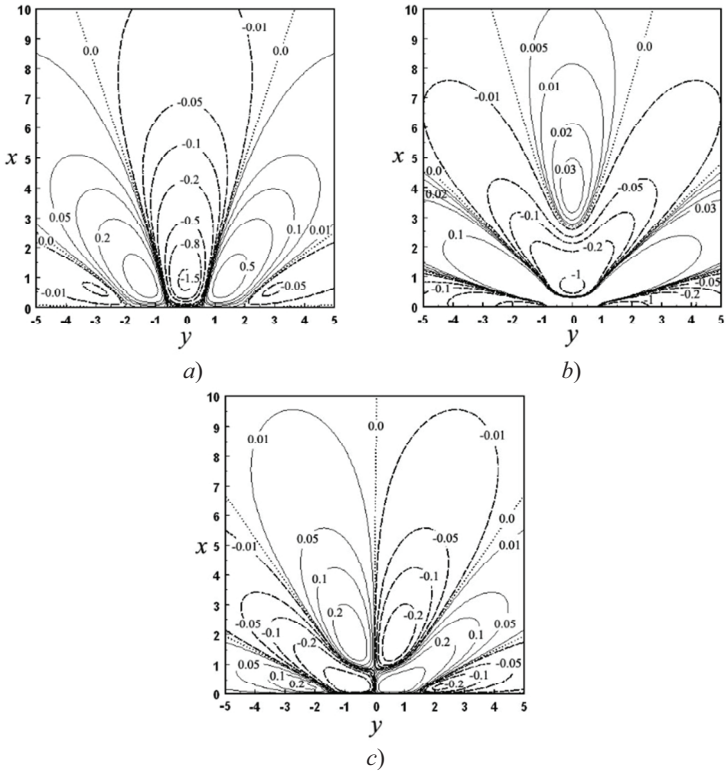

Figure 2.8. Distribution of the dimensionless thermal stresses (*a*) $10^{-2}\sigma_{yy}/(\alpha_\infty E_\infty \beta_1 \tau_0)$, (*b*) $10^{-2}\sigma_{xx}/(\alpha_\infty E_\infty \beta_1 \tau_0)$, and (*c*) $10^{-2}\sigma_{xy}(\alpha_\infty E_\infty \beta_1 \tau_0)$ in the half-plane for $\gamma_1 = 0$ and $\beta_2 = 1$ (adapted from our paper [239])

When analyzing the thermal stresses, we consider the plane stress case and assume the material properties in the form as follows:

$$E(y) = E_\infty \left(1 + \gamma_1 \exp(-\gamma_2 y)\right),$$

$$G(y) = G_\infty \left(1 + \gamma_1 \exp(-\gamma_2 y)\right),$$

$$\alpha(y) = \alpha_\infty \left(1 + \beta_1 \exp(-\beta_2 y)\right), \tag{2.5.55}$$

$$E_\infty, \gamma_1, \gamma_2 = \text{const}, \quad G_\infty = \frac{E_\infty}{2(1+\nu)},$$

$$\nu = \text{const}, \quad \alpha_\infty, \beta_1, \beta_2 = \text{const}.$$

All the constant parameters (2.5.55) are assumed to be not negative. Thus, for $y \to +\infty$, $E(y) \to E_\infty$, $G(y) \to G_\infty$, and $\alpha(y) \to \alpha_\infty$. At $y = 0$, these functions are equivalent to the constants $E_0 = (1+\gamma_1)E_\infty$, $G_0 = (1+\lambda)G_\infty$ and $\alpha_0 = (1+\beta_1)\alpha_\infty$. Thus, the assumption of material properties (2.5.55) meet the physical constrains adopted in linear elasticity theory [49].

In Fig. 2.8, the full-field analysis of the thermal stresses is shown for the case when $\gamma_1 = 0$ and $\beta_2 = 1$. As we can observe, thermal stresses arise in the half-plane even in the case if only the thermal expansion coefficient depends on the depth coordinate. Figure 2.9 shows how the thermal stresses depend on the inhomogeneity. As expected, the stresses are as more intensive as the material properties are of higher functional gradient. Plots in Fig. 2.8 *a* and *c*, as well as Fig. 2.9 *a* and *c* ensure that the stresses meet the condition of force-free boundary.

Consider the case of fixed boundary for an inhomogeneous isotropic strip $\mathfrak{D}_2$ with material properties

$$E = E_0 = \text{const}, \quad \nu = \nu_0 = 0.3,$$
$$\alpha = \alpha_0 (1 + y^m), \quad \alpha_0, m = \text{const}. \tag{2.5.56}$$

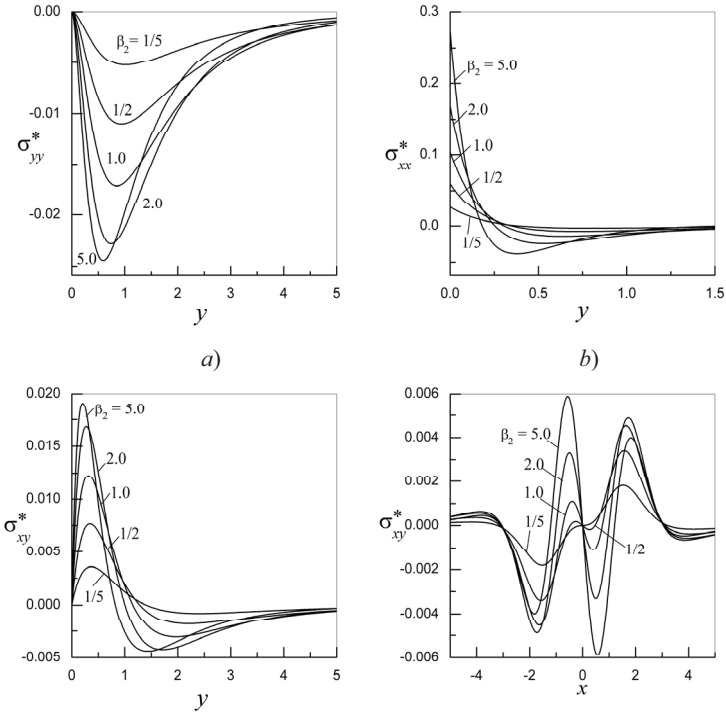

Figure 2.9. Comparison of thermal stresses in the half-plane for different cases on inhomogeneity, $\beta_2 = 1/5; 1/2; 1.0; 2.0; 3.0$ and $\lambda = 0$, showing: (*a*) $\sigma^*_{yy} = \sigma_{yy} / (\alpha_\infty E_\infty \beta_1 \tau_0)$ and (*b*) $\sigma^*_{xx} = \sigma_{xx} / (\alpha_\infty E_\infty \beta_1 \tau_0)$ at $x = 0$, and $\sigma^*_{xy} = \sigma_{xy} / (\alpha_\infty E_\infty \beta_1 \tau_0)$ at (*c*) $x = 1$ and (*d*) $y = 1$

The strip is under conditions (2.4.32), where

$$u_1(x) = v_1(x) = u_2(x) = v_2(x) = 0\,, \tag{2.5.57}$$

while subjected to the temperature field with Fourier mapping function

$$\overline{T}(y) = \tau_0 \sqrt{\pi} \exp\left(-\frac{s^2}{4}\right) \frac{\cosh sy}{\cosh s}\,, \tag{2.5.58}$$

where τ_0 is a constant parameter in the dimension of temperature. Temperature (2.5.58) has been obtained by solving the heat conduction equation with boundary conditions

$$T(x,\pm 1) = \tau_0 \exp\left(-x^2\right), \tag{2.5.59}$$

for materials with constant heat-conduction coefficient. Making use one-to-one relationships (2.4.46) and (2.4.50) between the given boundary displacements (2.5.57) and yet unknown boundary tractions $p_1(x)$, $p_2(x)$ and $q_1(x)$, $q_2(x)$, the latter ones can be evaluated and used for computing thermal stresses and displacements. In the Fig. 2.10, the temperature at $y = \pm 1$ and boundary tractions are shown for $m = 0$ (homogeneous material), $m = 1$, and $m = 3$ in (2.5.56). The tractions arise on the sides of strip in the zone, which approximately is twice wider than the zone of non-zero temperature distribution, and they vanish when moving away from it. The normal tractions are even functions of the longitudinal coordinate *x*, while the shearing tractions are odd functions. For homogenous material, $p_1 = p_2$ and $q_1 = -q_2$. If the linear thermal expansion coefficient depends on the transversal coordinate *y* in the form (2.5.56), then the tractions on sides $y = -1$ and $y = 1$ are different. As we can observe in the figure, the tractions on the side $y = -1$ are smaller in magnitude than the ones on the side $y = 1$. This can be explained by lesser thermal expansion of the side $y = -1$ and, thus, lower thermal stresses due to rigid fixation (2.5.57).

If the material of the inhomogeneous strip in the latter example is orthotropic with properties

$$E_y = \frac{E_x}{\delta_1} = \text{const}, \quad \frac{\nu_{xy}}{\delta_1} = \nu_{yx} = 0.3,$$

$$G_{xy} = \frac{E_x}{2(1+\nu_{xy})} = \text{const}, \tag{2.5.60}$$

$$\alpha_j = \alpha_j^0 (2+y)^k, \quad j = 1,2, \quad \frac{\alpha_2^0}{\delta_2} = \alpha_1^0.$$

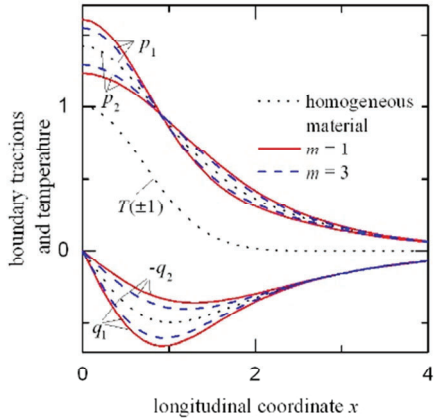

Figure 2.10. Boundary tractions and temperature on the sides $y = \pm 1$ of an isotropic inhomogeneous strip with material properties (2.5.56) due to temperature (2.5.60)

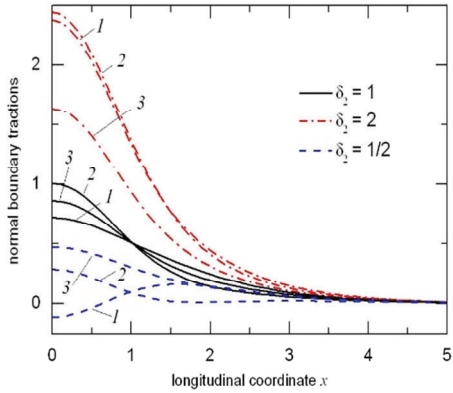

Figure 2.11. Dimensionless (normalized by $\alpha_1^0 E_x T_0$) normal tractions on the sides $y = \pm 1$ of the clamped orthotropic nonhomogeneous strip (curves *1*: p_1 at $k = 1$; curves *2*: p_2 at $k = 1$; curves *3*: p_1 and p_2 at $k = 0$)

then the boundary tractions those arise on the sides $y = \pm 1$ of the strip due to the temperature (2.5.58) and fixation condition (2.5.57) are shown in Fig. 2.11. As we can see, for the case of homogeneous material ($k = 0$), the tractions on both sides are equal for different ratio between the

constant elastic moduli. We can conclude that greater values of δ_2 cause the tractions of larger magnitude at $x = 0$. The anisotropy effects substantially in the distribution of tractions for both homogeneous and nonhomogeneous cases. Note that for the latter one, when $\delta_2 = \frac{1}{2}$ (dashed curve *1*), in contrast to the other cases, the traction p_1 is compressive in vicinity of $x = 0$. This can be explained by the fact that longitudinal thermal expansion is double of the transversal expansion, which leads to the contractions in transversal direction.

CHAPTER THREE

PLANE PROBLEMS FOR RADIALLY-INHOMOGENEOUS ELASTIC ANNULI

3.1. Governing equations and integral conditions

3.1.1. Governing equations in terms of stresses

Consider a plane problem (within the framework of either plane stress or plane strain) in an elastic annular domain $\Re = \{(\rho,\varphi): k \le \rho \le 1, \varphi \in [0,2\pi]\}$ using a dimensionless cylindrical-polar coordinate system (ρ,φ,z), where $z = \zeta / r_o$, $\rho = r / r_o$, $k = r_i / r_o$; r_i and r_o respectively indicate the inner and outer radii, and r and ζ are dimensional radial and axial coordinates. Assume that domain $\Re$ has cylindrically orthotropic material properties, which vary arbitrarily within the radial coordinate. The generalized strain-stress constitutive law for this plane problem is similar to (2.1.23), as follows:

$$\begin{aligned}
\varepsilon_{rr}(\rho,\varphi) &= a_{11}(\rho)\sigma_{rr}(\rho,\varphi) + a_{12}(\rho)\sigma_{\varphi\varphi}(\rho,\varphi) \\
&\quad +\varepsilon_1(\rho) + \alpha_1(\rho)T(\rho,\varphi), \\
\varepsilon_{\varphi\varphi}(\rho,\varphi) &= a_{12}(\rho)\sigma_{rr}(\rho,\varphi) + a_{22}(\rho)\sigma_{\varphi\varphi}(\rho,\varphi) \\
&\quad +\varepsilon_2(\rho) + \alpha_2(\rho)T(\rho,\varphi), \\
G_{r\varphi}(\rho)\varepsilon_{r\varphi}(\rho,\varphi) &= \sigma_{r\varphi}(\rho,\varphi).
\end{aligned} \tag{3.1.1}$$

Here, we assumed the initial temperature distribution of the stress-free state to be zero, i.e. $T_0 = 0$. Similar to (2.1.24),

$$a_{11}=\frac{1}{E_r}\begin{cases}1,\\ 1-\nu_{zr}\nu_{rz},\end{cases}\quad a_{22}=\frac{1}{E_\varphi}\begin{cases}1,\\ 1-\nu_{z\varphi}\nu_{\varphi z},\end{cases}$$

$$\varepsilon_1=\begin{cases}0,\\ -\nu_{zr}e_0,\end{cases}\quad \varepsilon_2=\begin{cases}0,\\ -\nu_{z\varphi}e_0,\end{cases}$$

$$a_{12}=-\frac{1}{E_\varphi}\begin{cases}\nu_{\varphi r},\\ \nu_{\varphi r}+\nu_{zr}\nu_{\varphi z},\end{cases}=-\frac{1}{E_r}\begin{cases}\nu_{r\varphi},\\ \nu_{r\varphi}+\nu_{rz}\nu_{z\varphi},\end{cases} \tag{3.1.2}$$

$$\alpha_1=\begin{cases}\alpha_r,\\ \alpha_r+\alpha_z\nu_{zr},\end{cases}\quad \alpha_2=\begin{cases}\alpha_\varphi,\\ \alpha_\varphi+\alpha_z\nu_{z\varphi}.\end{cases}$$

Furthermore, σ_{rr}, $\sigma_{\varphi\varphi}$, $\sigma_{r\varphi}$ and ε_{rr}, $\varepsilon_{\varphi\varphi}$, $\varepsilon_{r\varphi}$ are in-plane elastic stress- and strain-tensor components in the radial, circumferential, and tangential directions, respectively; and $E_r(\rho)$, $E_\varphi(\rho)$, and $E_z(\rho)$ are the Young moduli in the ρ, φ, and z directions, respectively; $\nu_{jk}(\rho)$ denotes the Poisson ratio describing the contraction in the j-direction under tension in the k-direction $\{j,k\}=\{r,\varphi,z\}$, $j\neq k$; $G_{r\varphi}(\rho)$ is the shear modulus within the (ρ,φ)-coordinate plane;; and $\alpha_j(\rho)$ is the linear thermal expansion coefficient in the j-direction. The orthotropic material properties represented by (3.1.2) meet the following symmetry conditions:

$$E_j\nu_{kj}=E_k\nu_{jk},\quad \{j,k\}=\{r,\varphi,z\},\quad j\neq k. \tag{3.1.3}$$

If the material of the considered domain is transversely isotropic, then coefficients (3.1.2) for the unified plane constitutive law (3.1.1) are as follows:

$$a_{11}=a_{22}=\frac{1}{E^*},\quad a_{12}=-\frac{\nu^*}{E^*},\quad \alpha_1=\alpha_2=\alpha^*,$$

$$\varepsilon_1=\varepsilon_2=-\varepsilon_0,\quad G_{r\varphi}=G, \tag{3.1.4}$$

$$E^* = \begin{cases} E, \\ \dfrac{EE'}{E' - \nu'^2 E}, \end{cases} \quad \nu^* = \begin{cases} \nu, \\ \dfrac{\nu E' + \nu'^2 E}{E' - \nu'^2 E}, \end{cases}$$
$$\alpha^* = \begin{cases} \alpha, \\ \alpha + \alpha'\nu', \end{cases} \quad \varepsilon_0 = \begin{cases} 0, \\ \nu' e_0. \end{cases} \tag{3.1.5}$$

Here, $E(\rho)$ and $E'(\rho)$ refer to the Young moduli under tension or compression respectively in the in-plane and out-of-plane directions; $\nu(\rho)$ is the Poisson ratio characterizing the out-of-plane contraction of ring $\mathfrak{R}$ in response to tension applied in the plane of isotropy; $\nu'(\rho)$ is the Poisson ratio characterizing in-plane contraction in response to tension applied in the out-of-plane direction; and $G(\rho)$, $\alpha(\rho)$ and $G'(\rho)$, $\alpha'(\rho)$ are the shear moduli and linear thermal expansion coefficients respectively in the in-plane and out-of-plane directions. Note that $2G = E^*/(1+\nu^*)$.

In the case of isotropic materials, coefficients (3.1.5) take the following form:

$$E^* = \begin{cases} E, \\ \dfrac{E}{1-\nu^2}, \end{cases} \quad \nu^* = \begin{cases} \nu, \\ \dfrac{\nu}{1-\nu}, \end{cases} \quad \alpha^* = \begin{cases} \alpha, \\ \alpha(1+\nu), \end{cases} \quad \varepsilon_0 = \begin{cases} 0, \\ \nu e_0. \end{cases} \tag{3.1.6}$$

Here, E and G are the Young and shear moduli, respectively, ν is the Poisson ratio, and α is the coefficient of linear thermal expansion.

In the case of plane strain, constant axial strain $\varepsilon_{zz} = e_0 = \text{const}$ either equals zero (when the end faces of a long hollow cylinder with cross-section $\mathfrak{R}$ are confined between two smooth rigid planes) or can be determined under following condition:

$$\iint_{\mathfrak{R}} \rho \sigma_{zz}(\rho,\varphi) d\rho d\varphi = p_{zz}^0, \tag{3.1.7}$$

where p_{zz}^0 is the resultant of normal stresses applied to the end-faces. If $p_{zz}^0 = 0$, then the end-faces are free of force loadings. Using the constitutive physical equation

$$\sigma_{zz}(\rho,\varphi) = E_z(\rho)e_0 + \nu_{zr}(\rho)\sigma_{rr}(\rho,\varphi)$$

$$+\nu_{z\varphi}(\rho)\sigma_{\varphi\varphi}(\rho,\varphi) - \alpha_z(\rho)E_z(\rho)T(\rho,\varphi), \tag{3.1.8}$$

condition (3.1.7) yields

$$e_0 = \frac{1}{2\pi e}\left(p_{zz}^0 - \iint_{\Re} \rho\left(\nu_{zr}(\rho)\sigma_{rr}(\rho,\varphi)\right)\right.$$

$$\left. + \nu_{z\varphi}(\rho)\sigma_{\varphi\varphi}(\rho,\varphi) - \alpha_z(\rho)E_z(\rho)T(\rho,\varphi)\right) d\rho d\varphi \Bigg), \tag{3.1.9}$$

where

$$e = \int_k^1 \rho E_z(\rho) d\rho\,. \tag{3.1.10}$$

The equilibrium equations (2.1.2) take the following form in the cylindrical-polar coordinate system (ρ,φ,z):

$$\frac{\partial\sigma_{rr}}{\partial\rho} + \frac{1}{\rho}\frac{\partial\sigma_{r\varphi}}{\partial\varphi} + \frac{\partial\sigma_{rz}}{\partial z} + \frac{\sigma_{rr}-\sigma_{\varphi\varphi}}{\rho} + F_r = 0,$$

$$\frac{\partial\sigma_{r\varphi}}{\partial\rho} + \frac{1}{\rho}\frac{\partial\sigma_{\varphi\varphi}}{\partial\varphi} + \frac{\partial\sigma_{\varphi z}}{\partial z} + 2\frac{\sigma_{r\varphi}}{\rho} + F_\varphi = 0, \tag{3.1.11}$$

$$\frac{\partial\sigma_{rz}}{\partial\rho} + \frac{1}{\rho}\frac{\partial\sigma_{\varphi z}}{\partial\varphi} + \frac{\partial\sigma_{zz}}{\partial z} + \frac{\sigma_{rz}}{\rho} + F_z = 0\,.$$

Here, F_r, F_φ, and F_z are projections of body forces onto the coordinate directions. In the cases of plane-stress and plane-strain, these equations take the following form:

$$\frac{1}{\rho}\frac{\partial}{\partial\rho}(\rho^2\sigma_{rr})+\frac{\partial\sigma_{r\varphi}}{\partial\varphi}+\rho F_r=\sigma,$$
$$\frac{1}{\rho}\frac{\partial}{\partial\rho}(\rho^2\sigma_{r\varphi})+\frac{\partial\sigma_{\varphi\varphi}}{\partial\varphi}+\rho F_\varphi=0. \tag{3.1.12}$$

The Cauchy equations (2.1.10) can be represented as follows:

$$\varepsilon_{rr}=\frac{\partial u_r}{\partial\rho},\quad \varepsilon_{r\varphi}=\frac{1}{\rho}\frac{\partial u_r}{\partial\varphi}+\frac{\partial u_\varphi}{\partial\rho}-\frac{u_\varphi}{\rho},$$
$$\varepsilon_{\varphi\varphi}=\frac{1}{\rho}\frac{\partial u_\varphi}{\partial\varphi}+\frac{u_r}{\rho},\quad \varepsilon_{\varphi z}=\frac{\partial u_\varphi}{\partial z}+\frac{1}{\rho}\frac{\partial u_z}{\partial\varphi}, \tag{3.1.13}$$
$$\varepsilon_{zz}=\frac{\partial u_z}{\partial z},\quad \varepsilon_{rz}=\frac{\partial u_z}{\partial r}+\frac{\partial u_r}{\partial z},$$

where u_r, u_φ, and u_z are the elastic displacements. Within the framework of plane formulation, equations (3.1.13) can be rewritten as follows:

$$\varepsilon_{rr}=\frac{\partial u_r}{\partial\rho},\qquad \varepsilon_{\varphi\varphi}=\frac{1}{\rho}\left(u_r+\frac{\partial u_\varphi}{\partial\varphi}\right),$$
$$\varepsilon_{r\varphi}=\frac{1}{\rho}\frac{\partial u_r}{\partial\varphi}+\rho\frac{\partial}{\partial\rho}\left(\frac{u_\varphi}{\rho}\right). \tag{3.1.14}$$

Note that the due to introduction of dimensionless coordinates, the right-hand sides of the latter equations are to be multiplied with $1/r_o$, which is omitted for the sake of brevity. By eliminating displacements from these equations, we can obtain the following strain-compatibility equation:

$$\frac{\partial^2(\rho\varepsilon_{r\varphi})}{\partial\rho\partial\varphi}=\frac{\partial^2\varepsilon_{rr}}{\partial\varphi^2}+\frac{\partial}{\partial\rho}\left(\rho^2\frac{\partial\varepsilon_{\varphi\varphi}}{\partial\rho}\right)-\rho\frac{\partial\varepsilon_{rr}}{\partial\rho}. \tag{3.1.15}$$

This equation corresponds to (2.1.19) in the Cartesian coordinate system.

Making use of constitutive equations (3.1.1) in conjunction with (3.1.8) permits the representation of compatibility equation (3.1.15) in terms of stresses, as follows:

$$\mathfrak{Q}\left(a_{22}\sigma+\alpha_2 T+\varepsilon_2\right)=\frac{1}{\rho}\frac{\partial}{\partial\rho}\left(\rho\sigma_{rr}\frac{d\beta_2}{d\rho}\right)$$

$$+\left\langle\frac{1}{\rho}\frac{\partial}{\partial\rho}-\frac{1}{\rho^2}\frac{\partial^2}{\partial\varphi^2}\right\rangle\left((\alpha_1-\alpha_2)T+\varepsilon_1-\varepsilon_2-\beta_3\sigma_{rr}\right)$$

$$+\frac{1}{\rho^2}\left(\frac{d}{d\rho}\left(\frac{\rho}{G_{r\varphi}}\right)-\frac{1}{\rho}\frac{d}{d\rho}\left(\rho^2\beta_2\right)\right)\frac{\partial\sigma_{r\varphi}}{\partial\varphi}$$

$$+\frac{1}{\rho}\left(\frac{1}{G_{r\varphi}}-2\beta_2\right)\frac{\partial^2\sigma_{r\varphi}}{\partial\rho\partial\varphi}\,. \tag{3.1.16}$$

Here,

$$\mathfrak{Q}=\frac{1}{\rho}\frac{\partial}{\partial\rho}\left(\rho\frac{\partial}{\partial\rho}\right)+\frac{1}{\rho^2}\frac{\partial^2}{\partial\varphi^2}\,, \tag{3.1.17}$$

$$\beta_j=a_{jj}-a_{12}\,,\quad \beta_3=a_{22}-a_{11}\,,\quad j=1,2\,, \tag{3.1.18}$$

and

$$\sigma=\sigma_{rr}+\sigma_{\varphi\varphi}\,. \tag{3.1.19}$$

We can use (3.1.19) to transform equilibrium equations (3.1.12) with the aim of expressing stress-tensor components in terms of the total stress (3.1.19), as follows:

$$\mathfrak{O}\sigma_{rr}(\rho,\varphi)=\frac{\partial}{\partial\rho}\left(\rho^2\sigma(\rho,\varphi)\right)+\rho\frac{\partial^2\sigma(\rho,\varphi)}{\partial\varphi^2},$$

$$\mathfrak{O}\sigma_{\varphi\varphi}(\rho,\varphi)=\rho\frac{\partial^2}{\partial\rho^2}\left(\rho^2\sigma(\rho,\varphi)\right), \tag{3.1.20}$$

$$\mathfrak{O}\sigma_{r\varphi}(\rho,\varphi)=-\rho\frac{\partial^2}{\partial\rho\partial\varphi}(\rho\sigma(\rho,\varphi)).$$

Note that the left side of equations (3.1.20) involves the same differential operator; i.e.,

$$\mathfrak{O}=\frac{\partial}{\partial\rho}\left(\rho\frac{\partial}{\partial\rho}\left(\rho^2\right)\right)+\rho\frac{\partial^2}{\partial\varphi^2}. \tag{3.1.21}$$

We can determine the steady-state temperature field $T(\rho,\varphi)$ distributed within orthotropic domain $\mathfrak{R}$ in which the material properties vary with radial coordinate ρ from the following equation of heat conduction [100, 124]:

$$\frac{1}{\rho}\frac{\partial}{\partial\rho}\left(\lambda_r(\rho)\rho\frac{\partial T(\rho,\varphi)}{\partial\rho}\right)$$

$$+\frac{1}{\rho^2}\frac{\partial}{\partial\varphi}\left(\lambda_\varphi(\rho)\frac{\partial T(\rho,\varphi)}{\partial\varphi}\right)=-w(\rho,\varphi), \tag{3.1.22}$$

where $w(\rho,\varphi)$ is the density of internal heat sources and $\lambda_r(\rho)$ and $\lambda_\varphi(\rho)$ are the heat-conduction coefficients in the radial and circumferential directions, respectively. This equation of heat conduction must be accompanied by thermal boundary conditions on the inner and outer surfaces of ring $\mathfrak{R}$.

3.1.2. Integral conditions of strain compatibility

Using the first equation in (3.1.14), the radial displacement can be determined as follows:

$$u_r(\rho,\varphi)=\frac{1}{2}U_r(\varphi)+\frac{1}{2}\int_k^1 \varepsilon_{rr}(\eta,\varphi)\,\mathrm{sgn}(\rho-\eta)d\eta\,, \tag{3.1.23}$$

where

$$U_r(\varphi)=u_r(k,\varphi)+u_r(1,\varphi)\,. \tag{3.1.24}$$

Inserting $\rho=k$ and $\rho=1$ into (3.1.23) yields the following condition:

$$\int_k^1 \varepsilon_{rr}(\rho,\varphi)d\rho=u_r(1,\varphi)-u_r(k,\varphi)\ . \tag{3.1.25}$$

By integrating the second equation in (3.1.14) over the angular coordinate φ in view of (3.1.23) and the angle-periodicity of the functions, we obtain the following expression for the circumferential displacement:

$$u_\varphi(\rho,\varphi)=u_\varphi(\rho,0)$$

$$+\frac{1}{4}\int_0^{2\pi}\Big(2\rho\varepsilon_{\varphi\varphi}(\rho,\xi)-U_r(\xi)\Big)\mathrm{sgn}(\varphi-\xi)d\xi$$

$$-\frac{1}{4}\iint_{\Re}\varepsilon_{rr}(\eta,\xi)\,\mathrm{sgn}(\rho-\eta)\,\mathrm{sgn}(\varphi-\xi)d\eta d\xi\,. \tag{3.1.26}$$

Inserting $\varphi=0$ or $\varphi=2\pi$ into (3.1.26) yields the following condition:

$$2\rho\int_0^{2\pi}\varepsilon_{\varphi\varphi}(\rho,\varphi)d\varphi-\iint_{\Re}\varepsilon_{rr}(\eta,\varphi)\,\mathrm{sgn}(\rho-\eta)d\eta d\varphi$$

$$=\int_0^{2\pi}U_r(\varphi)d\varphi\,. \tag{3.1.27}$$

If we substitute expressions (3.1.23) and (3.1.26) into the third equation in (3.1.14), we derive the following integro-differential equation:

$$4\varepsilon_{r\varphi}(\rho,\varphi)=\frac{2}{\rho}\frac{\partial}{\partial\varphi}\Bigg(U_r(\varphi)+\int_k^1\varepsilon_{rr}(\eta,\varphi)\operatorname{sgn}(\rho-\eta)d\eta\Bigg)$$

$$+\rho\frac{\partial}{\partial\rho}\Bigg(\frac{4}{\rho}u_\varphi(\rho,0)$$

$$+\int_0^{2\pi}\Big(2\varepsilon_{\varphi\varphi}(\rho,\xi)-\frac{1}{\rho}U_r(\xi)\Big)\operatorname{sgn}(\varphi-\xi)d\xi$$

$$-\frac{1}{\rho}\iint_{\Re}\varepsilon_{rr}(\eta,\xi)\operatorname{sgn}(\rho-\eta)\operatorname{sgn}(\varphi-\xi)d\eta d\xi\Bigg). \qquad (3.1.28)$$

This equation verbalizes the condition of strain compatibility within annular domain $\Re$. Applying differential operator $\frac{\partial^2}{\partial\rho\partial\varphi}(\rho\cdot)$ allows us to reduce this equation to the classical differential compatibility equation (3.1.15). However, deriving (3.1.28) from (3.1.15) requires that we fulfill the following fitting condition:

$$2\frac{\partial U_r(\varphi)}{\partial\varphi}+\int_0^{2\pi}U_r(\xi)\operatorname{sgn}(\varphi-\xi)d\xi+4\rho^2\frac{\partial}{\partial\rho}\Bigg(\frac{u_\varphi(\rho,0)}{\rho}\Bigg)$$

$$=2\Big(2\rho\varepsilon_{r\varphi}(\rho,0)+k\varepsilon_{r\varphi}(k,\varphi)$$

$$+\varepsilon_{r\varphi}(1,\varphi)-k\varepsilon_{r\varphi}(k,0)-\varepsilon_{r\varphi}(1,0)\Big)$$

$$+\int_0^{2\pi}\Bigg(k\varepsilon_{rr}(k,\xi)+\varepsilon_{rr}(1,\xi)$$

$$-k^2\left.\frac{\partial\varepsilon_{\varphi\varphi}(\rho,\xi)}{\partial\rho}\right|_{\rho=k}-\left.\frac{\partial\varepsilon_{\varphi\varphi}(\rho,\xi)}{\partial\rho}\right|_{\rho=1}\Bigg)\operatorname{sgn}(\varphi-\xi)d\xi$$

$$-2\int_k^1 \left.\frac{\partial \varepsilon_{rr}(\eta,\varphi)}{\partial \varphi}\right|_{\varphi=0} \operatorname{sgn}(\rho-\eta)d\eta\,. \tag{3.1.29}$$

By substituting $\varphi = 0$ into the third equation in (3.1.14) and making use of (3.1.23), we can obtain the following:

$$2\rho^2 \frac{\partial}{\partial \rho}\left(\frac{u_\varphi(\rho,0)}{\rho}\right) = 2\rho\varepsilon_{r\varphi}(\rho,0)$$

$$-\left.\frac{\partial U_r(\varphi)}{\partial \varphi}\right|_{\varphi=0} - \int_k^1 \left.\frac{\partial \varepsilon_{rr}(\eta,\varphi)}{\partial \varphi}\right|_{\varphi=0} \operatorname{sgn}(\rho-\eta)d\eta\,. \tag{3.1.30}$$

Substituting (3.1.30) in (3.1.27) and differentiating the result by φ to obtain the following:

$$\frac{d^2U_r(\varphi)}{d\varphi^2} + U_r(\varphi) = f(\varphi)\,, \tag{3.1.31}$$

where

$$f(\varphi) = \frac{d}{d\varphi}\Big(k\varepsilon_{r\varphi}(k,\varphi) + \varepsilon_{r\varphi}(1,\varphi)\Big)$$

$$+k\varepsilon_{rr}(k,\varphi) + \varepsilon_{rr}(1,\varphi)$$

$$-k^2 \left.\frac{\partial \varepsilon_{\varphi\varphi}(\rho,\varphi)}{\partial \rho}\right|_{\rho=k} - \left.\frac{\partial \varepsilon_{\varphi\varphi}(\rho,\varphi)}{\partial \rho}\right|_{\rho=1}\,. \tag{3.1.32}$$

The solution to equation (3.1.31) is derived as follows:

$$U_r(\varphi) = A\cos\varphi + B\sin\varphi + \frac{1}{2}\int_0^{2\pi} f(\xi)\sin|\varphi-\xi|\,d\xi\,, \tag{3.1.33}$$

where A and B are arbitrary constants of integration. The first derivative of this solution is

$$\frac{dU_r(\varphi)}{d\varphi} = -A\sin\varphi + B\cos\varphi$$

$$+\frac{1}{2}\int_0^{2\pi} f(\xi)\cos(\varphi-\xi)\,\mathrm{sgn}(\varphi-\xi)d\xi\,. \qquad (3.1.34)$$

If we substitute $\varphi = 0$ and $\varphi = 2\pi$ into (3.1.33) and (1.3.34) in view of the angle-periodicity of the functions, we obtain the following necessary conditions:

$$A = U_r(0), \quad B = \frac{dU_r(0)}{d\varphi}\,, \qquad (3.1.35)$$

$$\int_0^{2\pi} f\sin\varphi\, d\varphi = 0, \quad \int_0^{2\pi} f\cos\varphi\, d\varphi = 0\,. \qquad (3.1.36)$$

Within the context of (3.1.35), term $A\cos\varphi + B\sin\varphi$ in expression (3.1.33) describes radial translation of annular domain $\mathfrak{R}$ as a rigid solid. Thus, the constants (3.1.35) can be eliminated using of the corresponding fixation conditions.

In view of (3.1.32), conditions (3.1.36) imply the following strain-compatibility conditions:

$$\int_0^{2\pi}\Bigg(k\varepsilon_{rr}(k,\varphi) + \varepsilon_{rr}(1,\varphi)$$

$$-k^2\frac{\partial\varepsilon_{\varphi\varphi}(\rho,\varphi)}{\partial\rho}\bigg|_{\rho=k} - \frac{\partial\varepsilon_{\varphi\varphi}(\rho,\varphi)}{\partial\rho}\bigg|_{\rho=1}\Bigg)\sin\varphi d\varphi$$

$$= \int_0^{2\pi}\Big(k\varepsilon_{r\varphi}(k,\varphi) + \varepsilon_{r\varphi}(1,\varphi)\Big)\cos\varphi d\varphi, \qquad (3.1.37)$$

$$\int_0^{2\pi}\Bigg(k\varepsilon_{rr}(k,\varphi) + \varepsilon_{rr}(1,\varphi)$$

$$-k^2 \frac{\partial \varepsilon_{\varphi\varphi}(\rho,\varphi)}{\partial \rho}\bigg|_{\rho=k} - \frac{\partial \varepsilon_{\varphi\varphi}(\rho,\varphi)}{\partial \rho}\bigg|_{\rho=1}\Bigg)\cos\varphi d\varphi$$

$$= -\int_0^{2\pi} \Big(k\varepsilon_{r\varphi}(k,\varphi) + \varepsilon_{r\varphi}(1,\varphi)\Big)\sin\varphi d\varphi .$$

These conditions are important to the uniqueness of strains, stresses, and displacements in multiply-connected domain $\mathfrak{R}$ (see Section 3.2.3).

Determining function $U_r(\varphi)$ using (3.1.33) allows for the construction of radial displacement $u_r(\rho,\varphi)$ in the form (3.1.23). Moreover, in view of (3.1.35), expression (3.1.30) yields the following:

$$u_\varphi(\rho,0) = \frac{B}{2} + \rho C + \frac{\rho}{2}\int_k^1 \varepsilon_{r\varphi}(\eta,0)\frac{\operatorname{sgn}(\rho-\eta)}{\eta}d\eta$$

$$-\int_k^1 \frac{\partial \varepsilon_{rr}(\eta,\varphi)}{\partial \varphi}\bigg|_{\varphi=0}\left(\frac{\rho}{4}\left(1-\frac{1}{k}\right)+\frac{1}{2\eta}|\rho-\eta|\right)d\eta , \qquad (3.1.38)$$

where

$$C = \frac{1}{4k}\Big(2u_\varphi(k,0) + 2ku_\varphi(1,0) - (1+k)B\Big). \qquad (3.1.39)$$

Term $B + 2\rho C$ can be excluded from expression (3.1.38) to prevent rotation of ring $\mathfrak{R}$ as a rigid solid. In conjunction with (3.1.33) and (3.1.38), equation (3.1.26) makes it possible to determine the circumferential displacement using strain-tensor components.

3.2. Stress and displacement analysis

3.2.1. Solution representation and boundary conditions

Assume that radially-inhomogeneous annular domain $\mathfrak{R}$ is loaded by normal and shear forces on its inner and outer surfaces under the absence of body forces $F_\ell = 0$, $\ell = \{r,\varphi,z\}$:

$$\sigma_{rr}(k,\varphi) = -p_1(\varphi), \quad \sigma_{rr}(1,\varphi) = -p_2(\varphi),$$
$$\sigma_{r\varphi}(k,\varphi) = q_1(\varphi), \quad \sigma_{r\varphi}(1,\varphi) = q_2(\varphi). \tag{3.2.1}$$

Variables in the governing equations are separated by decomposing all of the angle-dependent functions into the Fourier series, as follows:

$$\sigma_{rr}(\rho,\varphi) = R_0(\rho) + \sum_{n=1}^{\infty}\left(R_n^1(\rho)\cos n\varphi + R_n^2(\rho)\sin n\varphi\right),$$

$$\sigma_{\varphi\varphi}(\rho,\varphi) = \Phi_0(\rho) + \sum_{n=1}^{\infty}\left(\Phi_n^1(\rho)\cos n\varphi + \Phi_n^2(\rho)\sin n\varphi\right),$$

$$\sigma(\rho,\varphi) = \sigma_0(\rho) + \sum_{n=1}^{\infty}\left(\sigma_n^1(\rho)\cos n\varphi + \sigma_n^2(\rho)\sin n\varphi\right),$$

$$T(\rho,\varphi) = T_0(\rho) + \sum_{n=1}^{\infty}\left(T_n^1(\rho)\cos n\varphi + T_n^2(\rho)\sin n\varphi\right), \tag{3.2.2}$$

$$p_j(\varphi) = p_{j0} + \sum_{n=1}^{\infty}\left(p_{jn}^1\cos n\varphi + p_{jn}^2(\rho)\sin n\varphi\right),$$

$$\sigma_{r\varphi}(\rho,\varphi) = S_0(\rho) + \sum_{n=1}^{\infty}\left(S_n^2(\rho)\cos n\varphi + S_n^1(\rho)\sin n\varphi\right),$$

$$q_j(\varphi) = q_{j0} + \sum_{n=1}^{\infty}\left(q_{jn}^2\cos n\varphi + q_{jn}^1(\rho)\sin n\varphi\right),$$

where $j = 1,2$ and

$$R_0(\rho) = \frac{1}{2\pi}\int_0^{2\pi}\sigma_{rr}(\rho,\varphi)d\varphi, \quad \Phi_0(\rho) = \frac{1}{2\pi}\int_0^{2\pi}\sigma_{\varphi\varphi}(\rho,\varphi)d\varphi,$$

$$\sigma_0(\rho)=\frac{1}{2\pi}\int_0^{2\pi}\sigma(\rho,\varphi)d\varphi,\quad T_0(\rho)=\frac{1}{2\pi}\int_0^{2\pi}T(\rho,\varphi)d\varphi,$$
$$S_0(\rho)=\frac{1}{2\pi}\int_0^{2\pi}\sigma_{r\varphi}(\rho,\varphi)d\varphi, \tag{3.2.3}$$
$$p_{j0}=\frac{1}{2\pi}\int_0^{2\pi}p_j(\varphi)d\varphi,\qquad q_{j0}=\frac{1}{2\pi}\int_0^{2\pi}q_j(\varphi)d\varphi,$$

and

$$R_n^1(\rho)=\frac{1}{\pi}\int_0^{2\pi}\sigma_{rr}(\rho,\varphi)\cos n\varphi d\varphi,$$
$$R_n^2(\rho)=\frac{1}{\pi}\int_0^{2\pi}\sigma_{rr}(\rho,\varphi)\sin n\varphi d\varphi,$$
$$\Phi_n^1(\rho)=\frac{1}{\pi}\int_0^{2\pi}\sigma_{\varphi\varphi}(\rho,\varphi)\cos n\varphi d\varphi,$$
$$\Phi_n^2(\rho)=\frac{1}{\pi}\int_0^{2\pi}\sigma_{\varphi\varphi}(\rho,\varphi)\sin n\varphi d\varphi,$$
$$\sigma_n^1(\rho)=\frac{1}{\pi}\int_0^{2\pi}\sigma(\rho,\varphi)\cos n\varphi d\varphi,$$
$$\sigma_n^2(\rho)=\frac{1}{\pi}\int_0^{2\pi}\sigma(\rho,\varphi)\sin n\varphi d\varphi,$$

$$T_n^1(\rho)=\frac{1}{\pi}\int_0^{2\pi}T(\rho,\varphi)\cos n\varphi d\varphi,$$

$$T_n^2(\rho)=\frac{1}{\pi}\int_0^{2\pi}T(\rho,\varphi)\sin n\varphi d\varphi,$$

$$S_n^1(\rho)=\frac{1}{\pi}\int_0^{2\pi}\sigma_{r\varphi}(\rho,\varphi)\sin n\varphi d\varphi,$$

$$S_n^2(\rho)=\frac{1}{\pi}\int_0^{2\pi}\sigma_{r\varphi}(\rho,\varphi)\cos n\varphi d\varphi,$$

$$p_{jn}^1=\frac{1}{\pi}\int_0^{2\pi}p_j(\varphi)\cos n\varphi d\varphi,$$

$$p_{jn}^2=\frac{1}{\pi}\int_0^{2\pi}p_j(\varphi)\sin n\varphi d\varphi,$$

$$q_{jn}^1=\frac{1}{\pi}\int_0^{2\pi}q_j(\varphi)\sin n\varphi d\varphi,$$

$$q_{jn}^2=\frac{1}{\pi}\int_0^{2\pi}q_j(\varphi)\cos n\varphi d\varphi. \qquad (3.2.4)$$

If external loadings (3.2.1) and the temperature field do not vary with angular coordinate φ, then stresses (3.2.2) can be represented only by the terms with subscript "0" given in (3.2.3). This represents the case of axial symmetry. If loadings (3.2.1) and the temperature vary with the angular coordinate, then stresses (3.2.2) necessarily involve the terms with subscript "*n*" given in (3.2.4). These two cases can be treated individually.

3.2.2. Solutions in the case of axial symmetry

Consider the case where the force and thermal loadings do not vary with the angular coordinate. Substituting expressions (3.2.2) into

equilibrium equations (3.1.12) and combining the terms with the subscript "0" yields

$$\frac{d}{d\rho}\left(\rho^2 R_0(\rho)\right) = \rho\sigma_0(\rho), \quad \frac{d}{d\rho}\left(\rho^2 S_0(\rho)\right) = 0. \tag{3.2.5}$$

Similarly, we can present compatibility equation (3.1.15) for the angle-independent parts of stresses as follows:

$$\begin{aligned}&\frac{d}{d\rho}\left(\rho\frac{d}{d\rho}\left(a_{22}(\rho)\sigma_0(\rho)+\varepsilon_2(\rho)+\alpha_2(\rho)T_0(\rho)\right)\right)\\ &=\frac{d}{d\rho}\left(\rho\frac{d}{d\rho}\left(\beta_2(\rho)R_0(\rho)\right)+\beta_1(\rho)R_0(\rho)-\beta_2(\rho)\Phi_0(\rho)\right.\\ &\left.+(\alpha_1(\rho)-\alpha_2(\rho))T_0(\rho)+\varepsilon_1(\rho)-\varepsilon_2(\rho)\right).\end{aligned} \tag{3.2.6}$$

Making use of (3.2.5) in conjunction with (3.1.19) and (3.1.3) allows us to represent equation (3.2.6) in the following form:

$$\begin{aligned}&\frac{d}{d\rho}\left(\rho\frac{d}{d\rho}\left(a_{22}\sigma_0(\rho)+\varepsilon_2(\rho)+\alpha_2(\rho)T_0(\rho)\right)\right)\\ &=\frac{d}{d\rho}\left(\left(\rho\frac{d\beta_2(\rho)}{d\rho}-\beta_3(\rho)\right)R_0(\rho)\right.\\ &\left.+(\alpha_1(\rho)-\alpha_2(\rho))T_0(\rho)+\varepsilon_1(\rho)-\varepsilon_2(\rho)\right).\end{aligned} \tag{3.2.7}$$

We then integrate it over the radial coordinate to obtain the following:

$$\begin{aligned}&\frac{d}{d\rho}\left(a_{22}(\rho)\sigma_0(\rho)+\varepsilon_2(\rho)+\alpha_2(\rho)T_0(\rho)\right)\\ &=\frac{1}{\rho}\left(\left(\rho\frac{d\beta_2(\rho)}{d\rho}-\beta_3(\rho)\right)R_0(\rho)\right.\end{aligned}$$

$$+(\alpha_1(\rho)-\alpha_2(\rho))T_0(\rho)+\varepsilon_1(\rho)-\varepsilon_2(\rho)\Big). \tag{3.2.8}$$

In the case of isotropic inhomogeneous materials, equation (3.2.8) complies with the compatibility equation in terms of stresses related to the one-dimensional thermoelasticity problem for a long hollow radially-inhomogeneous cylinder [252]. Note that we eliminate the constant of integration obtained when integrating equation (3.2.7) by imposing the condition of single-valuedness of displacement [282].

We solve equations (3.2.5) and (3.2.8) under the boundary conditions for radial stress

$$R_0(k)=-p_{10}, \qquad R_0(1)=-p_{20}, \tag{3.2.9}$$

and shear stress

$$S_0(k)=q_{10}, \qquad S_0(1)=q_{20}. \tag{3.2.10}$$

These conditions are obtained using (3.2.1) and (3.2.2).

A solution to the second equation in (3.2.5) under boundary conditions (3.2.10) can be derived as follows:

$$S_0(\rho)=\left(\frac{k}{\rho}\right)^2 q_{10}=\frac{q_{20}}{\rho^2}. \tag{3.2.11}$$

Similar to the case of a homogeneous isotropic material [298], solution (3.2.11) is irrespective of the material properties and temperature field. It is also easy to see that the condition

$$q_{20}=k^2 q_{10} \tag{3.2.12}$$

follows from (3.2.11), which in view of expressions (3.2.3) yields the following integral condition:

$$\int_0^{2\pi}\Big(q_2(\varphi)-k^2 q_1(\varphi)\Big)d\varphi=0 \tag{3.2.13}$$

for the shearing tractions on the inner and outer circumferences of annulus $\mathfrak{R}$. Note that solution (3.2.11) and condition (3.2.13) have been discussed in the literature on homogeneous isotropic materials [282, 298].

Integration of the first equation in (3.2.5) under the first condition in (3.2.9) yields the following expression for radial stress in the one-dimensional case:

$$R_0(\rho) = -\left(\frac{k}{\rho}\right)^2 p_{10} + \frac{1}{\rho^2}\int_k^\rho \eta\sigma_0(\eta)d\eta\,. \tag{3.2.14}$$

In view of the second condition in (3.2.9), expression (3.2.14) yields the following integral equilibrium condition:

$$\int_k^1 \rho\sigma_0(\rho)d\rho = k^2 p_{10} - p_{20}\,. \tag{3.2.15}$$

Note that expressions (3.2.11) and (3.2.14) are derived on the basis of equilibrium equations, which means that they remain the same for isotropic or anisotropic, homogeneous or inhomogeneous material properties.

By integrating equation (3.2.8) with expression (3.2.14) in mind, the following expression

$$\sigma_0(\rho) = \frac{1}{a_{22}(\rho)}\Bigg(A + \tilde{\varepsilon}_0(\rho) + \Theta_0(\rho) + p_{10}P_0(\rho)$$

$$+\int_k^\rho \frac{1}{\eta^2}\int_k^\eta \xi\sigma_0(\xi)d\xi\left(\frac{d\beta_2(\eta)}{d\eta} - \frac{\beta_3(\eta)}{\eta}\right)d\eta\Bigg) \tag{3.2.16}$$

can be obtained. Here, A is an arbitrary constant of integration and

$$\tilde{\varepsilon}_0(\rho) = -\varepsilon_2(\rho) + \int_k^\rho \frac{1}{\eta}\big(\varepsilon_1(\eta) - \varepsilon_2(\eta)\big)d\eta\,,$$

$$\Theta_0(\rho) = -\alpha_2(\rho)T_0(\rho) \tag{3.2.17}$$

$$+\int_k^\rho \frac{1}{\eta}\big((\alpha_1(\eta) - \alpha_2(\eta))T_0(\eta)\big)d\eta,$$

$$P_0(\rho) = k^2 \int_k^\rho \frac{1}{\eta^2}\left(\frac{\beta_3(\eta)}{\eta} - \frac{d\beta_2(\eta)}{d\eta}\right)d\eta\,.$$

Changing the order of integration in equation (3.2.16) yields the following Volterra integral equation of the second kind:

$$\sigma_0(\rho) = \frac{1}{a_{22}(\rho)}\Bigg(A + \tilde{\varepsilon}_0(\rho) + \Theta_0(\rho) + p_{10}P_0(\rho) + \int_k^\rho \sigma_0(\xi)\mathcal{K}_0(\rho,\xi)d\xi \Bigg), \tag{3.2.18}$$

where the kernel is given as

$$\mathcal{K}_0(\rho,\xi) = \xi\int_\xi^\rho \frac{1}{\eta^2}\left(\frac{d\beta_2(\eta)}{d\eta} - \frac{\beta_3(\eta)}{\eta}\right)d\eta\,. \tag{3.2.19}$$

Using the resolvent-kernel technique (see Chapter 2) allows us to obtain the following solution to equation (3.2.18):

$$\sigma_0(\rho) = \frac{1}{a_{22}(\rho)}\Bigg(Af(\rho) + \varepsilon(\rho) + \Theta_0(\rho) + p_{10}P_0(\rho) + \int_k^\rho \frac{\Theta_0(\xi) + p_{10}P_0(\xi)}{a_{22}(\xi)}\mathcal{R}_0(\rho,\xi)d\xi \Bigg). \tag{3.2.20}$$

Here,

$$\begin{aligned} f(\rho) &= 1 + \int_k^\rho \frac{\mathcal{R}_0(\rho,\xi)}{a_{22}(\xi)}d\xi, \\ \varepsilon(\rho) &= \tilde{\varepsilon}_0(\rho) + \int_k^\rho \frac{\tilde{\varepsilon}_0(\xi)}{a_{22}(\xi)}\mathcal{R}_0(\rho,\xi)d\xi, \end{aligned} \tag{3.2.21}$$

where the resolvent kernel can be computed as a series

$$\mathcal{R}_0(\rho,\xi)=\sum_{m=0}^{\infty}\mathcal{K}_{m+1}^0(\rho,\xi) \tag{3.2.22}$$

of recurring kernels

$$\begin{gathered}\mathcal{K}_1^0(\rho,\xi)=\mathcal{K}_0(\rho,\xi),\\ \mathcal{K}_{m+1}^0(\rho,\xi)=\int_{\xi}^{\rho}\frac{\mathcal{K}_1^0(\rho,\eta)\mathcal{K}_m^0(\eta,\xi)}{a_{22}(\eta)}d\eta.\end{gathered} \tag{3.2.23}$$

The constant of integration A can be eliminated by substituting (3.2.20) into integral condition (3.2.15). Then, expression (3.2.20) for the total stress component takes the following form:

$$\begin{aligned}\sigma_0(\rho)=\frac{1}{a_{22}(\rho)}\Bigg(&(k^2p_{10}-p_{20}-b_0)\frac{f(\rho)}{a_0}\\ &+\zeta(\rho)+\Theta_0(\rho)+p_{10}P_0(\rho)\\ &+\int_k^{\rho}\frac{\Theta_0(\xi)+p_{10}P_0(\xi)}{a_{22}(\xi)}\mathcal{R}_0(\rho,\xi)d\xi\Bigg),\end{aligned} \tag{3.2.24}$$

where

$$\begin{gathered}a_0=\int_k^1\frac{\rho f(\rho)}{a_{22}(\rho)}d\rho,\quad \zeta(\rho)=\varepsilon(\rho)-\frac{f(\rho)}{a_0}\int_k^1\frac{\rho\varepsilon(\rho)}{a_{22}(\rho)}d\rho,\\ b_0=\int_k^1\frac{\rho}{a_{22}(\rho)}\Bigg(\Theta_0(\rho)+p_{10}P_0(\rho)\\ +\int_k^{\rho}\frac{\Theta_0(\xi)+p_{10}P_0(\xi)}{a_{22}(\xi)}\mathcal{R}_0(\rho,\xi)d\xi\Bigg)d\rho.\end{gathered} \tag{3.2.25}$$

The total stress represented by (3.2.24) can also be written explicitly in terms of applied loadings:

$$\sigma_0(\rho) = p_{10}P_{10}(\rho) + p_{20}P_{20}(\rho) + \theta_0(\rho) + \frac{\zeta(\rho)}{a_{22}(\rho)}. \qquad (3.2.26)$$

Here,

$$P_{10}(\rho) = \frac{1}{a_{22}(\rho)}\left(\frac{f(\rho)}{a_0}\left(k^2 - \int_k^1 P_0(\xi)\varphi_0(\xi)d\xi\right)\right.$$

$$\left. + P_0(\rho) + \int_k^\rho \frac{P_0(\xi)}{a_{22}(\xi)}\mathcal{R}_0(\rho,\xi)d\xi\right),$$

$$P_{20}(\rho) = -\frac{f(\rho)}{a_0 a_{22}(\rho)}, \qquad (3.2.27)$$

$$\theta_0(\rho) = \frac{1}{a_{22}(\rho)}\left(\Theta_0(\rho) + \int_k^\rho \frac{\Theta_0(\xi)}{a_{22}(\xi)}\mathcal{R}_0(\rho,\xi)d\xi\right.$$

$$\left. - \frac{f(\rho)}{a_0}\int_k^1 \Theta_0(\xi)\varphi_0(\xi)d\xi\right),$$

$$\varphi_0(\xi) = \frac{1}{a_{22}(\xi)}\left(\xi + \int_\xi^1 \rho\frac{\mathcal{R}_0(\rho,\xi)}{a_{22}(\rho)}d\rho\right).$$

After finding the axisymmetric component of the total stress in form (3.2.26), we can use (3.2.14) and (3.1.19) to derive the following expressions for the radial and circumferential components:

$$\begin{aligned} R_0(\rho) &= p_{10}P_{10}^r(\rho) + p_{20}P_{20}^r(\rho) + \theta_0^r(\rho) + \zeta^r(\rho), \\ \Phi_0(\rho) &= p_{10}P_{10}^\varphi(\rho) + p_{20}P_{20}^\varphi(\rho) + \theta_0^\varphi(\rho) + \zeta^\varphi(\rho), \end{aligned} \qquad (3.2.28)$$

where

$$P_{j0}^r(\rho) = -\delta_{j1}\left(\frac{k}{\rho}\right)^2 + \frac{1}{\rho^2}\int_k^\rho \eta P_{j0}(\eta)d\eta,$$

$$P_{j0}^{\varphi}(\rho) = P_{j0}(\rho) - P_{j0}^{r}(\rho), \quad j = 1,2,$$

$$\theta_0^r(\rho) = \frac{1}{\rho^2}\int_k^\rho \eta\theta_0(\eta)d\eta, \quad \theta_0^\varphi(\rho) = \theta_0(\rho) - \theta_0^r(\rho), \tag{3.2.29}$$

$$\zeta^r(\rho) = \frac{1}{\rho^2}\int_k^\rho \eta\frac{\zeta(\eta)}{a_{22}(\eta)}d\eta, \quad \zeta^\varphi(\rho) = \frac{\zeta(\rho)}{a_{22}(\rho)} - \zeta^r(\rho),$$

and δ_{j1} is the Kronecker delta.

Expressions (3.2.26) and (3.2.28) contain undetermined terms $\zeta(\rho)$, $\zeta^r(\rho)$, and $\zeta^\varphi(\rho)$ expressed in terms of axial strain e_0 (see (3.1.2)). As mentioned in Section 3.1.1, this strain equals zero, $e_0 = 0$, in the case of plane stress or plane strain of an inhomogeneous cylinder whose end-faces are confined between two absolutely rigid smooth planes. In these cases, it is obvious that

$$\zeta(\rho) = \zeta^r(\rho) = \zeta^\varphi(\rho) = 0. \tag{3.2.30}$$

Thus, expressions (3.2.26) and (3.2.28) take the following forms:

$$\sigma_0(\rho) = p_{10}P_{10}(\rho) + p_{20}P_{20}(\rho) + \theta_0(\rho),$$

$$R_0(\rho) = p_{10}P_{10}^r(\rho) + p_{20}P_{20}^r(\rho) + \theta_0^r(\rho), \tag{3.2.31}$$

$$\Phi_0(\rho) = p_{10}P_{10}^\varphi(\rho) + p_{20}P_{20}^\varphi(\rho) + \theta_0^\varphi(\rho).$$

In the case of plane strain in a cylinder, the end-faces of which are subject to normal force loadings with resultant vector p_{zz}^0, we can use (3.1.9) in conjunction with (3.1.19), (3.2.2), (3.2.14), and (3.2.26) to obtain the following expressions:

$$\zeta(\rho) = e_0\zeta_0(\rho), \quad \zeta^r(\rho) = e_0\zeta_0^r(\rho), \quad \zeta^\varphi(\rho) = e_0\zeta_0^\varphi(\rho), \tag{3.2.32}$$

where

$$\zeta_0(\rho) = \varepsilon_{00}(\rho) - \frac{f(\rho)}{a_0}\int_k^1 \varepsilon_{00}(\xi)\varphi_0(\xi)d\xi$$

$$+\int_k^\rho \frac{\varepsilon_{00}(\xi)}{a_{22}(\xi)}\mathcal{R}_0(\rho,\xi)d\xi,$$

$$\zeta_0^r(\rho) = \frac{1}{\rho^2}\int_k^\rho \eta\frac{\zeta_0(\eta)}{a_{22}(\eta)}d\eta, \quad \zeta_0^\varphi(\rho) = \frac{\zeta_0(\rho)}{a_{22}(\rho)} - \zeta_0^r(\rho), \tag{3.2.33}$$

$$\varepsilon_{00}(\rho) = \nu_{z\varphi}(\rho) + \int_k^\rho \frac{1}{\eta}\left(\nu_{z\varphi}(\eta) - \nu_{zr}(\eta)\right)d\eta,$$

and

$$e_0 = \frac{p_{zz}^0}{2\pi(e+e_1)} + p_{10}P_{1e} + p_{20}P_{2e} + \theta_e. \tag{3.2.34}$$

Here,

$$P_{je} = -\frac{1}{e+e_1}\int_k^1 \rho\left(\nu_{zr}(\rho)P_{j0}^r(\rho) + \nu_{z\varphi}(\rho)P_{j0}^\varphi(\rho)\right)d\rho,$$

$$\theta_e = \frac{1}{e+e_1}\int_k^1 \rho\left(\alpha_z(\rho)E_z(\rho)T_0(\rho)\right.$$

$$\left.-\nu_{zr}(\rho)\theta_0^r(\rho) - \nu_{z\varphi}(\rho)\theta_0^\varphi(\rho)\right)d\rho, \tag{3.2.35}$$

$$e_1 = \int_k^1 \rho\left(\nu_{zr}(\rho)\zeta_0^r(\rho) + \nu_{z\varphi}(\rho)\zeta_0^\varphi(\rho)\right)d\rho,$$

and e is given by (3.1.10).

In view of (3.2.32) and (3.2.34), axisymmetric components (3.2.26) and (3.2.28) can be written as follows:

$$\sigma_0(\rho) = p_{10}\left(P_{10}(\rho) + \frac{P_{1e}\zeta_0(\rho)}{a_{22}(\rho)}\right) + p_{20}\left(P_{20}(\rho) + \frac{P_{2e}\zeta_0(\rho)}{a_{22}(\rho)}\right)$$

$$+\theta_0(\rho) + \frac{\theta_e\zeta_0(\rho)}{a_{22}(\rho)} + \frac{p^0_{zz}\zeta_0(\rho)}{2\pi(e+e_1)a_{22}(\rho)},$$

$$R_0(\rho) = p_{10}\left(P^r_{10}(\rho) + P_{1e}\zeta^r_0(\rho)\right)$$

$$+p_{20}\left(P^r_{20}(\rho) + P_{2e}\zeta^r_0(\rho)\right) \qquad (3.2.36)$$

$$+\theta^r_0(\rho) + \theta_e\zeta^r_0(\rho) + \frac{p^0_{zz}\zeta^r_0(\rho)}{2\pi(e+e_1)},$$

$$\Phi_0(\rho) = p_{10}\left(P^\varphi_{10}(\rho) + P_{1e}\zeta^\varphi_0(\rho)\right) + p_{20}\left(P^\varphi_{20}(\rho) + P_{2e}\zeta^\varphi_0(\rho)\right)$$

$$+\theta^\varphi_0(\rho) + \theta_e\zeta^\varphi_0(\rho) + \frac{p^0_{zz}\zeta^\varphi_0(\rho)}{2\pi(e+e_1)}.$$

If it is impossible to evaluate the resolvent kernel (3.2.22) for certain material properties, then it can be substituted in practical computations using the following approximation:

$$\mathcal{R}_0(\rho,\xi) \approx \mathcal{R}^N_0(\rho,\xi) = \sum_{m=0}^{N} \mathcal{K}^0_{m+1}(\rho,\xi), \qquad (3.2.37)$$

where natural digit N allows for satisfaction of equation (3.2.18) within the required degree of accuracy.

3.2.3. Angle-dependent (non-axisymmetric) components

In order to determine the angle-dependent parts of series (3.2.2), which are indicated by coefficients (3.2.4), the sine- and cosine-transforms (3.2.4) are to be applied to equations of equilibrium (3.1.12) to obtain

$$\frac{1}{\rho}\frac{d}{d\rho}\left(\rho^2 R_n^\ell(\rho)\right) - (-1)^\ell n S_n^\ell(\rho) = \sigma_n^\ell(\rho),$$
$$\frac{1}{\rho}\frac{d}{d\rho}\left(\rho^2 S_n^\ell(\rho)\right) + (-1)^\ell n \Phi_n^\ell(\rho) = 0, \tag{3.2.38}$$

where $\ell = 1, 2$. From (3.1.20), we can derive alternative equations:

$$\mathfrak{O}_n R_n^\ell(\rho) = \frac{d}{d\rho}\left(\rho^2 \sigma_n^\ell(\rho)\right) - n^2 \rho \sigma_n^\ell(\rho),$$
$$\mathfrak{O}_n \Phi_n^\ell(\rho) = \rho \frac{d^2}{\partial d^2}\left(\rho^2 \sigma_n^\ell(\rho)\right), \tag{3.2.39}$$
$$\mathfrak{O}_n(\rho) S_n^\ell(\rho) = (-1)^{\ell+1} n\rho \frac{d}{d\rho}\left(\rho \sigma_n^\ell(\rho)\right),$$

where

$$\mathfrak{O}_n = \frac{d}{d\rho}\left(\rho \frac{d}{d\rho}\left(\rho^2\right)\right) - n^2 \rho\,. \tag{3.2.40}$$

Similarly, equation (3.1.19) yields

$$\sigma_n^\ell(\rho) = R_n^\ell(\rho) + \Phi_n^\ell(\rho)\,. \tag{3.2.41}$$

We then obtain the following boundary conditions for the angle-dependent terms of expressions (3.2.2) using the transforms given in (3.2.4):

$$R_n^\ell(k) = -p_{1n}^\ell, \quad R_n^\ell(1) = -p_{2n}^\ell,$$
$$S_n^\ell(k) = q_{1n}^\ell, \quad S_n^\ell(1) = q_{2n}^\ell. \tag{3.2.42}$$

One solution to the third equation in (3.2.39) under the third and fourth conditions in (3.2.42) is

$$S_n^\ell(\rho) = \frac{(\rho^{-n} - \rho^n) k^2 q_{1n}^\ell}{(k^{-n} - k^n)\rho^2}$$

$$-\frac{(-1)^{\ell}}{2\rho^2}\int_k^{\rho}\eta\sigma_n^i(\eta)\left(n\chi_n^+(\rho,\eta)+\chi_n^-(\rho,\eta)\right)d\eta$$

$$-\frac{\chi_n^-(\rho,k)}{2\rho^2(k^{-n}-k^n)}\Bigg(2q_{2n}^{\ell}$$

$$+(-1)^{\ell}\int_k^1\rho\sigma_n^{\ell}(\rho)\left(\rho^{-n}(n-1)+\rho^n(n+1)\right)d\rho\Bigg), \tag{3.2.43}$$

where

$$\chi_n^{\pm}(x,y)=\left(\frac{y}{x}\right)^n\pm\left(\frac{x}{y}\right)^n, \tag{3.2.44}$$

and x and y are arbitrary arguments.

Using the second equation in (3.2.38) in conjunction with expression (3.2.43) yields

$$\Phi_n^{\ell}(\rho)=\frac{(-1)^{\ell}(\rho^{-n}+\rho^n)k^2q_{1n}^{\ell}}{(k^{-n}-k^n)\rho^2}$$

$$-\frac{1}{2\rho^2}\int_k^{\rho}\eta\sigma_n^{\ell}(\eta)\left(n\chi_n^-(\rho,\eta)+\chi_n^+(\rho,\eta)\right)d\eta+\sigma_n^{\ell}$$

$$-\frac{\chi_n^+(\rho,k)}{2\rho^2(k^{-n}-k^n)}\Bigg(2(-1)^{\ell}q_{2n}^{\ell}$$

$$+\int_k^1\rho\sigma_n^{\ell}(\rho)\left(\rho^{-n}(n-1)+\rho^n(n+1)\right)d\rho\Bigg). \tag{3.2.45}$$

Using (3.2.41) and (3.2.45), we can now express the coefficients of the angle-dependent part of radial stress through the corresponding angle-dependent part of total stress, as follows:

$$R_n^\ell(\rho) = -\frac{(-1)^\ell(\rho^{-n}+\rho^n)k^2 q_{1n}^\ell}{(k^{-n}-k^n)\rho^2}$$

$$+\frac{1}{2\rho^2}\int_k^\rho \eta\sigma_n^\ell(\eta)\left(n\chi_n^-(\rho,\eta)+\chi_n^+(\rho,\eta)\right)d\eta$$

$$+\frac{\chi_n^+(\rho,k)}{2\rho^2(k^{-n}-k^n)}\Bigg(2(-1)^\ell q_{2n}^\ell$$

$$+\int_k^1 \rho\sigma_n^\ell(\rho)\left(\rho^{-n}(n-1)+\rho^n(n+1)\right)d\rho\Bigg). \qquad (3.2.46)$$

Inserting (3.2.46) into the first and second conditions in (3.2.42) allows us to derive two integral conditions

$$(n+1)\int_k^1 \rho^{1+n}\sigma_n^\ell(\rho)d\rho$$

$$= k^{2+n}p_{1n}^\ell - p_{2n}^\ell + (-1)^\ell\left(k^{2+n}q_{1n}^\ell - q_{2n}^\ell\right), \qquad (3.2.47)$$

$$(n-1)\int_k^1 \rho^{1-n}\sigma_n^\ell(\rho)d\rho$$

$$= p_{2n}^\ell - k^{2-n}p_{1n}^\ell + (-1)^\ell\left(k^{2-n}q_{1n}^\ell - q_{2n}^\ell\right) \qquad (3.2.48)$$

for the coefficients $\sigma_n^\ell(\rho)$ of the angle-dependent parts of the total stress.

Note that condition (3.2.48) cannot be used for the first harmonic $n=1$, as the left-left side changes to zero. In this case, the right-hand side of (3.2.48) yields the following:

$$p_{21}^\ell - (-1)^\ell q_{21}^\ell = k\left(p_{11}^\ell - (-1)^\ell q_{11}^\ell\right). \qquad (3.2.49)$$

In view of expressions (3.2.4), we can rewrite this as follows:

$$\int_0^{2\pi}(p_2+q_2)\cos\varphi d\varphi = k\int_0^{2\pi}(p_1+q_1)\cos\varphi d\varphi,$$
$$\int_0^{2\pi}(p_2-q_2)\sin\varphi d\varphi = k\int_0^{2\pi}(p_1-q_1)\sin\varphi d\varphi. \tag{3.2.50}$$

Conditions (3.2.50) are well-known in elasticity theory (e.g., [282, p. 134]). They articulate the condition of equilibrium for the external normal and shear forces acting on the inner and outer circumferences of annular domain $\mathfrak{R}$ in projections onto the Cartesian axes.

In view of integral conditions (3.2.47) and (3.2.48), we can simplify expressions (3.2.43), (3.2.45), and (3.2.46) as follows:

$$S_n^{\ell}(\rho) = \frac{1}{2\rho^2}\left(k^2\chi_n^+(\rho,k)q_{1n}^{\ell} + (-1)^{\ell}k^2\chi_n^-(\rho,k)p_{1n}^{\ell} \right.$$
$$\left. -(-1)^{\ell}\int_k^{\rho}\eta\sigma_n^{\ell}(\eta)\left(n\chi_n^+(\rho,\eta)+\chi_n^-(\rho,\eta)\right)d\eta \right),$$
$$R_n^{\ell}(\rho) = \frac{1}{2\rho^2}\left((-1)^{\ell+1}k^2\chi_n^-(\rho,k)q_{1n}^{\ell} - k^2\chi_n^+(\rho,k)p_{1n}^{\ell} \right. \tag{3.2.51}$$
$$\left. +\int_k^{\rho}\eta\sigma_n^{\ell}(\eta)\left(n\chi_n^-(\rho,\eta)+\chi_n^+(\rho,\eta)\right)d\eta \right),$$
$$\Phi_n^{\ell}(\rho) = \sigma_n^{\ell} + \frac{1}{2\rho^2}\left((-1)^{\ell}k^2\chi_n^-(\rho,k)q_{1n}^{\ell} + k^2\chi_n^+(\rho,k)p_{1n}^{\ell} \right.$$
$$\left. -\int_k^{\rho}\eta\sigma_n^{\ell}(\eta)\left(n\chi_n^-(\rho,\eta)+\chi_n^+(\rho,\eta)\right)d\eta \right).$$

These expressions represent the angle-dependent constituents of normal and shear stresses in terms of the corresponding total-stress constituents. Along with conditions (3.2.47) – (3.2.50), they are derived on the basis of equilibrium equations. Thus, they do not depend on material properties and

can be used for homogeneous or inhomogeneous, isotropic or anisotropic materials. Ultimately, determining the constituents of the stress-tensor components requires that we calculate the total stress using equation (3.1.15) under conditions (3.2.47) and (3.2.48).

Making use of the transforms defined by expressions (3.2.4), the compatibility equation (3.1.15), in view of the equations in (3.2.39) for the shear stress, can be represented as

$$\mathfrak{Q}_n\left(a_{22}(\rho)\sigma_n^{\ell}(\rho)+\alpha_2(\rho)T_n^{\ell}(\rho)\right)$$

$$=\mathfrak{G}_n^{\rho}\left((\alpha_1(\rho)-\alpha_2(\rho))T_n^{\ell}(\rho)\right)$$

$$+\left(\frac{1}{\rho}\frac{d}{d\rho}\left(\frac{1}{\rho}\left(2\beta_2(\rho)-\frac{1}{G_{r\varphi}(\rho)}\right)\right)-\frac{\beta_3(\rho)}{\rho^3}\right)\frac{d}{d\rho}\left(\rho^2R_n^{\ell}(\rho)\right)$$

$$+\left(\rho\frac{d}{d\rho}\left(\frac{1}{\rho}\frac{d\beta_2(\rho)}{d\rho}-\frac{\beta_3(\rho)}{\rho^2}\right)\right.$$

$$\left.+\frac{n^2}{\rho^2}\left(\beta_1(\rho)+\beta_2(\rho)-\frac{1}{G_{r\varphi}(\rho)}\right)\right)R_n^{\ell}(\rho)$$

$$+\frac{1}{\rho}\left(\frac{d}{d\rho}\left(\frac{1}{G_{r\varphi}(\rho)}-\beta_2(\rho)\right)\right.$$

$$\left.+\frac{n^2-1}{\rho}\left(\frac{1}{G_{r\varphi}(\rho)}-2\beta_2(\rho)\right)\right)\sigma_n^{\ell}(\rho)\,. \qquad (3.2.52)$$

Here, $\beta_1(\rho)$ is given in (3.1.18) and

$$\mathfrak{Q}_n=\frac{1}{\rho}\frac{d}{d\rho}\left(\rho\frac{d}{d\rho}\right)-\left(\frac{n}{\rho}\right)^2,\qquad \mathfrak{G}_n^{\rho}=\frac{1}{\rho}\frac{d}{d\rho}+\left(\frac{n}{\rho}\right)^2. \qquad (3.2.53)$$

Inserting expression (3.2.51) for the radial stress into equation (3.2.52) allows us to represent the latter equation in the following form:

$$\mathfrak{Q}_n\left(a_{22}(\rho)\sigma_n^{\ell}(\rho)+\alpha_2(\rho)T_n^{\ell}(\rho)\right)=\mathfrak{G}_n^{\rho}\left((\alpha_1(\rho)-\alpha_2(\rho))T_n^{\ell}(\rho)\right)$$

$$+\frac{1}{\rho^2}\Bigg((-1)^\ell k^2 q_{1n}^\ell \left(k^n \rho^{-n}\psi_n^-(\rho)+k^{-n}\rho^n\psi_n^+(\rho)\right)$$

$$+k^2 p_{1n}^\ell \left(k^n \rho^{-n}\psi_n^-(\rho)-k^{-n}\rho^n\psi_n^+(\rho)\right)\Big)+2\rho^2\psi_n(\rho)\sigma_n^\ell(\rho)$$

$$-\int_k^\rho \eta\sigma_n^\ell(\eta)\left((n+1)\rho^{-n}\eta^n\psi_n^-(\rho)+(n-1)\rho^n\eta^{-n}\psi_n^+(\rho)\right)d\eta\Bigg), \quad (3.2.54)$$

where

$$\psi_n^\pm(\rho)=n\frac{d}{d\rho}\left(\frac{1}{\rho}\left(2\beta_2(\rho)-\frac{1}{G_{r\varphi}(\rho)}\right)\right)$$

$$-\frac{n\beta_3(\rho)}{\rho^2}\pm\rho\frac{d}{d\rho}\left(\frac{1}{\rho}\frac{d\beta_2(\rho)}{d\rho}-\frac{\beta_3(\rho)}{\rho^2}\right)$$

$$\pm\frac{n^2}{\rho^2}\left(\beta_1(\rho)+\beta_2(\rho)-\frac{1}{G_{r\varphi}(\rho)}\right), \quad (3.2.55)$$

$$\psi_n(\rho)=\frac{d}{d\rho}\left(\frac{\beta_2(\rho)}{\rho}\right)+\frac{\beta_1(\rho)}{\rho^2}$$

$$-\left(\frac{n}{\rho}\right)^2\left(2\beta_2(\rho)-\frac{1}{G_{r\varphi}(\rho)}\right).$$

Solving equation (3.2.54) with respect to its left-hand side returns the following Voltera integral equation of the second kind:

$$\sigma_n^\ell(\rho)=\frac{1}{a_{22}(\rho)}\Bigg(A_n^\ell\rho^{-n}+B_n^\ell\rho^n+p_{1n}^\ell P_n^\ell(\rho)$$

$$+q_{1n}^\ell Q_n^\ell(\rho)+\Theta_n^\ell(\rho)+\int_k^\rho \sigma_n^\ell(\eta)\mathcal{K}_n(\rho,\eta)d\eta\Bigg). \quad (3.2.56)$$

Here, A_n^ℓ and B_n^ℓ are arbitrary constants of integration,

$$P_n^\ell(\rho) = -\frac{k^2}{4n}\int_k^\rho \frac{1}{\xi}\Big(\xi^{-n}k^n\psi_n^-(\xi) - \xi^n k^{-n}\psi_n^+(\xi)\Big)\chi_n^-(\rho,\xi)d\xi\,,$$

$$Q_n^\ell(\rho) = -\frac{(-1)^\ell k^2}{4n}\int_k^\rho \frac{1}{\xi}\Big(\xi^{-n}k^n\psi_n^-(\xi) + \xi^n k^{-n}\psi_n^+(\xi)\Big)\chi_n^-(\rho,\xi)d\xi\,,$$

$$\begin{aligned}\Theta_n^\ell(\rho) &= -\alpha_2(\rho)T_n^\ell(\rho)\\ &-\frac{1}{2n}\int_k^\rho \xi\chi_n^-(\rho,\xi)\mathfrak{G}_n^\xi\Big(\big(\alpha_1(\xi)-\alpha_2(\xi)\big)T_n^i(\xi)\Big)d\xi,\end{aligned} \tag{3.2.57}$$

$$\mathcal{K}_n(\rho,\eta) = \frac{\eta}{4n}\Bigg(\int_\eta^\rho \frac{1}{\xi}\Big((n+1)\xi^{-n}\eta^n\psi_n^-(\xi)$$

$$+(n-1)(\xi)\xi^n\eta^{-n}\psi_n^+(\xi)\Big)\chi_n^-(\rho,\xi)d\xi - 2\psi_n(\eta)\chi_n^-(\rho,\eta)\Bigg).$$

Using the resolvent-kernel technique, we can derive the following solution to equation (3.2.56):

$$\begin{aligned}\sigma_n^\ell(\rho) &= \frac{1}{a_{22}(\rho)}\Big(a_n(\rho)A_n^\ell + b_n(\rho)B_n^\ell\\ &+ p_{1n}^\ell\overline{P}_n^\ell(\rho) + q_{1n}^\ell\overline{Q}_n^\ell(\rho) + \overline{\Theta}_n^\ell(\rho)\Big),\end{aligned} \tag{3.2.58}$$

where

$$\overline{P}_n^\ell(\rho) = P_n^\ell(\rho) + \int_k^\rho \frac{P_n^\ell(\eta)}{a_{22}(\eta)}\mathcal{R}_n(\rho,\eta)d\rho,$$

$$\overline{Q}_n^\ell(\rho) = Q_n^\ell(\rho) + \int_k^\rho \frac{Q_n^\ell(\eta)}{a_{22}(\eta)}\mathcal{R}_n(\rho,\eta)d\rho,$$

$$\bar{\Theta}_n^{\ell}(\rho) = \Theta_n^{\ell}(\rho) + \int_k^{\rho} \frac{\Theta_n^{\ell}(\eta)}{a_{22}(\eta)} \mathcal{R}_n(\rho,\eta) d\rho, \tag{3.2.59}$$

$$a_n(\rho) = \rho^{-n} + \int_k^{\rho} \frac{\eta^{-n}}{a_{22}(\eta)} \mathcal{R}_n(\rho,\eta) d\eta,$$

$$b_n(\rho) = \rho^{n} + \int_k^{\rho} \frac{\eta^{n}}{a_{22}(\eta)} \mathcal{R}_n(\rho,\eta) d\eta,$$

and the resolvent kernel can be expressed using the infinite series

$$\mathcal{R}_n(\rho,\eta) = \sum_{m=0}^{\infty} \mathcal{K}_{m+1}^n(\rho,\eta), \tag{3.2.60}$$

and

$$\begin{aligned} \mathcal{K}_1^n(\rho,\eta) &= \mathcal{K}_n(\rho,\eta), \\ \mathcal{K}_{m+1}^n(\rho,\eta) &= \int_{\eta}^{\rho} \frac{1}{a_{22}(\tau)} \mathcal{K}_1^n(\rho,\tau) \mathcal{K}_{m+1}^n(\tau,\eta) d\tau. \end{aligned} \tag{3.2.61}$$

We can substitute (3.2.58) into (3.2.47) and (3.2.48) for $n>1$ in order to determine the constants of integration A_n^{ℓ} and B_n^{ℓ}, as follows:

$$\begin{aligned} A_n^{\ell} &= \frac{1}{a_n^*}\left(F_{1n}^{\ell} b_n^- - F_{2n}^{\ell} b_n^+\right), \\ B_n^{\ell} &= \frac{1}{a_n^*}\left(F_{2n}^{\ell} a_n^+ - F_{1n}^{\ell} a_n^-\right). \end{aligned} \tag{3.2.62}$$

Here,

$$F_{1n}^{\ell} = k^{n+2} p_{1n}^{\ell} - p_{2n}^{\ell} + (-1)^{\ell}\left(k^{n+2} q_{1n}^{\ell} - q_{2n}^{\ell}\right)$$

$$-(n+1)\int_k^1 \frac{\rho^{1+n} f_n^\ell(\rho)}{a_{22}(\rho)} d\rho,$$

$$F_{2n}^\ell = p_{2n}^\ell - k^{2-n} p_{1n}^\ell + (-1)^\ell \left(k^{2-n} q_{1n}^\ell - q_{2n}^\ell\right)$$

$$-(n-1)\int_k^1 \frac{\rho^{1-n} f_n^\ell(\rho)}{a_{22}(\rho)} d\rho, \tag{3.2.63}$$

$$f_n^\ell(\rho) = p_{1n}^\ell \overline{P}_n^\ell(\rho) + q_{1n}^\ell \overline{Q}_n^\ell(\rho) + \overline{\Theta}_n^\ell(\rho),$$

$$a_n^\pm = (n \pm 1)\int_k^1 \frac{\rho^{1\pm n} a_n(\rho)}{a_{22}(\rho)} d\rho, \quad b_n^\pm = (n \pm 1)\int_k^1 \frac{\rho^{1\pm n} b_n(\rho)}{a_{22}(\rho)} d\rho,$$

$$a_n^* = a_n^+ b_n^- - a_n^- b_n^+, \qquad n > 1.$$

Note however that for $n = 1$, conditions (3.2.47) and (3.2.48) are insufficient to determine constants A_1^ℓ and B_1^ℓ since, as mentioned above, condition (3.2.48) degenerates. This problem can be attributed to the fact that this annular domain is multiply-connected [145]. It can be solved using displacement single-valuedness conditions [145, 282] or Michell conditions [124]. Herein, we apply an alternative and, in our opinion, more efficient method of implementing the strain-compatibility conditions (3.1.37). Making use of constitutive equations (3.1.1) and expressions (3.2.4) and (3.2.51) under conditions (3.2.42) along with (3.1.37) yields the following:

$$\begin{aligned} A_1^\ell &= \frac{1}{a_1^*}\left(F_{11}^\ell b_1^0 - F_{21}^{0\ell} b_1^+\right), \\ B_1^\ell &= \frac{1}{a_1^*}\left(F_{21}^{0\ell} a_1^+ - F_{11}^\ell a_1^0\right), \end{aligned} \tag{3.2.64}$$

where

$$a_1^0 = k^3 \frac{d}{d\rho}\left(\frac{a_1(\rho)}{\rho}\right)\Big|_{\rho=k} + \frac{d}{d\rho}\left(\frac{a_1(\rho)}{\rho}\right)\Big|_{\rho=1},$$

$$b_1^0 = k^3 \frac{d}{d\rho}\left(\frac{b_1(\rho)}{\rho}\right)\Big|_{\rho=k} + \frac{d}{d\rho}\left(\frac{b_1(\rho)}{\rho}\right)\Big|_{\rho=1},$$

$$\begin{aligned} F_{21}^{0\ell} = {} & kp_{11}^{\ell}\left(\beta_3(k) - k^2 \frac{d}{d\rho}\left(\frac{\beta_2(\rho)}{\rho}\right)\Big|_{\rho=k}\right) \\ & + p_{21}^{\ell}\left(\beta_3(1) - \frac{d}{d\rho}\left(\frac{\beta_2(\rho)}{\rho}\right)\Big|_{\rho=1}\right) \\ & + (-1)^{\ell} kq_{11}^{\ell}\left(\beta_2(k) - \frac{1}{G_{r\varphi}(k)}\right) \\ & + (-1)^{\ell} q_{21}^{\ell}\left(\beta_2(1) - \frac{1}{G_{r\varphi}(1)}\right) + k\alpha_1(k)T_1^{\ell}(k) \\ & - k^2 \frac{d}{d\rho}\left(\alpha_2(\rho)T_1^{\ell}(\rho) + \frac{k}{\rho} f_1^{\ell}(\rho)\right)\Big|_{\rho=k} \\ & + \alpha_1(1)T_1^{\ell}(1) - \frac{d}{d\rho}\left(\alpha_2(\rho)T_1^{\ell}(\rho) + \frac{1}{\rho} f_1^{\ell}(\rho)\right)\Big|_{\rho=1}, \end{aligned} \tag{3.2.65}$$

$$a_1^* = a_1^+ b_1^0 - a_1^0 b_1^+ .$$

In view of expressions (3.2.58) and (3.2.59), total stress can be presented in the form of explicit dependence on the force and thermal loadings as

$$\begin{aligned} \sigma_n^{\ell}(\rho) = {} & p_{1n}^{\ell} P_{1n}^{\ell}(\rho) + p_{2n}^{\ell} P_{2n}^{\ell}(\rho) \\ & + q_{1n}^{\ell} Q_{1n}^{\ell}(\rho) + q_{2n}^{\ell} Q_{2n}^{\ell}(\rho) + \mathrm{T}_n^{\ell}(\rho), \quad n = 1, 2, \ldots \end{aligned} \tag{3.2.66}$$

Here,

$$P_{1n}^{\ell}(\rho)=\frac{1}{a_{22}(\rho)}\left(\overline{P}_n^{\ell}(\rho)+\frac{a_n(\rho)}{a_n^*}\left(k^{2+n}b_n^-+k^{2-n}b_n^+\right.\right.$$

$$\left.-\int_k^1\frac{(n+1)\rho^n b_n^- -(n-1)\rho^{-n}b_n^+}{a_{22}(\rho)}\rho\overline{P}_n^{\ell}(\rho)d\rho\right)$$

$$-\frac{b_n(\rho)}{a_n^*}\left(k^{2+n}a_n^-+k^{2-n}a_n^+\right.$$

$$\left.\left.-\int_k^1\frac{(n+1)\rho^n a_n^- -(n-1)\rho^{-n}a_n^+}{a_{22}(\rho)}\rho\overline{P}_n^{\ell}(\rho)d\rho\right)\right),\ n>1,$$

$$P_{2n}^{\ell}(\rho)=-\frac{a_n(\rho)\left(b_n^+ +b_n^-\right)-b_n(\rho)\left(a_n^+ +a_n^-\right)}{a_n^* a_{22}(\rho)},\ n>1,$$

$$Q_{1n}^{\ell}(\rho)=\frac{1}{a_{22}(\rho)}\left(\overline{Q}_n^{\ell}(\rho)+\frac{a_n(\rho)}{a_n^*}\left((-1)^{\ell}k^2\left(k^n b_n^- -k^{-n}b_n^+\right)\right.\right.$$

$$\left.-\int_k^1\frac{(n+1)\rho^n b_n^- -(n-1)\rho^{-n}b_n^+}{a_{22}(\rho)}\rho\overline{Q}_n^{\ell}(\rho)d\rho\right)$$

$$-\frac{b_n(\rho)}{a_n^*}\left((-1)^{\ell}k^2\left(k^n a_n^- -k^{-n}a_n^+\right)\right.$$

$$\left.\left.-\int_k^1\frac{(n+1)\rho^n a_n^- -(n-1)\rho^{-n}a_n^+}{a_{22}(\rho)}\rho\overline{Q}_n^{\ell}(\rho)d\rho\right)\right),\ n>1,$$

$$Q_{2n}^{\ell}(\rho)=\frac{(-1)^{\ell}\left(a_n(\rho)\left(b_n^+ -b_n^-\right)-b_n(\rho)\left(a_n^+ +a_n^-\right)\right)}{a_n^* a_{22}(\rho)},\ n>1,$$

$$\mathrm{T}_n^{\ell}(\rho)=\frac{1}{a_{22}(\rho)}\Bigg(\bar{\Theta}_n^{\ell}(\rho)$$

$$-\frac{a_n(\rho)}{a_n^*}\int_k^1\frac{(n+1)\rho^n b_n^- -(n-1)\rho^{-n}b_n^+}{a_{22}(\rho)}\rho\bar{\Theta}_n^{\ell}(\rho)d\rho$$

$$+\frac{b_n(\rho)}{a_n^*}\int_k^1\frac{(n+1)\rho^n a_n^- -(n-1)\rho^{-n}a_n^+}{a_{22}(\rho)}\rho\bar{\Theta}_n^{\ell}(\rho)d\rho\Bigg),\ n>1,$$

$$P_{11}^{\ell}(\rho)=\frac{1}{a_{22}(\rho)}\Bigg(\bar{P}_1^{\ell}(\rho)+\frac{a_1(\rho)}{a_1^*}\Bigg(b_1^0\Bigg(k^3-2\int_k^1\frac{\rho^2\bar{P}_1^{\ell}(\rho)}{a_{22}(\rho)}d\rho\Bigg)$$

$$-b_1^+\Bigg(k\beta_3(k)-k^3\frac{d}{d\rho}\Bigg(\frac{\beta_1(\rho)+\bar{P}_1^{\ell}(\rho)}{\rho}\Bigg)\Bigg|_{\rho=k}$$

$$-\frac{d}{d\rho}\Bigg(\frac{\bar{P}_1^{\ell}(\rho)}{\rho}\Bigg)\Bigg|_{\rho=1}\Bigg)-\frac{b_1(\rho)}{a_1^*}\Bigg(a_1^0\Bigg(k^3-2\int_k^1\frac{\rho^2\bar{P}_1^{\ell}(\rho)}{a_{22}(\rho)}d\rho\Bigg)$$

$$-a_1^+\Bigg(k\beta_3(k)-k^3\frac{d}{d\rho}\Bigg(\frac{\beta_2(\rho)+\bar{P}_1^{\ell}(\rho)}{\rho}\Bigg)\Bigg|_{\rho=k}$$

$$-\frac{d}{d\rho}\Bigg(\frac{\bar{P}_1^{\ell}(\rho)}{\rho}\Bigg)\Bigg|_{\rho=1}\Bigg)\Bigg)\Bigg)\Bigg), \tag{3.2.67}$$

$$P_{21}^{\ell}(\rho)=\frac{1}{a_{22}(\rho)}\Bigg(\frac{b_1(\rho)}{a_1^*}$$

$$\times\Bigg(a_1^0+a_1^+\Bigg(\beta_3(1)-\frac{d}{d\rho}\Bigg(\frac{\beta_2(\rho)}{\rho}\Bigg)\Bigg|_{\rho=1}\Bigg)\Bigg)$$

$$-\frac{a_1(\rho)}{a_1^*}\left(b_1^0+b_1^+\left(\beta_3(1)-\frac{d}{d\rho}\left(\frac{\beta_2(\rho)}{\rho}\right)\Big|_{\rho=1}\right)\right)\Bigg),$$

$$Q_{11}^{\ell}(\rho)=\frac{1}{a_{22}(\rho)}\Bigg(\bar{Q}_1^{\ell}(\rho)$$

$$+\frac{a_1(\rho)}{a_1^*}\left(b_1^0\left((-1)^{\ell}k^3-2\int_k^1\frac{\rho^2\bar{Q}_1^{\ell}(\rho)}{a_{22}(\rho)}d\rho\right)\right.$$

$$-b_1^+\left((-1)^{\ell}k\left(\beta_2(k)-\frac{1}{G_{r\varphi}(k)}\right)\right.$$

$$\left.-k^3\frac{d}{d\rho}\left(\frac{\bar{Q}_1^{\ell}(\rho)}{\rho}\right)\Big|_{\rho=k}-\frac{d}{d\rho}\left(\frac{\bar{Q}_1^{\ell}(\rho)}{\rho}\right)\Big|_{\rho=1}\right)$$

$$-\frac{b_1(\rho)}{a_1^*}\left(a_1^0\left((-1)^{\ell}k^3-2\int_k^1\frac{\rho^2\bar{Q}_1^{\ell}(\rho)}{a_{22}(\rho)}d\rho\right)\right.$$

$$-a_1^+\left((-1)^{\ell}k\left(\beta_2(k)-\frac{1}{G_{r\varphi}(k)}\right)\right.$$

$$\left.\left.\left.-k^3\frac{d}{d\rho}\left(\frac{\bar{Q}_1^{\ell}(\rho)}{\rho}\right)\Big|_{\rho=k}-\frac{d}{d\rho}\left(\frac{\bar{Q}_1^{\ell}(\rho)}{\rho}\right)\Big|_{\rho=1}\right)\right)\right)\Bigg),$$

$$Q_{21}^{\ell}(\rho)=\frac{(-1)^{\ell}}{a_{22}(\rho)}\left(\frac{b_1(\rho)}{a_1^*}\left(a_1^0+a_1^+\left(\beta_2(1)-\frac{1}{G_{r\varphi}(1)}\right)\right)\right.$$

$$\left.-\frac{a_1(\rho)}{a_1^*}\left(b_1^0+b_1^+\left(\beta_2(1)-\frac{1}{G_{r\varphi}(1)}\right)\right)\right)\Bigg),$$

$$\mathrm{T}_1^{\ell}(\rho)=\frac{1}{a_{22}(\rho)}\Bigg(\overline{\Theta}_1^{\ell}(\rho)+\frac{b_1(\rho)}{a_1^*}\Bigg(2a_1^0\int_k^1\frac{\rho^2\overline{\Theta}_n^{\ell}(\rho)}{a_{22}(\rho)}d\rho$$

$$+a_1^+\Bigg(k\alpha_1(k)T_1^{\ell}(k)+\alpha_1(1)T_1^{\ell}(1)$$

$$-k^2\frac{d}{d\rho}\Bigg(\alpha_2(\rho)T_1^{\ell}(\rho)+\frac{k}{\rho}\overline{\Theta}_1^{\ell}(\rho)\Bigg)\Bigg|_{\rho=k}$$

$$-\frac{d}{d\rho}\Bigg(\alpha_2(\rho)T_1^{\ell}(\rho)+\frac{1}{\rho}\overline{\Theta}_1^{\ell}(\rho)\Bigg)\Bigg|_{\rho=1}\Bigg)\Bigg)$$

$$-\frac{a_1(\rho)}{a_1^*}\Bigg(2b_1^0\int_k^1\frac{\rho^2\overline{\Theta}_n^{\ell}(\rho)}{a_{22}(\rho)}d\rho+$$

$$b_1^+\Bigg(k\alpha_1(k)T_1^{\ell}(k)+\alpha_1(1)T_1^{\ell}(1)$$

$$-k^2\frac{d}{d\rho}\Bigg(\alpha_2(\rho)T_1^{\ell}(\rho)+\frac{k}{\rho}\overline{\Theta}_1^{\ell}(\rho)\Bigg)\Bigg|_{\rho=k}$$

$$-\frac{d}{d\rho}\Bigg(\alpha_2(\rho)T_1^{\ell}(\rho)+\frac{1}{\rho}\overline{\Theta}_1^{\ell}(\rho)\Bigg)\Bigg|_{\rho=1}\Bigg)\Bigg)\Bigg), \tag{3.2.68}$$

Deriving total stress in the form (3.2.66) allows us to find the stress-tensor components represented by (3.2.51) in the following form:

$$\begin{aligned}R_n^{\ell}(\rho)&=p_{1n}^{\ell}P_{1n}^{r\ell}(\rho)+p_{2n}^{\ell}P_{2n}^{r\ell}(\rho)\\&+q_{1n}^{\ell}Q_{1n}^{r\ell}(\rho)+q_{2n}^{\ell}Q_{2n}^{r\ell}(\rho)+\mathrm{T}_n^{r\ell}(\rho),\\\Phi_n^{\ell}(\rho)&=p_{1n}^{\ell}P_{1n}^{\varphi\ell}(\rho)+p_{2n}^{\ell}P_{2n}^{\varphi\ell}(\rho)\\&+q_{1n}^{\ell}Q_{1n}^{\varphi\ell}(\rho)+q_{2n}^{\ell}Q_{2n}^{\varphi\ell}(\rho)+\mathrm{T}_n^{\varphi\ell}(\rho),\end{aligned} \tag{3.2.69}$$

$$S_n^{\ell}(\rho) = p_{1n}^{\ell} P_{1n}^{r\varphi\ell}(\rho) + p_{2n}^{\ell} P_{2n}^{r\varphi\ell}(\rho)$$

$$+ q_{1n}^{\ell} Q_{1n}^{r\varphi\ell}(\rho) + q_{2n}^{\ell} Q_{2n}^{r\varphi\ell}(\rho) + \mathrm{T}_n^{r\varphi\ell}(\rho)\,,$$

where

$$P_{1n}^{r\ell}(\rho) = -k^2 \chi_n^{+}(\rho, k)$$

$$+ \frac{1}{2\rho^2} \int_k^{\rho} \eta P_{1n}^{\ell}(\eta) \left(n\chi_n^{-}(\rho,\eta) + \chi_n^{+}(\rho,\eta) \right) d\eta,$$

$$P_{2n}^{r\ell}(\rho) = \frac{1}{2\rho^2} \int_k^{\rho} \eta P_{2n}^{\ell}(\eta) \left(n\chi_n^{-}(\rho,\eta) + \chi_n^{+}(\rho,\eta) \right) d\eta,$$

$$Q_{1n}^{r\ell}(\rho) = \frac{1}{2\rho^2} \left(\int_k^{\rho} \eta Q_{1n}^{\ell}(\eta) \left(n\chi_n^{-}(\rho,\eta) + \chi_n^{+}(\rho,\eta) \right) d\eta \right.$$

$$\left. + (-1)^{\ell+1} k^2 \chi_n^{-}(\rho, k) \right),$$

$$Q_{2n}^{r\ell}(\rho) = \frac{1}{2\rho^2} \int_k^{\rho} \eta Q_{2n}^{\ell}(\eta) \left(n\chi_n^{-}(\rho,\eta) + \chi_n^{+}(\rho,\eta) \right) d\eta,$$

$$\mathrm{T}_n^{r\ell}(\rho) = \frac{1}{2\rho^2} \int_k^{\rho} \eta \mathrm{T}_n^{\ell}(\eta) \left(n\chi_n^{-}(\rho,\eta) + \chi_n^{+}(\rho,\eta) \right) d\eta\,,$$

$$P_{1n}^{\varphi\ell}(\rho) = P_{1n}^{\ell}(\rho) + \frac{1}{2\rho^2} \left(k^2 \chi_n^{+}(\rho, k) \right.$$

$$\left. - \int_k^{\rho} \eta P_{1n}^{\ell}(\eta) \left(n\chi_n^{-}(\rho,\eta) + \chi_n^{+}(\rho,\eta) \right) d\eta \right),$$

$$P_{2n}^{\varphi\ell}(\rho) = P_{2n}^{\ell}(\rho) - \frac{1}{2\rho^2}\int_k^\rho \eta P_{2n}^{\ell}(\eta)\Big(n\chi_n^-(\rho,\eta) + \chi_n^+(\rho,\eta)\Big)d\eta\,,$$

$$Q_{1n}^{\varphi\ell}(\rho) = Q_{1n}^{\ell}(\rho) + \frac{1}{2\rho^2}\Bigg((-1)^{\ell}k^2\chi_n^-(\rho,k)$$

$$-\int_k^\rho \eta Q_{1n}^{\ell}(\eta)\Big(n\chi_n^-(\rho,\eta) + \chi_n^+(\rho,\eta)\Big)d\eta\Bigg), \qquad (3.2.70)$$

$$Q_{2n}^{\varphi\ell}(\rho) = Q_{2n}^{\ell}(\rho)$$

$$-\frac{1}{2\rho^2}\int_k^\rho \eta Q_{2n}^{\ell}(\eta)\Big(n\chi_n^-(\rho,\eta) + \chi_n^+(\rho,\eta)\Big)d\eta\,,$$

$$\mathrm{T}_n^{\varphi\ell}(\rho) = \mathrm{T}_n^{\ell}(\rho) - \frac{1}{2\rho^2}\int_k^\rho \eta \mathrm{T}_n^{\ell}(\eta)\Big(n\chi_n^-(\rho,\eta) + \chi_n^+(\rho,\eta)\Big)d\eta\,,$$

$$P_{1n}^{r\varphi\ell}(\rho) = \frac{(-1)^{\ell}}{2\rho^2}\Bigg(k^2\chi_n^-(\rho,k)$$

$$-\int_k^\rho \eta P_{1n}^{\ell}(\eta)\Big(n\chi_n^+(\rho,\eta) + \chi_n^-(\rho,\eta)\Big)d\eta\Bigg),$$

$$P_{2n}^{r\varphi\ell}(\rho) = -\frac{(-1)^{\ell}}{2\rho^2}\int_k^\rho \eta P_{2n}^{\ell}(\eta)\Big(n\chi_n^+(\rho,\eta) + \chi_n^-(\rho,\eta)\Big)d\eta\,,$$

$$Q_{1n}^{r\varphi\ell}(\rho) = \frac{1}{2\rho^2}\Bigg(k^2\chi_n^+(\rho,k)$$

$$-(-1)^{\ell}\int_k^\rho \eta Q_{1n}^{\ell}(\eta)\Big(n\chi_n^+(\rho,\eta) + \chi_n^-(\rho,\eta)\Big)d\eta\Bigg),$$

$$Q_{2n}^{r\varphi\ell}(\rho) = -\frac{(-1)^{\ell}}{2\rho^2}\int_k^{\rho} \eta Q_{2n}^{\ell}(\eta)\left(n\chi_n^{+}(\rho,\eta) + \chi_n^{-}(\rho,\eta)\right)d\eta,$$

$$\mathrm{T}_n^{r\varphi\ell}(\rho) = -\frac{(-1)^{\ell}}{2\rho^2}\int_k^{\rho} \eta \mathrm{T}_n^{\ell}(\eta)\left(n\chi_n^{+}(\rho,\eta) + \chi_n^{-}(\rho,\eta)\right)d\eta.$$

We can use (3.2.2), (3.2.11), (3.2.26), (3.2.28), (3.2.36), and (3.2.69) to determine the in-plane thermal stresses in radially-inhomogeneous orthotropic annulus $\Re$ resulting from the force loading (3.2.1) and steady temperature field $T(\rho,\varphi)$.

3.2.4. Evaluation of axial stress and strain

After in-plane stresses are determined, axial stress can be computed for the case where ring $\Re$ is a cross-section of a long hollow cylinder under the condition of plane strain $\varepsilon_{zz}(\rho,\varphi) = e_0 = \text{const}$. This stress can be represented in the form of a periodic Fourier series, as follows:

$$\sigma_{zz}(\rho,\varphi) = Z_0(\rho) + \sum_{n=1}^{\infty}\left(Z_n^1(\rho)\cos n\varphi + Z_n^2(\rho)\sin n\varphi\right), \qquad (3.2.71)$$

where

$$Z_0(\rho) = \frac{1}{2\pi}\int_0^{2\pi} \sigma_{zz}(\rho,\varphi)d\varphi,$$

$$Z_n^1(\rho) = \frac{1}{\pi}\int_0^{2\pi} \sigma_{zz}(\rho,\varphi)\cos n\varphi d\varphi, \qquad (3.2.72)$$

$$Z_n^2(\rho) = \frac{1}{\pi}\int_0^{2\pi} \sigma_{zz}(\rho,\varphi)\sin n\varphi d\varphi.$$

We can use the constitutive equation in (3.1.8) for axial strain $\varepsilon_{zz}(\rho,\varphi) = e_0$ to deal with the considered orthotropic case in the polar coordinates under symmetry conditions (3.1.3), thereby deriving the following expression:

$$\sigma_{zz}(\rho,\varphi) = \nu_{zr}(\rho)\sigma_{rr}(\rho,\varphi) + \nu_{z\varphi}(\rho)\sigma_{\varphi\varphi}(\rho,\varphi)$$

$$+E_z(\rho)e_0 - \alpha_z(\rho)E_z(\rho)T(\rho,\varphi)\,. \tag{3.2.73}$$

In view of (3.2.2) and (3.2.71), we obtain the following:

$$\begin{gathered} Z_0(\rho) = \nu_{zr}(\rho)R_0(\rho) + \nu_{z\varphi}(\rho)\Phi_0(\rho) \\ +E_z(\rho)e_0 - \alpha_z(\rho)E_z(\rho)T_0(\rho), \\ Z_n^{\ell}(\rho) = \nu_{zr}(\rho)R_n^{\ell}(\rho) + \nu_{z\varphi}(\rho)\Phi_n^{\ell}(\rho) \\ -\alpha_z(\rho)E_z(\rho)T_n^{\ell}(\rho), \quad \ell = 1,2\,. \end{gathered} \tag{3.2.74}$$

In the case where the cylinder's end-faces are fixed by smooth rigid planes, $e_0 = 0$ and, hence, in view of (3.2.31), the elementary part of the axial stress can be expressed as

$$\begin{gathered} Z_0(\rho) = p_{10}\left(\nu_{zr}(\rho)P_{10}^{r}(\rho) + \nu_{z\varphi}(\rho)P_{10}^{\varphi}(\rho)\right) \\ +p_{20}\left(\nu_{zr}(\rho)P_{20}^{r}(\rho) + \nu_{z\varphi}(\rho)P_{20}^{\varphi}(\rho)\right) \\ +\nu_{zr}(\rho)\theta_0^{r}(\rho) + \nu_{z\varphi}(\rho)\theta_0^{\varphi}(\rho) - \alpha_z(\rho)E_z(\rho)T_0(\rho) \end{gathered} \tag{3.2.75}$$

with the coefficients given by formulae in (3.2.29).

If the end-faces are free of constraints and under load from normal forces with the resultant p_{zz}^0 given in (3.1.7), then the constant axial strain and elementary stresses can be found in the forms given in (3.2.34) and (3.2.36), respectively. Thus, making use of these expressions in conjunction with (3.2.74) yields

$$\begin{gathered} Z_0(\rho) = p_{10}\left(E_z(\rho)P_{1e} + \nu_{zr}(\rho)\left(P_{10}^{r}(\rho) + P_{1e}\zeta_0^{r}(\rho)\right)\right. \\ \left.+\nu_{z\varphi}(\rho)\left(P_{10}^{\varphi}(\rho) + P_{1e}\zeta_0^{\varphi}(\rho)\right)\right) \\ +p_{20}\left(E_z(\rho)P_{2e} + \nu_{zr}(\rho)\left(P_{20}^{r}(\rho) + P_{2e}\zeta_0^{r}(\rho)\right)\right. \end{gathered}$$

$$+\nu_{z\varphi}(\rho)\left(P_{20}^{\varphi}(\rho)+P_{2e}\zeta_0^{\varphi}(\rho)\right)\Big)$$

$$+p_{zz}^0\,\frac{E_z(\rho)+\nu_{zr}(\rho)\zeta_0^r(\rho)+\nu_{z\varphi}(\rho)\zeta_0^{\varphi}(\rho)}{2\pi(e+e_1)}+E_z(\rho)\theta_e$$

$$-\alpha_z(\rho)E_z(\rho)T_0(\rho)+\nu_{zr}(\rho)\left(\theta_0^r(\rho)+\theta_e\zeta_0^r(\rho)\right)$$

$$+\nu_{z\varphi}(\rho)\left(\theta_0^{\varphi}(\rho)+\theta_e\zeta_0^{\varphi}(\rho)\right). \qquad (3.2.76)$$

Here, the coefficients are given by (3.2.29) and (3.2.35).

Note that in the case of a homogeneous isotropic material at $p_{zz}^0=0$, the expressions (3.2.75) and (3.2.76) coincide with the following expressions obtained in [298]:

$$Z_0(\rho)=\frac{\alpha E}{1-\nu}\left(\frac{2}{1-k^2}\int_k^1\rho T_0(\rho)d\rho-T_0(\rho)\right) \qquad (3.2.77)$$

and

$$Z_0(\rho)=\frac{2\nu(k^2p_{10}-p_{20})}{1-k^2}$$

$$+\frac{\alpha E}{1-\nu}\left(\frac{2\nu}{1-k^2}\int_k^1\rho T_0(\rho)d\rho-T_0(\rho)\right), \qquad (3.2.78)$$

respectively.

In the case of axisymmetric force loadings associated with homogenous and isotropic annulus $\Re$, the term described in (3.2.77) represents the axial stress in the cylinder with cross-section $\Re$ and free end-faces. This stress is independent of the in-plane force loadings. In the case where the end-faces are fixed, the axial stress described in (3.2.78) depends on in-plane tractions, even for axisymmetric distributions.

In view of expressions (3.2.69), the angle-dependent part of axial stress represented by (3.2.74) can be derived as follows:

$$Z_n^{\ell}(\rho)=p_{1n}^{\ell}P_{1n}^{z\ell}(\rho)+p_{2n}^{\ell}P_{2n}^{z\ell}(\rho)$$

$$+q_{1n}^{\ell}Q_{1n}^{z\ell}(\rho)+q_{2n}^{\ell}Q_{2n}^{z\ell}(\rho)+\mathrm{T}_{n}^{z\ell}(\rho),\quad \ell=1,2\,. \tag{3.2.79}$$

Here,

$$\begin{gathered}
P_{jn}^{z\ell}(\rho)=\nu_{zr}(\rho)P_{jn}^{r\ell}(\rho)+\nu_{z\varphi}(\rho)P_{jn}^{\varphi\ell}(\rho),\\
Q_{jn}^{z\ell}(\rho)=\nu_{zr}(\rho)Q_{jn}^{r\ell}(\rho)+\nu_{z\varphi}(\rho)Q_{jn}^{\varphi\ell}(\rho),\\
\mathrm{T}_{n}^{z\ell}(\rho)=\nu_{zr}(\rho)\mathrm{T}_{n}^{r\ell}(\rho)+\nu_{z\varphi}(\rho)\mathrm{T}_{n}^{\varphi\ell}(\rho)\\
-\alpha_{z}(\rho)E_{z}(\rho)T_{n}^{\ell}(\rho),\quad j=1,2.
\end{gathered} \tag{3.2.80}$$

In the case where the end-faces of the cylinder with cross-section $\mathfrak{R}$ are free or when the end-faces are loaded by the normal force described in (3.1.7), we can see that axial stress induces the following bending moment:

$$M=\iint_{\mathfrak{R}}\rho^{2}\sigma_{zz}(\rho,\varphi)\cos\varphi\,d\varphi d\rho\,. \tag{3.2.81}$$

or, in view of (3.2.71),

$$M=\pi\int_{k}^{1}\rho^{2}Z_{1}^{1}(\rho)d\rho\,. \tag{3.2.82}$$

Thus, axial stress must be balanced by applying the opposite force to the end-faces of the cylinder as follows:

$$\begin{aligned}
M=-\pi\int_{k}^{1}\rho^{2}\Big(&p_{11}^{\ell}P_{11}^{z\ell}(\rho)+p_{21}^{\ell}P_{21}^{z\ell}(\rho)\\
&+q_{11}^{\ell}Q_{11}^{z\ell}(\rho)+q_{21}^{\ell}Q_{21}^{z\ell}(\rho)+\mathrm{T}_{1}^{z\ell}(\rho)\Big)d\rho\,.
\end{aligned} \tag{3.2.83}$$

The component of axial stress that emanates the moment (3.2.83) can be determined in the form

$$\sigma_{zz}^{M}(\rho,\varphi)=\Big(p_{11}^{\ell}\tilde{P}_{11}^{z\ell}(\rho)+p_{21}^{\ell}\tilde{P}_{21}^{z\ell}(\rho)+q_{11}^{\ell}\tilde{Q}_{11}^{z\ell}(\rho)$$

$$+q_{21}^{\ell}\tilde{Q}_{21}^{z\ell}(\rho)+\tilde{\mathrm{T}}_{1}^{z\ell}(\rho)\Big)\cos\varphi\,, \tag{3.2.84}$$

where

$$\tilde{P}_{j1}^{z\ell}(\rho)=-\frac{4\rho}{1-k^4}\int_{k}^{1}\rho^2 P_{j1}^{z\ell}(\rho)d\rho,$$

$$\tilde{Q}_{j1}^{z\ell}(\rho)=-\frac{4\rho}{1-k^4}\int_{k}^{1}\rho^2 Q_{j1}^{z\ell}(\rho)d\rho, \tag{3.2.85}$$

$$\tilde{\mathrm{T}}_{1}^{z\ell}(\rho)=-\frac{4\rho}{1-k^4}\int_{k}^{1}\rho^2 \mathrm{T}_{1}^{z\ell}(\rho)d\rho,\quad \ell=1,2,\quad j=1,2.$$

Ultimately, determining axial stress in a hollow orthotropic radially-inhomogeneous cylinder with free ends under the plane-strain condition involves adding term (3.2.84) to expression (3.2.71).

In the plane-stress case ($\sigma_{zz}=0$) for a thin plate (disk) with a midplane indicated by inhomogeneous orthotropic ring $\Re$, axial strain can be derived using (3.1.8) within polar coordinates under symmetry conditions (3.1.3). This yields the following:

$$\varepsilon_{zz}(\rho,\varphi)=-\frac{\nu_{zr}(\rho)}{E_z(\rho)}\sigma_{rr}(\rho,\varphi)$$

$$-\frac{\nu_{z\varphi}(\rho)}{E_z(\rho)}\sigma_{\varphi\varphi}(\rho,\varphi)+\alpha_z(\rho)T(\rho,\varphi)\,. \tag{3.2.86}$$

Thus, axial strain can be computed as follows:

$$\varepsilon_{zz}(\rho,\varphi)=\varepsilon_0(\rho)+\sum_{n=1}^{\infty}\Big(\varepsilon_n^1(\rho)\cos n\varphi+\varepsilon_n^2\sin n\varphi\Big), \tag{3.2.87}$$

where

$$\varepsilon_0(\rho)=-p_{10}\,\frac{\nu_{zr}(\rho)P_{10}^{r}(\rho)+\nu_{z\varphi}(\rho)P_{10}^{\varphi}(\rho)}{E_z(\rho)}$$

$$-p_{20}\frac{\nu_{zr}(\rho)P_{20}^{r}(\rho)+\nu_{z\varphi}(\rho)P_{20}^{\varphi}(\rho)}{E_z(\rho)}$$

$$+\alpha_z(\rho)T_0(\rho)-\frac{\nu_{zr}(\rho)\theta_0^{r}(\rho)+\nu_{z\varphi}(\rho)\theta_0^{\varphi}(\rho)}{E_z(\rho)},$$

$$\varepsilon_n^{\ell}(\rho)=-p_{1n}^{\ell}\frac{\nu_{zr}(\rho)P_{1n}^{r\ell}(\rho)+\nu_{z\varphi}(\rho)P_{1n}^{\varphi\ell}(\rho)}{E_z(\rho)}$$

$$-p_{2n}^{\ell}\frac{\nu_{zr}(\rho)P_{2n}^{r\ell}(\rho)+\nu_{z\varphi}(\rho)P_{2n}^{\varphi\ell}(\rho)}{E_z(\rho)} \qquad (3.2.88)$$

$$-q_{1n}^{\ell}\frac{\nu_{zr}(\rho)Q_{1n}^{r\ell}(\rho)+\nu_{z\varphi}(\rho)Q_{1n}^{\varphi\ell}(\rho)}{E_z(\rho)}$$

$$-q_{2n}^{\ell}\frac{\nu_{zr}(\rho)Q_{2n}^{r\ell}(\rho)+\nu_{z\varphi}(\rho)Q_{2n}^{\varphi\ell}(\rho)}{E_z(\rho)}$$

$$+\alpha_z(\rho)T_n^{\ell}(\rho)-\frac{\nu_{zr}(\rho)\mathrm{T}_n^{r\ell}(\rho)+\nu_{z\varphi}(\rho)\mathrm{T}_n^{\varphi\ell}(\rho)}{E_z(\rho)},\ \ \ell=1,2\,.$$

3.2.5. Analysis of elastic displacements

Consider the problem on determination of elastic displacements in inhomogeneous orthotropic annular domain $\mathfrak{R}$. We apply the formulae derived in Section 3.1.2 and the expressions for stress-tensor components outlined in Sections 3.2.2 and 3.2.3. Note that construction of function $U_r(\varphi)$, as expressed by (3.1.24), is key to the construction of explicit expressions for the displacements given in (3.1.23) and (3.1.26). To evaluate this function, let us represent function $f(\varphi)$ introduced in (3.1.32) as follows:

$$f(\varphi)=f_0+\sum_{n=2}^{\infty}\left(f_n^1\cos n\varphi+f_n^2\sin n\varphi\right), \qquad (3.2.89)$$

where

$$f_0 = \frac{1}{2\pi}\int\limits_0^{2\pi} f(\varphi)d\varphi,\ \ f_n^1 = \frac{1}{\pi}\int\limits_0^{2\pi} f(\varphi)\cos n\varphi d\varphi,$$
$$f_n^2 = \frac{1}{\pi}\int\limits_0^{2\pi} f(\varphi)\sin n\varphi d\varphi. \tag{3.2.90}$$

Note that the terms corresponding to $n=1$ are absent from expression (3.2.89) under conditions (3.1.36).

Making use of (3.1.1), (3.1.32), (3.2.36), and (3.2.69) allows us to derive the coefficients (3.2.90) of expression (3.2.89) as follows:

$$f_0 = p_{10}f_{p1}^0 + p_{20}f_{p2}^0 + f_T^0 + p_{zz}^0 f_z^0,$$
$$f_n^\ell = p_{1n}^\ell f_{1n}^\ell + p_{2n}^\ell f_{2n}^\ell + q_{1n}^\ell g_{1n}^\ell + q_{2n}^\ell g_{2n}^\ell + f_{Tn}^\ell,\ \ \ell = 1,2, \tag{3.2.91}$$

where

$$f_{p1}^0 = k\beta_3(k) - k^3\frac{d}{d\rho}\left(\frac{\beta_2(\rho) + a_{22}(\rho)P_{10}(\rho) + \delta P_{1e}\zeta_0(\rho)}{\rho}\right)\Bigg|_{\rho=k}$$
$$-\frac{d}{d\rho}\left(\frac{a_{22}(\rho)P_{10}(\rho) + \delta P_{1e}\zeta_0(\rho)}{\rho}\right)\Bigg|_{\rho=1}$$
$$+\delta\left(k^2\frac{d\nu_{z\varphi}(\rho)}{d\rho}\Bigg|_{\rho=k} - k\nu_{zr}(k) + \frac{d\nu_{z\varphi}(\rho)}{d\rho}\Bigg|_{\rho=1} - k\nu_{zr}(1)\right)P_{1e},$$
$$f_{p2}^0 = k\beta_3(1) - \frac{d}{d\rho}\left(\frac{\beta_2(\rho) - a_{22}(\rho)P_{20}(\rho) - \delta P_{2e}\zeta_0(\rho)}{\rho}\right)\Bigg|_{\rho=1}$$
$$-k^3\frac{d}{d\rho}\left(\frac{a_{22}(\rho)P_{20}(\rho) + \delta P_{2e}\zeta_0(\rho)}{\rho}\right)\Bigg|_{\rho=k}$$

$$+\delta\left(k^2\left.\frac{d\nu_{z\varphi}(\rho)}{d\rho}\right|_{\rho=k}-k\nu_{zr}(k)+\left.\frac{d\nu_{z\varphi}(\rho)}{d\rho}\right|_{\rho=1}-k\nu_{zr}(1)\right)P_{2e},$$

$$f_T^0=k\alpha_1(k)T_0(k)-k^2\frac{d}{d\rho}\big(\alpha_2(\rho)T_0(\rho)\big)\Big|_{\rho=k}$$

$$+\alpha_1(1)T_0(1)-\frac{d}{d\rho}\big(\alpha_2(\rho)T_0(\rho)\big)\Big|_{\rho=1}$$

$$-k^3\frac{d}{d\rho}\left(\frac{a_{22}(\rho)\theta_0(\rho)+\delta\theta_e\zeta_0(\rho)}{\rho}\right)\Bigg|_{\rho=k}$$

$$-\frac{d}{d\rho}\left(\frac{a_{22}(\rho)\theta_0(\rho)+\delta\theta_e\zeta_0(\rho)}{\rho}\right)\Bigg|_{\rho=1}$$

$$+\delta\left(k^2\left.\frac{d\nu_{z\varphi}(\rho)}{d\rho}\right|_{\rho=k}-k\nu_{zr}(k)+\left.\frac{d\nu_{z\varphi}(\rho)}{d\rho}\right|_{\rho=1}-k\nu_{zr}(1)\right)\theta_e,$$

$$f_z^0=\frac{\delta}{2\pi(e+e_1)}\left(k^2\left.\frac{d\nu_{z\varphi}(\rho)}{d\rho}\right|_{\rho=k}\right.$$

$$\left.-k\nu_{zr}(k)+\left.\frac{d\nu_{z\varphi}(\rho)}{d\rho}\right|_{\rho=1}-k\nu_{zr}(1)\right.$$

$$\left.-k^3\frac{d}{d\rho}\left(\frac{\zeta_0(\rho)}{\rho}\right)\Bigg|_{\rho=k}-\frac{d}{d\rho}\left(\frac{\zeta_0(\rho)}{\rho}\right)\Bigg|_{\rho=1}\right);\qquad(3.2.92)$$

$$f_{1n}^{\ell}=k\beta_3(k)-k^3\frac{d}{d\rho}\left(\frac{\beta_2(\rho)+a_{22}(\rho)P_{1n}^{\ell}(\rho)}{\rho}\right)\Bigg|_{\rho=k}$$

$$-\frac{d}{d\rho}\left(\frac{a_{22}(\rho)P_{1n}^{\ell}(\rho)}{\rho}\right)\Bigg|_{\rho=1},$$

$$f_{2n}^{\ell} = \beta_3(1) - \frac{d}{d\rho}\left(\frac{\beta_2(\rho) + a_{22}(\rho)P_{2n}^{\ell}(\rho)}{\rho}\right)\Bigg|_{\rho=1}$$

$$-k^3\frac{d}{d\rho}\left(\frac{a_{22}(\rho)P_{2n}^{\ell}(\rho)}{\rho}\right)\Bigg|_{\rho=k},$$

$$g_{1n}^{\ell} = (-1)^{\ell} nk\left(\beta_2(k) - \frac{1}{G_{r\varphi}(k)}\right)$$

$$-k^3\frac{d}{d\rho}\left(\frac{a_{22}(\rho)}{\rho}Q_{1n}^{\ell}(\rho)\right)\Bigg|_{\rho=k} - \frac{d}{d\rho}\left(\frac{a_{22}(\rho)}{\rho}Q_{1n}^{\ell}(\rho)\right)\Bigg|_{\rho=1},$$

$$g_{2n}^{\ell} = (-1)^{\ell} nk\left(\beta_2(1) - \frac{1}{G_{r\varphi}(1)}\right)$$

$$-k^3\frac{d}{d\rho}\left(\frac{a_{22}(\rho)}{\rho}Q_{2n}^{\ell}(\rho)\right)\Bigg|_{\rho=k} - \frac{d}{d\rho}\left(\frac{a_{22}(\rho)}{\rho}Q_{2n}^{\ell}(\rho)\right)\Bigg|_{\rho=1},$$

$$f_{Tn}^{\ell} = k\alpha_1(k)T_n^{\ell}(k) + \alpha_1(1)T_n^{\ell}(1)$$

$$-k^2\frac{d}{d\rho}\left(\alpha_2(\rho)T_n^{\ell}(\rho)\right)\Big|_{\rho=k} - \frac{d}{d\rho}\left(\alpha_2(\rho)T_n^{\ell}(\rho)\right)\Big|_{\rho=1}$$

$$-k^3\frac{d}{d\rho}\left(\frac{a_{22}(\rho)}{\rho}\mathrm{T}_n^{\ell}(\rho)\right)\Bigg|_{\rho=k} - \frac{d}{d\rho}\left(\frac{a_{22}(\rho)}{\rho}\mathrm{T}_n^{\ell}(\rho)\right)\Bigg|_{\rho=1}.$$

We now apply (3.2.92) and (3.1.33) in view of formulae

$$\int_0^{2\pi} \sin|\varphi-\xi|\,d\xi = 2(1-\cos\varphi),$$

$$\int_0^{2\pi} \cos n\xi \sin|\varphi-\xi|\,d\xi = 2\frac{\cos\varphi-\cos n\varphi}{n^2-1}, \tag{3.2.93}$$

$$\int_0^{2\pi} \sin n\xi \sin|\varphi-\xi|\,d\xi = 2\frac{n\sin\varphi-\sin n\varphi}{n^2-1}, \quad n\neq 1,$$

to derive the following expression:

$$U_r(\varphi) = f_0 + A^*\cos\varphi + B^*\sin\varphi$$

$$-\sum_{n=2}^{\infty}\left(\frac{f_n^1}{n^2-1}\cos n\varphi + \frac{f_n^2}{n^2-1}\sin n\varphi\right), \tag{3.2.94}$$

where

$$A^* = A - f_0 + \sum_{n=2}^{\infty}\frac{f_n^1}{n^2-1}, \qquad B^* = B + \sum_{n=2}^{\infty}\frac{nf_n^2}{n^2-1}. \tag{3.2.95}$$

The coefficients represented by (3.2.94) and (3.2.95) are given by formulae (3.2.92).

In the application of formula (3.1.23), we represent the radial strain by a Fourier series

$$\varepsilon_{rr}(\rho,\varphi) = \varepsilon_{rr}^0(\rho) + \sum_{n=1}^{\infty}\left(\varepsilon_{rrn}^1(\rho)\cos n\varphi + \varepsilon_{rrn}^2(\rho)\sin n\varphi\right). \tag{3.2.96}$$

Applying the corresponding constitutive equation given in (3.1.1) in conjunction with the expressions for the coefficients of stress-tensor components yields the following expressions for the coefficients of the foregoing series:

$$\varepsilon_{rr}^{0}(\rho) = p_{10}\varepsilon_{rp1}^{0}(\rho) + p_{20}\varepsilon_{rp2}^{0}(\rho)$$

$$+ p_{zz}^{0}\varepsilon_{rpz}^{0}(\rho) + \varepsilon_{rT}^{0}(\rho),$$

$$\varepsilon_{rrn}^{\ell}(\rho) = p_{1n}^{\ell}\varepsilon_{rnp}^{1\ell}(\rho) + p_{2n}^{\ell}\varepsilon_{rnp}^{2\ell}(\rho) \tag{3.2.97}$$

$$+ q_{1n}^{\ell}\varepsilon_{rnq}^{1\ell}(\rho) + q_{2n}^{\ell}\varepsilon_{rnq}^{2\ell}(\rho) + \varepsilon_{rnT}^{\ell}(\rho),$$

where

$$\varepsilon_{rpj}^{0}(\rho) = \left(P_{j0}^{r}(\rho) + \delta P_{je}\zeta_{0}^{r}(\rho)\right)\beta_{1}(\rho)$$

$$+ a_{12}(\rho)\left(P_{j0}(\rho) + \delta P_{je}\frac{\zeta_{0}(\rho)}{a_{22}(\rho)}\right) - \delta\nu_{zr}(\rho)P_{1e},$$

$$\varepsilon_{rT}^{0}(\rho) = \left(\theta_{0}^{r}(\rho) + \delta\theta_{e}\zeta_{0}^{r}(\rho)\right)\beta_{1}(\rho)$$

$$+ a_{12}(\rho)\left(\theta_{0}(\rho) + \delta\theta_{e}\frac{\zeta_{0}(\rho)}{a_{22}(\rho)}\right) - \delta\nu_{zr}(\rho)\theta_{e} + \alpha_{1}(\rho)T_{0}(\rho),$$

$$\varepsilon_{rpz}^{0}(\rho) = \frac{\delta}{2\pi(e+e_{1})}\left(\beta_{1}(\rho)\zeta_{0}^{r}(\rho)\right. \tag{3.2.98}$$

$$\left. + \frac{a_{12}(\rho)}{a_{22}(\rho)}\zeta_{0}(\rho) - \nu_{zr}(\rho)\right),$$

$$\varepsilon_{rnp}^{j\ell}(\rho) = \beta_{1}(\rho)P_{jn}^{r\ell}(\rho) + a_{12}(\rho)P_{jn}^{\ell}(\rho),$$

$$\varepsilon_{rnq}^{j\ell}(\rho) = \beta_{1}(\rho)Q_{jn}^{r\ell}(\rho) + a_{12}(\rho)Q_{jn}^{\ell}(\rho),$$

$$\varepsilon_{rnT}^{\ell}(\rho) = \beta_{1}(\rho)\mathrm{T}_{n}^{r\ell}(\rho) + a_{12}(\rho)\mathrm{T}_{n}^{\ell}(\rho), \quad j = 1,2; \ell = 1,2\,.$$

Deriving strain $\varepsilon_{rr}(\rho,\varphi)$ and function $U_{r}(\varphi)$ in terms of external force and thermal loadings allows us to compute radial displacement using (3.1.23), as follows:

$$u_r(\rho,\varphi) = u_r^0(\rho) + A_u^*(\rho)\cos\varphi + B_u^*(\rho)\sin\varphi$$

$$+\sum_{n=2}^{\infty}\left(u_{rn}^1(\rho)\cos n\varphi + u_{rn}^2(\rho)\sin n\varphi\right), \tag{3.2.99}$$

where

$$u_r^0(\rho) = p_{10}u_{rp1}^0(\rho) + p_{20}u_{rp2}^0(\rho) + p_{zz}^0 u_{rpz}^0(\rho) + u_{rT}^0(\rho),$$

$$u_{rn}^{\ell}(\rho) = p_{1n}^{\ell}u_{rnp}^{1\ell}(\rho) + p_{2n}^{\ell}u_{rnp}^{2\ell}(\rho)$$

$$+q_{1n}^{\ell}u_{rnq}^{1\ell}(\rho) + q_{2n}^{\ell}u_{rnq}^{2\ell}(\rho) + u_{rnT}^{\ell}(\rho), \tag{3.2.100}$$

$$A_u^*(\rho) = \frac{1}{2}\left(A^* + \int_k^1 \varepsilon_{r1p}^{1\ell}(\eta)\,\mathrm{sgn}(\rho-\eta)d\eta\right),$$

$$B_u^*(\rho) = \frac{1}{2}\left(B^* + \int_k^1 \varepsilon_{r1p}^{2\ell}(\eta)\,\mathrm{sgn}(\rho-\eta)d\eta\right),$$

and

$$u_{rpj}^0(\rho) = \frac{1}{2}\left(f_{pj}^0 + \int_k^1 \varepsilon_{rpj}^0(\eta)\,\mathrm{sgn}(\rho-\eta)d\eta\right),$$

$$u_{rpz}^0(\rho) = \frac{1}{2}\left(f_z^0 + \int_k^1 \varepsilon_{rpz}^0(\eta)\,\mathrm{sgn}(\rho-\eta)d\eta\right),$$

$$u_{rT}^0(\rho) = \frac{1}{2}\left(f_T^0 + \int_k^1 \varepsilon_{rT}^0(\eta)\,\mathrm{sgn}(\rho-\eta)d\eta\right),$$

$$u_{rnp}^{j\ell}(\rho) = \frac{1}{2}\left(\frac{f_{jn}^{\ell}}{1-n^2} + \int_k^1 \varepsilon_{rnp}^{j\ell}(\eta)\,\mathrm{sgn}(\rho-\eta)d\eta\right), \tag{3.2.101}$$

$$u_{rnq}^{j\ell}(\rho)=\frac{1}{2}\left(\frac{g_{jn}^{\ell}}{1-n^2}+\int_k^1 \varepsilon_{rnq}^{j\ell}(\eta)\,\mathrm{sgn}(\rho-\eta)d\eta\right),$$

$$u_{rnT}^{\ell}(\rho)=\frac{1}{2}\left(\frac{f_{Tn}^{\ell}}{1-n^2}+\int_k^1 \varepsilon_{rnT}^{\ell}(\eta)\,\mathrm{sgn}(\rho-\eta)d\eta\right),\quad j=1,2;\ell=1,2.$$

In such a manner, radial displacement $u_r(\rho,\varphi)$ is expressed using Fourier series in (3.2.99), the coefficients of which can be found explicitly through the force loadings applied to the inner and outer circumferences of the annulus and the thermal field distribution in its interior. Similarly, the circumferential displacement $u_\varphi(\rho,\varphi)$ can be derived using formula (3.1.26). This yields the following expression:

$$\begin{aligned}u_\varphi(\rho,\varphi)=&\frac{B}{2}+\rho C+\frac{\rho}{2}\int_k^1 \varepsilon_{r\varphi}(\eta,0)\frac{\mathrm{sgn}(\rho-\eta)}{\eta}d\eta\\&-\int_k^1\frac{\partial\varepsilon_{rr}(\eta,0)}{\partial\varphi}\left(\frac{\rho}{4}\left(1-\frac{1}{k}\right)+\frac{|\rho-\eta|}{2\eta}\right)d\eta\\&+\frac{1}{4}\int_0^{2\pi}\left(2\rho\varepsilon_{\varphi\varphi}(\rho,\xi)-U_r(\xi)\right)\mathrm{sgn}(\varphi-\xi)d\xi\\&-\frac{1}{4}\iint_{\Re}\varepsilon_{rr}(\eta,\xi)\,\mathrm{sgn}(\rho-\eta)\,\mathrm{sgn}(\varphi-\xi)d\eta d\xi,\end{aligned}\qquad(3.2.102)$$

where constants B and C can be eliminated by anchoring the ring from the rotation as a rigid solid [328].

Due to the fact that the displacements represented by (3.2.99) and (3.2.102) are found explicitly through the applied thermal and force loadings, the one-to-one relationship between the tractions and displacements on the inner and outer boundaries of annular domain $\Re$ can be established using the approach proposed in Section 2.3.4. This allows for the analysis of boundary conditions in terms of displacements, as well as mixed-type boundary conditions.

3.3. Steady-state temperature field

Consider the problem of steady-state temperature field in an orthotropic inhomogeneous annular domain $\mathfrak{R}$. We solve the heat-conduction equation (3.1.22) within the following boundary conditions:

$$\ell_1 T(1,\varphi) + \ell_2 \left.\frac{\partial T(\rho,\varphi)}{\partial \rho}\right|_{\rho=1} = t(\varphi),$$
$$\text{æ}_1 T(k,\varphi) + \text{æ}_2 \left.\frac{\partial T(\rho,\varphi)}{\partial \rho}\right|_{\rho=k} = \tau(\varphi), \tag{3.3.1}$$

where $t(\varphi)$ and $\tau(\varphi)$ are given functions and constants ℓ_m and æ_m, $m = 1,2$, define the type of boundary condition (similarly to (2.3.65) in Section 2.3.5). Using the temperature representation (3.2.2) and representing the heat sources density and right-hand sides of conditions (3.3.1) as follows:

$$w(\rho,\varphi) = w_0(\rho) + \sum_{n=1}^{\infty}\left(w_n^1(\rho)\cos n\varphi + w_n^2(\rho)\sin n\varphi\right),$$
$$t(\varphi) = t_0 + \sum_{n=1}^{\infty}\left(t_n^1\cos n\varphi + t_n^2\sin n\varphi\right), \tag{3.3.2}$$
$$\tau(\varphi) = \tau_0 + \sum_{n=1}^{\infty}\left(\tau_n^1\cos n\varphi + \tau_n^2\sin n\varphi\right),$$

we can separate variables in the formulated heat-conduction problem (3.1.22) and (3.3.1) to determine the coefficients of corresponding series representations separately. Here,

$$w_0(\rho) = \frac{1}{2\pi}\int_0^{2\pi} w(\rho,\varphi)d\varphi,$$
$$w_n^1(\rho) = \frac{1}{\pi}\int_0^{2\pi} w(\rho,\varphi)\cos n\varphi d\varphi,$$

$$w_n^2(\rho)=\frac{1}{\pi}\int_0^{2\pi} w(\rho,\varphi)\sin n\varphi d\varphi,$$

$$t_0=\frac{1}{2\pi}\int_0^{2\pi} t(\varphi)d\varphi,$$

$$t_n^1=\frac{1}{\pi}\int_0^{2\pi} t(\varphi)\cos n\varphi d\varphi, \tag{3.3.3}$$

$$t_n^2=\frac{1}{\pi}\int_0^{2\pi} t(\varphi)\sin n\varphi d\varphi,$$

$$\tau_0=\frac{1}{2\pi}\int_0^{2\pi} \tau(\varphi)d\varphi,$$

$$\tau_n^1=\frac{1}{\pi}\int_0^{2\pi} \tau(\varphi)\cos n\varphi d\varphi,$$

$$\tau_n^2=\frac{1}{\pi}\int_0^{2\pi} \tau(\varphi)\sin n\varphi d\varphi.$$

For constituent $T_0(\rho)$ of the temperature series representation (3.2.2), equation (3.1.22) and boundary conditions (3.3.1) take the forms

$$\frac{d}{d\rho}\left(\rho\frac{dT_0(\rho)}{d\rho}\right)=-\rho\left(\frac{w_0(\rho)}{\lambda_r(\rho)}+\frac{d\ln\lambda_r(\rho)}{d\rho}\frac{dT_0(\rho)}{d\rho}\right) \tag{3.3.4}$$

and

$$\begin{aligned}\ell_1 T_0(1)+\ell_2\left.\frac{dT_0(\rho)}{d\rho}\right|_{\rho=1}&=t_0,\\ æ_1 T_0(k)+æ_2\left.\frac{dT_0(\rho)}{d\rho}\right|_{\rho=k}&=\tau_0,\end{aligned} \tag{3.3.5}$$

respectively. Solving equation (3.3.4) with respect to its left-hand side yields

$$T_0(\rho) = A_0 \ln\frac{\rho^2}{k} + B_0 - \frac{1}{2}\int_k^1 \eta \frac{w_0(\eta)}{\lambda_r(\eta)}\left|\ln\frac{\rho}{\eta}\right| d\eta$$

$$+\frac{1}{2}\int_k^1 T_0(\eta)\left(\frac{d}{d\eta}\left(\eta\frac{d\ln\lambda_r(\eta)}{d\eta}\right)\left|\ln\frac{\rho}{\eta}\right|\right.$$

$$\left.-\frac{d\ln\lambda_r(\eta)}{d\eta}\operatorname{sgn}(\rho-\eta)\right) d\eta\,. \qquad (3.3.6)$$

The constants of integration, A_0 and B_0, can be computed by inserting (3.3.6) into conditions (3.3.5), which yields the expression for the temperature in the case of thermal loading independent of the angular coordinate, in the following form:

$$T_0(\rho) = \frac{\alpha_{22}\ln\frac{\rho^2}{k} - 2\alpha_{21}}{2\alpha_0} t_0 + \frac{2\alpha_{11} - \alpha_{12}\ln\frac{\rho^2}{k}}{2\alpha_0}\tau_0$$

$$+W_0(\rho) + \int_k^1 T_0(\eta)\mathcal{L}_0(\rho,\eta)d\eta, \qquad (3.3.7)$$

where

$$W_0(\rho) = \int_k^1 \eta\frac{w_0(\eta)}{\lambda_r(\eta)}\left(\frac{\psi_1(\eta)}{\alpha_0}\left(\alpha_{21} - \frac{\alpha_{22}}{2}\ln\frac{\rho^2}{k}\right)\right.$$

$$\left.+\frac{\psi_k(\eta)}{\alpha_0}\left(\alpha_{11} - \frac{\alpha_{12}}{2}\ln\frac{\rho^2}{k}\right) - \frac{1}{2}\left|\ln\frac{\rho}{k}\right|\right) d\eta\,,$$

$$\mathcal{L}_0(\rho,\eta) = \frac{d}{d\eta}\left(\eta\frac{d\ln\lambda_r(\eta)}{d\eta}\right)\left(\frac{1}{2}\left|\ln\frac{\rho}{k}\right|\right.$$

$$+\frac{\psi_1(\eta)}{\alpha_0}\left(\frac{\alpha_{22}}{2}\ln\frac{\rho^2}{k}-\alpha_{21}\right)+\frac{\psi_k(\eta)}{\alpha_0}\left(\frac{\alpha_{12}}{2}\ln\frac{\rho^2}{k}-\alpha_{11}\right)\Bigg)$$

$$+\frac{d\ln\lambda_r(\eta)}{d\eta}\left(\frac{\ell_0}{\alpha_0}\left(\frac{\alpha_{22}}{2}\ln\frac{\rho^2}{k}-\alpha_{21}\right)\right.$$

$$\left.+\frac{æ_0}{\alpha_0}\left(\frac{\alpha_{12}}{2}\ln\frac{\rho^2}{k}-\alpha_{11}\right)-\frac{\operatorname{sgn}(\rho-\eta)}{2}\right),$$

$$\ell_0=\frac{1}{2}\left(\ell_1-\ell_2\left.\frac{d\ln\lambda_r(\rho)}{d\rho}\right|_{\rho=1}\right),$$

$$æ_0=\frac{1}{2}\left(æ_1-æ_2\left.\frac{d\ln\lambda_r(\rho)}{d\rho}\right|_{\rho=k}\right), \tag{3.3.8}$$

$$\alpha_{11}=-\frac{\ell_1}{2}\ln k+\ell_2\left(1+\frac{\ln k}{2}\left.\frac{d\ln\lambda_r(\rho)}{d\rho}\right|_{\rho=1}\right),$$

$$\alpha_{12}=\ell_1-\ell_2\left.\frac{d\ln\lambda_r(\rho)}{d\rho}\right|_{\rho=1},$$

$$\alpha_{21}=\frac{æ_1}{2}\ln k+æ_2\left(\frac{1}{k}-\frac{\ln k}{2}\left.\frac{d\ln\lambda_r(\rho)}{d\rho}\right|_{\rho=k}\right),$$

$$\alpha_{22}=-æ_1+æ_2\left.\frac{d\ln\lambda_r(\rho)}{d\rho}\right|_{\rho=k},$$

$$\psi_1(\eta)=\frac{1}{2}\big(\ell_1-\ell_2\varphi(1,\eta)\big),$$

$$\psi_k(\eta)=\frac{1}{2}\big(æ_1-æ_2\varphi(k,\eta)\big),$$

$$\alpha_0=\alpha_{11}\alpha_{22}-\alpha_{12}\alpha_{21},$$

$$\varphi(j,\eta)=\frac{1}{j}+\ln\eta\left.\frac{d\ln\lambda_r(\rho)}{d\rho}\right|_{\rho=j}\qquad j=1,k\,.$$

A solution to integral equation (3.3.7) can be written explicitly as follows:

$$T_0(\rho)=t_0\tilde{t}_0(\rho)+\tau_0\tilde{\tau}_0(\rho)+\tilde{w}_0(\rho)\,, \tag{3.3.9}$$

where

$$\tilde{t}_0(\rho)=\alpha_{22}\tau_2^0(\rho)-\alpha_{21}\tau_1^0(\rho),$$

$$\tilde{\tau}_0(\rho)=\alpha_{11}\tau_1^0(\rho)-\alpha_{12}\tau_2^0(\rho),$$

$$\tilde{w}_0(\rho)=W_0(\rho)+\int_k^1 W_0(\eta)\mathcal{T}_0(\rho,\eta)d\eta, \tag{3.3.10}$$

$$\tau_1^0(\rho)=\frac{1}{2\alpha_0}\left(1+\int_k^1\mathcal{T}_0(\rho,\eta)d\eta\right),$$

$$\tau_2^0(\rho)=\frac{1}{2\alpha_0}\left(\ln\frac{\rho^2}{k}+\int_k^1\ln\frac{\eta^2}{k}\mathcal{T}_0(\rho,\eta)d\eta\right),$$

and the resolvent kernel can be evaluated as

$$\mathcal{T}_0(\rho,\eta)=\sum_{m=0}^{\infty}\mathcal{L}_0^{m+1}(\rho,\eta)\,, \tag{3.3.11}$$

where

$$\begin{gathered}\mathcal{L}_0^1(\rho,\eta)=\mathcal{L}_0(\rho,\eta),\\ \mathcal{L}_0^{m+1}(\rho,\eta)=\int_k^1\mathcal{L}_0^1(\rho,t)\mathcal{L}_0^m(t,\eta)dt,\quad m=1,2,...\end{gathered} \tag{3.3.12}$$

Constituents $T_n^{\ell}(\rho)$, $\ell = 1,2$; $n = 1,2,\ldots$, of the temperature series representation (3.2.2) satisfy the following equation:

$$\frac{d^2T_n^{\ell}(\rho)}{d\rho^2} + \frac{1}{\rho}\frac{dT_n^{\ell}(\rho)}{d\rho} - \frac{n^2}{\rho^2}T_n^{\ell}(\rho)$$

$$= \frac{n^2}{\rho^2}\frac{\lambda_{\varphi}(\rho) - \lambda_r(\rho)}{\lambda_r(\rho)}T_n^{\ell}(\rho)$$

$$- \frac{d\ln\lambda_r(\rho)}{d\rho}\frac{dT_n^{\ell}(\rho)}{d\rho} - \frac{w_n^{\ell}(\rho)}{\lambda_r(\rho)} \tag{3.3.13}$$

and boundary conditions

$$\ell_1 T_n^{\ell}(1) + \ell_2 \left.\frac{dT_n^{\ell}(\rho)}{d\rho}\right|_{\rho=1} = t_n^{\ell},$$

$$æ_1 T_n^{\ell}(k) + æ_2 \left.\frac{dT_n^{\ell}(\rho)}{d\rho}\right|_{\rho=k} = \tau_n^{\ell}, \tag{3.3.14}$$

which follow from equation (3.1.22) and conditions (3.3.1) in view of (3.2.2) and (3.3.2). Solving (3.3.13) with respect to its left-hand side yields the following integral equation:

$$T_n^{\ell}(\rho) = A_n^{\ell}\rho^{-n} + B_n^{\ell}\rho^{n}$$

$$+ \frac{1}{4n}\int_k^1 \frac{w_n^{\ell}(\eta)}{\lambda_r(\eta)}\chi_n^{-}(\rho,\eta)\,\mathrm{sgn}(\rho-\eta)\,d\eta$$

$$+ \frac{1}{4n}\int_k^1 T_n^{\ell}(\eta)\left(\left(\frac{n^2}{\eta^2}\frac{\lambda_r(\eta) - \lambda_{\varphi}(\eta)}{\lambda_r(\eta)} - \frac{d^2\ln\lambda_r(\eta)}{d\eta^2}\right)\chi_n^{-}(\rho,\eta)\right.$$

$$\left. - \frac{n}{\eta}\frac{d\ln\lambda_r(\eta)}{d\eta}\chi_n^{+}(\rho,\eta)\right)\mathrm{sgn}(\rho-\eta)\,d\eta, \tag{3.3.15}$$

where functions $\chi_n^{\pm}(\rho,\eta)$ are given by formula (3.2.44). We can substitute (3.3.15) into (3.3.14) to eliminate the constants of integration A_n^{ℓ} and B_n^{ℓ} in order to obtain the following:

$$T_n^{\ell}(\rho)=\frac{l_{22}\rho^{-n}-l_{21}\rho^{n}}{\alpha_n}t_n^{\ell}+\frac{l_{11}\rho^{n}-l_{12}\rho^{-n}}{\alpha_n}\tau_n^{\ell}$$

$$+W_n^{\ell}(\rho)+\int_k^1 T_n^{\ell}(\eta)\mathcal{L}_n(\rho,\eta)d\eta, \tag{3.3.16}$$

where

$$W_n^{\ell}(\rho)=\frac{1}{4n}\int_k^1\frac{w_n^{\ell}(\eta)}{\lambda_r(\eta)}\left(\frac{l_{22}\rho^{-n}-l_{21}\rho^{n}}{\alpha_n}\right.$$

$$\times\left(\ell_2\left(n\chi_n^{+}(1,\eta)+\left.\frac{d\ln\lambda_r(\rho)}{d\rho}\right|_{\rho=1}\chi_n^{-}(1,\eta)\right)-\ell_1\chi_n^{-}(1,\eta)\right)$$

$$+\frac{l_{12}\rho^{-n}-l_{11}\rho^{n}}{\alpha_n}\left(\frac{æ_2}{k}\left(n\chi_n^{+}(k,\eta)+\left.\frac{d\ln\lambda_r(\rho)}{d\rho}\right|_{\rho=k}\chi_n^{-}(k,\eta)\right)-æ_1\chi_n^{-}(k,\eta)\right)$$

$$\left.+\chi_n^{-}(\rho,\eta)\,\mathrm{sgn}(\rho-\eta)\right)d\eta,$$

$$\mathcal{L}_n(\rho,\eta)=\frac{1}{4n}\left(\left(\frac{n^2}{\eta^2}\frac{\lambda_r(\eta)-\lambda_\varphi(\eta)}{\lambda_r(\eta)}-\frac{d^2\ln\lambda_r(\eta)}{d\eta^2}\right)\right.$$

$$\times\left(\frac{l_{21}\rho^{n}-l_{22}\rho^{-n}}{\alpha_n}\left(-\ell_2 n\chi_n^{+}(1,\eta)+\left(\ell_1-\ell_2\left.\frac{d\ln\lambda_r(\rho)}{d\rho}\right|_{\rho=1}\right)\chi_n^{-}(1,\eta)\right)\right.$$

$$+\frac{l_{11}\rho^{n}-l_{12}\rho^{-n}}{\alpha_n}\left(-\frac{æ_2}{k}n\chi_n^{+}(k,\eta)+\left(æ_1-æ_2\left.\frac{d\ln\lambda_r(\rho)}{d\rho}\right|_{\rho=k}\right)\chi_n^{-}(k,\eta)\right)$$

$$+\chi_n^-(\rho,\eta)\operatorname{sgn}(\rho-\eta)\Bigg)+\frac{n}{\eta}\frac{d\ln\lambda_r(\eta)}{d\eta} \tag{3.3.17}$$

$$\times\Bigg(\frac{l_{21}\rho^n-l_{22}\rho^{-n}}{\alpha_n}\Bigg(\ell_2 n\chi_n^-(1,\eta)-\Bigg(\ell_1-\ell_2\frac{d\ln\lambda_r(\rho)}{d\rho}\Bigg|_{\rho=1}\Bigg)\chi_n^+(1,\eta)\Bigg)$$

$$+\frac{l_{11}\rho^n-l_{12}\rho^{-n}}{\alpha_n}\Bigg(\frac{æ_2}{k}n\chi_n^-(k,\eta)-\Bigg(æ_1-\frac{æ_2}{k}\frac{d\ln\lambda_r(\rho)}{d\rho}\Bigg|_{\rho=k}\Bigg)\chi_n^+(k,\eta)\Bigg)$$

$$-\chi_n^+(\rho,\eta)\operatorname{sgn}(\rho-\eta)\Bigg)\Bigg),\ l_{11}=\ell_1-\ell_2 d_n^+(1),\quad l_{12}=\ell_1+\ell_2 d_n^-(1),$$

$$l_{21}=\big(æ_1-æ_2 d_n^+(k)\big)k^{-n},\quad l_{22}=\big(æ_1+æ_2 d_n^-(k)\big)k^n,$$

$$\alpha_n=l_{11}l_{22}-l_{12}l_{21},\quad d_n^{\pm}(\rho)=\frac{1}{\rho}\Bigg(n\pm\frac{d\ln\lambda_r(\rho)}{d\rho}\Bigg).$$

A solution to integral equation (3.3.16) can be given in an explicit form

$$T_n^\ell(\rho)=t_n^\ell\tilde{t}_n^\ell(\rho)+\tau_n^\ell\tilde{\tau}_n^\ell(\rho)+\tilde{w}_n^\ell(\rho)\,, \tag{3.3.18}$$

where

$$\tilde{t}_n^\ell(\rho)=\frac{1}{\alpha_n}\Bigg(l_{22}\rho^{-n}-l_{21}\rho^n+\int_k^1\big(l_{22}\eta^{-n}-l_{21}\eta^n\big)\mathcal{T}_n(\rho,\eta)d\eta\Bigg),$$

$$\tilde{\tau}_n^\ell(\rho)=\frac{1}{\alpha_n}\Bigg(l_{11}\rho^n-l_{12}\rho^{-n}+\int_k^1\big(l_{11}\eta^n-l_{12}\eta^{-n}\big)\mathcal{T}_n(\rho,\eta)d\eta\Bigg), \tag{3.3.19}$$

$$\tilde{w}_n^\ell(\rho)=W_n^\ell(\rho)+\int_k^1 W_n^\ell(\eta)\mathcal{T}_n(\rho,\eta)d\eta,$$

and the resolvent kernel can be evaluated as

$$\mathcal{T}_n(\rho,\eta)=\sum_{m=0}^{\infty}\mathcal{L}_n^{m+1}(\rho,\eta)\,, \tag{3.3.20}$$

where

$$\mathcal{L}_n^1(\rho,\eta)=\mathcal{L}_n(\rho,\eta),$$
$$\mathcal{L}_n^{m+1}(\rho,\eta)=\int_k^1\mathcal{L}_n^1(\rho,t)\mathcal{L}_n^m(t,\eta)dt,\quad m=1,2,... \tag{3.3.21}$$

3.4. Specific material properties and solutions

3.4.1. Trivial resolvent kernels

Similar to the plane problem in the Cartesian coordinate system considered in Chapter 2, the major challenge in the analysis of stresses, displacements, and temperature in an inhomogeneous orthotropic ring lies in the evaluation of resolvent kernels (3.2.22), (3.2.60), (3.3.11), and (3.3.20). Thus, it is reasonable to analyze the cases where the latter functions are either absent or have a relatively simple form.

To eliminate resolvent kernels (3.2.22) and (3.2.60) respectively for the axisymmetric and angle-dependent parts of the stresses, it is enough to make sure that the corresponding kernels (3.2.19) and (3.2.57) of integral equations (3.2.18) and (3.2.56) equal zero for all possible values of their variables. From (3.2.19), we see that $\mathcal{K}_0(\rho,\eta)\equiv 0$ if

$$\rho\frac{d\beta_2(\rho)}{d\rho}=\beta_3(\rho)\,. \tag{3.4.1}$$

In view of (3.2.57), kernel $\mathcal{K}_n(\rho,\eta)\equiv 0$ can be eliminated as long as $\psi_n^{\pm}(\rho)=\psi_n(\rho)\equiv 0$. The latter condition in conjunction with (3.2.55) and the obvious restriction that the material properties must be independent of the Fourier harmonic number n yield the following relations:

$$\frac{d}{d\rho}\left(\frac{\beta_2(\rho)}{\rho}\right)+\frac{\beta_1(\rho)}{\rho^2}=2\beta_2(\rho)-\frac{1}{G_{r\varphi}(\rho)}=0,$$

$$\frac{d}{d\rho}\left(\frac{1}{\rho}\left(2\beta_2(\rho)-\frac{1}{G_{r\varphi}(\rho)}\right)\right)=\frac{\beta_3(\rho)}{\rho^2}, \tag{3.4.2}$$

$$\beta_1(\rho)+\beta_2(\rho)=\frac{1}{G_{r\varphi}(\rho)},$$

along with one more condition

$$\frac{d}{d\rho}\left(\frac{1}{\rho}\frac{d\beta_2(\rho)}{d\rho}-\frac{\beta_3(\rho)}{\rho^2}\right)=0\,, \tag{3.4.3}$$

which is satisfied in view of (3.4.1). Conditions (3.4.1) and (3.4.2) imply that

$$\beta_1(\rho)=\beta_2(\rho)=\frac{1}{2G_{r\varphi}(\rho)}\,, \tag{3.4.4}$$

or, in view of (3.1.18),

$$a_{11}(\rho)=a_{22}(\rho)=a_{12}(\rho)+\frac{1}{2G_{r\varphi}(\rho)}\,, \tag{3.4.5}$$

and

$$\frac{d}{d\rho}\left(\frac{1}{G_{r\varphi}(\rho)}\right)=0\,. \tag{3.4.6}$$

Condition (3.4.6) implies that shear modulus $G_{r\varphi}(\rho)$ is a constant (i.e., $G_{r\varphi}(\rho)=G_0=\text{const}$), which modifies condition (3.4.5) as follows:

$$a_{11}(\rho)=a_{22}(\rho)=a_{12}(\rho)+\frac{1}{2G_0}. \tag{3.4.7}$$

Condition (3.4.7) when considered with expressions (3.1.2) for the case of plane stress imposes the following restrictions on the elastic moduli:

$$\frac{E_r(\rho)}{1+\nu_{r\varphi}(\rho)}=\frac{E_\varphi(\rho)}{1+\nu_{\varphi r}(\rho)}=2G_{r\varphi}=G_0=\text{const}. \tag{3.4.8}$$

As we can see from the latter formula, if $E_r=\text{const}$, then necessarily $\nu_{r\varphi}=\text{const}$, and vice versa. The same conclusion can be drawn for the pair of moduli E_φ and $\nu_{\varphi r}$.

For the case of plane strain, conditions (3.4.7) and (3.1.2) yield

$$\frac{E_r(\rho)}{1+\nu_{r\varphi}(\rho)+\nu_{rz}(\rho)(\nu_{z\varphi}(\rho)-\nu_{zr}(\rho))}$$

$$=\frac{E_\varphi(\rho)}{1+\nu_{\varphi r}(\rho)+\nu_{\varphi z}(\rho)(\nu_{zr}(\rho)-\nu_{z\varphi}(\rho))}$$

$$=2G_{r\varphi}=2G_0=\text{const}. \tag{3.4.9}$$

3.4.2. Isotropic and transversely isotropic materials

As can be concluded from expressions (3.1.4) – (3.1.6), conditions (3.4.5) are always valid for transversely isotropic and isotropic materials. In both cases, the axially symmetric part of the total stress at $e_0=0$ can be derived using (3.2.31), where

$$P_{10}(\rho)=kE^*(\rho)\left(\frac{f(\rho)}{a_0}\left(k+\int_k^1\mathcal{K}_0(\xi,k)\varphi_0(\xi)d\xi\right)\right.$$

$$\left.-\mathcal{K}_0(\rho,k)+\int_k^\rho E^*(\xi)\mathcal{K}_0(\xi,k)\mathcal{R}_0(\rho,\xi)d\xi\right),$$

$$P_{20}(\rho) = -E^*(\rho)\frac{f(\rho)}{a_0},$$

$$\theta_0(\rho) = E^*(\rho)\left(\frac{f(\rho)}{a_0}\int_k^1 \alpha^*(\xi)T_0(\xi)\varphi_0(\xi)d\xi \right.$$

$$\left. -\alpha^*(\rho)T_0(\rho) - \int_k^\rho \alpha^*(\xi)E^*(\xi)T_0(\xi)\mathcal{R}_0(\rho,\xi)d\xi \right), \qquad (3.4.10)$$

$$f(\rho) = 1 + \int_k^\rho E^*(\xi)\mathcal{R}_0(\rho,\xi)d\xi,$$

$$\varphi_0(\xi) = E^*(\rho)\left(\xi + \int_\xi^1 \rho E^*(\rho)\mathcal{R}_0(\rho,\xi)d\rho \right),$$

$$a_0 = \int_k^1 \rho E^*(\rho)f(\rho)d\rho\,.$$

In this case, the integral kernel given in (3.2.19) takes a form by which the resolvent kernel given in (3.2.22) is originated in accordance with (3.2.23), as follows:

$$\mathcal{K}_0(\rho,\xi) = \frac{\xi}{2}\int_\xi^\rho \frac{1}{\eta^2}\frac{d}{d\eta}\left(\frac{1}{G(\eta)}\right)d\eta\,. \qquad (3.4.11)$$

Moduli $E^*(\rho)$ and $\alpha^*(\xi)$ are represented by expressions (3.1.5) for transversely isotropic materials and using (3.1.6) for isotropic materials. The axisymmetric components of the radial and circumferential stresses have the form of (3.2.28) with coefficients (3.2.29) as computed using (3.4.10). The component for shear stress given in (3.2.11) does not change its appearance.

The angle-dependent components of the total stress (3.2.58) where the coefficients (3.2.59) are expressed by

$$P_n^{\ell}(\rho) = -\frac{k}{4}\left(\frac{\chi_n^{-}(\rho,k)}{n} \frac{d}{dr}\left(\frac{1}{G(\rho)} \right) \right|_{\rho=k}$$

$$+k\int_k^{\rho} \frac{d}{d\eta}\left(\frac{1}{G(\eta)} \right)\left(k^{-n}\rho^{-n}\eta^{2(n-1)} + k^n\rho^n\eta^{-2(n+1)} \right) d\eta \Bigg),$$

$$Q_n^{\ell}(\rho) = \frac{(-1)^{\ell}k^2}{4}\int_k^{\rho} \frac{d}{d\eta}\left(\frac{1}{G(\eta)} \right)$$

$$\times\left(k^{-n}\rho^{-n}\eta^{2(n-1)} - k^n\rho^n\eta^{-2(n+1)} \right) d\eta, \qquad (3.4.12)$$

$$\Theta_n^{\ell}(\rho) = -\alpha^*(\rho)T_n^{\ell}(\rho),$$

$$a_n(\rho) = \rho^{-n} + \int_k^{\rho} \eta^{-n}E^*(\eta)\mathcal{R}_n(\rho,\eta)d\eta,$$

$$b_n(\rho) = \rho^n + \int_k^{\rho} \eta^n E^*(\eta)\mathcal{R}_n(\rho,\eta)d\eta\,.$$

Integral kernel (3.2.57) has the form

$$\mathcal{K}_n(\rho,\eta) = \frac{\eta}{4}\int_{\eta}^{\rho} \frac{d}{d\xi}\left(\frac{1}{G(\xi)} \right)\left((n+1)\rho^n\eta^n\xi^{-2(n+1)} \right.$$

$$\left. -(n-1)\rho^{-n}\eta^{-n}\xi^{2(n-1)} \right) d\xi\,, \qquad (3.4.13)$$

and constants A_n^{ℓ} and B_n^{ℓ} for $n>1$ are given by expressions (3.2.62) with the following coefficients:

$$F_{1n}^{\ell} = k^{n+2}p_{1n}^{\ell} - p_{2n}^{\ell} + (-1)^{\ell}\left(k^{n+2}q_{1n}^{\ell} - q_{2n}^{\ell} \right)$$

$$-(n+1)\int_k^1 \rho^{1+n}E^*(\rho)f_n^{\ell}(\rho)d\rho\,,$$

$$F_{2n}^{\ell} = p_{2n}^{\ell} - k^{2-n} p_{1n}^{\ell} + (-1)^{\ell} \left(k^{2-n} q_{1n}^{\ell} - q_{2n}^{\ell} \right)$$

$$-(n-1)\int_{k}^{1} \rho^{1-n} E^{*}(\rho) f_{n}^{\ell}(\rho) d\rho, \tag{3.4.14}$$

$$f_{n}^{\ell}(\rho) = p_{1n}^{\ell} \overline{P}_{n}^{\ell}(\rho) + q_{1n}^{\ell} \overline{Q}_{n}^{\ell}(\rho) + \overline{\Theta}_{n}^{\ell}(\rho),$$

$$a_{n}^{\pm} = (n \pm 1)\int_{k}^{1} \rho^{1\pm n} E^{*}(\rho) a_{n}(\rho) d\rho,$$

$$b_{n}^{\pm} = (n \pm 1)\int_{k}^{1} \rho^{1\pm n} E^{*}(\rho) b_{n}(\rho) d\rho .$$

Here, $\chi_{n}^{-}(\rho, k)$ is given by (3.2.44) and resolvent kernel (3.2.60) is computed by means of the formulae (3.2.61) with account for the kernel (3.4.13). Constants A_{1}^{ℓ} and B_{1}^{ℓ} are given by (3.2.64) with coefficients (3.2.65) expressed as follows:

$$a_{1}^{0} = k^{3} \frac{d}{d\rho}\left(\frac{a_{1}(\rho)}{\rho} \right)\Bigg|_{\rho=k} + \frac{d}{d\rho}\left(\frac{a_{1}(\rho)}{\rho} \right)\Bigg|_{\rho=1},$$

$$b_{1}^{0} = k^{3} \frac{d}{d\rho}\left(\frac{b_{1}(\rho)}{\rho} \right)\Bigg|_{\rho=k} + \frac{d}{d\rho}\left(\frac{b_{1}(\rho)}{\rho} \right)\Bigg|_{\rho=1},$$

$$F_{21}^{0\ell} = -\frac{k^{3} p_{11}^{\ell}}{2} \frac{d}{d\rho}\left(\frac{1}{\rho G(\rho)} \right)\Bigg|_{\rho=k}$$

$$-\frac{p_{21}^{\ell}}{2} \frac{d}{d\rho}\left(\frac{1}{\rho G(\rho)} \right)\Bigg|_{\rho=1} - \frac{(-1)^{\ell} k q_{11}^{\ell}}{G(k)} - \frac{(-1)^{\ell} k q_{21}^{\ell}}{G(1)} \tag{3.4.15}$$

$$+k\alpha^{*}(k) T_{1}^{\ell}(k) - k^{2} \frac{d}{d\rho}\left(\alpha^{*}(\rho) T_{1}^{\ell}(\rho) + \frac{k}{\rho} f_{1}^{\ell}(\rho) \right)\Bigg|_{\rho=k}$$

$$+\alpha^*(1)T_1^\ell(1)-\frac{d}{d\rho}\left(\alpha^*(\rho)T_1^\ell(\rho)+\frac{1}{\rho}f_1^\ell(\rho)\right)\Big|_{\rho=1}.$$

The angle-dependent parts of stresses can be computed by substituting the found total stress into expressions (3.2.51).

If the shear modulus meets condition (3.4.6), kernels (3.4.11) and (3.4.13) are equal to zero which allows for simplification of expressions (3.4.10) and (3.4.12).

If all the material properties in expressions (3.1.5) and (3.1.6) are constant, then the components of total stress are as follows:

$$\begin{gathered}\sigma_0(\rho)=\frac{2}{1-k^2}\left(k^2p_{10}-p_{20}+\frac{\alpha E}{1-\nu}\int_k^1\rho T_0(\rho)d\rho\right)\\ -\frac{\alpha E}{1-\nu}T_0(\rho),\\ \sigma_n^\ell(\rho)=A_n^\ell\rho^{-n}+B_n^\ell\rho^n-\frac{\alpha E}{1-\nu}T_n^\ell(\rho),\\ \ell=1,2;n=1,2,3,\ldots,\end{gathered}\tag{3.4.16}$$

where constants A_n^ℓ and B_n^ℓ, $n>1$, have the form

$$\begin{gathered}A_n^\ell=\frac{2}{\mu}\left(\left(k^{-n}+nk^n(1-k^2)-k^n\right)k^2p_{1n}^\ell\right.\\ -\left(n(1-k^2)+k^2(1-k^{2n})\right)p_{2n}^\ell\\ +\left(nk^n(1-k^2)-k^n-k^{-n}+2k^{2+n}\right)(-1)^\ell k^2q_{1n}^\ell\\ +\left(2-n(1-k^2)-k^2(1+k^{2n})\right)(-1)^\ell q_{2n}^\ell\\ +(n-1)\frac{\alpha E}{1-\nu}\left((n+1)(1-k^2)\int_k^1\rho^{1+n}T_n^\ell(\rho)d\rho\right.\end{gathered}$$

$$-(1-k^{2+2n})\int_k^1 \rho^{1-n}T_n^\ell(\rho)d\rho\Bigg)\Bigg),$$

$$B_n^\ell = \frac{2}{\mu}\Bigg(\left(k^n - nk^{-n}(1-k^2) - k^{-n}\right)k^2 p_{1n}^\ell \tag{3.4.17}$$

$$+\left(n(1-k^2) - k^2(1-k^{-2n})\right)p_{2n}^\ell$$

$$+\left(nk^{-n}(1-k^2) + k^n + k^{-n} - 2k^{2-n}\right)(-1)^\ell k^2 q_{1n}^\ell$$

$$-\left(2 + n(1-k^2) - k^2(1+k^{-2n})\right)(-1)^\ell q_{2n}^\ell$$

$$+(n+1)\frac{\alpha E}{1-\nu}\Bigg((n-1)(1-k^2)\int_k^1 \rho^{1-n}T_n^\ell(\rho)d\rho$$

$$+(1-k^{2-2n})\int_k^1 \rho^{1+n}T_n^\ell(\rho)d\rho\Bigg)\Bigg),$$

$$\mu = k^2\left(n^2(k-k^{-1})^2 - (k^n - k^{-n})^2\right),$$

and constants A_1^ℓ and B_1^ℓ take the form

$$A_1^\ell = \frac{(-1)^\ell q_{21}^\ell - p_{21}^\ell}{2(1-\nu)},$$

$$B_1^\ell = \frac{2}{k^4-1}\Bigg[\frac{1-2\nu+k^2}{2(1-\nu)}k\left(p_{11}^\ell - (-1)^\ell q_{11}^\ell\right) \tag{3.4.18}$$

$$-k^3\left(p_{11}^\ell + (-1)^\ell q_{11}^\ell\right) + 2(-1)^\ell q_{21}^\ell$$

$$-\frac{2\alpha E}{1-\nu}\int_k^1 \rho^2 T_1^\ell(\rho)d\rho\Bigg], \quad \ell = 1,2.$$

The expression for the stress-tensor components in this case can be found as follows:

$$S_0(\rho)=\left(\frac{k}{\rho}\right)^2 q_{10}=\frac{1}{\rho^2}q_{20},$$

$$R_0(\rho)=-\frac{k^2\left(1-\rho^2\right)}{\rho^2\left(1-k^2\right)}p_{10}-\frac{\rho^2-k^2}{\rho^2\left(1-k^2\right)}p_{20}$$

$$+\frac{\alpha E}{2(1-\nu)\rho^2}\int_k^1 \eta T_0(\eta)\left(\frac{2\rho^2-k^2-1}{1-k^2}-\operatorname{sgn}(\rho-\eta)\right)d\eta, \qquad (3.4.19)$$

$$\Phi_0(\rho)=\frac{k^2\left(1+\rho^2\right)}{\rho^2\left(1-k^2\right)}p_{10}-\frac{\rho^2+k^2}{\rho^2\left(1-k^2\right)}$$

$$+\frac{\alpha E}{1-\nu}\left(\frac{1}{2\rho^2}\int_k^1 \eta T_0(\eta)\left(\frac{2\rho^2+k^2+1}{1-k^2}+\operatorname{sgn}(\rho-\eta)\right)d\eta-T_0(\rho)\right),$$

and

$$S_n^\ell(\rho)=\frac{k^2}{2\rho^2}\chi^+(\rho,k)q_{1n}^\ell+(-1)^\ell\frac{k^2}{2\rho^2}\chi^-(\rho,k)p_{1n}^\ell$$

$$+\frac{(-1)^\ell A_n^\ell}{4\rho^2}\left(k^{2-n}\chi^-(\rho,k)+n\rho^{-n}(k^2-\rho^2)\right)$$

$$+\frac{(-1)^\ell B_n^\ell}{4\rho^2}\left(k^{2+n}\chi^-(\rho,k)+n\rho^{n}(k^2-\rho^2)\right)$$

$$+\frac{(-1)^\ell}{2\rho^2}\frac{\alpha E}{1-\nu}\int_k^r \eta T_n^i(\eta)\left(n\chi^+(\rho,\eta)+\chi^-(\rho,\eta)\right)d\eta,$$

$$R_n^\ell(\rho)=(-1)^{\ell+1}\frac{k^2}{2\rho^2}\chi^-(\rho,k)q_{1n}^\ell-\frac{k^2}{2\rho^2}\chi^+(\rho,k)p_{1n}^\ell$$

$$-\frac{A_n^\ell}{4\rho^2}\left(k^{2-n}\chi^+(\rho,k)+n\rho^{-n}(k^2-\rho^2)-2\rho^{2-n}\right)$$

$$-\frac{B_n^\ell}{4\rho^2}\left(k^{2+n}\chi^+(\rho,k)-nr^n(k^2-\rho^2)-2\rho^{2+n}\right)$$

$$-\frac{1}{2\rho^2}\frac{\alpha E}{1-\nu}\int_k^\rho \eta T_n^\ell(\eta)\left(n\chi^-(\rho,\eta)+\chi^+(\rho,\eta)\right)d\eta, \tag{3.4.20}$$

$$\Phi_n^\ell(\rho)=(-1)^\ell\frac{k^2}{2\rho^2}\chi^-(\rho,k)q_{1n}^\ell+\frac{k^2}{2\rho^2}\chi^+(\rho,k)p_{1n}^\ell$$

$$+\frac{A_n^\ell}{4\rho^2}\left(k^{2-n}\chi^+(\rho,k)+n\rho^{-n}(k^2-\rho^2)+2\rho^{2-n}\right)$$

$$+\frac{B_n^\ell}{4\rho^2}\left(k^{2+n}\chi^+(\rho,k)-n\rho^{n}(k^2-\rho^2)+2\rho^{2+n}\right)$$

$$+\frac{\alpha E}{1-\nu}\left(\frac{1}{2\rho^2}\int_k^\rho \eta T_n^\ell(\eta)\left(n\chi^-(\rho,\eta)+\chi^+(\rho,\eta)\right)d\eta-T_n^\ell(\rho)\right).$$

3.4.3. Michell's potential

The in-plane stress tensor components in a homogeneous isotropic ring can be determined using the following formulae:

$$\sigma_{rr}(\rho,\varphi)=\frac{1}{\rho}\left(\frac{\partial W(\rho,\varphi)}{\partial\rho}+\frac{1}{\rho}\frac{\partial^2 W(\rho,\varphi)}{\partial\varphi^2}\right),$$

$$\sigma_{\varphi\varphi}(\rho,\varphi)=\frac{\partial^2 W(\rho,\varphi)}{\partial\rho^2}, \tag{3.4.21}$$

$$\sigma_{r\varphi}(\rho,\varphi)=-\frac{\partial}{\partial\rho}\left(\frac{1}{\rho}\frac{\partial W(\rho,\varphi)}{\partial\varphi}\right),$$

where $W(\rho,\varphi)$ is biharmonic Michell's potential [26]

$$W(\rho,\varphi) = a_0 \ln\rho + \rho^2\left(b_0 + c_0\ln\rho + d_0\varphi\right) + a_0'\varphi$$

$$+\frac{a_1^1}{2}\rho\varphi\sin\varphi + \left(b_1^1\rho^3 + \frac{c_1^1}{\rho} + d_1^1\rho\ln\rho\right)\cos\varphi$$

$$-\frac{a_1^2}{2}\rho\varphi\cos\varphi + \left(b_1^2\rho^3 + \frac{c_1^2}{\rho} + d_1^2\rho\ln\rho\right)\sin\varphi$$

$$+\sum_{n=2}^{\infty}\left(a_n^1\rho^n + b_n^1\rho^{n+2} + c_n^1\rho^{-n} + d_n^1\rho^{-n+2}\right)\cos n\varphi$$

$$+\sum_{n=2}^{\infty}\left(a_n^2\rho^n + b_n^2\rho^{n+2} + c_n^2\rho^{-n} + d_n^2\rho^{-n+2}\right)\sin n\varphi\,, \qquad (3.4.22)$$

where $a_0, b_0, c_0, d_0, a'_0, a_n^i, b_n^i, c_n^i, d_n^i$ $(n = 1,2..., \ i = 1,2)$ are arbitrary constants which can be determined from additional conditions. Substituting (3.4.22) into (3.4.21) allows for expression of the stress tensor components in the following form:

$$\sigma_{rr}(\rho,\varphi) = a_0\rho^{-2} + 2b_0 + c_0\left(1 + 2\ln\rho\right)$$

$$+2d_0\varphi + \left(\frac{a_1^1 + d_1^1}{\rho} + 2b_1^1\rho - \frac{2c_1^1}{r\rho^3}\right)\cos\varphi$$

$$+\left(\frac{a_1^2 + d_1^2}{\rho} + 2b_1^2\rho - \frac{2c_1^2}{\rho^3}\right)\sin\varphi$$

$$-\sum_{n=2}^{\infty}(n-1)\left[na_n^1\rho^{n-2} + (n+2)d_n^1\rho^{-n}\right]\cos n\varphi$$

$$-\sum_{n=2}^{\infty}(n+1)\left[nc_n^1\rho^{-n-2} + (n-2)b_n^1\rho^n\right]\cos n\varphi$$

$$-\sum_{n=2}^{\infty}(n-1)\left[na_n^2\rho^{n-2}+(n+2)d_n^2\rho^{-n}\right]\sin n\varphi$$

$$-\sum_{n=2}^{\infty}(n+1)\left[nc_n^2\rho^{-n-2}+(n-2)b_n^2\rho^{n}\right]\sin n\varphi,$$

$$\sigma_{\varphi\varphi}(\rho,\varphi)=-a_0\rho^{-2}+2b_0+c_0\left(3+2\ln\rho\right)$$

$$+2d_0\varphi+\left(6\rho b_1^1+\frac{2c_1^1}{\rho^3}+\frac{d_1^1}{\rho}\right)\cos\varphi$$

$$+\left(6\rho b_1^2+\frac{2c_1^2}{\rho^3}+\frac{d_1^2}{\rho}\right)\sin\varphi$$

$$+\sum_{n=2}^{\infty}(n-1)\left[na_n^1\rho^{n-2}+(n-2)d_n^1\rho^{-n}\right]\cos n\varphi \qquad (3.4.23)$$

$$+\sum_{n=2}^{\infty}(n+1)\left[nc_n^1\rho^{-n-2}+(n+2)b_n^1\rho^{n}\right]\cos n\varphi$$

$$+\sum_{n=2}^{\infty}(n-1)\left[na_n^2\rho^{n-2}+(n-2)d_n^2\rho^{-n}\right]\sin n\varphi$$

$$+\sum_{n=2}^{\infty}(n+1)\left[nc_n^2r^{-n-2}+(n+2)b_n^2r^{n}\right]\sin n\theta,$$

$$\sigma_{r\varphi}(\rho,\varphi)=-d_0+\frac{a'_0}{\rho^2}+\left(2\rho b_1^1-2\frac{c_1^1}{\rho^3}+\frac{d_1^1}{\rho}\right)\sin\varphi$$

$$-\left(2\rho b_1^2-2\frac{c_1^2}{\rho^3}+\frac{d_1^2}{\rho}\right)\cos\varphi$$

$$+\sum_{n=2}^{\infty}n(n-1)\left(a_n^1\rho^{n-2}-d_n^1\rho^{-n}\right)\sin n\varphi$$

$$-\sum_{n=2}^{\infty} n(n+1)\left(c_n^1\rho^{-n-2} - b_n^1\rho^n\right)\sin n\varphi$$

$$-\sum_{n=2}^{\infty} n(n-1)\left(a_n^2\rho^{n-2} - d_n^2\rho^{-n}\right)\cos n\varphi$$

$$+\sum_{n=2}^{\infty} n(n+1)\left(c_n^2\rho^{-n-2} - b_n^2\rho^n\right)\cos n\varphi.$$

It can be shown that the stresses given by (3.4.23) coincide with those given by (3.4.19) and (3.4.20) in view of (3.2.2) disregarding the temperature under the following relations:

$$c_0 = d_0 = 0, \qquad a_0 = \frac{k^2(p_{20} - p_{10})}{1-k^2},$$

$$b_0 = \frac{k^2 p_{10} - p_{20}}{2(1-k^2)}, \qquad a_0' = q_{20},$$

$$a_1^\ell + d_1^\ell = \frac{1}{2}\left(k\left((-1)^\ell q_{11}^\ell - p_{11}^\ell\right) + A_1^\ell\right),$$

$$b_1^\ell = \frac{1}{8}B_1^\ell,$$

$$c_1^\ell = \frac{k^2}{8}\left(2k\left(p_{11}^\ell + (-1)^\ell q_{11}^\ell\right) + 2A_1^\ell + k^2 B_1^\ell\right), \tag{3.4.24}$$

$$a_n^\ell = \frac{k^2}{4n(n-1)}\left(2k^{-n}\left(p_{1n}^\ell - (-1)^\ell q_{1n}^\ell\right)\right.$$

$$\left. + k^{-2n}A_n^\ell - (n-1)B_n^\ell\right),$$

$$c_n^\ell = \frac{k^2}{4n(n+1)}\left(2k^n\left(p_{1n}^\ell + (-1)^\ell q_{1n}^\ell\right)\right.$$

$$\left. + k^{2n}B_n^\ell + (n+1)A_n^\ell\right),$$

$$b_n^{\ell} = \frac{1}{4(n+1)} B_n^{\ell}, \qquad d_n^{\ell} = -\frac{1}{4(n-1)} A_n^{\ell}, \qquad \ell = 1, 2.$$

The integral of a biharmonic equation in polar coordinates was first given in its most general form in [70] and later translated into English [71]. It is worth noting that the completeness and feasibility of the solutions based on biharmonic potential has been the subject of discussion in a series of comments [31, 114, 334] on the paper [241]. From this standpoint, the solution constructed here via direct integration method appear to be a superior approach, due to the fact that it deals with physical functions and does not call for increments of differential order of the governing equations and therefore does not required additional unfeasible terms to be dealt with through the imposition of additional conditions pertaining to feasibility.

In the next section, we consider various applications of the proposed solution for use in analyzing a number of important cases related to force and thermal loadings.

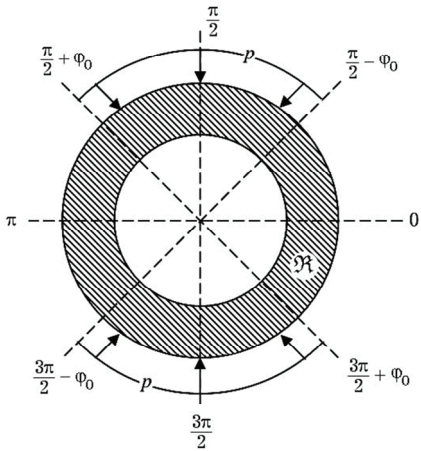

Figure 3.1. Loading scheme of diametrically-compressed annular domain

3.4.4. Special cases of loading

Consider the case where the effect of temperature is disregarded (i.e., $T = 0$) and the external force loading (3.2.1) is given by

$$p_1(\varphi)=q_1(\varphi)=q_2(\varphi)=0,$$
$$p_2(\varphi)=\begin{cases}p,\varphi\in\left[\left(\ell+\frac{1}{2}\right)\pi-\varphi_0,\left(\ell+\frac{1}{2}\right)\pi+\varphi_0\right],\\0,\text{elsewhere.}\end{cases} \tag{3.4.25}$$

In (3.4.25), $\ell=0,1$, $\varphi_0\in(0,\pi/2]$, and $p=\text{const}$ is a uniform pressure in the dimension of stress. A loading scheme for (3.4.25) is shown in Fig. 3.1.

In the case of homogeneous isotropic material, the stress field represented by (3.4.19) and (3.4.20) for the loading given in (3.4.25) can be expressed as follows [291]:

$$\sigma_{rr}(\rho,\varphi)=\frac{p}{\pi}\Bigg(-2\frac{\rho^2-k^2}{1-k^2}\frac{\varphi_0}{\rho^2}$$
$$+\sum_{m=1}^{\infty}\frac{(-1)^m R_m(\rho)}{m}\sin(2m\varphi_0)\cos(2m\varphi)\Bigg),$$
$$\sigma_{\varphi\varphi}(\rho,\varphi)=\frac{p}{\pi}\Bigg(-2\frac{\rho^2+k^2}{1-k^2}\frac{\varphi_0}{\rho^2} \tag{3.4.26}$$
$$+\sum_{m=1}^{\infty}\frac{(-1)^m \Phi_m(\rho)}{m}\sin(2m\varphi_0)\cos(2m\varphi)\Bigg),$$
$$\sigma_{r\varphi}(\rho,\varphi)=\frac{p}{\pi}\sum_{m=1}^{\infty}\frac{(-1)^m S_m(\rho)}{m}\sin(2m\varphi_0)\sin(2m\varphi),$$

where

$$R_m(\rho)=\Big(2(m+1)\rho^{-2m}-(2m+1)k^2\rho^{-2(1+m)}$$
$$-k^{2(1-2m)}\rho^{-2(1-m)}\Big)A_m$$
$$-\Big(2(m-1)\rho^{2m}-(2m-1)k^2\rho^{-2(1-m)}$$

$$+k^{2(1+2m)}\rho^{-2(1+m)}\Big)B_m,$$

$$\Phi_m(\rho)=\Big((2m+1)k^2\rho^{-2(1+m)}-2(m-1)\rho^{-2m}$$

$$+k^{2(1-2m)}\rho^{-2(1-m)}\Big)A_m$$

$$-\Big((2m-1)k^2\rho^{-2(1-m)}-2(m+1)\rho^{2m} \tag{3.4.27}$$

$$-k^{2(1+2m)}\rho^{-2(1+m)}\Big)B_m,$$

$$S_m(\rho)=\Big(2m\rho^{-2m}-(2m+1)k^2\rho^{-2(1+m)}$$

$$+k^{2(1-2m)}\rho^{-2(1-m)}\Big)A_m$$

$$+\Big(2m\rho^{2m}-(2m-1)k^2\rho^{-2(1-m)}$$

$$-k^{2(1+2m)}\rho^{-2(1+m)}\Big)B_m,$$

$$A_m=\frac{k^{2(1+m)}(k^{2m}-k^{-2m})-2m(1-k^2)}{4m^2(1-k^2)^2-k^2(k^{2m}-k^{-2m})^2},$$

$$B_m=\frac{2m(1-k^2)-k^{2(1-m)}(k^{2m}-k^{-2m})}{4m^2(1-k^2)^2-k^2(k^{2m}-k^{-2m})^2}.$$

Figure 3.2 presents the full-field distribution of dimensionless radial stress $\sigma_{rr}(\rho,\varphi)/p$ for various inner radii $k=0.25;0.50;0.75$ where $\varphi_0=\pi/4$. In annulus sectors corresponding to the loaded arches of the rim, this stress is naturally compressive near the loaded surface (considering the boundary conditions). However, in the same sectors, the radial stress is tensile in zones near the inner surface, and the size of the zones and stress magnitude grow with an increase in the value of k. This produced high stress gradients versus a ring wall of reduced thickness. On the inner surfaces, the stress is equal to zero in accordance with the imposed boundary conditions (3.2.1) and (3.4.25).

Figure 3.3 illustrates the effect of narrowing the loading area in the radial stress. The case when angle φ_0 is comparatively small is of considerable importance, due to its wide applicability in materials science (e.g., measurement of tensile strength and toughness) and engineering (e.g., diametrical compression of rollers and tubes or chain links under tension). The problem of diametric compression of circular and annular disks is the basis of the so-called "Brazilian experiment". This dominant indirect measurement technique by which to assess the tensile strength of brittle materials [10, 45] generally involves a cylindrical specimen resting upon a horizontal flat and rigid support under the effects of compression by an upper pressure platen. In terms of stresses, the problem is governed by the case when the specimen is compressed by two equivalent forces applied to opposing places along the periphery. Due to the symmetry associated with the diameter passing through the centers of the loaded parts of the boundary and in the perpendicular direction, there is no particular need to fix the specimen at the top or bottom. This simplifies both the experimental and theoretical treatment. In some cases, however, the top and bottom pressure platens are substituted with curved jaws [144], which can alter the loading profile. Nonetheless, the Saint-Venant principle [282] stipulates that the actual profile of loading affects the stress-strain state of the specimen in the vicinity of the zones of the rim under load. These zones are comparatively small; therefore, the stress-strain field in the specimen is the same for all the statically-equivalent loadings (i.e., loadings of the same resultant force and moment [282]) at a given distance from the loaded zones. An exhaustive review of the existing literature on the diametrical compression of cylinders and discs has been presented in a recent monograph [105], including some new results. In [291], we discussed the application of the direct integration method to the analysis of stresses and displacements in a thin isotropic and homogeneous disk under diametric compression, and compared the results with the photoelastic experiment. The two sets of results were in perfect agreement (Fig. 3.4).

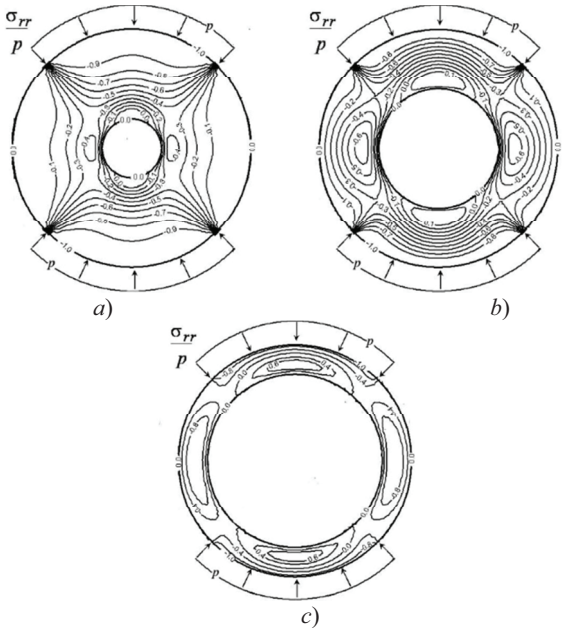

Figure 3.2. Full-field distributions of dimensionless radial stress in diametrically-compressed isotropic homogeneous ring of inner radius: a) $k = 0.25$, b) $k = 0.50$, and c) $k = 0.75$, when $\varphi_0 = \pi / 4$ (adapted from our paper [291])

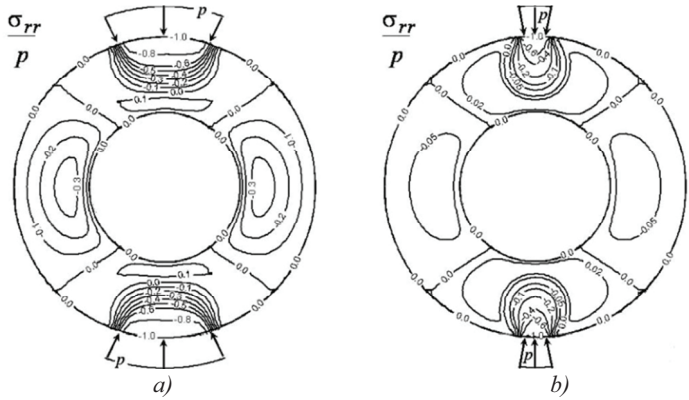

Figure 3.3. Full-field radial stress in diametrically-compressed isotropic homogeneous ring with inner radius $k = 0.50$: a) $\varphi_0 = \pi / 10$ and b) $\varphi_0 = \pi / 40$ (adapted from our paper [291])

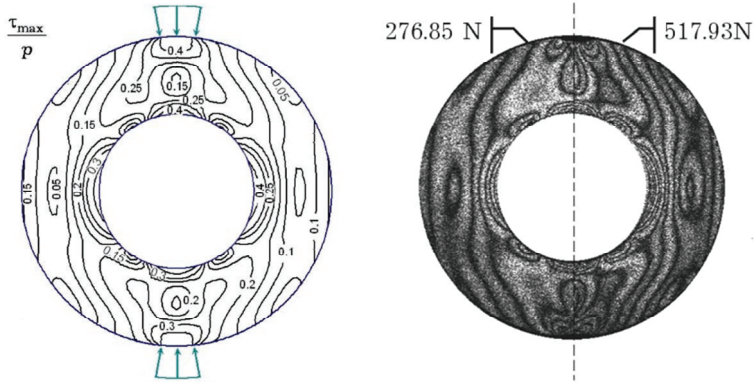

a) *b)*

Figure 3.4. *a*) Theoretical predictions of maximum shear stress

$$\tau_{\max}=\frac{1}{2}\begin{cases}\sigma_1-\sigma_2, & \sigma_1\sigma_2\le 0,\\ \sigma_1, & \sigma_1>0,\ \sigma_2>0,\\ |\sigma_2|, & \sigma_1<0,\ \sigma_2<0,\end{cases}\quad\text{where}\quad \sigma_{1,2}=\frac{\sigma}{2}\pm\sqrt{\left(\sigma_{rr}-\frac{\sigma}{2}\right)^2+\sigma_{r\varphi}^2},$$

and *b*) photoelastic fringe patterns in an annular disk of inner radius $k=0.50$ subject to loading (3.4.25) under two different compressive force values when $\varphi_0=\pi/40$ (adapted from our paper [291])

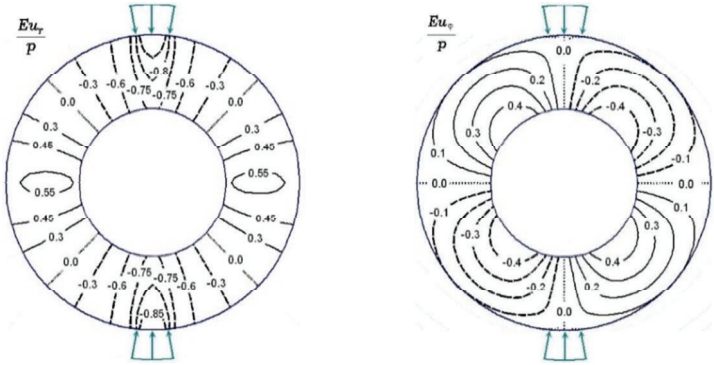

a) *b)*

Figure 3.5. Full-field elastic displacements in annular disk with inner radius $k=0.50$ subject to loading (3.4.25) when $\varphi_0=\pi/40$ (adapted from our paper [291])

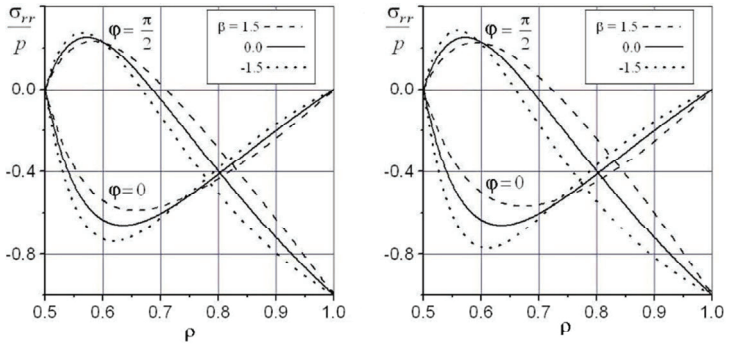

a) *b)*

Figure 3.6. Effect of material inhomogeneity on radial stresses in isotropic annulus with inner radius $k = 0.50$ under constant Poisson's ratio where $E_0, \beta = \text{const}$ and $\varphi_0 = \pi / 4$ in (3.4.24) and variable Young's modulus: *a)* $E(\rho) = E_0 \exp(\beta\rho)$ and *b)* $E(\rho) = E_0 \rho^{\beta}$ (adapted from our paper [298])

We also computed the elastic displacement corresponding to stress field (3.4.26) under condition of plane stress [291], as follows:

$$\frac{Eu_r(\rho,\varphi)}{p} = \frac{1}{\pi}\left(-\frac{2\varphi_0}{1-k^2}\frac{(1+\nu)k^2 + (1-\nu)\rho^2}{\rho} \right.$$

$$\left. + \sum_{m=1}^{\infty} \frac{(-1)^m u_m(\rho)}{m(4m^2-1)} \sin(2m\varphi_0)\cos(2m\varphi) \right), \qquad (3.4.28)$$

$$\frac{Eu_\varphi(\rho,\varphi)}{p} = \frac{1}{\pi}\sum_{m=1}^{\infty} \frac{(-1)^m}{m^2} v_m(\rho)\sin(2m\varphi_0)\sin(2m\varphi),$$

where

$$u_m(\rho) = \lambda_m - 4\nu\rho\left(4m\rho^{2m}B_m - (2m+1)\sigma_m\right),$$

$$v_m(\rho) = \rho\left(2\sigma_m\left(1 - \frac{\nu}{2m-1}\right) - \frac{1+\nu}{2}R_m\right)$$

$$+\frac{1}{4m^2-1}\left(8\nu m\rho^{2m+1}B_m-\frac{\lambda_m}{2}\right),$$

$$\lambda_m=(1+\nu)\left(\frac{\gamma_m}{2}-2f_m-1\right),$$

$$f_m=(2m+1)l_m-4m(1+k^{2m+1})B_m,$$

$$l_m=\frac{k(k^{2m}-k^{-2m})}{2m(1-k^2)-k(k^{2m}-k^{-2m})}, \tag{3.4.29}$$

$$\gamma_m=3(2m+1)l_m+\frac{2(2m+1)\sigma_m}{\rho}\left((2m-1)k^2-2(m+1)\rho^2\right)$$

$$+(2m+1)A_m\left((2m-1)(1-k^2)-k^{2(1-2m)}\left(2\rho^{2m-1}-1-k^{2m-1}\right)\right)$$

$$+(2m-1)B_m\left((2m+1)(1-k^2)+k^{2(1+2m)}\left(2\rho^{-2m-1}-1-k^{-2m-1}\right)\right)$$

$$+12mB_m\left(2\rho^{2m+1}-1-k^{2m+1}\right),$$

$$\sigma_m=\frac{2+k\left(k^{2m}+k^{-2m}\right)}{2m\left(1-k^2\right)+k\left(k^{2m}-k^{-2m}\right)}$$

$$+\frac{2k\left(1-k^2\right)\left(k^{2m}-k^{-2m}\right)}{4m^2\left(1-k^2\right)-k^2\left(k^{2m}-k^{-2m}\right)^2}.$$

Figure 3.5 presents the numerical analysis results of elastic displacements (3.4.28).

If an isotropic elastic ring exhibits radial inhomogeneity, the stress field can be computed using (3.4.10) – (3.4.15). Although the stresses computed for this case qualitatively resemble the stresses for the homogeneous case, there is a quantitative difference, as shown in Fig. 3.6.

Further details on the analysis of stress and displacement in homogeneous and inhomogeneous elastic annuli under the load described in (3.4.25) can be found in [291, 294, 298].

Consider the case where $T = 0$ and the external force loading (3.2.1) is given by (see Fig. 3.7)

$$p_1(\varphi) = q_1(\varphi) = q_2(\varphi) = 0,$$
$$p_2(\varphi) = P_0 \begin{cases} 1, & \varphi \in \left[\dfrac{\pi-\alpha}{2}, \dfrac{\pi+\alpha}{2}\right], \\ k_0, & \varphi \in \left[\dfrac{3\pi \pm \theta - \beta}{2}, \dfrac{3\pi \pm \theta + \beta}{2}\right], \\ 0, & \text{elsewhere.} \end{cases} \tag{3.4.30}$$

Here, in order to fulfill the condition of equilibrium, $k_0 = \dfrac{\sin(\alpha/2)}{2\sin(\beta/2)\cos(\theta/2)}$. In the case where $\alpha = \beta$, $k_0 = \dfrac{1}{2\cos(\theta/2)}$, and if $\theta = 0$, then $k_0 = \dfrac{\sin(\alpha/2)}{2\sin(\beta/2)}$.

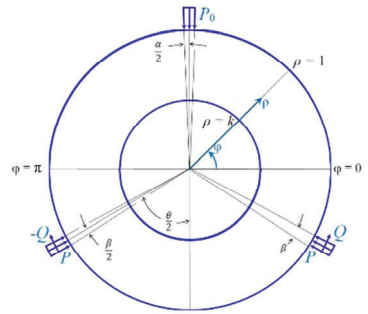

Figure 3.7. Scheme of loading given in (3.4.30)

Using analytical solution (3.4.19) and (3.4.20), we can express radial stress in the case of the loading given in (3.4.30) in the following form:

$$\frac{\sigma_r(\rho,\varphi)}{P_0} = -\left(1 - \frac{k^2}{\rho^2}\right)\frac{\alpha + 2k_0\beta}{2\pi(1-k^2)}$$

$$+\sum_{n=1}^{\infty}\frac{(-1)^n}{n\pi}\left(\left(r_{2n}^{+} + \frac{q_{2n}^{+}}{\rho^2}\right)\rho^{2n} + \left(r_{2n}^{-} + \frac{q_{2n}^{-}}{\rho^2}\right)\rho^{-2n}\right)$$

$$\times\left(\sin n\alpha + 2k_0 \sin n\beta \cos n\theta\right)\cos 2n\varphi$$

$$-\sum_{n=1}^{\infty}\frac{2(-1)^n}{(2n-1)\pi}\left(\left(r_{2n-1}^{+}+\frac{q_{2n-1}^{+}}{\rho^2}\right)\rho^{2n-1}+\left(r_{2n-1}^{-}+\frac{q_{2n-1}^{-}}{\rho^2}\right)\rho^{-2n+1}\right),$$

$$\frac{\sigma_{\varphi}(\rho,\varphi)}{P_0}=-\left(1+\frac{k^2}{\rho^2}\right)\frac{\alpha+2k_0\beta}{2\pi(1-k^2)}$$

$$-\sum_{n=1}^{\infty}\frac{(-1)^n}{n\pi}\left(\left(\frac{n+1}{n-1}r_{2n}^{+}+\frac{q_{2n}^{+}}{\rho^2}\right)\rho^{2n}+\left(\frac{n-1}{n+1}r_{2n}^{-}+\frac{q_{2n}^{-}}{\rho^2}\right)\rho^{-2n}\right)$$

$$\times\left(\sin n\alpha + 2k_0 \sin n\beta \cos n\theta\right)\cos 2n\varphi \qquad (3.4.31)$$

$$+\sum_{n=1}^{\infty}\frac{2(-1)^n}{(2n-1)\pi}\left(\left(\frac{2n+1}{2n-3}r_{2n-1}^{+}+\frac{q_{2n-1}^{+}}{\rho^2}\right)\rho^{2n-1}\right.$$

$$\left.+\left(\frac{2n-3}{2n+1}r_{2n-1}^{-}+\frac{q_{2n-1}^{-}}{\rho^2}\right)\rho^{-2n+1}\right)$$

$$\times\left(\sin\frac{2n-1}{2}\alpha-2k_0\sin\frac{2n-1}{2}\beta\cos\frac{2n-1}{2}\theta\right)\sin(2n-1)\varphi\,,$$

$$\frac{\sigma_{r\varphi}(\rho,\varphi)}{P_0}=-\sum_{n=1}^{\infty}\frac{(-1)^n}{n\pi}\left(\left(\frac{n}{n-1}r_{2n}^{+}+\frac{q_{2n}^{+}}{\rho^2}\right)\rho^{2n}\right.$$

$$\left.-\left(\frac{n}{n+1}r_{2n}^{-}+\frac{q_{2n}^{-}}{\rho^2}\right)\rho^{-2n}\right)$$

$$\times\left(\sin n\alpha + 2k_0 \sin n\beta \cos n\theta\right)\sin 2n\varphi$$

$$-\sum_{n=1}^{\infty}\frac{2(-1)^n}{(2n-1)\pi}\left(\left(\frac{2n-1}{2n-3}r_{2n-1}^{+}+\frac{q_{2n-1}^{+}}{\rho^2}\right)\rho^{2n-1}\right.$$

$$-\left(\frac{2n-1}{2n+1}r_{2n-1}^{-}+\frac{q_{2n-1}^{-}}{\rho^2}\right)\rho^{-2n+1}\Bigg)$$

$$\times\left(\sin\frac{2n-1}{2}\alpha-2k_0\sin\frac{2n-1}{2}\beta\cos\frac{2n-1}{2}\theta\right)\cos(2n-1)\varphi,$$

where

$$r_m^{\pm}=\frac{-m\pm 2}{2\omega_m}\left(m\left(1-k^2\right)\mp k^2\left(1-k^{\mp 2m}\right)\right),$$

$$q_m^{\pm}=\frac{mk^2}{2\omega_m}\left(m\left(1-k^2\right)\mp 1\pm k^{\mp 2m}\right), \tag{3.4.32}$$

$$\omega_m=m^2(1-k^2)^2-k^2(k^m-k^{-m})^2.$$

Note that when $\theta=0$ and $\alpha=\beta$, the term $\sin\frac{2n-1}{2}\alpha-2k_0\sin\frac{2n-1}{2}\beta\cos\frac{2n-1}{2}\theta$ is zero, such that formulae (3.4.31) correspond to the case of an annular plate compressed by the diametrical forces presented in (3.4.26).

The solution (3.4.31) is discussed in our recent paper [292]. These findings are in strong agreement with photoelastic measurement results (see Fig. 3.8).

Consider computation of thermal stresses in annular domain subject to a uniform temperature distribution τ on its inner circumference $\rho=k$ and the temperature $\tau(1+\cos\varphi)$ on the outer circumference $\rho=1$. In the case of homogeneous isotropic material properties, a solution to the heat-transfer equation (3.1.22) can be given in the following form:

$$\frac{T(\rho,\varphi)}{\tau}=1+\frac{\rho^2-k^2}{(1-k^2)\rho}\cos\varphi. \tag{3.4.33}$$

Distributions of temperature (3.4.33) and thermal stresses (3.2.2) with components given by formulae (3.4.19) and (3.4.20) are shown in Fig. 3.9.

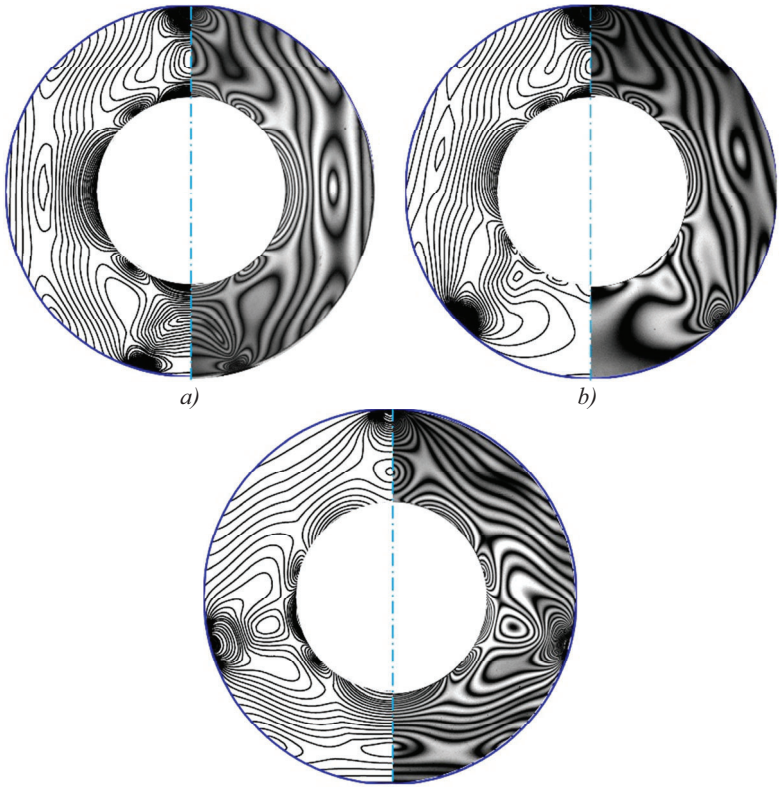

Figure 3.8. Theoretical prediction of (left sides) maximum shear stress, based on (3.4.31) and (right sides) photoelastic fringe patterns in homogeneous isotropic ring of inner radius $k = 0.5$ under (3.4.30) where $\alpha = \beta = \pi / 36$: *a*) $\theta = \pi / 6$, *b*) $\theta = \pi / 2$, and *c*) $\theta = 5\pi / 6$ (adapted from our paper [292])

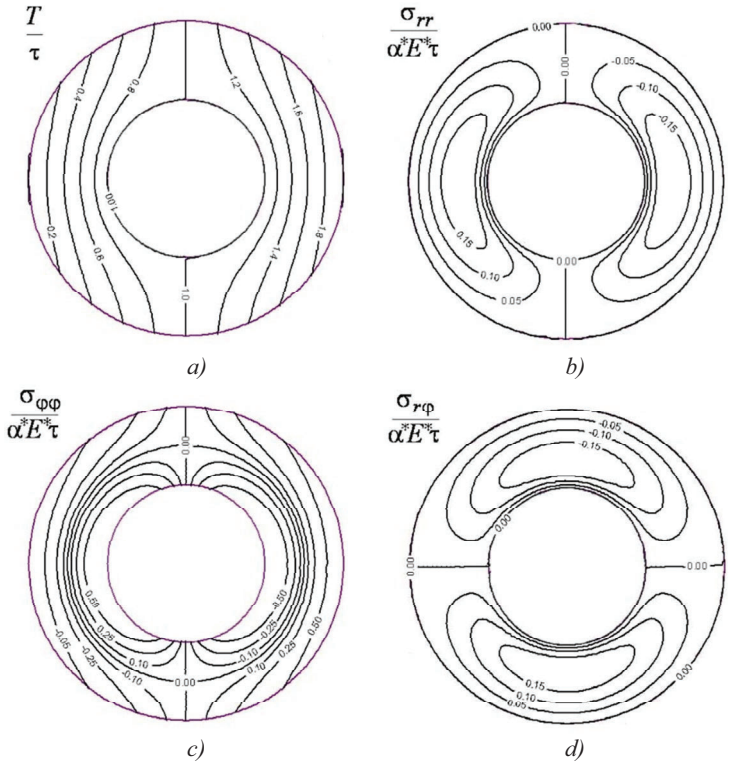

Figure 3.9. Dimensionless distributions of *a)* temperature (3.4.33) and corresponding thermal b) radial, c) circumferential, and d) shear stresses in an isotropic homogeneous annular domain of inner radius $k = 0.5$ (adapted from our paper [292])

If assuming the thermal loading of the inner and outer circumferences of an isotropic annulus to be $T(k,\varphi) = \tau = \text{const}$ and $T(1,\varphi) = \tau(1+\cos 2\varphi)$, respectively, the temperature field for the case of constant heat conduction coefficient takes the form

$$\frac{T(\rho,\varphi)}{\tau} = 1 + \frac{\rho^4 - k^4}{(1-k^4)\rho^2}\cos 2\varphi\,. \tag{3.4.34}$$

The distribution of temperature (3.4.34) is shown in Fig. 3.10*a*. If all the elastic moduli of the annular domain are constant, temperature (3.4.34) does not induce any thermal stresses. If, however, all or some of the elastic

moduli depend on the radial coordinate (for example, $\alpha(\rho) = \alpha^* \exp(\beta\rho)$, $\beta = \text{const}$ and $\alpha^* = \text{const}$), then thermal stresses can arise even for the harmonic temperature distribution (3.4.34) (see Fig. 3.10*b,c,d*). The effect of inhomogeneity, which in the considered case is verbalized by parameter β is essential, which can be seen from Fig. 3.11.

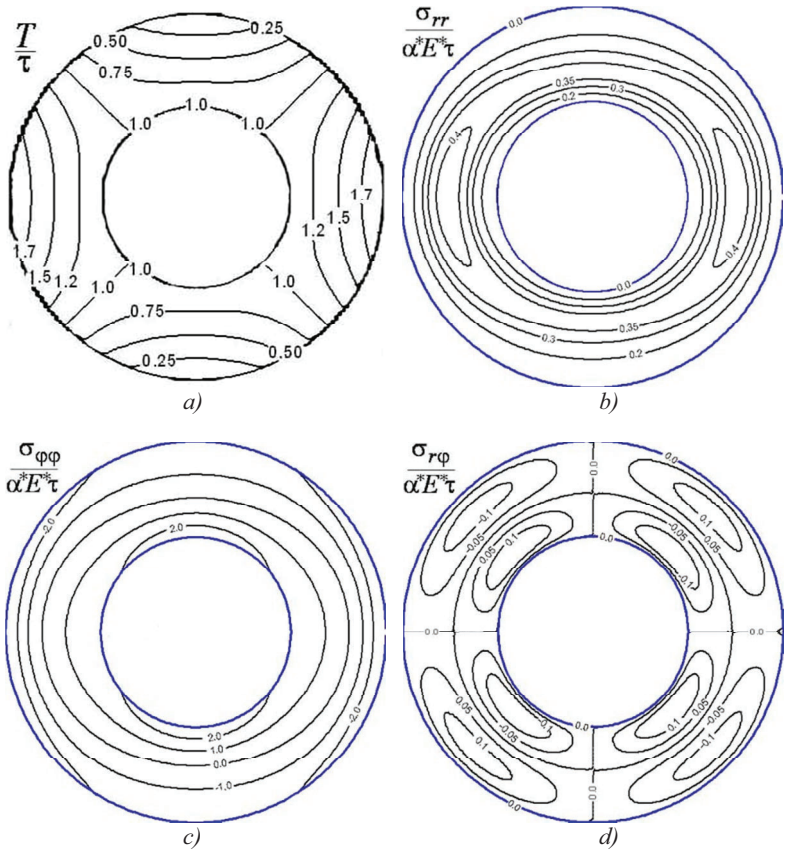

Figure 3.10. Dimensionless distributions of *a)* temperature (3.4.34) and corresponding thermal b) radial, c) circumferential, and d) shear stresses in an isotropic annular domain of inner radius $k = 0.5$ with the coefficient of linear thermal expansion $\alpha(\rho) = \alpha^* \exp(2\rho)$

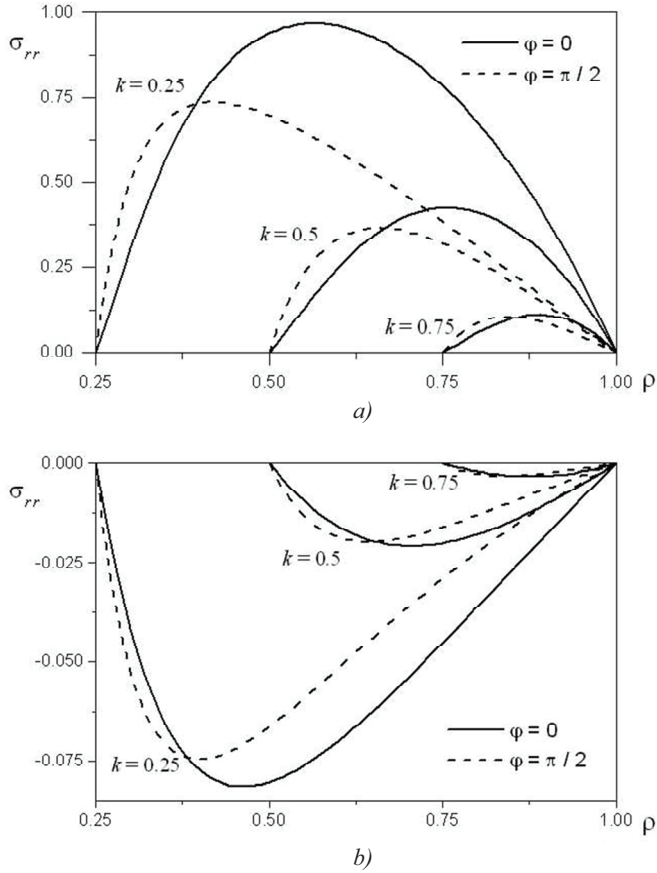

Figure 3.11. Dimensionless radial stress for annuli of different inner radius with constant elastic moduli and variable coefficient of linear thermal expansion $\alpha(\rho) = \alpha^* \exp(\beta\rho)$, where *a)* $\beta = 2$ and *b)* $\beta = -2$

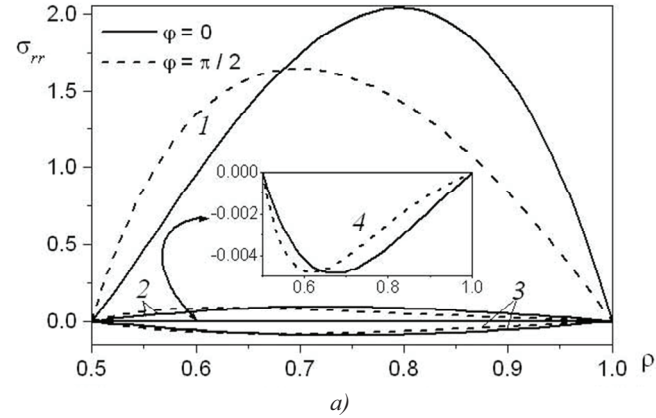

a)

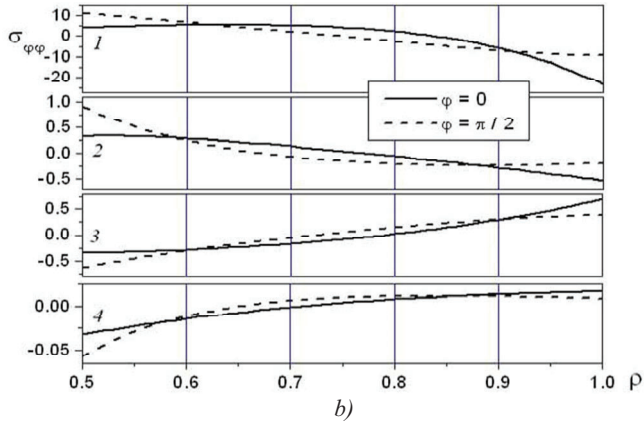

b)

Figure 3.12. Dimensionless radial *a*) and circumferential *b*) stress distribution in an isotropic inhomogeneous ring of inner radius $k = 0.5$ with $\nu = 0.3$, $E(\rho) = E^* \exp(\gamma\rho)$, $G(\rho) = G^* \exp(\gamma\rho)$, $\alpha(\rho) = \alpha^* \exp(\beta\rho)$, where *1* – $\beta = 2,\ \gamma = 2$; *2* – $\beta = 2,\ \gamma = -2$; *3* – $\beta = -2,\ \gamma = 2$; *4* – $\beta = -2,\ \gamma = -2$;

The effect of simultaneous dependence of the linear thermal expansion coefficient and the Young and shear moduli on the radial coordinate is illustrated in Fig. 3.12

CHAPTER FOUR

AXISYMMETRIC THERMOELASTICITY OF INHOMOGENEOUS SOLIDS

4.1. Formulation of thermoelasticity problems

Consider an isotropic elastic space $\mathcal{A}_0 = \{(\rho,\varphi,z): 0 \le \rho < +\infty, \varphi \in [0,2\pi), |z| < +\infty\}$, half-space $\mathcal{A}_1 = \{(\rho,\varphi,z): 0 \le \rho < +\infty, \varphi \in [0,2\pi), z \ge 0\}$, and layer $\mathcal{A}_2 = \{(\rho,\varphi,z): 0 \le \rho < +\infty, \varphi \in [0,2\pi), |z| \le 1\}$ within a dimensionless cylindrical-polar coordinate system (ρ,φ,z). Assume that the force and thermal loadings of the considered solids are symmetric about the z-axis. The elastic equilibrium of these solids can be expressed using equations (3.1.11), which take the following form under the foregoing assumption of axial symmetry in the absence of body forces:

$$\frac{\partial(\rho\sigma_{rr})}{\partial\rho} + \rho\frac{\partial\sigma_{rz}}{\partial z} = \sigma_{\varphi\varphi}, \quad \frac{\partial(\rho\sigma_{rz})}{\partial\rho} + \rho\frac{\partial\sigma_{zz}}{\partial z} = 0. \tag{4.1.1}$$

The Cauchy equations (3.1.13) for the axisymmetric case can be written as follows:

$$\varepsilon_{rr} = \frac{\partial u_r}{\partial\rho}, \quad \varepsilon_{\varphi\varphi} = \frac{u_r}{\rho}, \quad \varepsilon_{zz} = \frac{\partial u_z}{\partial z}, \quad \varepsilon_{rz} = \frac{\partial u_z}{\partial r} + \frac{\partial u_r}{\partial z}. \tag{4.1.2}$$

By eliminating the elastic displacements from the later equations, the strain-compatibility equations can be obtained in the following forms:

$$\rho\frac{\partial\varepsilon_{\varphi\varphi}}{\partial\rho} = \varepsilon_{rr} - \varepsilon_{\varphi\varphi}, \quad \rho\frac{\partial^2\varepsilon_{\varphi\varphi}}{\partial z^2} - \frac{\partial\varepsilon_{rz}}{\partial z} + \frac{\partial\varepsilon_{zz}}{\partial\rho} = 0. \tag{4.1.3}$$

Assume that in the constitutive equations

$$E\varepsilon_{rr} = \sigma_{rr} - \nu\left(\sigma_{\varphi\varphi} + \sigma_{zz}\right) + \alpha ET,$$

$$E\varepsilon_{\varphi\varphi} = \sigma_{\varphi\varphi} - \nu\left(\sigma_{rr} + \sigma_{zz}\right) + \alpha ET, \tag{4.1.4}$$

$$E\varepsilon_{zz} = \sigma_{zz} - \nu\left(\sigma_{rr} + \sigma_{\varphi\varphi}\right) + \alpha ET, \quad G\varepsilon_{rz} = \sigma_{rz},$$

the Young and shear moduli, $E = E(z)$ and $G = E(z)/(2 + 2\nu(z))$, the Poisson ratio, $\nu = \nu(z)$, and the coefficient of linear thermal expansion, $\alpha = \alpha(z)$, are arbitrary functions of z.

By making use of the constitutive equations (4.1.4), the strain-compatibility equations (4.1.3) can be given in terms of stresses:

$$\rho\frac{\partial}{\partial\rho}\left(\sigma_{\varphi\varphi}(\rho,z) - \nu(z)(\sigma_{rr}(\rho,z) + \sigma_{zz}(\rho,z)) + \alpha(z)E(z)T(\rho,z)\right)$$

$$+(1+\nu(z))\left(\sigma_{\varphi\varphi}(\rho,z) - \sigma_{rr}(\rho,z)\right) = 0,$$

$$\rho\frac{\partial^2}{\partial z^2}\left(\frac{\sigma_{\varphi\varphi}(\rho,z)}{E(z)} - \frac{\nu(z)}{E(z)}\left(\sigma_{rr}(\rho,z) + \sigma_{zz}(\rho,z)\right) + \alpha(z)T(\rho,z)\right) \tag{4.1.5}$$

$$-2\frac{\partial}{\partial z}\left(\frac{1+\nu(z)}{E(z)}\sigma_{rz}(\rho,z)\right)$$

$$+\frac{\partial}{\partial\rho}\left(\frac{\sigma_{zz}(\rho,z)}{E(z)} - \frac{\nu(z)}{E(z)}(\sigma_{rr}(\rho,z) + \sigma_{\varphi\varphi}(\rho,z)) + \alpha(z)T(\rho,z)\right) = 0.$$

Boundary $z = 0$ of half-space $\mathcal{A}_1$ is subjected to external force loadings:

$$\sigma_{zz}(\rho,0) = -p(\rho), \quad \sigma_{rz}(\rho,0) = q(\rho), \tag{4.1.6}$$

where $p(\rho)$ and $q(\rho)$ are given functions and $\lim\limits_{\rho\to+\infty} p(\rho) = \lim\limits_{\rho\to+\infty} q(\rho) = 0$.

Limiting planes $z = \pm 1$ of layer $\mathcal{A}_2$ are exposed to normal and shear forces:

$$\sigma_{zz}(\rho,1)=-p_1(\rho),\quad \sigma_{zz}(\rho,-1)=-p_2(\rho),$$
$$\sigma_{rz}(\rho,1)=q_1(\rho),\qquad \sigma_{rz}(\rho,-1)=q_2(\rho), \tag{4.1.7}$$

where $p_\ell(\rho)$ and $q_\ell(\rho)$ are given functions and $\lim\limits_{\rho\to+\infty} p_\ell(\rho)=\lim\limits_{\rho\to+\infty} q_\ell(\rho)=0$, $\ell=1,2$.

The axisymmetric steady-state temperature field $T(\rho,z)$ distributed within the considered inhomogeneous solids $\mathcal{A}_k$, $k=0,1,2$, material properties of which that vary with axial coordinate z, can be determined from the following heat-transfer equation:

$$\frac{\lambda(z)}{\rho}\frac{\partial}{\partial\rho}\left(\rho\frac{\partial T(\rho,z)}{\partial\rho}\right)+\frac{\partial}{\partial z}\left(\lambda(z)\frac{\partial T(\rho,z)}{\partial z}\right)=-w(\rho,z), \tag{4.1.8}$$

where $w(\rho,z)$ is the density of internal heat sources and $\lambda(z)$ is the heat conduction coefficient.

For inhomogeneous space $\mathcal{A}_0$, this heat-transfer equation must be solved under the condition that the temperature vanishes when $\rho+z^2\to+\infty$. For half-space $\mathcal{A}_1$, a solution to this equation must be constructed under the following general thermal condition of the limiting plane $z=0$:

$$\ell_0 T(\rho,0)+\ell_1\frac{\partial T(\rho,z)}{\partial z}\bigg|_{z=0}=T_0(\rho). \tag{4.1.9}$$

Finally, a solution to the same heat-transfer equation in layer $\mathcal{A}_2$ is constructed with the following conditions imposed on the limiting plane $z=\pm1$:

$$\ell_{11}T(\rho,z)+\ell_{12}\frac{\partial T(\rho,z)}{\partial z}=T_1(\rho),\quad z=1,$$
$$\ell_{21}T(\rho,z)+\ell_{22}\frac{\partial T(\rho,z)}{\partial z}=T_2(\rho),\quad z=-1. \tag{4.1.10}$$

Constants ℓ_0 and ℓ_1 in (4.1.9) and ℓ_{11}, ℓ_{12}, ℓ_{21}, and ℓ_{22} in (4.1.10) indicate the type of boundary condition, similarly to (2.4.52).

4.2. Governing equations in terms of stresses

To reduce compatibility equations (4.1.5) to the governing equations for the key functions, we introduce the total stress using the following formula:

$$\sigma(\rho,z)=\sigma_{rr}(\rho,z)+\sigma_{\varphi\varphi}(\rho,z)+\sigma_{zz}(\rho,z)\,. \tag{4.2.1}$$

Note that total stress $\sigma(\rho,z)$ introduced by (4.2.1) coincides with the first invariant of the stress tensor in the cylindrical polar coordinate system [26]. Now implementing the first equation in (4.1.1) and expression (4.2.1) allows us to rewrite the first equation in (4.1.5) as follows:

$$\rho\frac{\partial}{\partial\rho}\big(\sigma(\rho,z)-(1+\nu(z))\sigma_{zz}(\rho,z)+\alpha(z)E(z)T(\rho,z)\big)$$

$$+\rho(1+\nu(z))\frac{\partial\sigma_{rz}(\rho,z)}{\partial z}=0\,. \tag{4.2.2}$$

Integration of the second equation in (4.1.1) over the radial coordinate yields the following formula:

$$\rho\sigma_{rz}(\rho,z)=-\int_0^{\rho}\eta\frac{\partial\sigma_{zz}(\eta,z)}{\partial z}d\eta\,. \tag{4.2.3}$$

In view of this, equation (4.2.2) takes the following form:

$$\rho\frac{\partial\sigma_{zz}(\rho,z)}{\partial\rho}+\int_0^{\rho}\eta\frac{\partial^2\sigma_{zz}(\eta,z)}{\partial z^2}d\eta$$

$$=\frac{\rho}{1+\nu(z)}\frac{\partial}{\partial\rho}\big(\sigma(\rho,z)+\alpha(z)E(z)T(\rho,z)\big)\,. \tag{4.2.4}$$

Differentiating equation (4.2.4) by the radial coordinate, we arrive at the first governing equation:

$$\Delta\sigma_{zz}(\rho,z)=\frac{1}{1+\nu(z)}\frac{1}{\rho}\frac{\partial}{\partial\rho}\left(\rho\frac{\partial}{\partial\rho}\big(\sigma(\rho,z)+\alpha(z)E(z)T(\rho,z)\big)\right), \tag{4.2.5}$$

where

$$\Delta = \frac{1}{\rho}\frac{\partial}{\partial\rho}\left(\rho\frac{\partial}{\partial\rho}\right) + \frac{\partial^2}{\partial z^2}. \tag{4.2.6}$$

Equation (4.2.5) allows for expressing the axial stress $\sigma_{zz}(\rho, z)$ in terms of total stress $\sigma(\rho, z)$ given by formula (4.2.1). To derive the second governing equation for these two functions, we use (4.2.1) and (4.2.3) to represent the second equation in (4.1.5) in the following form:

$$\rho^2\frac{\partial^2}{\partial z^2}\left(\frac{\sigma_{\varphi\varphi}(\rho, z)}{E(z)} - \frac{\nu(z)}{E(z)}\left(\sigma_{rr}(\rho, z) + \sigma_{zz}(\rho, z)\right) + \alpha(z)T(\rho, z)\right)$$

$$= -2\frac{\partial}{\partial z}\left(\frac{1+\nu(z)}{E(z)}\int_0^\rho \eta\frac{\partial\sigma_{zz}(\eta, z)}{\partial z}d\eta\right)$$

$$-\rho\frac{\partial}{\partial\rho}\left(\frac{1+\nu(z)}{E(z)}\sigma_{zz}(\rho, z) - \frac{\nu(z)}{E(z)}\sigma(\rho, z) + \alpha(z)T(\rho, z)\right). \tag{4.2.7}$$

Note that the first equation in (4.1.5) can be presented in an alternative form to that given in (4.2.2), as follows:

$$(1+\nu(z))\frac{\partial}{\partial\rho}\left(\rho^2\sigma_{rr}(\rho, z)\right)$$

$$= \rho(1+\nu(z))\left(\sigma_{rr}(\rho, z) + \sigma_{\varphi\varphi}(\rho, z)\right)$$

$$+\rho^2\frac{\partial}{\partial\rho}\left(\sigma_{rr}(\rho, z) + \sigma_{\varphi\varphi}(\rho, z)\right.$$

$$\left.-\nu(z)\sigma_{zz}(\rho, z) + \alpha(z)E(z)T(\rho, z)\right). \tag{4.2.8}$$

Integrating this over the radial coordinate from 0 to ρ yields

$$\rho^2\left(\sigma_{\varphi\varphi}(\rho, z) - \nu(z)\left(\sigma_{rr}(\rho, z) + \sigma_{zz}(\rho, z)\right) + \alpha(z)E(z)T(\rho, z)\right)$$

$$= \int_0^\rho \eta\left((1-\nu(z))\sigma(\eta, z) - (1+\nu(z))\sigma_{zz}(\eta, z)\right.$$

$$+2\alpha(z)E(z)T(\eta,z))d\eta\,. \tag{4.2.9}$$

Applying differential operator $\frac{\partial^2}{\partial z^2}\left(\frac{1}{E(z)}\cdot\right)$ to equation (4.2.9), we obtain

$$\rho^2\frac{\partial^2}{\partial z^2}\left(\frac{\sigma_{\varphi\varphi}(\rho,z)}{E(z)}-\frac{\nu(z)}{E(z)}\left(\sigma_{rr}(\rho,z)+\sigma_{zz}(\rho,z)\right)+\alpha(z)T(\rho,z)\right)$$

$$=\frac{\partial^2}{\partial z^2}\int_0^\rho\eta\left(\frac{1-\nu(z)}{E(z)}\sigma(\eta,z)\right.$$

$$\left.-\frac{1+\nu(z)}{E(z)}\sigma_{zz}(\eta,z)+2\alpha(z)T(\eta,z)\right)d\eta\,. \tag{4.2.10}$$

Comparing the left-hand sides of equations (4.2.7) and (4.2.10), we arrive at the following equation:

$$\frac{\partial^2}{\partial z^2}\int_0^\rho\eta\left(\frac{1-\nu(z)}{E(z)}\sigma(\eta,z)\right.$$

$$\left.-\frac{1+\nu(z)}{E(z)}\sigma_{zz}(\eta,z)+2\alpha(z)T(\eta,z)\right)d\eta$$

$$+2\frac{\partial}{\partial z}\left(\frac{1+\nu(z)}{E(z)}\int_0^\rho\eta\frac{\partial\sigma_{zz}(\eta,z)}{\partial z}d\eta\right)$$

$$+\rho\frac{\partial}{\partial\rho}\left(\frac{1+\nu(z)}{E(z)}\sigma_{zz}-\frac{\nu(z)}{E(z)}\sigma+\alpha(z)T\right)=0\,. \tag{4.2.11}$$

Dividing equation (4.2.4) by $E(z)$, we obtain

$$\frac{\rho}{E(z)}\frac{\partial\sigma_{zz}(\rho,z)}{\partial\rho}+\int_0^\rho\frac{\eta}{E(z)}\frac{\partial^2\sigma_{zz}(\eta,z)}{\partial z^2}d\eta$$

$$=\frac{\rho}{1+\nu(z)}\frac{\partial}{\partial\rho}\left(\frac{\sigma(\rho,z)}{E(z)}+\alpha(z)T(\rho,z)\right). \tag{4.2.12}$$

Summing up equations (4.2.11) and (4.2.12), the following equation can be derived

$$\rho\frac{\partial}{\partial\rho}\left(\frac{1-\nu(z)}{E(z)}\sigma(\rho,z)+2\alpha(z)T(\rho,z)\right)$$

$$+\frac{\partial^2}{\partial z^2}\int_0^\rho \eta\left(\frac{1-\nu(z)}{E(z)}\sigma(\eta,z)+2\alpha(z)T(\eta,z)\right)d\eta$$

$$=\frac{1}{2}\frac{d^2}{dz^2}\left(\frac{1}{G(z)}\right)\int_0^\rho \eta\sigma_z(\eta,z)d\eta\,. \qquad (4.2.13)$$

Finally, differentiating this by the radial coordinate yields the second governing equation:

$$\Delta\left(\frac{1-\nu(z)}{E(z)}\sigma(\rho,z)+2\alpha(z)T(\rho,z)\right)$$

$$=\frac{\sigma_{zz}(\rho,z)}{2}\frac{d^2}{dz^2}\left(\frac{1}{G(z)}\right). \qquad (4.2.14)$$

Here, Δ is given in (4.2.6).

This second governing equation determines total stress $\sigma(\rho,z)$ in terms of axial stress $\sigma_{zz}(\rho,z)$. Thus, the two key functions can be determined entirely from the governing equations (4.2.5) and (4.2.14) within the context of the corresponding axisymmetric boundary conditions for considered inhomogeneous solids and the temperature field computed from the heat-conduction problem (4.1.8) and the relevant thermal vanishing or boundary conditions. Shear stress $\sigma_{rz}(\rho,z)$ can then be calculated using formula (4.2.3). Radial stress $\sigma_{rr}(\rho,z)$ can be determined from the first equation in (4.1.1), which in view of (4.2.1) takes the following form:

$$\frac{\partial\sigma_{rr}(\rho,z)}{\partial\rho}+2\sigma_{rr}(\rho,z)$$

$$=\sigma(\rho,z)-\sigma_{zz}(\rho,z)-\rho\frac{\partial\sigma_{rz}(\rho,z)}{\partial z}\,. \qquad (4.2.15)$$

Finally, circumferential stress $\sigma_{\varphi\varphi}$ can be computed using the formula

$$\sigma_{\varphi\varphi}(\rho,z)=\sigma(\rho,z)-\sigma_{rr}(\rho,z)-\sigma_{zz}(\rho,z), \tag{4.2.16}$$

which follows from the expression for total stress given in (4.2.1).

To separate the variables in equations (4.2.5) and (4.2.14), we represent the stress-tensor components and temperature using the inverse Hankel integral-transform [228, 305] as follows:

$$\begin{aligned}
\sigma_{rr}(\rho,z)&=\int_0^{+\infty} s\left(\left(J_0(\rho s)-\frac{1}{s\rho}J_1(\rho s)\right)\overline{\sigma}_{rr}(z)\right.\\
&\left.+\frac{1}{s\rho}J_1(\rho s)\overline{\sigma}_{\varphi\varphi}(z)\right)ds,\\
\sigma_{\varphi\varphi}(\rho,z)&=\int_0^{+\infty} s\left(\left(J_0(\rho s)-\frac{1}{s\rho}J_1(\rho s)\right)\overline{\sigma}_{\varphi\varphi}(z)\right.\\
&\left.+\frac{1}{s\rho}J_1(\rho s)\overline{\sigma}_{rr}(z)\right)ds,\\
\sigma(\rho,z)&=\int_0^{+\infty} s\overline{\sigma}(z)J_0(\rho s)ds,\\
\sigma_{zz}(\rho,z)&=\int_0^{+\infty} s\overline{\sigma}_{zz}(z)J_0(\rho s)ds,\\
\sigma_{rz}(\rho,z)&=\int_0^{+\infty} s\overline{\sigma}_{rz}(\eta,z)J_1(\rho s)ds,\\
T(\rho,z)&=\int_0^{+\infty} s\overline{T}(z)J_0(\rho s)ds,
\end{aligned} \tag{4.2.17}$$

where J_0 and J_1 are the zero- and first-order Bessel functions of the first kind, s is the transformation parameter, and the overlined functions are the unknown transformants with a parametric dependence on s.

In view of (4.2.17), the governing equations (4.2.5) and (4.2.14) take the following forms:

$$\overline{\Delta}\overline{\sigma}_{zz}(z) = -\frac{s^2}{1+\nu(z)}\left(\overline{\sigma}(z) + \alpha(z)E(z)\overline{T}(z)\right), \tag{4.2.18}$$

and

$$\overline{\Delta}\left(\frac{1-\nu(z)}{E(z)}\overline{\sigma}(z) + 2\alpha(z)\overline{T}(z)\right) = \frac{\overline{\sigma}_{zz}(z)}{2}\frac{d^2}{dz^2}\left(\frac{1}{G(z)}\right). \tag{4.2.19}$$

Here,

$$\overline{\Delta} = \frac{d^2}{dz^2} - s^2. \tag{4.2.20}$$

Similarly, equations (4.1.1) and (4.2.1) can be transformed as follows:

$$\overline{\sigma}_{rz}(z) = -\frac{1}{s}\frac{d\overline{\sigma}_{zz}(z)}{dz}, \tag{4.2.21}$$

$$\overline{\sigma}_{rr}(z) = \frac{1}{s}\frac{d\overline{\sigma}_{rz}(z)}{dz}, \tag{4.2.22}$$

and

$$\sigma(z) = \overline{\sigma}_{rr}(z) + \overline{\sigma}_{\varphi\varphi}(z) + \overline{\sigma}_{zz}(z). \tag{4.2.23}$$

Below we consider the application of the proposed solution strategy to problems of thermoelasticity in inhomogeneous elastic space $\mathcal{A}_0$, half-space $\mathcal{A}_1$, and layer $\mathcal{A}_2$.

4.3. Thermal stresses in an inhomogeneous elastic space

For inhomogeneous space $\mathcal{A}_0$, a solution to equation (4.2.18) can be derived as:

$$\overline{\sigma}_{zz}(z) = \frac{s}{2}\int_{-\infty}^{+\infty}\left(\frac{\overline{\sigma}(\zeta)}{1+\nu(\zeta)} + 2\alpha(\zeta)G(\zeta)\overline{T}(\zeta)\right)\exp\left(-s\,|\,z-\zeta\,|\right)d\zeta. \tag{4.3.1}$$

As we can see, this solution vanishes at $z^2 \to \infty$.

A solution to equation (4.2.19) with respect to the total stress mapping function can be obtained as follows:

$$\bar{\sigma}(z) = -2\frac{\alpha(z)E(z)}{1-\nu(z)}\bar{T}(z)$$

$$+\frac{E(z)}{4s(1-\nu(z))}\int_{-\infty}^{+\infty}\bar{\sigma}_{zz}(\zeta)\frac{d^2}{d\zeta^2}\left(\frac{1}{G(\zeta)}\right)\exp(-s\,|\,z-\zeta\,|)\,d\zeta\,. \qquad (4.3.2)$$

If we substitute (4.3.1) into (4.3.2) and change the order of integration, we derive the following integral equation:

$$\bar{\sigma}(z) = \theta_0(z) + \int_{-\infty}^{+\infty}\bar{\sigma}(\zeta)\mathcal{K}_0(z,\zeta)d\zeta, \qquad (4.3.3)$$

where

$$\mathcal{K}_0(z,\zeta) = \frac{E(z)}{8(\nu(z)-1)(\nu(\zeta)+1)}\int_{-\infty}^{+\infty}\frac{d^2}{d\xi^2}\left(\frac{1}{G(\xi)}\right)$$

$$\times\exp(-s(|\,z-\xi\,|+|\,\xi-\zeta\,|))\,d\xi\,, \qquad (4.3.4)$$

$$\theta_0(z) = \frac{2E(z)}{\nu(z)-1}\left(\alpha(z)\bar{T}(z)+\frac{1}{8}\int_{-\infty}^{+\infty}\alpha(\zeta)G(\zeta)\bar{T}(\zeta)\right.$$

$$\left.\times\int_{-\infty}^{+\infty}\frac{d^2}{d\xi^2}\left(\frac{1}{G(\xi)}\right)\exp(-s(|\,z-\xi\,|+|\,\xi-\zeta\,|))\,d\xi d\zeta\right). \qquad (4.3.5)$$

A solution to integral equation (4.3.3) can be computed using the resolvent-kernel formula, as follows:

$$\bar{\sigma}(z) = \theta_0(z) + \int_{-\infty}^{+\infty}\theta_0(\zeta)\mathcal{R}_0(z,\zeta)d\zeta, \qquad (4.3.6)$$

where

$$\mathcal{R}_0(z,\zeta) = \sum_{n=0}^{\infty} \mathcal{R}_{n+1}^0(z,\zeta) \tag{4.3.7}$$

and

$$\begin{gathered} \mathcal{R}_1^0(z,\zeta) = \mathcal{K}_0(z,\zeta), \\ \mathcal{R}_{n+1}^0(z,\zeta) = \int_{-\infty}^{+\infty} \mathcal{R}_1^0(z,t)\mathcal{R}_n^0(t,\zeta)dt, \quad n = 1,2,... \end{gathered} \tag{4.3.8}$$

The use of solution (4.3.6) and expression (4.3.5) allows us to write the Hankel mapping function for total stress in isotropic inhomogeneous space $\mathcal{A}_0$ in the form of an explicit expression of temperature:

$$\overline{\sigma}(z) = -2\frac{\alpha(z)E(z)}{1-\nu(z)}\overline{T}(z) - \int_{-\infty}^{+\infty} \overline{T}(\zeta)\Theta_0(z,\zeta)d\zeta, \tag{4.3.9}$$

where

$$\begin{aligned} \Theta_0(z,\zeta) &= 2\frac{\alpha(\zeta)E(\zeta)}{1-\nu(\zeta)}\mathcal{R}_0(z,\zeta) \\ &+ \frac{\alpha(\zeta)G(\zeta)}{4}\int_{-\infty}^{+\infty} \frac{d^2}{d\xi^2}\left(\frac{1}{G(\xi)}\right) \\ &\times\left(\frac{E(z)}{1-\nu(z)}\exp\left(-s\left(|z-\xi|+|\xi-\zeta|\right)\right)\right. \\ &\left. + \int_{-\infty}^{+\infty} \frac{E(\eta)}{1-\nu(\eta)}\exp\left(-s\left(|\eta-\xi|+|\xi-\zeta|\right)\right)\mathcal{R}_0(z,\eta)d\eta\right)d\xi. \end{aligned} \tag{4.3.10}$$

Inserting (4.3.9) into (4.3.1) yields

$$\overline{\sigma}_{zz}(z) = -\frac{s}{2}\int_{-\infty}^{+\infty} \overline{T}(\zeta)\left(\frac{\alpha(\zeta)E(\zeta)}{1-\nu(\zeta)}\exp(-s|z-\zeta|)\right.$$

$$+\int_{-\infty}^{+\infty}\frac{\Theta_0(\eta,\zeta)}{1+\nu(\eta)}\exp(-s\,|\,z-\eta\,|)d\eta\Bigg)d\zeta. \qquad (4.3.11)$$

Using (4.2.21) in conjunction with (4.3.11) allows us to derive the following expression for shear stress:

$$\overline{\sigma}_{rz}(z)=-\frac{s}{2}\int_{-\infty}^{+\infty}\overline{T}(\zeta)\Bigg(\frac{\alpha(\zeta)E(\zeta)}{1-\nu(\zeta)}\exp(-s\,|\,z-\zeta\,|)\operatorname{sgn}(z-\zeta)$$

$$+\int_{-\infty}^{+\infty}\frac{\Theta_0(\eta,\zeta)}{1+\nu(\eta)}\exp(-s\,|\,z-\eta\,|)\operatorname{sgn}(z-\eta)d\eta\Bigg)d\zeta. \qquad (4.3.12)$$

Finally, implementing (4.2.22) with (4.3.12) yields

$$\overline{\sigma}_{rr}(z)=-\frac{\alpha(z)E(z)}{1-\nu(z)}\overline{T}(z)-\frac{s}{2}\int_{-\infty}^{+\infty}\overline{T}(\zeta)\Bigg(\frac{2}{s}\frac{\Theta_0(z,\zeta)}{1+\nu(z)}$$

$$-\frac{\alpha(\zeta)E(\zeta)}{1-\nu(\zeta)}\exp(-s\,|\,z-\zeta\,|)$$

$$-\int_{-\infty}^{+\infty}\frac{\Theta_0(\eta,\zeta)}{1+\nu(\eta)}\exp(-s\,|\,z-\eta\,|)d\eta\Bigg)d\zeta. \qquad (4.3.13)$$

Circumferential stress can be computed using (4.2.23), (4.3.11), and (4.3.13) as follows:

$$\overline{\sigma}_{\varphi\varphi}(z)=-\frac{\alpha(z)E(z)}{1-\nu(z)}\overline{T}(z)-\frac{\nu(z)}{1+\nu(z)}\int_{-\infty}^{+\infty}\overline{T}(\zeta)\Theta_0(z,\zeta)d\zeta\,. \qquad (4.3.14)$$

Computing the stresses in the physical domain requires that we substitute the Hankel images of the stresses represented by (4.3.11) – (4.3.13) into the inverse transform formulae in (4.2.17).

4.4. Thermal stresses in an inhomogeneous elastic half-space

For inhomogeneous half-space $\mathcal{A}_1$, equations (4.2.18) and (4.2.19) must be solved under conditions (4.1.6). Using the second equation in (4.1.1) allows us to transform the condition for the shear stress represented by (4.1.6) into the one for normal stress, as follows:

$$\left.\frac{\partial \sigma_{zz}(\rho, z)}{\partial z}\right|_{z=0} = -\frac{1}{\rho}\frac{\partial(\rho q(\rho))}{\partial \rho}. \tag{4.4.1}$$

In the mapping domain of the Hankel transform (4.2.17), condition (4.4.1) along with the first condition in (4.1.6) take the following form:

$$\overline{\sigma}_{zz}(0) = -\overline{p}, \qquad \left.\frac{d\overline{\sigma}_{zz}(z)}{dz}\right|_{z=0} = -s\overline{q}, \tag{4.4.2}$$

where

$$\overline{p} = \int_0^{+\infty} \rho p(\rho) J_0(\rho s) d\rho, \qquad \overline{q} = \int_0^{+\infty} \rho q(\rho) J_1(\rho s) d\rho. \tag{4.4.3}$$

A solution to equation (4.2.18) under the first condition in (4.4.2) can be given as follows:

$$\overline{\sigma}_{zz}(z) = -\overline{p}\exp(-sz)$$

$$+\frac{s}{2}\int_0^{+\infty} \frac{\overline{\sigma}(\zeta) + \alpha(\zeta)E(\zeta)\overline{T}(\zeta)}{1+\nu(\zeta)}$$

$$\times\left(\exp(-s\,|\,z-\zeta\,|) - \exp(-s(z+\zeta))\right)d\zeta. \tag{4.4.4}$$

Submitting (4.4.4) to the second condition in (4.4.2) yields the following integral condition:

$$s\int_0^{+\infty} \frac{\overline{\sigma}(z) + \alpha(z)E(z)\overline{T}(z)}{1+\nu(z)}\exp(-sz)\,dz = -\overline{p} - \overline{q}. \tag{4.4.5}$$

Within the context of condition (4.4.5), the integral in expression for normal stress (4.4.4) can be presented in a simplified form, as follows:

$$\bar{\sigma}_{zz}(z) = \frac{\bar{q} - \bar{p}}{2} \exp(-sz)$$

$$+ \frac{s}{2} \int_0^{+\infty} \frac{\bar{\sigma}(\zeta) + \alpha(\zeta) E(\zeta) \bar{T}(\zeta)}{1 + \nu(\zeta)} \exp(-s \mid z - \zeta \mid) d\zeta . \qquad (4.4.6)$$

A solution to equation (4.2.19) with respect to the Hankel mapping function of the total stress can be given as follows:

$$\bar{\sigma}(z) = A \frac{E(z) \exp(-sz)}{1 - \nu(z)} - 2 \frac{\alpha(z) E(z)}{1 - \nu(z)} \bar{T}(z)$$

$$- \frac{E(z)}{4s(1 - \nu(z))} \int_0^{+\infty} \bar{\sigma}_{zz}(\zeta) \frac{d^2}{d\zeta^2} \left(\frac{1}{G(\zeta)} \right) \exp(-s \mid z - \zeta \mid) d\zeta . \qquad (4.4.7)$$

Substituting (4.4.6) into (4.4.7) yields an integral equation of the second kind:

$$\bar{\sigma}(z) = A \frac{E(z) \exp(-sz)}{1 - \nu(z)} + (\bar{p} - \bar{q}) \varphi_1(z)$$

$$+ \theta_1(z) + \int_0^{+\infty} \bar{\sigma}(\zeta) \mathcal{K}_1(z, \zeta) d\zeta . \qquad (4.4.8)$$

Here,

$$\varphi_1(z) = \frac{E(z)}{8(1 - \nu(z)) s} \int_0^{+\infty} \frac{d^2}{d\xi^2} \left(\frac{1}{G(\xi)} \right) \exp(-s(\xi + \mid z - \xi \mid)) d\xi ,$$

$$\mathcal{K}_1(z,\zeta)=\frac{E(z)}{8(\nu(z)-1)(\nu(\zeta)+1)}\int_0^{+\infty}\frac{d^2}{d\xi^2}\left(\frac{1}{G(\xi)}\right)$$

$$\times\exp\left(-s\left(|\,z-\xi\,|+|\,\xi-\zeta\,|\right)\right)d\xi, \tag{4.4.9}$$

$$\theta_1(z)=\frac{2E(z)}{\nu(z)-1}\left(\alpha(z)\overline{T}(z)+\frac{1}{8}\int_0^{+\infty}\alpha(\zeta)G(\zeta)\overline{T}(\zeta)\right.$$

$$\left.\times\int_0^{+\infty}\frac{d^2}{d\xi^2}\left(\frac{1}{G(\xi)}\right)\exp\left(-s\left(|\,z-\xi\,|+|\,\xi-\zeta\,|\right)\right)d\xi d\zeta\right),$$

and A is a constant of integration. The resolvent-kernel solution to the integral equation (4.4.8) can be given as

$$\overline{\sigma}(z)=A\Psi_1(z)+(\overline{p}-\overline{q})\Phi_1(z)+\Theta_1(z)\,, \tag{4.4.10}$$

where

$$\Psi_1(z)=\frac{E(z)\exp(-sz)}{1-\nu(z)}+\int_0^{+\infty}\frac{E(\zeta)\exp(-s\zeta)}{1-\nu(\zeta)}\mathcal{R}_1(z,\zeta)d\zeta,$$

$$\Phi_1(z)=\varphi_1(z)+\int_0^{+\infty}\varphi_1(\zeta)\mathcal{R}_1(z,\zeta)d\zeta,$$

$$\Theta_1(z)=\theta_1(z)+\int_0^{+\infty}\theta_1(\zeta)\mathcal{R}_1(z,\zeta)d\zeta, \tag{4.4.11}$$

$$\mathcal{R}_1(z,\zeta)=\sum_{n=0}^{\infty}\mathcal{R}_{n+1}^1(z,\zeta),\quad \mathcal{R}_1^1(z,\zeta)=\mathcal{K}_1(z,\zeta),$$

$$\mathcal{R}_{n+1}^1(z,\zeta)=\int_0^{+\infty}\mathcal{R}_1^1(z,t)\mathcal{R}_n^1(t,\zeta)dt.$$

Constant A can be computed by substituting (4.4.10) into the integral condition (4.4.5), which yields

$$\overline{\sigma}(z) = \overline{p}\left(\Phi_1(z) - \frac{1+b}{a}\Psi_1(z)\right)$$

$$-\overline{q}\left(\Phi_1(z) + \frac{1-b}{a}\Psi_1(z)\right) + \Theta_1(z) - \frac{c}{a}\Psi_1(z)\,. \qquad (4.4.12)$$

Here,

$$a = s\int_0^{+\infty} \frac{\Psi_1(z)}{1+\nu(z)}\exp(-sz)\,dz,$$

$$b = s\int_0^{+\infty} \frac{\Phi_1(z)}{1+\nu(z)}\exp(-sz)\,dz,$$

$$c = s\int_0^{+\infty} \left(\frac{\Theta_1(z)}{1+\nu(z)} + 2\alpha(z)G(z)\overline{T}(z)\right)\exp(-sz)\,dz\,. \qquad (4.4.13)$$

If we substitute (4.4.12) into (4.4.6), we can derive transversal stress in the following form:

$$\overline{\sigma}_{zz}(z) = \frac{\overline{p}}{2}\Bigg(-\exp(-sz)$$

$$+\frac{s}{a}\int_0^{+\infty} \frac{a\Phi_1(\zeta) - (1+b)\Psi_1(\zeta)}{1+\nu(\zeta)}\exp(-s\,|\,z-\zeta\,|)\,d\zeta\Bigg)$$

$$+\frac{\overline{q}}{2}\Bigg(\exp(-sz)$$

$$-\frac{s}{a}\int_0^{+\infty} \frac{a\Phi_1(\zeta) + (1-b)\Psi_1(\zeta)}{1+\nu(\zeta)}\exp(-s\,|\,z-\zeta\,|)\,d\zeta\Bigg)$$

$$+\frac{s}{2a}\int_0^{+\infty} \frac{a\left(\alpha(\zeta)E(\zeta)\overline{T}(\zeta) + \Theta_1(\zeta)\right) - c\Psi_1(\zeta)}{1+\nu(\zeta)}$$

$$\times \exp\left(-s \mid z-\zeta \mid\right) d\zeta \tag{4.4.14}$$

It can be shown through direct computation that

$$\frac{s}{a} \int_0^{+\infty} \frac{a\Phi_1(\zeta)-(1+b)\Psi_1(\zeta)}{1+\nu(\zeta)} \exp\left(-s\zeta\right) d\zeta = -1,$$

$$\frac{s}{a} \int_0^{+\infty} \frac{a\Phi_1(\zeta)+(1-b)\Psi_1(\zeta)}{1+\nu(\zeta)} \exp\left(-s\zeta\right) d\zeta = 1, \tag{4.4.15}$$

$$\frac{s}{2a} \int_0^{+\infty} \frac{a\left(\alpha(\zeta)E(\zeta)\overline{T}(\zeta)+\Theta_1(\zeta)\right)-c\Psi_1(\zeta)}{1+\nu(\zeta)} \exp\left(-s\zeta\right) d\zeta = 0.$$

Equalities (4.4.15) ensure the axial stress (4.4.14) satisfies the boundary conditions (4.4.2).

Substituting (4.4.14) into (4.2.21), we can determine the shear stress as follows:

$$\begin{aligned}
\overline{\sigma}_{rz}(z) = {} & \frac{\overline{p}}{2}\Bigg(-\exp\left(-sz\right) + \frac{s}{a} \int_0^{+\infty} \frac{a\Phi_1(\zeta)-(1+b)\Psi_1(\zeta)}{1+\nu(\zeta)} \\
& \times \exp\left(-s \mid z-\zeta \mid\right) \operatorname{sgn}(z-\zeta) d\zeta \Bigg) \\
& + \frac{\overline{q}}{2}\Bigg(\exp\left(-sz\right) - \frac{s}{a} \int_0^{+\infty} \frac{a\Phi_1(\zeta)+(1-b)\Psi_1(\zeta)}{1+\nu(\zeta)} \\
& \times \exp\left(-s \mid z-\zeta \mid\right) \operatorname{sgn}(z-\zeta) d\zeta \Bigg) \\
& + \frac{s}{2a} \int_0^{+\infty} \frac{a\left(\alpha(\zeta)E(\zeta)\overline{T}(\zeta)+\Theta_1(\zeta)\right)-c\Psi_1(\zeta)}{1+\nu(\zeta)} \\
& \times \exp\left(-s \mid z-\zeta \mid\right) \operatorname{sgn}(z-\zeta) d\zeta.
\end{aligned} \tag{4.4.16}$$

Similarly, implementing (4.4.16) in conjunction with (4.2.22) yields the following equation for radial stress:

$$\overline{\sigma}_{rr}(z)=\frac{\overline{p}}{a}\Bigg(\frac{a\Phi_1(z)-(1+b)\Psi_1(z)}{1+\nu(z)}+\frac{a\exp(-sz)}{2}$$

$$-\frac{s}{2}\int_0^{+\infty}\frac{a\Phi_1(\zeta)-(1+b)\Psi_1(\zeta)}{1+\nu(\zeta)}\exp(-s\,|\,z-\zeta\,|)\,d\zeta\Bigg)$$

$$-\frac{\overline{q}}{a}\Bigg(\frac{a\Phi_1(z)+(1-b)\Psi_1(z)}{1+\nu(z)}+\frac{a\exp(-sz)}{2}$$

$$-\frac{s}{2}\int_0^{+\infty}\frac{a\Phi_1(\zeta)+(1-b)\Psi_1(\zeta)}{1+\nu(\zeta)}\exp(-s\,|\,z-\zeta\,|)\,d\zeta\Bigg)$$

$$-\frac{s}{2a}\int_0^{+\infty}\frac{a\big(\alpha(\zeta)E(\zeta)\overline{T}(\zeta)+\Theta_1(\zeta)\big)-c\Psi_1(\zeta)}{1+\nu(\zeta)}$$

$$\times\exp(-s\,|\,z-\zeta\,|)\,d\zeta$$

$$+\frac{\alpha(z)E(z)}{1+\nu(z)}\overline{T}(z)+\frac{a\Theta_1(z)-c\Psi_1(z)}{a(1+\nu(z))}. \qquad (4.4.17)$$

Finally, circumferential stress can be found using (4.2.23) in conjunction with (4.4.12), (4.4.14), and (4.4.17), as follows:

$$\overline{\sigma}_{\varphi\varphi}(z)=\Bigg(\Big(\Phi_1(z)-\frac{1+b}{a}\Psi_1(z)\Big)\overline{p}$$

$$-\Big(\Phi_1(z)+\frac{1-b}{a}\Psi_1(z)\Big)\overline{q}$$

$$+\Theta_1(z)-\frac{c}{a}\Psi_1(z)-\frac{\alpha(z)E(z)}{\nu(z)}\overline{T}(z)\Bigg)\frac{\nu(z)}{1+\nu(z)}. \qquad (4.4.18)$$

Using the Hankel representations given in (4.2.17) in conjunction with (4.4.12) and (4.4.16) – (4.4.18) allows for the construction of stress-tensor

components in an inhomogeneous elastic half-space due to force loadings (4.1.6) and a steady-state temperature field.

4.5. Thermal stresses in an inhomogeneous elastic layer

For isotropic transversely-inhomogeneous layer $\mathcal{A}_2$, solutions to equations (4.2.18) and (4.2.19) must be found under boundary conditions (4.1.7). The conditions for shear stress can be replaced with the following conditions for the derivatives of normal stress:

$$\left.\frac{\partial \sigma_{zz}(\rho,z)}{\partial z}\right|_{z=1} = -\frac{1}{\rho}\frac{\partial(\rho q_1)}{\partial \rho}, \qquad \left.\frac{\partial \sigma_{zz}(\rho,z)}{\partial z}\right|_{z=-1} = -\frac{1}{\rho}\frac{\partial(\rho q_2)}{\partial \rho}. \tag{4.5.1}$$

These conditions are derived on the basis of the second equation in (4.1.1). In view of the Hankel transform represented by (4.2.17), we can set the conditions in the mapping domain as follows:

$$\left.\frac{d\overline{\sigma}_{zz}(z)}{dz}\right|_{z=1} = -s\overline{q}_1, \quad \left.\frac{d\overline{\sigma}_{zz}(z)}{dz}\right|_{z=-1} = -s\overline{q}_2. \tag{4.5.2}$$

Similarly, boundary conditions (4.1.7) for normal stress appear as

$$\overline{\sigma}_{zz}(1) = -\overline{p}_1, \quad \overline{\sigma}_{zz}(-1) = -\overline{p}_2. \tag{4.5.3}$$

Here,

$$\overline{p}_\ell = \int_0^{+\infty} \rho p_\ell(\rho) J_0(\rho s) d\rho, \qquad \overline{q}_\ell = \int_0^{+\infty} \rho q_\ell(\rho) J_1(\rho s) d\rho, \quad \ell = 1,2. \tag{4.5.4}$$

A solution to equation (4.2.18) under boundary conditions (4.5.3) can be derived as follows:

$$\overline{\sigma}_{zz}(z)=\left(-\overline{p}_1+s\int_{-1}^{1}\frac{\overline{\sigma}(\zeta)+\alpha(\zeta)E(\zeta)\overline{T}(\zeta)}{1+\nu(\zeta)}\sinh s(1-\zeta)d\zeta\right)$$

$$\times\frac{\sinh s(1+z)}{\sinh 2s}-\overline{p}_2\frac{\sinh s(1-z)}{\sinh 2s}$$

$$-s\int_{-1}^{z}\frac{\overline{\sigma}(\zeta)+\alpha(\zeta)E(\zeta)\overline{T}(\zeta)}{1+\nu(\zeta)}\sinh s(z-\zeta)d\zeta\ . \tag{4.5.5}$$

For solution (4.5.5) to meet conditions (5.4.2) requires that the following integral conditions be satisfied:

$$\begin{aligned}&\int_{-1}^{1}\frac{\overline{\sigma}(z)+\alpha(z)E(z)\overline{T}(z)}{1+\nu(z)}\sinh szdz\\&=-\frac{\overline{p}_1-\overline{p}_2}{s}\cosh s+\frac{\overline{q}_1+\overline{q}_2}{s}\sinh s,\\&\int_{-1}^{1}\frac{\overline{\sigma}(z)+\alpha(z)E(z)\overline{T}(z)}{1+\nu(z)}\cosh szdz\\&=-\frac{\overline{p}_1+\overline{p}_2}{s}\sinh s+\frac{\overline{q}_1-\overline{q}_2}{s}\cosh s.\end{aligned} \tag{4.5.6}$$

These conditions allow us to derive the following:

$$s\int_{-1}^{1}\frac{\overline{\sigma}(\zeta)+\alpha(\zeta)E(\zeta)\overline{T}(\zeta)}{1+\nu(\zeta)}\sinh s(1-\zeta)d\zeta$$

$$=\overline{p}_1-\overline{p}_2\cosh 2s-\overline{q}_2\sinh 2s\,. \tag{4.5.7}$$

Under this formula, (4.5.5) can be simplified as follows:

$$\overline{\sigma}_{zz}(z)=-\overline{p}_2\cosh s(1+z)-\overline{q}_2\sinh s(1+z)$$

$$-s\int_{-1}^{z}\frac{\overline{\sigma}(\zeta)+\alpha(\zeta)E(\zeta)\overline{T}(\zeta)}{1+\nu(\zeta)}\sinh s(z-\zeta)d\zeta\,. \tag{4.5.8}$$

A solution to equation (4.2.19) with respect to its left-hand side can be given as

$$\frac{1-\nu(z)}{E(z)}\bar{\sigma}(z)+2\alpha(z)\bar{T}(z)=A\cosh sz+B\sinh sz$$

$$+\frac{1}{2s}\int_{-1}^{z}\bar{\sigma}_{zz}(\xi)\frac{d^2}{d\xi^2}\left(\frac{1}{G(\xi)}\right)\sinh s(z-\xi)d\xi\,, \tag{4.5.9}$$

where A and B are arbitrary constants.

Substituting (4.5.8) into (4.5.9) yields (after some algebra) the following Volterra integral equation of the second kind:

$$\bar{\sigma}(z)=A\frac{E(z)\cosh sz}{1-\nu(z)}+B\frac{E(z)\sinh sz}{1-\nu(z)}+\bar{p}_2\tilde{p}(z)$$

$$+\bar{q}_2\tilde{q}(z)+\theta(z)+\int_{-1}^{z}\bar{\sigma}(\zeta)\mathcal{K}(z,\zeta)d\zeta\,, \tag{4.5.10}$$

where

$$\tilde{p}(z)=-\frac{1}{2s}\frac{E(z)}{1-\nu(z)}\int_{-1}^{z}\frac{d^2}{d\xi^2}\left(\frac{1}{G(\xi)}\right)$$

$$\times\sinh s(z-\xi)\cosh s(1+\xi)d\xi\,,$$

$$\tilde{q}(z)=-\frac{1}{2s}\frac{E(z)}{1-\nu(z)}\int_{-1}^{z}\frac{d^2}{d\xi^2}\left(\frac{1}{G(\xi)}\right)$$

$$\times\sinh s(z-\xi)\sinh s(1+\xi)d\xi\,,$$

$$\theta(z)=-\frac{E(z)}{1-\nu(z)}\left(2\alpha(z)\bar{T}(z)\right. \tag{4.5.11}$$

$$\left.+\int_{-1}^{z}\frac{d^2}{d\xi^2}\left(\frac{1}{G(\xi)}\right)\sinh s(z-\xi)\right.$$

$$\times \int_{-1}^{\xi} \alpha(\zeta) G(\zeta) \overline{T}(\zeta) \sinh s(\xi - \zeta) d\zeta d\xi \Bigg),$$

$$\mathcal{K}(z,\zeta) = -\frac{E(z)}{2(1+\nu(\zeta))(1-\nu(z))}$$

$$\times \int_{\zeta}^{z} \frac{d^2}{d\xi^2}\left(\frac{1}{G(\xi)}\right) \sinh s(z-\xi) \sinh s(\xi - \zeta) d\xi \,.$$

A resolvent-kernel solution to equation (4.5.10) can be given in the following form:

$$\overline{\sigma}(z) = A f^A(z) + B f^B(z) + \overline{p}_2 P(z) + \overline{q}_2 Q(z) + \Theta(z), \qquad (4.5.12)$$

where

$$f^A(z) = \frac{E(z)}{1-\nu(z)} \cosh sz$$

$$+ \int_{-1}^{z} \frac{E(\zeta)}{1-\nu(\zeta)} \cosh s\zeta \mathcal{R}(z,\zeta) d\zeta,$$

$$f^B(z) = \frac{E(z)}{1-\nu(z)} \sinh sz$$

$$+ \int_{-1}^{z} \frac{E(\zeta)}{1-\nu(\zeta)} \sinh s\zeta \mathcal{R}(z,\zeta) d\zeta, \qquad (4.5.13)$$

$$P(z) = \tilde{p}(z) + \int_{-1}^{z} \tilde{p}(\zeta) \mathcal{R}(z,\zeta) d\zeta,$$

$$Q(z) = \tilde{q}(z) + \int_{-1}^{z} \tilde{q}(\zeta) \mathcal{R}(z,\zeta) d\zeta,$$

$$\Theta(z) = \theta(z) + \int_{-1}^{z} \theta(\zeta)\mathcal{R}(z,\zeta)d\zeta\,.$$

The resolvent-kernel is given as

$$\mathcal{R}(z,\zeta) = \sum_{n=0}^{\infty} \mathcal{R}_{n+1}(z,\zeta), \tag{4.5.14}$$

where

$$\begin{gathered}\mathcal{R}_1(z,\zeta) = \mathcal{K}(z,\zeta),\\ \mathcal{R}_{n+1}(z,\zeta) = \int_{\zeta}^{z} \mathcal{R}_1(z,t)\mathcal{R}_n(t,\zeta)dt, \quad n = 1,2,...\end{gathered} \tag{4.5.15}$$

Substituting solution (4.5.12) into the integral conditions (4.5.6) allows us to determine constants A and B in the following form:

$$A = \frac{b_1 a_{22} - b_2 a_{12}}{\gamma}, \quad B = \frac{b_2 a_{11} - b_1 a_{21}}{\gamma}, \tag{4.5.16}$$

where

$$a_{11} = \int_{-1}^{1} f^A(z)\frac{\sinh sz}{1+\nu(z)}dz, \quad a_{21} = \int_{-1}^{1} f^A(z)\frac{\cosh sz}{1+\nu(z)}dz,$$

$$a_{12} = \int_{-1}^{1} f^B(z)\frac{\sinh sz}{1+\nu(z)}dz, \quad a_{22} = \int_{-1}^{1} f^B(z)\frac{\cosh sz}{1+\nu(z)}dz,$$

$$b_1 = -\frac{\overline{p}_1 - \overline{p}_2}{s}\cosh s + \frac{\overline{q}_1 + \overline{q}_2}{s}\sinh s$$

$$-\int_{-1}^{1} \frac{\overline{p}_2 P(z) + \overline{q}_2 Q(z) + \Theta(z) + \alpha(z)E(z)\overline{T}(z)}{1+\nu(z)}\sinh szdz\,, \tag{4.5.17}$$

$$b_2 = -\frac{\overline{p}_1 + \overline{p}_2}{s}\sinh s + \frac{\overline{q}_1 - \overline{q}_2}{s}\cosh s$$

$$-\int_{-1}^{1} \frac{\overline{p}_2 P(z) + \overline{q}_2 Q(z) + \Theta(z) + \alpha(z) E(z) \overline{T}(z)}{1 + \nu(z)} \cosh szdz ,$$

$$\gamma = a_{11} a_{22} - a_{12} a_{21}.$$

Inserting (4.5.16) into (4.5.12) yields

$$\overline{\sigma}(z) = \overline{p}_1 P_1(z) + \overline{p}_2 P_2(z) + \overline{q}_1 Q_1(z) + \overline{q}_2 Q_2(z) + \mathrm{T}(z) , \qquad (4.5.18)$$

where

$$P_1(z) = \frac{a_{12} \sinh s - a_{22} \cosh s}{s\gamma} f^A(z)$$

$$+ \frac{a_{21} \cosh s - a_{11} \sinh s}{s\gamma} f^B(z) ,$$

$$P_2(z) = P(z) + \frac{a_{12} \sinh s + a_{22} \cosh s}{s\gamma} f^A(z)$$

$$- \frac{a_{21} \cosh s + a_{11} \sinh s}{s\gamma} f^B(z)$$

$$- \int_{-1}^{1} \frac{P(\zeta)}{1 + \nu(\zeta)} \left(\frac{a_{22} \sinh s\zeta - a_{12} \cosh s\zeta}{\gamma} f^A(z) \right.$$

$$\left. + \frac{a_{11} \cosh s\zeta - a_{21} \sinh s\zeta}{\gamma} f^B(z) \right) d\zeta ,$$

$$Q_1(z) = \frac{a_{22}\sinh s - a_{12}\cosh s}{s\gamma} f^A(z)$$

$$+\frac{a_{11}\cosh s - a_{21}\sinh s}{s\gamma} f^B(z),$$

$$Q_2(z) = Q(z) + \frac{a_{22}\sinh s + a_{12}\cosh s}{s\gamma} f^A(z) \tag{4.5.19}$$

$$-\frac{a_{11}\cosh s + a_{21}\sinh s}{s\gamma} f^B(z)$$

$$-\int_{-1}^{1} \frac{Q(\zeta)}{1+\nu(\zeta)}\left(\frac{a_{22}\sinh s\zeta - a_{12}\cosh s\zeta}{\gamma} f^A(z)\right.$$

$$\left.+\frac{a_{11}\cosh s\zeta - a_{21}\sinh s\zeta}{\gamma} f^B(z)\right)d\zeta,$$

$$\mathrm{T}(z) = \Theta(z) - \int_{-1}^{1} \frac{\Theta(\zeta) + \alpha(\zeta)E(\zeta)\overline{T}(\zeta)}{1+\nu(\zeta)}$$

$$\times\left(\frac{a_{22}\sinh s\zeta - a_{12}\cosh s\zeta}{\gamma} f^A(z)\right.$$

$$\left.+\frac{a_{11}\cosh s\zeta - a_{21}\sinh s\zeta}{\gamma} f^B(z)\right)d\zeta.$$

In view of the explicit expression (4.5.18), transversal stress can be determined using (4.5.8) as follows:

$$\overline{\sigma}_{zz}(z) = \overline{p}_1 P_1^z(z) + \overline{p}_2 P_2^z(z)$$

$$+\overline{q}_1 Q_1^z(z) + \overline{q}_2 Q_2^z(z) + \mathrm{T}^z(z), \tag{4.5.20}$$

where

$$P_1^z(z) = -s\int_{-1}^{z} \frac{P_1(\zeta)\sinh s(z-\zeta)}{1+\nu(\zeta)}d\zeta\,,$$

$$P_2^z(z) = -\cosh s(1+z) - s\int_{-1}^{z} \frac{P_2(\zeta)\sinh s(z-\zeta)}{1+\nu(\zeta)}d\zeta\,,$$

$$Q_1^z(z) = -s\int_{-1}^{z} \frac{Q_1(\zeta)\sinh s(z-\zeta)}{1+\nu(\zeta)}d\zeta\,,$$

$$Q_2^z(z) = -\sinh s(1+z) - s\int_{-1}^{z} \frac{Q_2(\zeta)\sinh s(z-\zeta)}{1+\nu(\zeta)}d\zeta\,, \qquad (4.5.21)$$

$$\mathrm{T}^z(z) = -s\int_{-1}^{z} \frac{\mathrm{T}(\zeta)+\alpha(\zeta)E(\zeta)\overline{T}(\zeta)}{1+\nu(\zeta)}\sinh s(z-\zeta)d\zeta\,.$$

Now, we can use (4.2.21) – (4.2.23) to determine radial, circumferential, and shear stresses in the Hankel mapping domain, as follows:

$$\begin{aligned}
&\overline{\sigma}_{rr}(z) = \overline{p}_1 P_1^r(z) + \overline{p}_2 P_2^r(z)\\
&+\overline{q}_1 Q_1^r(z) + \overline{q}_2 Q_2^r(z) + \mathrm{T}^r(z),\\
&\overline{\sigma}_{\varphi\varphi}(z) = \overline{p}_1 P_1^{\varphi}(z) + \overline{p}_2 P_2^{\varphi}(z)\\
&+\overline{q}_1 Q_1^{\varphi}(z) + \overline{q}_2 Q_2^{\varphi}(z) + \mathrm{T}^{\varphi}(z),\\
&\overline{\sigma}_{rz}(z) = \overline{p}_1 P_1^{rz}(z) + \overline{p}_2 P_2^{rz}(z)\\
&+\overline{q}_1 Q_1^{rz}(z) + \overline{q}_2 Q_2^{rz}(z) + \mathrm{T}^{rz}(z)\,.
\end{aligned} \qquad (4.5.22)$$

Here,

$$P_\ell^{rz}(z) = -\frac{1}{s}\frac{dP_\ell^z(z)}{dz}, \quad P_\ell^r(z) = \frac{1}{s}\frac{dP_\ell^{rz}(z)}{dz},$$

$$Q_\ell^r(z)=\frac{1}{s}\frac{dQ_\ell^{rz}(z)}{dz},\quad Q_\ell^{rz}(z)=-\frac{1}{s}\frac{dQ_\ell^{z}(z)}{dz},$$

$$\mathrm{T}^r(z)=\frac{1}{s}\frac{d\mathrm{T}^{rz}(z)}{dz},\quad \mathrm{T}^{rz}(z)=-\frac{1}{s}\frac{d\mathrm{T}^{z}(z)}{dz}, \tag{4.5.23}$$

$$Q_\ell^{\varphi}(z)=Q_\ell(z)-Q_\ell^r(z)-Q_\ell^z(z),$$

$$P_\ell^{\varphi}(z)=P_\ell(z)-P_\ell^r(z)-P_\ell^z(z),$$

$$\mathrm{T}^{\varphi}(z)=\mathrm{T}(z)-\mathrm{T}^r(z)-\mathrm{T}^z(z).$$

Using the Hankel representations given in (4.2.17) in conjunction with (4.5.20) and (4.4.22) allows for the construction of stress-tensor components in an inhomogeneous elastic layer due to force loadings (4.1.7) and the steady-state temperature field.

4.6. Displacement determination

4.6.1. Integration of Cauchy equations

To determine elastic displacements u_r and u_z from the Cauchy equations (4.1.2), the displacements can be represented using the Hankel integrals [147]:

$$u_r(\rho,z)=\int_0^{+\infty} s\overline{u}_r(z)J_1(s\rho)ds,$$
$$u_z(\rho,z)=\int_0^{+\infty} s\overline{u}_z(z)J_0(s\rho)ds. \tag{4.6.1}$$

These expressions combined with the first and second equations in (4.1.2) give us

$$\varepsilon_{rr}(\rho,z)+\varepsilon_{\varphi\varphi}(\rho,z)=\int_0^{+\infty} s^2\overline{u}_r(z)J_0(s\rho)ds\,. \tag{4.6.2}$$

We substitute the first and second equations of the constitutive law represented by (4.1.4) into (4.6.2), while taking into account the stress representations given in (4.2.17). This gives the following expression for radial displacement in the Hankel mapping domain:

$$s\overline{u}_r(z) = \frac{1-\nu(z)}{E(z)}\overline{\sigma}(z) - \frac{1}{2G(z)}\overline{\sigma}_{zz}(z) + 2\alpha(z)\overline{T}(z)\,. \qquad (4.6.3)$$

Similarly, using expressions (4.2.17) and (4.6.1) together with the fourth Cauchy equation in (4.1.2) and the constitutive equation for the shear stress in (4.1.4) yields the following expression for axial displacement:

$$s\overline{u}_z(z) = \frac{d\overline{u}_r(z)}{dz} - \frac{1}{G(z)}\overline{\sigma}_{rz}(z)\,. \qquad (4.6.4)$$

We can use (4.6.3) and (4.6.4) to determine elastic displacements in terms of stress-tensor components. These components were presented in the foregoing sections in the form of Hankel integrals (4.2.17) along with (4.3.11) – (4.3.13) for considered space $\mathcal{A}_0$, (4.4.13), (4.4.16) – (4.4.18) for half-space $\mathcal{A}_1$, and (4.5.20) and (4.4.22) for layer $\mathcal{A}_2$. Thus, the displacements can be expressed explicitly through the temperature field in the corresponding elastic solids along with the force loadings applied to the boundary of half-space $\mathcal{A}_1$ and layer $\mathcal{A}_2$. In the presentation of boundary conditions in terms of displacement, expressions (4.6.3) and (4.6.4) provide a perfect tool for establishing a one-to-one relationship between the boundary tractions and boundary displacements for the corresponding inhomogeneous elastic solids.

4.6.2. Axisymmetric elastic displacements in an inhomogeneous space

To compute the radial elastic displacement in inhomogeneous elastic space $\mathcal{A}_0$, we substitute (4.3.9) and (4.3.11) into (4.6.3) to obtain

$$\overline{u}_r(z) = \frac{1}{4G(z)}\int_{-\infty}^{+\infty}\overline{T}(\zeta)\left(\frac{\alpha(\zeta)E(\zeta)}{1-\nu(\zeta)}\exp(-s\,|\,z-\zeta\,|\,)\right.$$

$$-\frac{2}{s}\frac{1-\nu(z)}{1+\nu(z)}\Theta_0(z,\zeta)+\int_{-\infty}^{+\infty}\frac{\Theta_0(\eta,\zeta)}{1+\nu(\eta)}\exp(-s\,|\,z-\eta\,|)d\eta\Bigg)d\zeta\,. \quad (4.6.5)$$

In view of this, combining (4.6.4) with (4.3.12) yields

$$\overline{u}_z(z)=\frac{1}{4s}\int_{-\infty}^{+\infty}\overline{T}(\zeta)\Bigg(\frac{\alpha(\zeta)E(\zeta)}{1-\nu(\zeta)}\Bigg(\frac{d}{dz}\Bigg(\frac{1}{G(z)}\Bigg)+\frac{s\,\mathrm{sgn}(z-\zeta)}{G(z)}\Bigg)$$

$$\times\exp\left(-s\,|\,z-\zeta\,|\right)-\frac{4}{s}\frac{\partial}{\partial z}\Bigg(\frac{1-\nu(z)}{E(z)}\Theta_0(z,\zeta)\Bigg)$$

$$+\int_{-\infty}^{+\infty}\frac{\Theta_0(\eta,\zeta)}{1+\nu(\eta)}\Bigg(\frac{d}{dz}\Bigg(\frac{1}{G(z)}\Bigg)+\frac{s\,\mathrm{sgn}(z-\eta)}{G(z)}\Bigg)$$

$$\times\exp\left(-s\,|\,z-\eta\,|\right)d\eta\Bigg)d\zeta\,. \quad (4.6.6)$$

Function $\Theta_0(z,\zeta)$ in (4.6.5) and (4.6.6) is given by (4.3.18).

Displacement in the physical domain is computed by substituting (4.6.5) and (4.6.6) into the Hankel formulation in (4.6.1).

4.6.3. Axisymmetric elastic displacements in an inhomogeneous half-space

The radial displacement in inhomogeneous elastic half-space $\mathcal{A}_1$ can be computed by substituting (4.4.10) and (4.4.14) into (4.6.3), which yields the following formula:

$$\overline{u}_r(z)=\overline{p}P_r(z)+\overline{q}Q_r(z)+\mathrm{T}_r(z)\,. \quad (4.6.7)$$

Here,

$$P_r(z)=\frac{1-\nu(z)}{sE(z)}\Bigg(\Phi_1(z)-\frac{1+b}{a}\Psi_1(z)\Bigg)$$

$$+\frac{1}{4sG(z)}\Bigg(\exp(-sz)$$

$$-\frac{s}{a}\int_0^{+\infty}\frac{a\Phi_1(\zeta)-(1+b)\Psi_1(\zeta)}{1+\nu(\zeta)}\exp\left(-s\,|\,z-\zeta\,|\right)d\zeta\Bigg),$$

$$Q_r(z)=-\frac{1-\nu(z)}{sE(z)}\left(\Phi_1(z)+\frac{1-b}{a}\Psi_1(z)\right)$$

$$+\frac{1}{4sG(z)}\Bigg(\exp(-sz) \tag{4.6.8}$$

$$-\frac{s}{a}\int_0^{+\infty}\frac{a\Phi_1(\zeta)+(1-b)\Psi_1(\zeta)}{1+\nu(\zeta)}\exp\left(-s\,|\,z-\zeta\,|\right)d\zeta\Bigg),$$

$$\mathrm{T}_r(z)=\frac{1-\nu(z)}{sE(z)}\left(\Theta_1(z)-\frac{c}{a}\Psi_1(z)\right)+\frac{2}{s}\alpha(z)\overline{T}(z)$$

$$-\frac{1}{4aG(z)}\int_0^{+\infty}\frac{a\left(\alpha(\zeta)E(\zeta)\overline{T}(\zeta)+\Theta_1(\zeta)\right)-c\Psi_1(\zeta)}{1+\nu(\zeta)}$$

$$\times\exp\left(-s\,|\,z-\zeta\,|\right)d\zeta\,.$$

Implementing (4.6.4) in conjunction with (4.6.7) and (4.4.16) allows us to determine axial displacement as follows:

$$\overline{u}_z(z)=\overline{p}P_z(z)+\overline{q}Q_z(z)+\mathrm{T}_z(z)\,. \tag{4.6.9}$$

Here,

$$P_z(z)=\frac{1}{s}\frac{dP_r(z)}{dz}+\frac{1}{2G(z)}\Bigg(\frac{\exp(-sz)}{s}$$

$$-\frac{1}{a}\int_0^{+\infty}\frac{a\Phi_1(\zeta)-(1+b)\Psi_1(\zeta)}{1+\nu(\zeta)}$$

$$\times\exp\left(-s\,|\,z-\zeta\,|\right)\mathrm{sgn}(z-\zeta)d\zeta\Bigg),$$

$$Q_z(z)=\frac{1}{s}\frac{dQ_r(z)}{dz}-\frac{1}{2G(z)}\Bigg(\frac{\exp(-sz)}{s}$$

$$-\frac{1}{a}\int_0^{+\infty}\frac{a\Phi_1(\zeta)+(1-b)\Psi_1(\zeta)}{1+\nu(\zeta)} \tag{4.6.10}$$

$$\times\exp(-s\,|\,z-\zeta\,|)\operatorname{sgn}(z-\zeta)d\zeta\Bigg),$$

$$\mathrm{T}_z(z)=\frac{1}{s}\frac{d\mathrm{T}_r(z)}{dz}$$

$$-\frac{1}{2aG(z)}\int_0^{+\infty}\frac{a\big(\alpha(\zeta)E(\zeta)\overline{T}(\zeta)+\Theta_1(\zeta)\big)-c\Psi_1(\zeta)}{1+\nu(\zeta)}$$

$$\times\exp(-s\,|\,z-\zeta\,|)\operatorname{sgn}(z-\zeta)d\zeta\,.$$

Functions $\Phi_1(\zeta)$, $\Psi_1(\zeta)$, and $\Theta_1(\zeta)$ are given in (4.4.11); and constants a, b, and c are described in (4.4.13).

To compute displacement in the physical domain, we use the Hankel formulae in (4.6.1) together with (4.6.7) and (4.6.9).

The expressions given in (4.6.7) and (4.6.9) are explicit representations of the elastic displacements in half-space $\mathcal{A}_1$ in terms of force loadings (4.1.6) on its plane limiting surface $z=0$. This fact allows for simple analysis of various types of boundary condition. Consider, for example, the case when the boundary displacements are imposed on surface $z=0$:

$$u_r(\rho,0)=u_r^0(\rho),\qquad u_z(\rho,0)=u_z^0(\rho)\,. \tag{4.6.11}$$

Here, $u_r^0(\rho)$ and $u_z^0(\rho)$ are given functions for which the Hankel integrals (4.6.1) exist. Then, formulae (4.6.7), (4.6.9), and (4.6.11) provide the following system of equations:

$$\begin{aligned}\overline{u}_r^0 &= \overline{p}P_r(0)+\overline{q}Q_r(0)+\mathrm{T}_r(0),\\ \overline{u}_z^0 &= \overline{p}P_z(0)+\overline{q}Q_z(0)+\mathrm{T}_z(0).\end{aligned} \tag{4.6.12}$$

These equations make it possible to determine the normal and shear forces at the boundary in terms of boundary displacements:

$$\overline{p} = \frac{Q_z(0)\left(\overline{u}_r^0 - \mathrm{T}_r(0)\right) - Q_r(0)\left(\overline{u}_z^0 - \mathrm{T}_z(0)\right)}{P_r(0)Q_z(0) - P_z(0)Q_r(0)},$$
$$\overline{q} = \frac{P_r(0)\left(\overline{u}_z^0 - \mathrm{T}_z(0)\right) - P_z(0)\left(\overline{u}_r^0 - \mathrm{T}_r(0)\right)}{P_r(0)Q_z(0) - P_z(0)Q_r(0)}. \tag{4.6.13}$$

Now, we substitute (4.6.13) into (4.4.10), (4.4.16) – (4.4.18), (4.6.11), and (4.6.7) and (4.4.22) to determine the elastic stresses and displacements using the boundary displacements given in (4.6.11).

The case of mixed boundary conditions can be treated similarly. If, for example, the boundary $z = 0$ of half-space $\mathcal{A}_1$ exists under conditions of a sliding support, then the transversal displacement and shear stress are zero [149]:

$$\sigma_{rz}(\rho, 0) = q(\rho) \equiv 0, \qquad u_z(\rho, 0) = u_z^0(\rho) \equiv 0. \tag{4.6.14}$$

The system of equations (4.6.12) can be used to determine the two unknown functions at the boundary (i.e., normal traction and radial displacement), as follows:

$$\overline{p} = -\frac{\mathrm{T}_z(0)}{P_z(0)}, \qquad \overline{u}_r^0 = \frac{P_z(0)\mathrm{T}_r(0) - P_r(0)\mathrm{T}_z(0)}{P_z(0)}. \tag{4.6.15}$$

Inserting $\overline{p}$ and $\overline{q}$ presented in (4.6.14) and (4.6.15) into (4.4.14), (4.4.16) – (4.4.18), (4.6.11), and (4.6.7) and (4.4.22) allows us to determine the elastic stresses and displacements in inhomogeneous elastic half-space $\mathcal{A}_1$ under the sliding support of its boundary.

4.6.4. Axisymmetric elastic displacements in a transversely-inhomogeneous layer

Elastic displacements in layer $\mathcal{A}_2$ can be determined from formulae (4.6.3) and (4.6.4) in conjunction with (4.5.18), (4.5.20), and (4.5.22), as follows:

$$\begin{aligned}\overline{u}_r(z) &= \overline{p}_1 P_{1u}^r(z) + \overline{p}_2 P_{2u}^r(z)\\ &+\overline{q}_1 Q_{1u}^r(z) + \overline{q}_2 Q_{2u}^r(z) + \mathrm{T}_u^r(z),\\ \overline{u}_z(z) &= \overline{p}_1 P_{1u}^z(z) + \overline{p}_2 P_{2u}^z(z)\\ &+\overline{q}_1 Q_{1u}^z(z) + \overline{q}_2 Q_{2u}^z(z) + \mathrm{T}_u^z(z),\end{aligned} \tag{4.6.14}$$

where

$$\begin{aligned}P_{\ell u}^r(z) &= \frac{1-\nu(z)}{sE(z)} P_\ell(z) - \frac{1}{2sG(z)} P_\ell^z(z),\\ Q_{\ell u}^r(z) &= \frac{1-\nu(z)}{sE(z)} Q_\ell(z) - \frac{1}{2sG(z)} Q_\ell^z(z),\\ \mathrm{T}_u^r(z) &= \frac{1-\nu(z)}{sE(z)} \mathrm{T}(z) - \frac{1}{2sG(z)} \mathrm{T}^z(z) + 2\alpha(z)\overline{T}(z),\\ P_{\ell u}^z(z) &= \frac{1}{s}\frac{dP_{\ell u}^r(z)}{dz} - \frac{1}{sG(z)} P_\ell^{rz}(z),\\ Q_{\ell u}^z(z) &= \frac{1}{s}\frac{dQ_{\ell u}^r(z)}{dz} - \frac{1}{sG(z)} Q_\ell^{rz}(z),\\ \mathrm{T}_u^z(z) &= \frac{1}{s}\frac{d\mathrm{T}^r(z)}{dz} - \frac{1}{sG(z)} \mathrm{T}^{rz}(z), \quad \ell = 1,2\,.\end{aligned} \tag{4.6.15}$$

Displacements in the physical domain are computed using (4.6.14) in conjunction with the Hankel formulae given in (4.6.1).

The explicit expressions given in (4.6.14) for the elastic displacements through the force loadings (4.1.7) make it possible to establish a one-to-one relationship between boundary displacements and boundary tractions. Assume the boundary displacements to be imposed on the limiting planes $z = \pm 1$ of layer $\mathcal{A}_2$:

$$u_r(\rho,1)=u_r^+(\rho),\qquad u_z(\rho,1)=u_z^+(\rho),$$
$$u_r(\rho,-1)=u_r^-(\rho),\qquad u_z(\rho,-1)=u_z^-(\rho), \tag{4.6.16}$$

where $u_r^{\pm}(\rho)$ and $u_z^{\pm}(\rho)$ are given functions whose Hankel integrals (4.6.1) exist. Substituting (4.6.14) into (4.6.16), while taking into account (4.6.1) yields the following system of equations:

$$\begin{aligned}
\overline{u}_r^+ &= \overline{p}_1 P_{1u}^r(1)+\overline{p}_2 P_{2u}^r(1)\\
&+\overline{q}_1 Q_{1u}^r(1)+\overline{q}_2 Q_{2u}^r(1)+\mathrm{T}_u^r(1),\\
\overline{u}_r^- &= \overline{p}_1 P_{1u}^r(-1)+\overline{p}_2 P_{2u}^r(-1)\\
&+\overline{q}_1 Q_{1u}^r(-1)+\overline{q}_2 Q_{2u}^r(-1)+\mathrm{T}_u^r(-1),\\
\overline{u}_z^+ &= \overline{p}_1 P_{1u}^z(1)+\overline{p}_2 P_{2u}^z(1)\\
&+\overline{q}_1 Q_{1u}^z(1)+\overline{q}_2 Q_{2u}^z(1)+\mathrm{T}_u^z(1),\\
\overline{u}_z^- &= \overline{p}_1 P_{1u}^z(-1)+\overline{p}_2 P_{2u}^z(-1)\\
&+\overline{q}_1 Q_{1u}^z(-1)+\overline{q}_2 Q_{2u}^z(-1)+\mathrm{T}_u^z(-1).
\end{aligned} \tag{4.6.17}$$

These equations establish one-to-one relationships between the four displacement components $u_r^{\pm}(\rho)$ and $u_z^{\pm}(\rho)$ and four force-loading components p_ℓ and q_ℓ, $\ell=1,2$, on the limiting planes $z=\pm1$ of layer $\mathcal{A}_2$. Thus, in situations where there is a need in solving a thermoelasticity problem with boundary conditions in terms of displacements (4.6.16), equations (4.6.17) can be used to determine the unknown boundary tractions p_ℓ and q_ℓ, $\ell=1,2$, and then implement them for the determination of stresses (4.5.20) and (4.5.22), and displacements (4.6.14). The same strategy can be used in the case of the mixed-type boundary conditions. If, for example, the limiting planes of layer $\mathcal{A}_2$ are under the conditions of a sliding support

$$\sigma_{rz}(\rho,1)=q_1(\rho)=0,\qquad u_z(\rho,1)=u_z^{+}(\rho)=0,$$
$$\sigma_{rz}(\rho,-1)=q_2(\rho)=0,\qquad u_z(\rho,-1)=u_z^{-}(\rho)=0, \tag{4.6.18}$$

then system of equations (4.6.17) yields

$$\begin{aligned}
\overline{u}_r^{+} &= \overline{p}_1 P_{1u}^{r}(1)+\overline{p}_2 P_{2u}^{r}(1)+\mathrm{T}_u^{r}(1),\\
\overline{u}_r^{-} &= \overline{p}_1 P_{1u}^{r}(-1)+\overline{p}_2 P_{2u}^{r}(-1)+\mathrm{T}_u^{r}(-1),\\
\overline{p}_1 P_{1u}^{z}(1)&+\overline{p}_2 P_{2u}^{z}(1)=-\mathrm{T}_u^{z}(1),\\
\overline{p}_1 P_{1u}^{z}(-1)&+\overline{p}_2 P_{2u}^{z}(-1)=-\mathrm{T}_u^{z}(-1).
\end{aligned} \tag{4.6.19}$$

Solving third and fourth equations in (4.6.19) with respect to the as-yet unknown functions p_ℓ, $\ell=1,2$, gives the following boundary tractions:

$$\begin{aligned}
\overline{p}_1 &= \frac{\mathrm{T}_u^{z}(-1)P_{2u}^{z}(1)-\mathrm{T}_u^{z}(1)P_{2u}^{z}(-1)}{P_{1u}^{z}(1)P_{2u}^{z}(-1)-P_{1u}^{z}(-1)P_{2u}^{z}(1)},\\
\overline{p}_2 &= \frac{\mathrm{T}_u^{z}(1)P_{1u}^{z}(-1)-\mathrm{T}_u^{z}(-1)P_{1u}^{z}(1)}{P_{1u}^{z}(1)P_{2u}^{z}(-1)-P_{1u}^{z}(-1)P_{2u}^{z}(1)}.
\end{aligned} \tag{4.6.20}$$

The tractions can now be used in conjunction with $\overline{q}_1=\overline{q}_2=0$ to determine the stresses (4.5.20) and (4.4.22), as well as displacements (4.6.14) for inhomogeneous elastic layer $\mathcal{A}_2$ under the condition of sliding support (4.6.19) along its boundaries $z=\pm 1$.

4.7. Axisymmetric steady-state temperature field in inhomogeneous elastic solids

To determine the temperature field in inhomogeneous space $\mathcal{A}_0$, half-space $\mathcal{A}_1$, and layer $\mathcal{A}_2$, we use the heat-transfer equation (4.1.8) under the following conditions: vanishing temperature and heat-source density at $z^2\to+\infty$ for space $\mathcal{A}_0$; vanishing temperature, heat-source density at

$z \to +\infty$, and condition (4.1.9) for half-space $\mathcal{A}_1$; and conditions (4.1.10) for layer $\mathcal{A}_2$. We can apply the Hankel representation for temperature given in (4.2.17) to transform equation (4.1.8) as follows:

$$\frac{d^2\overline{T}(z)}{dz^2} - s^2\overline{T}(z) = -\frac{\overline{w}(z)}{\lambda(z)} - \frac{d\ln\lambda(z)}{dz}\frac{d\overline{T}(z)}{dz}, \tag{4.7.1}$$

where $\overline{w}(z)$ is the Hankel image of the heat-source density:

$$w(\rho, z) = \int_0^{+\infty} \overline{w}(z) J_0(\rho s)\, ds\,. \tag{4.7.2}$$

Clearly, equation (4.7.1) is similar to (2.2.62), which presents the heat-transfer equation in the Fourier mapping domain for plane problems of thermoelasticity. For the latter, we set $\lambda_x = \lambda_y = \lambda$ and change the variable from y to z. Thus, solutions of equation (2.2.62) for plane $\mathfrak{D}_0$, half-plane $\mathfrak{D}_1$, and strip $\mathfrak{D}_2$ can be adopted here as solutions to equation (4.7.1) in the mapping domain of transform (4.2.17) for space $\mathcal{A}_0$, half-space $\mathcal{A}_1$, and layer $\mathcal{A}_2$.

A solution to equation (4.7.1) for space $\mathcal{A}_0$ can be obtained using (2.2.66) as follows:

$$\overline{T}(z) = w_{\mathrm{SP}}(z) + \int_{-\infty}^{+\infty} w_{\mathrm{SP}}(\eta)\mathcal{T}_{\mathrm{SP}}(z,\zeta)\, d\zeta\,, \tag{4.7.3}$$

where

$$w_{\mathrm{SP}}(z) = \frac{1}{2s}\int_{-\infty}^{+\infty} \frac{\overline{w}(\zeta)}{\lambda(\zeta)} \exp\left(-s\,|\,z-\zeta\,|\right) d\zeta\,, \tag{4.7.4}$$

and

$$\mathcal{T}_{\mathrm{SP}}(z,\zeta) = \sum_{n=0}^{\infty} \mathcal{T}_{n+1}^{\mathrm{SP}}(z,\zeta)\,, \tag{4.7.5}$$

$$\mathcal{T}_1^{\mathrm{SP}}(z,\zeta) = \mathcal{L}_{\mathrm{SP}}(z,\zeta),$$
$$\mathcal{T}_{n+1}^{\mathrm{SP}}(z,\zeta) = \int_{-\infty}^{+\infty} \mathcal{T}_1^{\mathrm{SP}}(z,\xi)\mathcal{T}_n^{\mathrm{SP}}(\xi,\zeta)d\xi, \tag{4.7.6}$$

$$\mathcal{L}_{\mathrm{SP}}(z,\zeta) = -\frac{1}{2s}\left(s\frac{d\ln\lambda(\zeta)}{d\zeta}\operatorname{sgn}(z-\zeta) + \frac{d^2\ln\lambda(\zeta)}{d\zeta^2}\right)\exp\left(-s\,|\,z-\zeta\,|\right) \quad . \tag{4.7.7}$$

To solve equation (4.7.1) under boundary condition (4.1.9) for half-space $\mathcal{A}_1$, we adopt solution (2.3.88) in the following form:

$$\overline{T}(z) = \overline{T}_0 t_{\mathrm{HS}}^0(z) + w_{\mathrm{HS}}(z)\,, \tag{4.7.8}$$

where

$$t_{\mathrm{HS}}^0(z) = \frac{1}{\text{æ}^-}\left(\exp(-sz) + \int_0^{+\infty}\exp(-s\zeta)\mathcal{T}_{\mathrm{HS}}(z,\zeta)d\zeta\right),$$
$$w_{\mathrm{HS}}(z) = W_{\mathrm{HS}}(z) + \int_0^{+\infty} W_{\mathrm{HS}}(\zeta)\mathcal{T}_{\mathrm{HS}}(z,\zeta)d\zeta, \tag{4.7.9}$$

and

$$W_{\mathrm{HS}}(z) = \frac{1}{2s}\int_0^{+\infty}\frac{\overline{w}(\zeta)}{\lambda(\zeta)}\left(\exp(-s\,|\,z-\zeta\,|) - \frac{\text{æ}^+}{\text{æ}^-}\exp(-s(z+\zeta))\right)d\zeta,$$
$$\text{æ}^+ = \ell_0 + \ell_1\left(|\,s\,| - \text{æ}_0\right), \quad \text{æ}^- = \ell_0 - \ell_1\left(|\,s\,| + \text{æ}_0\right), \tag{4.7.10}$$
$$\text{æ}_0 = \frac{1}{\lambda(0)}\left.\frac{d\lambda(z)}{dz}\right|_{z=0}.$$

The resolvent-kernel in this case has the following form:

$$\mathcal{T}_{\mathrm{HS}}(z,\zeta)=\sum_{n=0}^{\infty}\mathcal{T}_{n+1}^{\mathrm{HS}}(z,\zeta)\,, \tag{4.7.11}$$

where

$$\mathcal{T}_{1}^{\mathrm{HS}}(z,\zeta)=\mathcal{L}_{\mathrm{HS}}(z,\zeta),$$

$$\mathcal{T}_{n+1}^{\mathrm{HS}}(z,\zeta)=\int_{0}^{+\infty}\mathcal{T}_{1}^{\mathrm{HS}}(z,\xi)\mathcal{T}_{n}^{\mathrm{HS}}(\xi,\zeta)d\xi\,,\ n=1,2,...,$$

$$\mathcal{L}_{\mathrm{HS}}(z,\zeta)=-\frac{1}{2s}\frac{d^{2}\ln\lambda(\zeta)}{d\zeta^{2}}$$

$$\times\left(\exp(-s\,|\,z-\zeta\,|)-\frac{æ^{+}}{æ^{-}}\exp(-s\,|\,z+\zeta\,|)\right) \tag{4.7.12}$$

$$-\frac{1}{2}\frac{d\ln\lambda(\zeta)}{d\zeta}\left(\exp(-s\,|\,z-\zeta\,|)\mathrm{sgn}(z-\zeta)\right.$$

$$\left.+\frac{æ^{+}}{æ^{-}}\exp(-s(z+\zeta))\right).$$

Finally, the Hankel mapping function for the temperature in elastic transversely-inhomogeneous layer $\mathcal{A}_2$ can be found using (2.4.68), leading to the following equation:

$$\overline{T}(z)=\overline{T}_{1}\tau_{1,\mathrm{LR}}(z)+\overline{T}_{2}\tau_{2,\mathrm{LR}}(z)+w_{\mathrm{LR}}(z)\,. \tag{4.7.13}$$

Here,

$$\tau_{1,\mathrm{LR}}(z)=\frac{\gamma_{22}\overline{\tau}_{\mathrm{c}}(z)-\gamma_{21}\overline{\tau}_{\mathrm{s}}(z)}{\gamma},$$

$$\tau_{2,\mathrm{LR}}(z)=\frac{\gamma_{11}\overline{\tau}_{\mathrm{s}}(z)-\gamma_{12}\overline{\tau}_{\mathrm{c}}(z)}{\gamma},$$

$$\overline{\tau}_{\mathrm{c}}(z) = \cosh sz + \int_{-1}^{1} \cosh s\zeta \mathcal{T}_{\mathrm{LR}}(z,\zeta)d\zeta,$$

$$\overline{\tau}_{\mathrm{s}}(z) = \sinh sz + \int_{-1}^{1} \sinh s\zeta \mathcal{T}_{\mathrm{LR}}(z,\zeta)d\zeta,$$

$$w_{\mathrm{LR}}(z) = w^{*}_{\mathrm{LR}}(z) + \int_{-1}^{1} w^{*}_{\mathrm{LR}}(\zeta)\mathcal{T}_{\mathrm{LR}}(z,\zeta)d\zeta,$$

$$w^{*}_{\mathrm{LR}}(z) = \frac{1}{2s}\int_{-1}^{1} \frac{\overline{w}(\zeta)}{\lambda(\zeta)}\Bigg[-\sinh s\,|\,z-\zeta\,|$$

$$+\Bigg[\gamma_{22}\ell_{11}\sinh s(1-\zeta)$$

$$+\gamma_{22}\ell_{12}\left(s\cosh s(1-\zeta) - \left.\frac{d\ln\lambda(z)}{dz}\right|_{z=1}\sinh s(1-\zeta)\right)$$

$$-\gamma_{12}\ell_{21}\sinh s(1+\zeta) + \gamma_{12}\ell_{22}\left(s\cosh s(1+\zeta)\right.$$

$$\left.+\left.\frac{d\ln\lambda(z)}{dz}\right|_{z=-1}\sinh s(1+\zeta)\right)\Bigg]\frac{\cosh sz}{\gamma}$$

$$+\Bigg[\gamma_{11}\ell_{21}\sinh s(1+\zeta) - \gamma_{11}\ell_{22}\left(s\cosh s(1+\zeta)\right. \tag{4.7.14}$$

$$\left.+\left.\frac{d\ln\lambda(z)}{dz}\right|_{z=-1}\sinh s(1+\zeta)\right)$$

$$-\gamma_{21}\ell_{11}\sinh s(1-\zeta) - \gamma_{21}\ell_{12}\left(s\cosh s(1-\zeta)\right.$$

$$\left.-\left.\frac{d\ln\lambda(z)}{dz}\right|_{z=1}\sinh s(1-\zeta)\right)\Bigg]\frac{\sinh sz}{\gamma}\Bigg]d\zeta,$$

,

$$\gamma_{11} = \left(\ell_{11} - \ell_{12} \frac{d \ln \lambda(z)}{dz}\bigg|_{z=1} \right) \cosh s + \ell_{12} s \sinh s,$$

$$\gamma_{12} = \left(\ell_{11} - \ell_{12} \frac{d \ln \lambda(z)}{dz}\bigg|_{z=1} \right) \sinh s + \ell_{12} s \cosh s,$$

$$\gamma_{21} = \left(\ell_{21} - \ell_{22} \frac{d \ln \lambda(z)}{dz}\bigg|_{z=-1} \right) \cosh s - \ell_{22} s \sinh s,$$

$$\gamma_{22} = -\left(\ell_{21} - \ell_{22} \frac{d \ln \lambda(z)}{dz}\bigg|_{z=-1} \right) \sinh s + \ell_{22} s \cosh s,$$

$$\gamma = \gamma_{11}\gamma_{22} - \gamma_{12}\gamma_{21}.$$

The resolvent-kernel takes the form of the series

$$\mathcal{T}_{\mathrm{LR}}(z,\zeta) = \sum_{n=0}^{\infty} \mathcal{L}_{n+1}^{\mathrm{LR}}(z,\zeta) \tag{4.7.15}$$

of the following recurring kernels:

$$\begin{aligned} \mathcal{L}_1^{\mathrm{LR}}(z,\zeta) &= \mathcal{L}_{\mathrm{LR}}(z,\zeta), \\ \mathcal{L}_{n+1}^{\mathrm{LR}}(z,\zeta) &= \int_{-1}^{1} \mathcal{L}_1^{\mathrm{LR}}(z,\xi)\mathcal{L}_n^{\mathrm{LR}}(\xi,\zeta)d\xi, \quad n = 1,2,..., \end{aligned} \tag{4.7.16}$$

where

$$\mathcal{L}_{\mathrm{LR}}(z,\zeta) = \frac{1}{2s}\left\{ \frac{d^2 \ln \lambda(\zeta)}{d\zeta^2}\left[\sinh s \mid z-\zeta \mid \right.\right.$$

$$-\left[\gamma_{22}\ell_{11} \sinh s(1-\zeta) + \gamma_{22}\ell_{12}\left(s\cosh s(1-\zeta) \right.\right.$$

$$\left.\left.\left. -\frac{d \ln \lambda(z)}{dz}\bigg|_{z=1} \sinh s(1-\zeta) \right) \right.\right.$$

$$+\gamma_{12}\ell_{21}\sinh s(1+\zeta)+\gamma_{12}\ell_{22}\left(s\cosh s(1+\zeta)\right.$$

$$\left.+\frac{d\ln\lambda(z)}{dz}\bigg|_{z=-1}\sinh s(1+\zeta)\right)\Bigg]\frac{\cosh sz}{\gamma}$$

$$-\Bigg[\gamma_{11}\ell_{21}\sinh s(1+\zeta)-\gamma_{11}\ell_{22}\left(s\cosh s(1+\zeta)\right.$$

$$\left.+\frac{d\ln\lambda(z)}{dz}\bigg|_{z=-1}\sinh s(1+\zeta)\right)$$

$$-\gamma_{21}\ell_{11}\sinh s(1-\zeta)-\gamma_{21}\ell_{12}\left(s\cosh s(1-\zeta)\right.$$

$$\left.-\frac{d\ln\lambda(z)}{dz}\bigg|_{z=1}\sinh s(1-\zeta)\right)\Bigg]\frac{\sinh sz}{\gamma}\Bigg] \tag{4.7.18}$$

$$-s\frac{d\ln\lambda(\zeta)}{d\zeta}\Bigg[\cosh s(z-\zeta)\operatorname{sgn}(z-\zeta)$$

$$-\Bigg[\gamma_{22}\ell_{11}\cosh s(1-\zeta)+\gamma_{22}\ell_{12}\left(s\sinh s(1-\zeta)\right.$$

$$\left.-\frac{d\ln\lambda(z)}{dz}\bigg|_{z=1}\cosh s(1-\zeta)\right)$$

$$+\gamma_{12}\ell_{21}\cosh s(1+\zeta)-\gamma_{12}\ell_{22}\left(s\sinh s(1+\zeta)\right.$$

$$\left.+\frac{d\ln\lambda(z)}{dz}\bigg|_{z=-1}\cosh s(1+\zeta)\right)\Bigg]\frac{\cosh sz}{\gamma}$$

$$+\left[\gamma_{11}\ell_{21}\cosh s(1+\zeta)-\gamma_{11}\ell_{22}\left(s\sinh s(1+\zeta)\right.\right.$$

$$\left.+\frac{d\ln\lambda(z)}{dz}\bigg|_{z=-1}\cosh s(1+\zeta)\right)$$

$$+\gamma_{21}\ell_{11}\cosh s(1-\zeta)+\gamma_{21}\ell_{12}\left(s\sinh s(1-\zeta)\right.$$

$$\left.\left.\left.-\frac{d\ln\lambda(z)}{dz}\bigg|_{z=1}\cosh s(1-\zeta)\right)\right]\frac{\sinh sz}{\gamma}\right]\Bigg\}.$$

To compute temperature in the physical domain, we use formulae (4.2.17) and (4.7.2) in conjunction with (4.7.3) for space $\mathcal{A}_0$, (4.7.8) for half-space $\mathcal{A}_1$, and (4.7.13) for layer $\mathcal{A}_2$.

This makes it possible to utilize the analogy between the plane and axisymmetric heat conduction solutions to represent axisymmetric thermal fields in the considered inhomogeneous solids. These representations are in the form of explicit dependencies on thermal loadings, either in interior points (i.e., internal heat sources) or at the boundaries (i.e., boundary temperature, heat flux through the surface, or complex conditions of heat exchange). Computational accuracy depends on evaluations of the resolvent-kernels given in (4.7.5), (4.7.11), and (4.7.15).

4.8. Stress analysis and special cases of inhomogeneity

The axisymmetric stress-tensor and displacement-vector components constructed above in the form of explicit dependencies on the steady-state temperature field (for inhomogeneous elastic space $\mathcal{A}_0$) and the steady-state temperature field and force loadings imposed on the boundary (for inhomogeneous elastic half-space $\mathcal{A}_1$ and layer $\mathcal{A}_2$). Under the assumption that the temperature field is known, the computational accuracy of these components depends on the evaluation of resolvent kernels $\mathcal{R}_0(z,\zeta)$, $\mathcal{R}_1(z,\zeta)$, and $\mathcal{R}(z,\zeta)$. These are presented respectively by formulae (4.3.7), (4.4.11), and (4.5.14) as infinite series of corresponding recurring kernels originated by the kernels (4.3.4), (4.4.9), and (4.5.11) of the integral equations (4.3.3), (4.4.8), and (4.5.10) for total

stress in the mapping domain of the Hankel transform (4.2.17). These kernels depend on the material properties and in some cases can be evaluated analytically. However, when analytical evaluation presents a challenge, these series can be truncated for practical purposes to be represented by corresponding finite sums of initial terms.

As can be seen from the corresponding expressions for the integral kernels (4.3.4), (4.4.9), and (4.5.11), they can be zeros for certain inhomogeneous materials, for which

$$G(z) = \frac{E(z)}{2(1+\nu(z))} = \frac{G_0}{1+a_0 z}, \tag{4.8.1}$$

where G_0 is a constant in the dimension of stresses and a_0 is a dimensionless constant ensuring that the material moduli remain within the physical constraints implied by the mathematical model for the entire range of variation of coordinate *z*.

For inhomogeneous elastic space $\mathcal{A}_0$, the condition of positivity for the shear modulus (i.e., $G(z) > 0$) for $z \in (-\infty, +\infty)$ implies $a_0 = 0$ and $G_0 > 0$. This yields

$$E(z) = 2(1+\nu(z))G_0 \tag{4.8.2}$$

or

$$\nu(z) = \frac{E(z)}{2G_0} - 1. \tag{4.8.3}$$

Thus, if the Young modulus and the Poisson ratio in isotropic inhomogeneous space $\mathcal{A}_0$ meet conditions (4.8.2) or (4.8.3), i.e., $E(z)$ varies proportionally to $1+\nu(z)$ for $z \in (-\infty, +\infty)$, then resolvent kernel $\mathcal{R}_0(z,\zeta)$ given by (4.3.7) equals zero. Furthermore, corresponding stress-tensor components (4.3.11) – (4.3.14) can be obtained explicitly as follows:

$$\overline{\sigma}_{zz}(z) = -sG_0 \int_{-\infty}^{+\infty} \frac{1+\nu(\zeta)}{1-\nu(\zeta)} \alpha(\zeta)\overline{T}(\zeta) \exp(-s\,|\,z-\zeta\,|)d\zeta,$$

$$\bar{\sigma}_{rr}(z) = G_0 \left(-2\frac{1+\nu(z)}{1-\nu(z)}\alpha(z)\bar{T}(z) \right.$$

$$\left. +s\int_{-\infty}^{+\infty}\frac{1+\nu(\zeta)}{1-\nu(\zeta)}\alpha(\zeta)\bar{T}(\zeta)\exp(-s\,|\,z-\zeta\,|)d\zeta \right), \qquad (4.8.4)$$

$$\bar{\sigma}_{\varphi\varphi}(z) = -2G_0\frac{1+\nu(z)}{1-\nu(z)}\alpha(z)\bar{T}(z),$$

$$\bar{\sigma}_{rz}(z) = -sG_0\int_{-\infty}^{+\infty}\frac{1+\nu(\zeta)}{1-\nu(\zeta)}\alpha(\zeta)\bar{T}(\zeta)\exp(-s\,|\,z-\zeta\,|)\,\mathrm{sgn}(z-\zeta)d\zeta\,,$$

or

$$\bar{\sigma}_{zz}(z) = sG_0\int_{-\infty}^{+\infty}\frac{\alpha(\zeta)E(\zeta)}{E(\zeta)-4G_0}\bar{T}(\zeta)\exp(-s\,|\,z-\zeta\,|)d\zeta\,,$$

$$\bar{\sigma}_{rr}(z) = G_0 \left(2\frac{\alpha(z)E(z)}{E(z)-4G_0}\bar{T}(z) \right.$$

$$\left. -s\int_{-\infty}^{+\infty}\frac{\alpha(\zeta)E(\zeta)}{E(\zeta)-4G_0}\bar{T}(\zeta)\exp(-s\,|\,z-\zeta\,|)d\zeta \right), \qquad (4.8.6)$$

$$\bar{\sigma}_{\varphi\varphi}(z) = 2G_0\frac{\alpha(z)E(z)}{E(z)-4G_0}\bar{T}(z),$$

$$\bar{\sigma}_{rz}(z) = sG_0\int_{-\infty}^{+\infty}\frac{\alpha(\zeta)E(\zeta)}{E(\zeta)-4G_0}\bar{T}(\zeta)$$

$$\times\exp(-s\,|\,z-\zeta\,|)\,\mathrm{sgn}(z-\zeta)d\zeta\,.$$

At the same time, feasible material moduli satisfying (4.8.2) or (4.8.3) are required to assume finite values at $z \to \pm\infty$. Moreover, due to the restrictions of the elasticity model, the Poisson ratio varies within the

following constraint: $-1 < \nu(z) \le 1/2$, $z \in (-\infty, +\infty)$. Thus, in view of (4.8.3), we obtain the following:

$$0 < E(z) \le 3G_0 . \tag{4.8.7}$$

For example, if we designate that

$$E(z) = \big(2 + \big(\exp(-m\,|\,z\,|) - 1\big)\,\mathrm{sgn}(z)\big)\,G_0 , \tag{4.8.8}$$

or, in view of (4.8.3),

$$\nu(z) = \frac{1}{2}\big(\exp(-m\,|\,z\,|) - 1\big)\,\mathrm{sgn}(z) , \tag{4.8.9}$$

then the condition given in (4.8.7) is satisfied and the limit values of $E(z)$ and $\nu(z)$ at $z \to \pm\infty$ are constant. When the material moduli are represented by (4.8.8) and (4.8.9), inhomogeneous elastic space $\mathcal{A}_0$ comprises two homogeneous half-spaces with dissimilar material properties ("material A" and "material B"), which are connected via a transversally-inhomogeneous intermediate layer with smoothly-varying properties from one interface to another (Fig. 4.1).

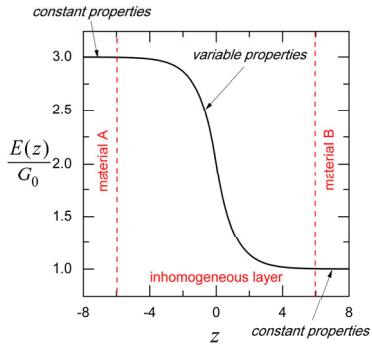

Figure 4.1. Young's modulus (4.8.8) of inhomogeneous elastic space $\mathcal{A}_0$ for $m = 1$

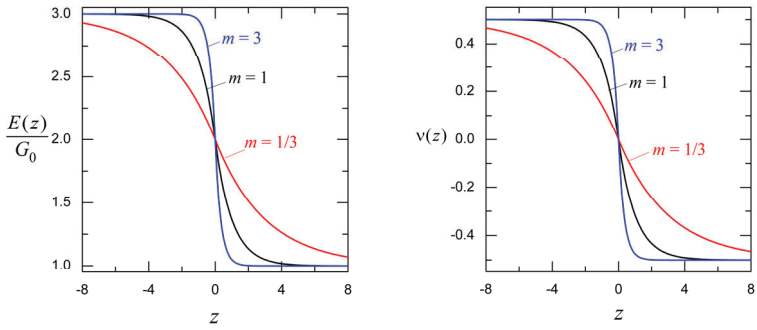

a) *b*)

Figure 4.2. *a*) Young's modulus (4.8.8) and *b*) Poisson's ratio (4.8.9) of inhomogeneous elastic space $\mathcal{A}_0$ for $m = 1/3; 1; 3$

Parameter m in (4.8.8) and (4.8.9) makes it possible for us to control the width of the intermediate inhomogeneous layer and the "steepness" of the variation in the material properties across it (see Fig. 4.2). If $m = 0$, then $E(z) = E_0 = \text{const}$ and $\nu(z) = \nu_0 = \text{const}$, and the inhomogeneity of elastic space $\mathcal{A}_0$ is indicated only by the z-dependence of the coefficient of linear thermal expansion. Then,

$$\sigma_{zz}(z) = -\frac{s}{2}\frac{E_0}{1-\nu_0}\int_{-\infty}^{+\infty}\alpha(\zeta)\overline{T}(\zeta)\exp(-s\,|\,z-\zeta\,|)d\zeta\,,$$

$$\overline{\sigma}_{rr}(z) = \frac{E_0}{1-\nu_0}\left(-\alpha(z)\overline{T}(z)\right.$$

$$\left.+\frac{s}{2}\int_{-\infty}^{+\infty}\alpha(\zeta)\overline{T}(\zeta)\exp(-s\,|\,z-\zeta\,|)d\zeta\right), \qquad (4.8.10)$$

$$\overline{\sigma}_{\varphi\varphi}(z) = -\frac{\alpha(z)E_0}{1-\nu_0}\overline{T}(z),$$

$$\overline{\sigma}_{rz}(z) = -\frac{s}{2}\frac{E_0}{1-\nu_0}\int_{-\infty}^{+\infty}\alpha(\zeta)\overline{T}(\zeta)\exp(-s\,|\,z-\zeta\,|)\,\mathrm{sgn}(z-\zeta)d\zeta\,.$$

Expressions (4.8.10) can be regarded as a benchmark analytical solution for capturing the thermal effect of the variable linear thermal expansion coefficient $\alpha(z)$.

Finally, if in (4.8.10) coefficient $\alpha(z) = \alpha_0 = \text{const}$, then the isotropic elastic space $\mathcal{A}_0$ can be regarded as homogeneous.

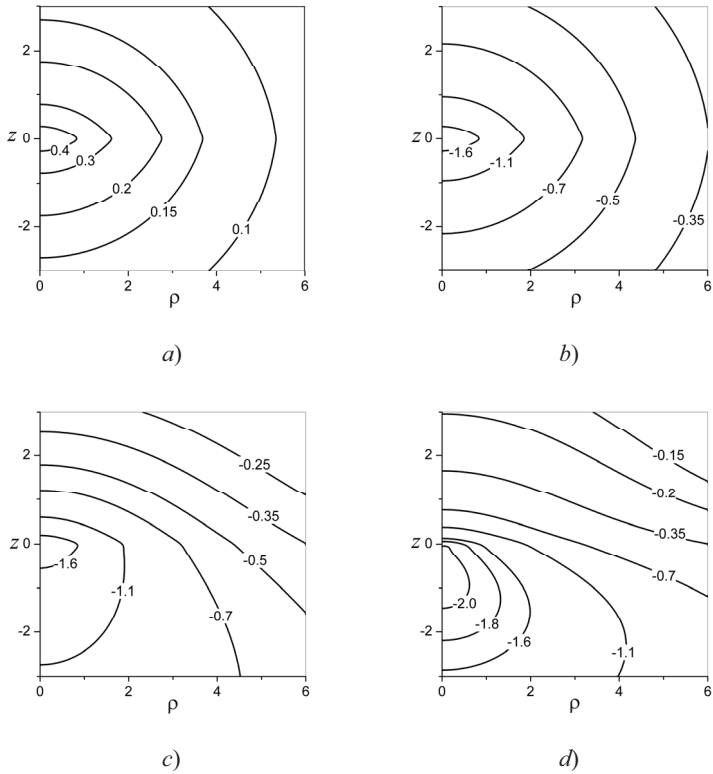

a) *b*)

c) *d*)

Figure 4.3. Full-field distributions of *a*) temperature $\lambda_0 T(\rho, z)/w_0$ and total stress $\lambda_0 \sigma(\rho, z)/(\alpha_0 G_0 w_0)$ for *b*) $m = 0$ (homogeneous material), *c*) $m = 1/3$ and *d*) $m = 1$ in (4.8.8) and (4.8.9)

Consider computation of the thermal stresses (4.8.4) for space $\mathcal{A}_0$ using material moduli (4.8.8) and (4.8.9) and a constant coefficient of linear thermal expansion, $\alpha(z) = \alpha_0 = \text{const}$, under a temperature

imposed by internal heat sources of density $w(\rho,z)=w_0\exp(-\rho)\delta(z)$ acting in plane $z=0$ and exponentially decaying when moving away from the symmetry axis for the case of constant heat-conduction coefficient $\lambda(z)=\lambda_0=\text{const}$. Here, $w_0=\text{const}$ and $\delta(z)$ is the Dirac delta-function. We compute temperature $\lambda_0 T(\rho,z)/w_0$ as a solution to heat-conduction equation (4.7.1) in the physical domain of transfer (4.2.17). This is depicted in Fig. 4.3*a*. The effect of material inhomogeneity (3.8.8) and (3.8.9) in total stress $\lambda_0\sigma(\rho,z)/(\alpha_0 G_0 w_0)$ is illustrated in Fig. 4.3. Total stress in the case of homogeneous material $m=0$ is proportional to the temperature; therefore, the distribution of stress in Fig. 4.3*b* echoes that of temperature in Fig. 4. 3*a.* It is also symmetric about the plane $z=0$, which is not the case for inhomogeneous materials where $m=1/3$ (Fig. 4.3*c*) and $m=1$ (Fig. 4.3*d*). Similar analysis can be applied to the case where the linear coefficient of thermal expansion depends on the axial coordinate.

For inhomogeneous elastic half-space $\mathcal{A}_1$, the condition that the shear modulus is positive and described in the form (4.8.1) implies that $G_0>0$ and $a_0\geq 0$. Thus, the type of inhomogeneity covered by formula (4.8.1) can be referred to as "Gibson soil" (see formula (1.2.5) in Chapter 1). In this case,

$$E(z)=2\frac{1+\nu(z)}{1+a_0 z}G_0 \tag{4.8.11}$$

and

$$\nu(z)=\frac{E(z)}{2G_0}(1+a_0 z)-1. \tag{4.8.12}$$

The physical constraints on Poisson's ratio impose the following limitations pertaining to variations in the elastic moduli:

$$0<(1+a_0 z)E(z)\leq 3G_0. \tag{4.8.13}$$

The stress-tensor components (4.4.14), (4.4.16) – (4.4.18) in this case take the following form:

$$\overline{\sigma}_{zz}(z) = -\frac{\overline{p}}{2}\left(\exp(-sz) \right.$$

$$\left. + \frac{s}{a}\int_0^{+\infty} \frac{E(\zeta)}{1-\nu^2(\zeta)} \exp\left(-s\left(\zeta + |z-\zeta|\right)\right) d\zeta \right)$$

$$+ \frac{\overline{q}}{2}\left(\exp(-sz) - \frac{s}{a}\int_0^{+\infty} \frac{E(\zeta)}{1-\nu^2(\zeta)} \exp\left(-s\left(\zeta + |z-\zeta|\right)\right) d\zeta \right)$$

$$-\frac{s}{2a}\int_0^{+\infty} \frac{c\exp(-s\zeta) + a\left(1-\nu(\zeta)\right)\alpha(\zeta)\overline{T}(\zeta)}{1-\nu^2(\zeta)}$$

$$\times \exp\left(-s\,|z-\zeta|\right) d\zeta\,,$$

$$\overline{\sigma}_{rr}(z) = \frac{\overline{p}}{a}\left(\left(\frac{a}{2} - \frac{E(z)}{1-\nu^2(z)} \right) \exp(-sz) \right.$$

$$\left. + \frac{s}{2}\int_0^{+\infty} \frac{E(\zeta)}{1-\nu^2(\zeta)} \exp\left(-s\left(\zeta + |z-\zeta|\right)\right) d\zeta \right)$$

$$-\frac{\overline{q}}{a}\left(\left(\frac{a}{2} + \frac{E(z)}{1-\nu^2(z)} \right) \exp(-sz) \right.$$

$$\left. - \frac{s}{2}\int_0^{+\infty} \frac{E(\zeta)}{1-\nu^2(\zeta)} \exp\left(-s\left(\zeta + |z-\zeta|\right)\right) d\zeta \right)$$

$$+\frac{s}{2a}\int_0^{+\infty} \frac{c\exp(-s\zeta) + a\left(1-\nu(\zeta)\right)\alpha(\zeta)\overline{T}(\zeta)}{1-\nu^2(\zeta)}$$

$$\times \exp\left(-s\,|z-\zeta|\right) d\zeta \qquad (4.8.14)$$

$$-\frac{\alpha(z)E(z)}{1-\nu(z)}\overline{T}(z) - \frac{c}{a}\frac{E(z)\exp(-sz)}{1-\nu^2(z)}\,,$$

$$\bar{\sigma}_{\varphi\varphi}(z)=\left(-\frac{\bar{p}+\bar{q}+c}{a}\exp(-sz)\right.$$

$$\left.-\alpha(z)\frac{1+\nu(z)}{\nu(z)}\bar{T}(z)\right)\frac{\nu(z)E(z)}{1-\nu^2(z)},$$

$$\bar{\sigma}_{rz}(z)=-\frac{\bar{p}}{2}\left(\exp(-sz)\right.$$

$$\left.+\frac{s}{a}\int_0^{+\infty}\frac{E(\zeta)}{1-\nu^2(\zeta)}\exp\left(-s\left(\zeta+|z-\zeta|\right)\right)\operatorname{sgn}(z-\zeta)d\zeta\right)$$

$$+\frac{\bar{q}}{2}\left(\exp(-sz)\right.$$

$$\left.-\frac{s}{a}\int_0^{+\infty}\frac{E(\zeta)}{1-\nu^2(\zeta)}\exp\left(-s\left(\zeta+|z-\zeta|\right)\right)\operatorname{sgn}(z-\zeta)d\zeta\right.$$

$$\left.-\frac{s}{2a}\int_0^{+\infty}\frac{c\exp(-s\zeta)+a\left(1-\nu(\zeta)\right)\alpha(\zeta)\bar{T}(\zeta)}{1-\nu^2(\zeta)}\right.$$

$$\left.\times\exp\left(-s\,|z-\zeta|\right)\operatorname{sgn}(z-\zeta)d\zeta\right),$$

where

$$a=s\int_0^{+\infty}\frac{E(z)}{1-\nu^2(z)}\exp\left(-2sz\right)dz,$$

$$c=-s\int_0^{+\infty}\frac{\alpha(z)E(z)}{1-\nu(z)}\bar{T}(z)\exp\left(-sz\right)dz \tag{4.8.15}$$

and the Young modulus and Poisson ratio are related via (4.8.11) or (4.8.12).

It is important to note however that in view of expression (4.8.11), the Young modulus breaks the lower limit set in (4.8.13) for $z\to+\infty$, due to

the fact that the Poisson ratio is limited in terms of variability, and thus $E(z) \underset{z\to+\infty}{\to} 0$. However, if we focus on the local near-boundary effects in an inhomogeneous elastic half-space, then the assumption of Gibson soil (as represented by (4.8.11)) can be accounted for in the analysis of elastic and thermoelastic properties.

Consider, for example, the case of constant Poisson's ratio $\nu(z) = \nu_0 = \text{const}$ and introduce a constant $E_0 = 2(1+\nu_0)G_0$. Under these assumptions and within the context of equation (4.8.11), the Young modulus takes the following form:

$$E(z) = \frac{E_0}{1 + a_0 z}. \tag{4.8.16}$$

If $a_0 = 0$ in equation (4.8.16), then only the inhomogeneity in the material is affected by the coefficient of linear thermal expansion, while all the other material moduli are constant.

Figure 4.4 illustrates the effect of this type of inhomogeneity in the axial stress, when the limiting surface $z = 0$ of half-space $\mathcal{A}_1$ suffers from the action of locally-uniform normal pressure (4.1.6), where

$$p(\rho) = \begin{cases} p_0, \rho \le 1, \\ 0, \rho > 1, \end{cases} \qquad q(\rho) = 0 \tag{4.8.17}$$

at a temperature of zero $T(\rho, z) = 0$. Here, p_0 is a constant in the dimension of stresses. Due to the absence of temperature, the effect of the linear thermal expansion coefficient is disregarded, such that setting $a_0 = 0$ in (4.8.16) means that the material is homogeneous. As seen in Figure 4.4, material inhomogeneity in this case has only a quantitative impact, while the qualitative behavior of stresses remains similar.

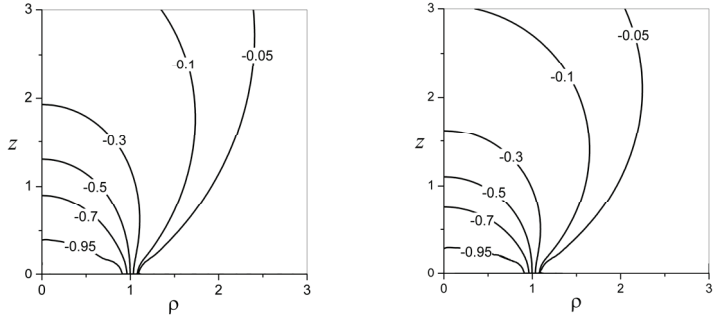

a) *b)*

Figure 4.4. Full-field distributions of axial stress σ_{zz} / p_0 in half-space computed using (4.8.14) and (4.2.17) for loading (4.8.17) and Young's modulus (4.8.16) for *a)* $a_0 = 0$ (homogeneous material) and *b)* $a_0 = 1$ (inhomogeneous material)

The validity of assumption (4.8.1) in the case of inhomogeneous elastic layer $\mathcal{A}_2$ implies that $G_0 > 0$ and $|a_0| < 1$. Thus, the conditions presented in (4.8.11) – (4.8.13) hold for the full range of axial coordinates within $[-1,1]$. The stress-tensor components in this case take the form given in (4.5.20) and (4.5.22) with coefficients represented using (4.5.19) as follows:

$$P_1(z) = \frac{1}{s\gamma_0}\big(I_c \sinh s(1+z)$$

$$-I_0 \sinh s(1-z) - I_s \cosh s(1-z)\big)\frac{E(z)}{1-\nu(z)},$$

$$P_2(z) = \frac{1}{s\gamma_0}\big(I_c \sinh s(1-z)$$

$$-I_0 \sinh s(1+z) + I_s \cosh s(1-z)\big)\frac{E(z)}{1-\nu(z)},$$

$$Q_1(z)=\frac{1}{s\gamma_0}\big(I_s\sinh s(1+z)$$

$$-I_c\cosh s(1+z)+I_0\cosh s(1+z)\big)\frac{E(z)}{1-\nu(z)}, \tag{4.8.18}$$

$$Q_2(z)=\frac{1}{s\gamma_0}\big(I_s\sinh s(1-z)$$

$$+I_c\cosh s(1-z)-I_0\cosh s(1+z)\big)\frac{E(z)}{1-\nu(z)},$$

$$\mathrm{T}(z)=\frac{E(z)}{1-\nu(z)}\Bigg(2\alpha(z)\overline{T}(z)$$

$$-\frac{1}{\gamma_0}\int_{-1}^{1}\frac{\alpha(\zeta)E(\zeta)\overline{T}(\zeta)}{1-\nu(\zeta)}\big(I_s\sinh s(\zeta+z)$$

$$-I_c\cosh s(\zeta+z)+I_0\cosh s(\zeta+z)\big)d\zeta\Bigg),$$

where

$$I_s=G_0\int_{-1}^{1}\frac{E(z)\sinh 2sz}{1-\nu(z)}dz,$$

$$I_c=G_0\int_{-1}^{1}\frac{E(z)\cosh 2sz}{1-\nu(z)}dz, \tag{4.8.19}$$

$$I_0=G_0\int_{-1}^{1}\frac{E(z)}{1-\nu(z)}dz,\qquad \gamma_0=I_0^2+I_s^2-I_c^2.$$

Let us consider the case where (4.8.1) does not hold. Assume that the material properties of half-space $\mathcal{A}_1$ are given in the following form:

$$E(z) = E_0\left(1 + \mu_1 \exp(-\mu_0 z)\right),$$
$$G(z) = G_0\left(1 + \mu_1 \exp(-\mu_0 z)\right), \quad \nu(z) = \nu_0 = 0.3. \tag{4.8.20}$$

Here, $G_0 = E_0/(2 + 2\nu_0)$ and $\mu_1 > -1$ and $\mu_0 \geq 0$ are dimensionless parameters. The material properties in (4.8.20) represent the case where the deposit of the half-space, which is distant from its surface $z = 0$, is homogeneous in terms of a constant Young's modulus and shear modulus (i.e., E_0 and G_0). When approaching the surface $z = 0$, elastic moduli (4.8.20) increase to their maximum values at $\mu_1 > 0$, or decrease to the minimum at the surface where $\mu_1 < 0$. Parameter μ_0 describes the growth (decrement) value of the elastic moduli when approaching the surface. When $\mu_0 = \mu_1 = 0$, half-space $\mathcal{A}_1$ is homogeneous. If we assume that the half-space is loaded with local pressure (4.8.17) at zero temperature, then keeping only three terms in the series (4.4.11) makes it possible to compute the stresses within 0.1%. The effect of inhomogeneity in the axial and radial stresses is illustrated in Fig. 4.5 (see [289] for more detail).

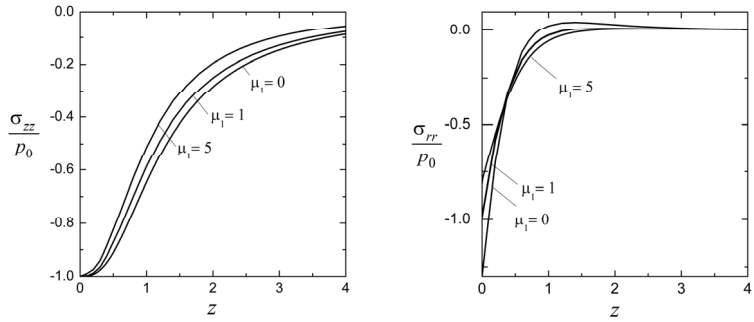

a) *b*)

Figure 4.5. Depth variation of the axial (*a*) and radial (*b*) stresses on symmetry axis $\rho = 0$ of elastic half-space $\mathcal{A}_1$ due to force loading (4.8.18) when $\mu_0 = 1$ and $\mu_1 = 0;1;5$ in (4.8.20) (adapted from our paper [303])

To verify the accuracy of the proposed solution, we consider the computation of stresses in elastic layer $\mathcal{A}_2$ in which the Young modulus

and shear modulus are exponential functions of the thickness coordinate and Poisson's ratio is constant:

$$\frac{E(z)}{E_0} = \frac{G(z)}{G_0} = \exp(\kappa z), \quad \nu(z) = \nu_0 = 0.3 . \tag{4.8.21}$$

Here, $G_0 = E_0 / (2 + 2\nu_0)$ and κ is a real number. When we disregard the effects of temperature, the case where $\kappa = 0$ in (4.8.21) corresponds to a homogeneous material. Then formulae (4.5.20) and (4.5.22) do not involve the resolvent kernel and present the exact solution to the problem.

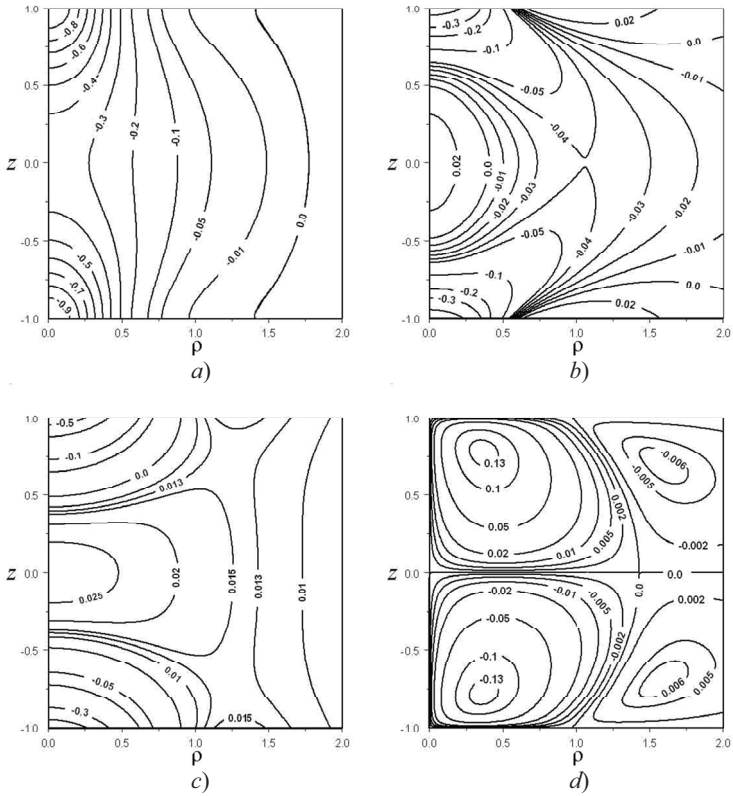

Figure 4.6. Full-field distributions of dimensionless *a*) axial, *b*) radial, *c*) circumferential, and *d*) shear stresses due to force loading (4.8.22), normalized by p_0 in homogeneous layer, when $\kappa = 0$ in (4.8.21) (adapted from our paper [303])

In Fig. 4.6, the full-field distributions of the dimensionless stress-tensor components due to the force loading (4.1.7), where

$$p_1(\rho) = p_2(\rho) = p_0 \exp(-m\rho^2), \quad q_1(\rho) = q_2(\rho) = 0\,, \qquad (4.8.22)$$

components in homogeneous ($\kappa = 0$) layer $\mathcal{A}_2$ are depicted. Due to the locally-distributed loading (4.8.22), the stress fields are local in character, gradually vanishing with an increase in the radial coordinate. Due to the equality of the non-zero normal tractions $p_1 = p_2$ and the homogeneity of the material, normal stresses are symmetric about the mid-plane $z = 0$ and attain the maximum negative values on boundaries $z = \pm 1$ at the central point $\rho = 0$. Axial stress (*a*) precisely satisfies the boundary conditions (4.1.7) with the normal tractions represented by (4.8.22). The stress is compressive within the zone of distribution $\rho < 2$ and vanishes beyond this zone. Radial stress (*b*) is positive in the central area $\rho < 1/2$ and $|z| < 1/2$ and is negative for the same range of ρ when $1/2 < |z| \le 1$. This stress is also positive in the near-surface area for $1/2 < \rho < 3$. Circumferential stress (*c*) is negative in the near-surface area $1/2 < |z| \le 1$, $\rho < 0.8$ and positive elsewhere. Shear stress (*d*) is antisymmetric about the mid-plane $z = 0$ and reaches its maximum values in the regions $0.36 < \rho < 0.38$ and $0.76 < |z| < 0.78$. This stress exactly satisfies the homogeneous boundary conditions given in (4.1.7) and (4.8.22).

Under the assumption of elastic moduli in the form of (4.8.21), it is possible to construct a closed-form analytical solution even for $\kappa \neq 0$ [303]. If we substitute the material properties (4.8.21) into (4.5.18) and (4.5.19) and eliminate total stress, we derive the following fourth-order ordinary differential equation for axial stress:

$$\frac{d^4\overline{\sigma}_{zz}(z)}{dz^4} - 2\kappa\left(\frac{d^3\overline{\sigma}_{zz}(z)}{dz^3} - s^2\frac{d\overline{\sigma}_{zz}(z)}{dz}\right)$$

$$+\left(\kappa^2 - 2s^2\right)\frac{d^2\overline{\sigma}_{zz}(z)}{dz^2} + s^2\left(\frac{\kappa^2\nu_0}{1-\nu_0} + s^2\right)\overline{\sigma}_{zz}(z) = 0\,. \qquad (4.8.23)$$

A solution to this equation for layer $\mathcal{A}_2$ can be found in the following form:

$$\overline{\sigma}_{zz}(z) = \sum_{\ell=1}^{4} C_\ell \exp(\vartheta_\ell z), \tag{4.8.24}$$

where ϑ_ℓ are the roots of the characteristic equation

$$\vartheta^4 + \left(\kappa^2 - 2s^2\right)\vartheta^2 - 2\kappa\left(\vartheta^3 - s^2\vartheta\right) + s^2\left(\frac{\nu_0\kappa}{1-\nu_0} + s^2\right) = 0\,. \tag{4.8.25}$$

These roots can be presented as follows:

$$\begin{aligned}
\vartheta_1 &= \frac{1}{2}\left(\kappa + \sqrt{\kappa^2 + 4s^2 + 4is\kappa\sqrt{\frac{\nu_0}{1-\nu_0}}}\right),\\
\vartheta_2 &= \frac{1}{2}\left(\kappa + \sqrt{\kappa^2 + 4s^2 - 4is\kappa\sqrt{\frac{\nu_0}{1-\nu_0}}}\right),\\
\vartheta_3 &= \frac{1}{2}\left(\kappa - \sqrt{\kappa^2 + 4s^2 + 4is\kappa\sqrt{\frac{\nu_0}{1-\nu_0}}}\right),\\
\vartheta_4 &= \frac{1}{2}\left(\kappa - \sqrt{\kappa^2 + 4s^2 - 4is\kappa\sqrt{\frac{\nu_0}{1-\nu_0}}}\right).
\end{aligned} \tag{4.8.26}$$

Constants of integration C_ℓ can be determined by inserting (4.8.24) into boundary conditions (4.1.7) and (4.8.22).

The axial stress computed using formulae (4.8.23) and (4.2.17) for $\kappa = 0$ (homogeneous material) and $\kappa = 1$ (inhomogeneous material) at $\rho = 0$ is depicted in Fig. 4.7. Qualitatively, distribution of this stress-tensor component is similar for both cases; however, axial stress in not symmetric around the plane $z = 0$ in the case where $\kappa = 1$ due to inhomogeneity. The same conclusion holds for all the stress-tensor components.

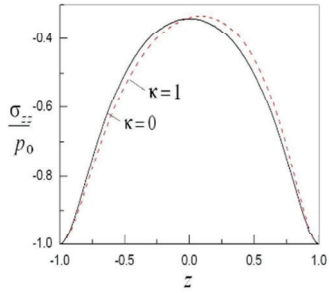

Fig 4.7. Distributions of axial stress across layer at $\rho = 0$ for $\kappa = 0$ and $\kappa = 1$ in (4.8.21) (adapted from our paper [301])

Table 4.1. Comparison of solution (4.5.11) computed for approximate resolvent kernel (4.5.14) with three initial terms and the exact solution (4.8.24) for exponentially-inhomogeneous material (4.8.21) [303]

z	Solution (4.8.24)	Solution (4.5.11)	ε (%)
-0.9	-0.833	-0.842	1.13
-0.5	-0.537	-0.550	2.47
0	-0.337	-0.339	0.39
0.5	-0.459	-0.457	0.41
0.9	-0.781	-0.763	2.23

To verify solution (4.5.18) for the case of inhomogeneous material (i.e., (4.8.21)) where $\kappa = 1$, we compare it with the exact solution represented in (4.8.24). For the material properties (4.8.21), the kernel (4.5.11) takes the following form:

$$\mathcal{K}(z,\zeta) = -\frac{\kappa^2 \exp(\kappa z)}{1-\nu_0}\left(\frac{\exp(\kappa z)-\exp(\kappa\zeta)}{2\kappa}\cosh s(z-\zeta)\right.$$

$$+\frac{\exp(-(\kappa+2s)z)-\exp(-(\kappa+2s)\zeta)}{4(\kappa+2s)}\exp(s(z+\zeta))$$

$$\left.-\frac{\exp(-(\kappa-2s)z)-\exp(-(\kappa-2s)\zeta)}{4(\kappa-2s)}\exp(-s(z+\zeta))\right). \qquad (4.8.27)$$

This expression can be used to compute recurring kernels (4.5.15) and use the truncated series (4.5.14) in order to compute the resolvent-kernel at a satisfactory level of accuracy. Table 4.1 presents values of stress σ_{zz} / p_0 calculated for $\kappa = 1$ at $\rho = 0$ using exact solution (4.8.24). It also presents the resolvent solution given in (4.5.11) with resolvent kernel (4.5.14) containing three ($N = 3$) constituents computed using the first iterative kernel (4.8.27). Clearly, the three terms in (4.5.14) are enough to compute the axial stress within 2.5% of relative error. Using four terms reduced the error to within 1 %. This kind of convergence can be explained using the theory of Volterra integral equations of the second kind. According to this theory, a resolvent-kernel solution can be constructed using Picard's successive approximation method. The efficiency of this method depends strongly on the initial approximation, which, in our case, is the solution of the original integral equation with $\mathcal{K}(z,\zeta) \equiv 0$.

In Fig. 4.8 [303], the distribution of axial stress in layer $\mathcal{A}_2$ can be attributed to force loading (4.1.7) and (4.8.22) based on the following elastic moduli:

$$\frac{E(z)}{E_0} = \frac{G(z)}{G_0} = (2+z)^{-\kappa},$$

$$\nu(z) = \nu_0 = 0.3, \quad G_0 = \frac{E_0}{2(1+\nu_0)}, \tag{4.8.28}$$

where $\kappa = 0;1;2$ at $\rho = 0$ versus thickness coordinate z. In the case where $\kappa = 2$, stress is computed by setting $N = 4$ in formula (4.5.14). From a qualitative perspective, behavior of the stress is similar to the above case. For a homogeneous material ($\kappa = 0$), stress is symmetric about the mid-plane $z = 0$. Decreasing κ moves the local minimum (which is at $z = 0$ for homogeneous material) of the compressive axial stress in the direction of increment of the Young and shearing moduli (see Fig. 2). At the same time, the absolute value of local minimum of this stress decreases slightly with an increase in κ.

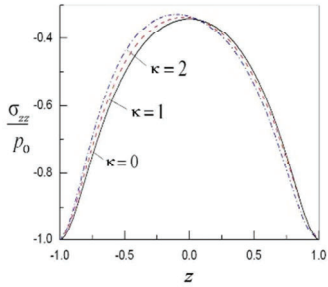

Fig. 4.8. Distributions of axial stresses across layer at $\rho = 0$ for $\kappa = 0;1;2$ in (4.8.28) (adapted from our paper [303])

Let us consider the computation of temperature and thermal stresses in inhomogeneous layer $\mathcal{A}_2$ with the following properties:

$$\frac{E(z)}{E_0} = \frac{G(z)}{G_0} = (2+z)^{l_1}, \ \frac{\alpha(z)}{\alpha_0} = (2+z)^{l_2}, \\ \frac{\lambda(z)}{\lambda_0} = \exp(kz), \quad \nu(z) = \nu_0 = 0.3, \tag{4.8.29}$$

where $G_0 = E_0 / (2+\nu_0)$, l_1, l_2, and k are real numbers and E_0, α_0, and λ_0 are constants of corresponding dimensions. The layer is free of force loadings, as follows:

$$p_1(\rho) = p_2(\rho) = q_1(\rho) = q_2(\rho) = 0. \tag{4.8.30}$$

It is also subjected to local heating, as follows:

$$T(\rho, h) = T_1(\rho), \ T(\rho, -h) = T_2(\rho), \\ T_1(\rho) = T_2(\rho) = t_0 \varphi \exp(-m\rho^2), \tag{4.8.31}$$

where t_0 is a constant in the temperature dimension and m is a positive real number.

Full-field distribution of dimensionless temperature $T(\rho, z)/t_0$ computed using (4.2.17) and (4.7.13) for $k = 0$ in (4.8.29) is shown in

Fig. 4.9. In this case, the temperature is symmetric about mid-plane $z = 0$ and reaches its maximum on the limiting surface.

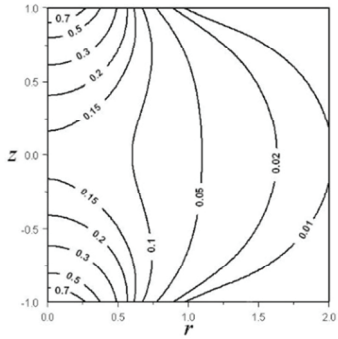

Fig 4.9. Full-field distribution of dimensionless temperature T / t_0 computed using formula (4.7.13) for homogeneous layer subjected to local heating (4.8.31) (adapted from our paper [303])

The effect of material inhomogeneity ($k \neq 0$) on temperature is illustrated in Fig. 4.10. Clearly, increases in parameter k shift the local minimum with coordinates $(0, z_{\min})$ towards the side $z = -1$ ($z_{\min} = -0.11$ for $k = 1$ and $z_{\min} = -0.22$ for $k = 2$), which can be explained by the fact that the heat-conductivity is lower for a lower value of z. It is also clear that the local minimum is slightly greater for $k = 1, 2$ than for $k = 0$. The maximum deviation is within 1 % for $k = 1$ and 8 % for $k = 2$.

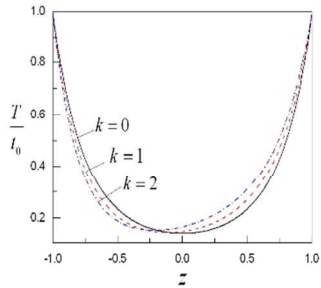

Fig. 4.10. Distribution of dimensionless temperature field T / t_0 at $\rho = 0$ as a function of the value of parameter k in (4.8.29) (adapted from our paper [303])

Note that in the case where $l_1 = l_2 = k = 0$ in (4.8.29), the harmonic temperature field (4.7.13) does not induce thermal stresses (see, e.g., [145]) in the layer with free limiting planes, as established by conditions (4.8.30). However, if l_2 or k in (4.8.29) are not zero, then the stresses occur necessarily.

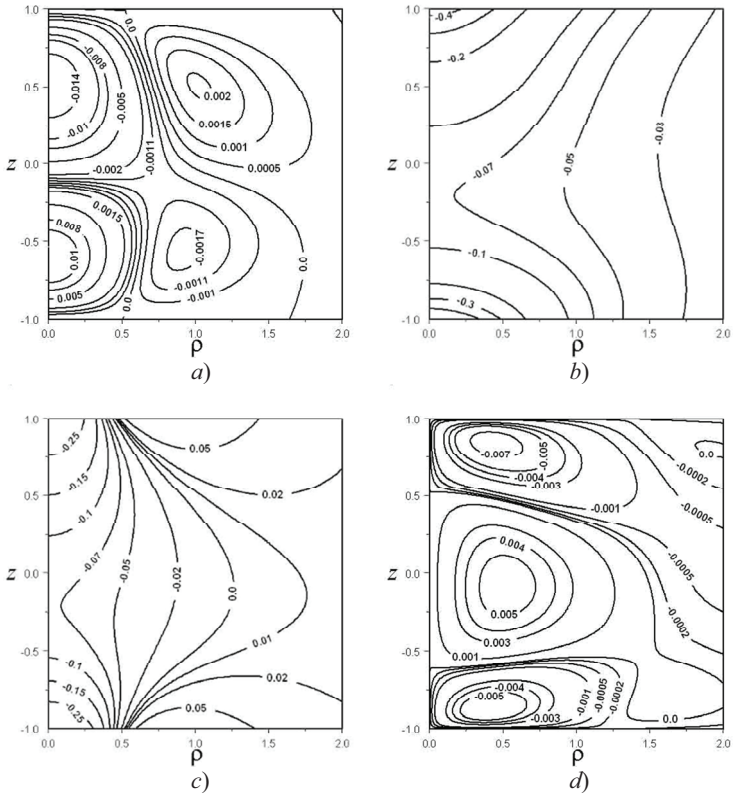

Fig. 4.11. Full-field distributions of dimensionless stresses *a)* $\sigma_{zz}/(\alpha_0 E_0 t_0)$, *b)* $\sigma_{rr}/(\alpha_0 E_0 t_0)$, c) $\sigma_{\varphi\varphi}/(\alpha_0 E_0 t_0)$, *d)* $\sigma_{rz}/(\alpha_0 E_0 t_0)$ due to the temperature field (4.7.13) under the effects of thermal loading (4.8.31) in layer with material properties (4.8.30), where $l_1 = l_2 = 0,\ k = 1$ (adapted from our paper [303])

Figure 4.11 presents the full-field distributions of the dimensionless thermal stresses computed for the case where $l_1 = l_2 = 0,\ k = 1$. The

normal stresses change from tensile to compressive as a function of thickness due to variations in the linear coefficient of thermal expansion. Note that the maximum radial and circumferential stresses are ten orders of magnitude higher than the maximum axial and shear stresses.

Thus, the direct integration method can be used to reduce problems of elasticity and thermoelasticity to two governing equations pertaining to total and axial stresses. These equations can be derived from the compatibility equations and the relations connecting the stress-tensor components (obtained through the integration of equilibrium equations). The governing equations are then reduced to the solution of an integral equation of the second kind with accompanying integral conditions. We use the resolvent-kernel technique to suggest an explicit functional solution to the latter equation. Note that the resolvent kernel is expressed only in terms of material properties; i.e., it does not depend on the loading factors. The resolvent kernel is presented using an infinite series of kernels, which can be truncated to provide an approximate formula for practical computation. Sufficient accuracy can be achieved using even a small number of summands. The efficiency of this approach depends on the selection of the initial kernel. If the shear modulus is inversely proportional to a linear function, then the kernel of the integral equation is equal to zero and, such that solution appears to be an exact analytical solution.

The fact that the solution is given in the form of explicit analytical expressions through the given boundary tractions makes it possible to establish a one-to-one relationship between the tractions and the boundary displacements for an arbitrarily inhomogeneous layer. This makes it possible to apply the proposed solution procedure to the analysis of various types of boundary condition involving stresses, displacements, or a combination of the two.

BIBLIOGRAPHY

1. **Abovski NP, Andreyev NP, and Deruga AP** (1978) *Variational Principles in Elasticity and Shell Theory*. Moscow: Nauka [in Russian].
2. **Agmon S, Douglis A, and Nirenberg L** (1964) Estimates near the boundary for solutions of elliptic partial differential equations satisfying general boundary conditions II. *Communications on Pure and Applied Mathematics* **17**(1), 35–92.
3. **Aichi K** (1922) On the transversal seismic waves travelling upon the surface of heterogeneous material. *Proceedings of the Physico-Mathematical Society of Japan. 3rd Series* **4**(4–5), 137–142.
4. **Aizikovich SM** (1992) An asymptotic solution of one class of dual equations for large values of the parameter. *Soviet Mathematics Doklady* **44**(1), 252–256.
5. **Aizikovich SM, Alexandrov VM, Kalker JJ, Krenev LI, and Trubchik IS** (2002) Analytical solution of the spherical indentation problem for a half-space with gradient with the depth elastic properties," *International Journal of Solids and Structures* **39**(10), 2745–2772.
6. **Aizikovich S, Krenev L, Sevostianov I, Trubchik I, and Evich L** (2011) Evaluation of the elastic properties of a functionally-graded coating from the indentation measurements. *Zeitschrift für Angewandte Mathematik und Mechanik* **91**(6), 493–515.
7. **Aizikovich SM, Krenev LI, and Trubchik IS** (2000) Asymptotic analysis of the indentation of a half-space with depth-varying properties by a sphere. *Mechanics of Solids* **35**(5), 87–96.
8. **Aizikovich SM and Vasiliev AS** (2013) A bilateral asymptotic method of solving the integral equation of the contact problem of the Torsion of an elastic half-space inhomogeneous in depth. *Journal of Applied Mathematics and Mechanics* **77,** 91–97.
9. **Aizikovich S, Vasiliev A, and Seleznev N** (2010) Inverse analysis for evaluation of the shear modulus of inhomogeneous media by torsion experiments. *International Journal of Engineering Science* **48**, 936–942.

10. **Akazawa T** (1943) New test method for evaluating internal stress due to compression of concrete (the splitting tension test) (part 1). *Journal of Japanese Civil Engineering Institute* **29**, 777–787.
11. **Alshits VI and Kirchner HOK** (2001) Cylindrically anisotropic, radially inhomogeneous elastic materials. *Proceedings of the Royal Society of London A* **457**, 671–693.
12. **Ambatsumyan SA** (1970) *Theory of Anisotropic Plates. Strength, Stability, and Vibration.* Stamfort: Technomic.
13. **Andrianov IV and Awrejcewicz J** (2002) A comment on the problem of elasticity. *Facta Universitatis* **3**(12), 475–478.
14. **Andrianov IV and Awrejcewicz J** (2003) Compatibility equations in the theory of elasticity. *Journal of Vibration and Acoustics* **125**(2). 244–245.
15. **Andrianov IV, Shevchenko VV, and Kholod EG** (1995) Asymptotic methods in the statics and dynamics of perforated plates and shells with periodic structures. *Technische Mechanik* **15**(2), 141 – 157.
16. **Arai Y, Kobayashi K, and Tamura M** (1991) Elastic–plastic thermal stresses analysis for optimum design of FGM. In *Proceedings of Fourth National Symposium on Functionally Gradient Materials (FGM'91)*, Kawasaki, pp. 19–30.
17. **Arsenin VI** (1968) Basic Equations and Special Functions of Mathematical Physics. London: Iliffe.
18. **Awaji H and Sivakumar R** (2001) Temperature and stress distributions in a hollow cylinder of functionally graded material: the case of temperature-independent material properties. *Journal of the American Ceramic Society* **84**(5), 1059–1065.
19. **Awojobi AO** (1972) Vertical vibration of a rigid circular foundation on Gibson soil. *Géotechnique* **22**(2), 333–343.
20. **Awojobi AO** (1974) The invariance of Gibson's law for a stratum on a frictionless base. *Géotechnique* **24**(3), 359–366.
21. **Awojobi AO** (1975) The settlement of a foundation on Gibson soil of the second kind. *Géotechnique* **25**(2), 221–228.
22. **Awojobi AO and Gibson RE** (1973) Plane strain and axially symmetric problems of a linearly nonhomogeneous elastic half-space. *The Quarterly Journal of Mechanics and Applied Mathematics* **26**(3), 285–302.
23. **Babich VM** (1961) Fundamental solutions of the dynamical equations of elasticity for nonhomogeneous media. *Journal of Applied Mathematics and Mechanics* **25**(1), 49–60.

24. **Babich VM** (1960) Fundamental solutions of hyperbolic equations with variable coefficients. *Matematicheskiy Sbornik* **52**(2), 709–738 [in Russian].
25. **Bakhvalov N and Panasenko G** (1989) *Homogenization: Averaging Processes in Periodic Media. Mathematical Problems in Mechanics of Composite Materials*. Dordrecht: Kluwert Academic Publishers.
26. **Barber JR** (2010) *Elasticity*, Dordrecht: Springer.
27. **Bartoshevich MA** (1975) A heat-conduction problem. *Journal of Engineering Physics and Thermophysics* **28**(2), 240–244.
28. **Belik GI and Protsenko VS** (1967) The contact problem of a half-plane for which the modulus of elasticity of the material is expressed by a power function of the depth. *International Applied Mechanics* **3**(6), 80–82.
29. **Belik VD, Uryukov BA, Frolov GA, and Tkachenko GV** (2008) Numerical-analytical method of solution of a nonlinear unsteady heat-conduction equation. *Journal of Engineering Physics and Thermophysics* **81**(6), 1099–1103.
30. **Berdichevsky VL** (1983) *Variational Principles of the Continuum Mechanics*. Moscow: Nauka. [in Russian].
31. **Bert CW** (1968) Comments on "A note to the general solution of the two-dimensional linear elasticity problem in polar coordinates". *AIAA Journal* **6**(3).
32. **Bezukhov NI and Louzhin OV** (1974) *Application of Methods of Elasticity and Plasticity Theory to Solution of Engineering Problems*. Moscow: Vysshaya Shkola [in Russian].
33. **Birman V and Byrd LW** (2007) Modeling and analysis of functionally graded materials and structures. *Applied Mechanics Reviews* **60**(5), 195–216.
34. **Bois PA** (2007) Joseph Boussinesq (1842–1929): a pioneer of mechanical modelling at the end of the 19th century. *Comptes Rendus Mécanique* 335, 479–495.
35. **Bolotin VV, Goldenblat II, and Smirnov AF** (1972) *Structural Mechanics: State-of-Art and Development Perspectives*. Moscow: Stroyizdat [in Russian].
36. **Bolotin VV and Novichkov YN** (1980) *Mechanics of Multilayer Structures*. Moscow: Mashinostroenie [in Russian].
37. **Borodachev NM** (1995) Three-dimensional elasticity-theory problem in terms of the stress. *International Applied Mechanics* **31**(12), 991–996.

38. **Brown PT and Gibson RE** (1973) Rectangular loads on inhomogeneous elastic soil. *Journal of the Soil Mechanics and Foundation Division* **99**, 917–920.
39. **Brown PT and Gibson RE** (1979) Surface settlement of a finite elastic layer whose modulus increases linearly with depth. *International Journal for Numerical and Analytical Methods in Geomechanics* **3**(1), 37–47.
40. **Bryant Moodie T** (1973) Elastic waves in a nonhomogeneous medium – a high-frequency approximation involving turning points. *The Quarterly Journal of Mechanics and Applied Mathematics* **26**(3), 265–284.
41. **Brychkov YA and Prudnikov AP** (1989) Integral transforms of generalized functions. New York : Gordon and Breach Science Publishers
42. **Burmister DM** (1945) The general theory of stresses and displacements in layered systems. I. *Journal of Applied Physics* **16**, 89–94.
43. **Burmister DM** (1945). The general theory of stresses and displacements in layered soil systems. II. *Journal of Applied Physics* **16**, 126–127.
44. **Burmister DM** (1945) The general theory of stresses and displacements in layered soil systems. III. *Journal of Applied Physics* **16**, 296–302.
45. **Carneiro F** (1943) A new method to determine the tensile strength of concrete. In *Proceedings of the 5th Meeting of the Brazilian Association for Technical Rules*, Sao Paulo, Brazil, September 16, The Brazilian Association of Technical Norms (ABNT), pp. 126–129.
46. **Carrier WD and Christian JT** (1973) Rigid circular plate resting on a non-homogeneous elastic half-space. *Géotechnique* **23**(1), 67–84.
47. **Caviglia G and Morro A** (1991) Wave propagation in inhomogeneous viscoelastic solids. *The Quarterly Journal of Mechanics and Applied Mathematics* **44**(1), 45–54.
48. **Chen P and Chen S** (2013) Thermo-mechanical contact behavior of a finite graded layer under a sliding punch with heat generation. *International Journal of Solids and Structures* **50**(7–8), 1108–1119.
49. **Chernykh KF** (1998) *An Introduction to Modern Anisotropic Elasticity*. New York: Begell House.
50. **Choi HJ and Paulino GH** (2008) Thermoelastic contact mechanics for a flat punch sliding over a graded coating/substrate system with frictional heat generation. *Journal of Mechanics and Physics of Solids* **56**, 1673–1692.

51. **Chou PC and Gordon PF** (1967) Radial propagation of axial shear waves in nonhomogeneous elastic media. *Journal of the Acoustical Society of America* **42**(1), 36–41.
52. **Chou SC and Greif R** (1968) Numerical solution of stress waves in layered media. *AIAA Journal* **6**(6): 1067–1074.
53. **Chou SC, Greif R, and Johnson DE** (1969) Stress-wave propagation in a class of nonhomogeneous elastic media. *AIAA Journal* **7**(9), 1710–1716.
54. **Choules BD and Kokini K** (1996) Architecture of functionally graded ceramic coatings against surface thermal fracture. *Journal of Engineering Materials and Technology* **118**(1), 522–528.
55. **Christensen RM** (1979) *Mechanics of Composite Materials*. New York: Wiley.
56. **Chuaprasert MF and Kassir MK** (1974) Displacements and stresses in nonhomogeneous solid. *Journal of the Engineering Mechanics Division* **100**(5), 861–872.
57. **Chuong TL** (1971) Sur les Contraintes et les Déplacements d'un Semi-Espace non Homogène. *Comptes Rendus Hebdomadaires des Séances de L'Académies des Sciences* **273**(4), 254–257.
58. **Clements DL and Rogers C** (1974) On wave propagation in inhomogeneous elastic media. *International Journal of Solids and Structures* **10**(6), 661–669.
59. **Clements DL and Rogers C** (1978) On the Bergman operator method and anti-plane contact problems involving an inhomogeneous half-space. *SIAM Journal of Applied Mathematics* **34**(4), 764–773.
60. **Cournat R and Hilbert D** (1937) *Methoden der Mathematischen Physik.* II. Berlin: Springer Verlag.
61. **Courant R and Lax PD** (1956) The propagation of discontinuities in wave motion. *Proceedings of the National Academy of Sciences of the United States of America* **42**(11), 872–876.
62. **Cristescu ND, Craciun EM, and Soós E** (2004) *Mechanics of Elastic Composites*. New York: Chapman & Hall / CRC.
63. **Dai HL, Rao YN and Dai T** (2016) A review of recent researches on FGM cylindrical structures under coupled physical interactions, 2000–2015. *Composite Structures* **152**, 199–225.
64. **Domke K and Hącia L** (2007) Integral equations in some thermal problems. *International Journal of Mathematics and Computers IN Simulation* **1**(2), 184–188.
65. **Duan ZP, Eischen JW, and Herrmann G** (1986) Harmonic wave propagation in nonhomogeneous layered composites. *Journal of Applied Mechanics Transactions of ASME* **53**(1), 108–115.

66. **El-Naggar AM, Abd-Alla AM, Fahmy MA, and Ahmed SM** (2002) Thermal stresses in a rotating non-homogeneous orthotropic hollow cylinder. *Heat and Mass Transfer* **39**, 41–46.
67. **Ewing WM, Jardetzki WS and Press F** (1957) *Elastic Waves in Layered Media*. New York, Toronto, London: McGraw Hill Book Company Inc.
68. **Fedotkin IM, Verlan EV, Chebotaresku ID, and Evtukhovich SV** (1983) Heat conductivity of the adjoining plates with a plane heat source between them. *Journal of Engineering Physics and Thermophysics* **45**(3), 1071–1075.
69. **Fichera G** (1961) Linear elliptic equations of higher order in two independent variables and singular integral equations, with applications to anisotropic inhomogeneous elasticity. In Langer RE (ed), *Partial Differential Equations and Continuum Mechanics*. Madison: Univ. Wisconsin Press, pp. 55–80.
70. **Filonenko-Borodich M** (1959) Theory of Elasticity. Moscow: Fizmatgiz [in Russian]
71. **Filonenko-Borodich M** (1963) Theory of Elasticity. Moscow: Peace Publishers
72. **Föppl A** (1897) Versuche über die Elastizität des Erdbodens. *Zentralblatt der Bauverwaltung* **17**, 276–278.
73. **Frankel JI** (1991) A nonlinear heat transfer problem: solution of nonlinear, weakly singular Volterra integral equations of the second kind. *Engineering Analysis with Boundary Elements* **8**(5), 231–238.
74. **Fröhlich OK** (1934) *Druckverteilung im Baugrunde mit Besonderer Berüksichtigung der Plastischen Erscheinungen*. Wien: Springer.
75. **Furuhashi R** (1972) On the uniqueness and the existence of solution in elastostatic for inhomogeneous materials. *The Japan Society of Mechanical Engineers: Bulletin of the JSME* **15**(83), 657–662.
76. **Furuhashi R** (1972) On Green's function in elastostatics for inhomogeneous materials. *Research Reports of the Faculty of Engineering, Meiji University* (26/27), 11–19.
77. **Furuhashi R and Kataoka M** (1967) On the integral equations of the basic boundary value problems of elasticity of inhomogeneous media. *Transactions of the Japan Society of Mechanical Engineers* **33**(253), 1331–1343.
78. **Furuhashi R and Kataoka M** (1968) Theory of elastic potential of inhomogeneous materials. *The Japan Society of Mechanical Engineers: Bulletin of the JSME* **11**(48), 972–982.

79. **Giannakopoulos AE and Pallot P** (2000) Two-dimensional contact analysis of elastic graded materials. *Journal of Mechanics and Physics of Solids* **48**, 1597–1631.
80. **Gibson RE** (1967) Some results concerning displacements and stresses in a non-homogeneous elastic halfspace. *Géotechnique* **17**, 58–67.
81. **Gibson RE** (1974) Fourteenth Rankine lecture: the analytical method in soil mechanics. *Géotechnique* **24**(2), 115–140.
82. **Gibson RE** (1974) The analytical method in soil mechanics. *Géotechnique* **24**(2), 115–140.
83. **Gibson RE, Brown PT, and Andrews KRF** (1971) Some results concerning displacements in a non-homogeneous elastic layer. *Zeitschrift für Angewandte Mathematik und Physik* **22**(5), 855–864.
84. **Gibson RE and Kalsi GS** (1974) The surface settlement of a linearly inhomogeneous cross-anisotropic elastic half-space. *Zeitschrift für angewandte Mathematik und Physik* **25**(6), 843–847.
85. **Gibson RE and Sills GC** (1969) On the loaded elastic half-space with a depth varying Poisson's ratio. *Zeitschrift für Angewandte Mathematik und Physik* **20**(5), 691–695.
86. **Gibson RE and Sills GC** (1975) Settlement of a strip load on a nonhomogeneous orthotropic incompressible elastic half-space. *The Quarterly Journal of Mechanics and Applied Mathematics* **28**(2), 233–243.
87. **Gibson RF** (2016) *Principles of Composite Material Mechanics*. Boca Raton London New York: CRC Press.
88. **Golecki JJ** (1971) On non-radial stress distribution in non-homogeneous elastic half-plane under concentrated load. *Meccanica* **6**(3), 147–156.
89. **Golecki J** (1968) Elastic half-plane with variable Poisson's ratio. Displacement boundary problems. *Bulletin L'Académie Polonaise des Science, Série des Sciences Techniques* **16**(4), 175–182.
90. **Golecki J and Knops RJ** (1969) Introduction to linear elastoplastics with variable Poisson's ratio. *Zeszyty Naukowe Akademii Górniczo Hutniczej* **30**, 81 – 91.
91. **Gontarovskii VP, Kozlov IA, and Gontarovskaya TN** (1975) Stress and strain calculations on inhomogeneous bodies of rotation by finite-element methods. *Strength of Materials* **7**(8), 991–995.
92. **Gorbachev VI** (1979) Elastic equilibrium of a cylindrical tube with nonuniform thickness under the action of surface loads and displacements. *Strength of Materials* **11**(5), 538–542.

93. **Gorbachev VI and Pobedria BI** (1979) On elastic equilibrium of nonhomogeneous strips. *Mekhanika Tverdogo Tela* **5**, 111–118 [in Russian].
94. **Greif R and Chou SC** (1971) The propagation of radially symmetric stress waves in anisotropic non-homogeneous elastic media. *Journal of Applied Mechanics Transactions of ASME* **38**(1), 51–57.
95. **Grigorenko YM, Grits'ko EG, and Zhuravchak LM** (1995) Application of the method of boundary Elements to the problem of the stressed state of inhomogeneous bodies with allowance for physical nonlinearity. *International Applied Mechanics* **31**(11), 873 – 879.
96. **Grinchenko VT** (1978) *Equilibrium and Steady Vibrations of Finite Elastic Solids*. Kiev: Naukova Dumla [in Russian]
97. **Gryts'ko EH, Gudz' RV, and Zhuravchak LM** (1999) Method of boundary elements and Hermitian finite elements in problems of elasticity for bodies with inhomogeneities. *Materials Science* **35**(5), 716–719.
98. **Guo LC and Noda N** (2007) Modeling method for a crack problem of functionally graded materials with arbitrary properties – piecewise-exponential model. *International Journal of Solids and Structures* **44**, 6768–6790.
99. **Hącia L** (2007) Iterative-collocation method for integral equations of heat conduction problems. *Numerical Methods and Applications, Lecture Notes in Computer Science* **4310**, 378–385.
100. **Hahn D and Özişik MN** (2012) *Heat Conduction*. New Jersey: John Wiley & Sons, Inc.
101. **Hamming RW** (1962) *Numerical Methods for Scientists and Engineers*. New York: McGraw-Hill Book Company.
102. **Han X, Liu GR, Xi ZC, and Lam KY** (2001) Transient waves in a functionally graded cylinder. *International Journal of Solids and Structures* **38**(17), 3021–3037.
103. **Hashin Z** (1964) Theory of mechanical behavior of heterogeneous media. *Applied Mechanics Reviews* **17**(1), 1–9.
104. **Hashin Z** (1983) Analyzis of composite materials – a survey. *Journal of Applied Mechanics* **50**, 481–505.
105. **Hemsley JA** (2016) *Glass in Engineering Science. Vol. 2 Glass under Load*. Chapeltown: Society of Glass Technology.
106. **Hilton HH** (2017) Elastic and viscoelastic Poisson's ratios: the theoretical mechanics perspective. *Materials Sciences and Applications* **8**, 291–332.

107. **Hilton HH** (1952) Thermal stresses in bodies exhibiting temperature-dependent elastic properties. *Journal of Applied Mechanics, Transactions of ASME* **19**, 350–354.
108. **Hook JF** (1961) Separation of the vector wave equation of elasticity for certain types of inhomogeneous, isotropic media. *Journal of the Acoustical Society of America* **33**(3), 302–313.
109. **Hook JF** (1962) Green's function for axially symmetric elastic waves in unbounded inhomogeneous media having constant velocity gradients. *Journal of Applied Mechanics Transactions of ASME* **29**(2), 293–298.
110. **de Hoop MV and de Hoop AT** (1994) Elastic wave up/down decomposition in inhomogeneous and anisotropic media: an operator approach and its approximations. *Wave Motion* **20**(1), 57–82.
111. **Horgan CO and Chan AM** (1999) The pressurized hollow cylinder or disk problem for functionally graded isotropic linearly elastic materials. *Journal of Elasticity* **55**, 43–59.
112. **Horgan CO and Chan AM** (1999) The stress response of functionally graded isotropic linearly elastic rotating disks. *Journal of Elasticity* **55**, 219–230.
113. **Hryts'ko BY** (2017) "Numerical-analytic technique for the solution of nonstationary problems of heat conduction in locally inhomogeneous media. *Journal of Mathematical Sciences*, **226**(1), pp. 41–51.
114. **Hyman BI** (1968) Comment on "A note to the general solution of the two-dimensional linear elasticity problem in polar coordinates. *AIAA Journal* **6**(3), 568–569.
115. **Ilschner B** (1997) Lessons learnt in 7 years of FGM research at Lausanne. In Shiota I and Miyamoto MY (eds), *Functionally Graded Materials 1996*. Amsterdam: Elsevier, pp. 15–20.
116. **Ilyushin AA** (1971) *Basic Directions of the Development in Problems of Durability and Plasticity*. Moscow, Nauka (1971).
117. **Jabbari M, Sohrabpour S, and Eslami MR** (2002) Mechanical and thermal stresses in a functionally graded hollow cylinder due to radially symmetric loads. *International Journal of Pressure Vessels and Piping* **79**, 493–497.
118. **Jabbari M, Sohrabpour S, and Eslami MR** (2003) General solution for mechanical and thermal stresses in a functionally graded hollow cylinder due to nonaxisymmetric steady-state loads. *Journal of Applied Mechanics* **70**, 111–118.

119. **Jasinsky FS** (1904) *Collection of Papers* **3**, St-Petersburg, Izd. Instituta Inzhenerov Putey Soobscheniy Imperatora Aleksandra I [in Russian].
120. **Jeffreys H** (1928) The effect on Love waves of heterogeneity in the lower layer. *Monthly Notices of the Astronomical Society of London. Geophysical Supplement (Geophysical Journal International)* **2**, 101–111.
121. **Jha DK, Kant T, and Singh RK** (2013) A critical review of recent research on functionally graded plates. *Composite Structures* **96**, 883–849.
122. **Jiang L and Haddow JB** (1995) A finite element solution of plane wave propagation in inhomogeneous linear viscoelastic solids. *Journal of Sound and Vibration* **184**(3), 429–438.
123. **Jones RM** (1999) *Mechanics of Composite Materials*. Philadelphia: Taylor & Francisc.
124. **Kalam MA and Tauchert TR** (1978) Stresses in an orthotropic elastic cylinder due to a plane temperature distribution $T(r,\Theta)$. *Journal of Thermal Stresses* **1**, 13–24.
125. **Kalynyak BM** (2000) Integration of equations of one-dimensional problems of elasticity and thermoelasticity for inhomogeneous cylindrical bodies. *Journal of Mathematical Sciences* **99**(5), 1662–1670.
126. **Kalynyak BM, Tokovyy YV, and Yasinskyy AV** (2019) Direct and inverse problems of thermomechanics concerning the optimization and identification of the thermal stressed state of deformed solids. *Journal of Mathematical Sciences* **236**(1), 21–34.
127. **Kashtalyan M and Rushchitsky JJ** (2009) Revisiting displacement functions in three-dimensional elasticity of inhomogeneous media. *International Journal of Solids and Structures* **46**, 3463–3470.
128. **Kassir MK** (1970) The Reissner-Sagoci problem for a non-homogeneous solid. *International Journal of Engineering Science* **8**(10), 875–885.
129. **Kassir MK** (1972) Boussinesq problems for nonhomogeneous solid. *Journal of the Engineering Mechanics Division* **98**(2), 457–470.
130. **Kassir MK** (1974) A note on mixed boundary-value problems in nonhomogeneous elasticity. *Journal of Elasticity* **4**(4), 317–321.
131. **Kassir MK and Chuaprasert MF** (1974) A rigid punch in contact with a nonhomogeneous elastic solid. *Journal of Applied Mechanics Transactions of ASME* **41**(4), 1019–1024.

132. **Kawasaki A and Watanabe R** (2002) Thermal fracture behavior of metal/ceramic functionally graded materials. *Engineering Fracture Mechanics* **69**(14–16), 1713–1728.
133. **Ke LL and Wang YS** (2006) Two-dimensional contact mechanics of functionally graded materials with arbitrary spatial variations of material properties. *International Journal of Solids and Structures* **43**(18–19), 5779–5798.
134. **Khan KA and Hilton** HH (2010) On inconstant Poisson's ratios in non-homogeneous elastic media. *Journal of Thermal Stresses* **33**(1), 29–36.
135. **Kim KS and Noda N** (2001) Green's function approach to three-dimensional heat conduction equation of functionally graded materials. *Journal of Thermal Stresses* **24**(5), 457–477.
136. **Kim KS and Noda N** (2002) Green's function approach to unsteady thermal stresses in an infinite hollow cylinder of functionally graded material. *Acta Mechanica* **156**, 145–161.
137. **Klein GK** (1956) Study of non-homogeneity of discontinuities in deformations and of other mechanical properties of the soil in the design of structures on solid foundations. *Sbornik Trudov Moskovskogo Inzhenerno-stroitelnogo Instituta* **14**, 168–180 [in Russian]
138. **Klimenko NI** (1999) Solution of problems on the stress state of rotating anisotropic hollow cylinders that are nonuniform in the circumferential direction. *International Applied Mechanics* **35**(12), 1246–1253.
139. **Kniazev PN** (1969) *Integral Transforms*. Minsk: Vysheishaya Shkola.
140. **Kogan BI** (1953) Stresses and strains in multilayered coatings, *Trudy Kharkovskogo Automobile-Dorozhnogo Instituta* **14**, 33–46 [in Russian]
141. **Koizumi M** (1997) FGM activities in Japan. *Composites Part B: Engineering* **28**(1–2), 1–4.
142. **Kolchin GB** (1971) *Computation of the Structural Elements from Elastic Nonhomogeneous Materials.* Kishinau: Kartya Moldovenyasce [in Russian].
143. **Korenev BG** (1957) A die resting on an elastic half-space, the modulus of elasticity of which is an exponential function of the depth. *Doklady Akademii Nauk SSSR* **112**(5), 823–826 [in Russian].
144. **Kourkoulis SK and Markides CF** (2014) Stresses and displacements in a circular ring under parabolic diametral

compression. *International Journal of Rock Mechanics and Mining Sciences* **71**, 272–292.
145. **Kovalenko AD** (1969) *Thermoelasticity: Basic Theory and Applications*. Groningen: Wolters-Noordhoff.
146. **Kozák I and Szeidl G** (1997) Complete solution for stresses in terms of stress functions. Part I. Derivation from the principle of virtual work. *Technische Mechanik* **16**(2), 147–168.
147. **Krenev LI, Aizikovich SM, Tokovyy YV, and Wang YC** (2015) Axisymmetric problem on the indentation of a hot circular punch into an arbitrarily nonhomogeneous half-space. *International Journal of Solids and Structures* **59**, 18–28.
148. **Krenev LI, Tokovyy YV, Aizikovich SM, Seleznev NM, and Gorokhov SV** (2016) A numerical-analytical solution to the mixed boundary-value problem of the heat-conduction theory for arbitrarily inhomogeneous coatingsю *International Journal of Thermal Sciences*, **107**, 56–65.
149. **Kupradze VD, Gegelia TG, Basheleishvili MO, and Burchuladze TV** (1979) *Three-Dimensional Problems of the Mathematical Theory of Elasticity and Thermoelasticity*. Amsterdam, Oxford, New York: North-Holland Publishing Company.
150. **Kushnir RM and Popovych VS** (2006) Stressed state of a thermosensitive plate in a central-symmetric temperature field. *Materials Science* **42**(2), 145–154.
151. **Kushnir RM and Popovych VS** (2011) Heat Conduction Problems of Thermosensitive Solids under Complex Heat Exchange. In Vikhrenko VS (ed), *Heat Conduction – Basic Research.* Rijeka: IntechOpen, pp. 131–154.
152. **Kushnir RM, Protsyuk BV, and Synyuta VM** (2002) Temperature stresses and displacements in a multilayer plate with nonlinear conditions of heat exchange. *Materials Science* **38**(6), 798–808.
153. **Lax PD** (1957) Asymptotic solutions of oscillatory initial value problems. *Duke Mathematical Journal* **24**(4), 627–646.
154. **Lekhnitskii SG** (1968) *Anisotropic Plates*. New York: Gordon and Breach.
155. **Lekhnitskii SG** (1962) Radial distribution of stresses in a wedge and in a half-plane with variable modulus of elasticity. *Journal of Applied Mathematics and Mechanics* **26**, 199–206.
156. **Lekhnitskii SG** (1981) *Theory of Elasticity of an Anisotropic Body*. Moscow: Mir Publishers.

157. **Li XF, Peng XL, and Lee KY** (2010) Radially polarized functionally graded piezoelectric hollow cylinders as sensors and actuators. *European Journal of Mechanics A Solids* **29**(4), 413–437.
158. **Liew KM, Kitipornchai S, Zhang XZ, and Lim CW** (2003), "Analysis of the thermal stress behaviour of functionally graded hollow circular cylinders. *International Journal of Solids and Structures* **40**, 2355–2380.
159. **Liu J, Ke LL and Wang YS** (2011) "Thermoelastic contact analysis of functionally graded materials with properties varying exponentially. *Advanced Materials Research* **189-193**, 988–992.
160. **Liu J, Ke LL, Wang YS, Yang J, and Alam F** (2012) "Thermoelastic frictional contact of functionally graded materials with arbitrarily varying properties. *International Journal of Mechanical Sciences* **63,** 86–98.
161. **Lock MH** (1963) Axially symmetric elastic waves in an unbounded inhomogeneous medium with exponentially varying properties. *Bulletin of the Seismological Society of America* **53**(3), pp. 527–538.
162. **Lopatynsky YB** (1953) On a class of reduction of boundary-value problems for a system of differential equations of elliptic type to regular integral equations. *Ukrainian Mathematical Journal* **5**(2), 123–151.
163. **Luciano R and Sacco E** (1998) Variational methods for the homogenization of periodic heterogeneous media. *European Journal of Mechanics A Solids* **17**(4), 599–617.
164. **Lurie SA and Vasiliev VV** (1995) *The Biharmonic Problem in the Theory of Elasticity*. Luxembourg: Gordon and Breach.
165. **Mahamood RM and Akinlabi ET** (2017) Functionally graded materials. In Bergmann CP (ed), *Topics in Mining, Metallurgy and Materials Engineering*. Cham: Springer, 118 p.
166. **Malyi VI** (1986) One representation of the conditions of the compatibility of deformations. *Journal of Applied Mathematics and Mechanics* **50**(5), 679–681.
167. **Mao JJ, Ke LL, and Wang YS** (2014) Thermoelastic contact instability of a functionally graded layer and a homogeneous half-plane. *International Journal of Solids and Structures* **51**(23-24), 3962–3972.
168. **Markworth AJ, Ramesh KS, and Parks WP** (1995) Modelling studies applied to functionally graded materials. *Journal of Materials Science* **30** (9), 2183–2193.
169. **Maugin GA** (1993) *Material Inhomogeneities in Elasticity*. London, Chapman and Hall.

170. **Maxwell JC** (1873) *A Treatise on Electricity and Magnetism*, **1**. Oxford, Clarendon Press.
171. **Meguid SA and Zhu ZH** (1995) A novel finite element for treating inhomogeneous solids. *International Journal for Numerical Methods in Engineering* **38**(9), 1579–1592.
172. **Meissner E** (1921) Elastische Oberflächenwellen mit Dispersion in einem inhomogenen Medium. *Vierteljahrsschrift der Naturforschenden Gesellschaft in Zürich* **66**, 181–195.
173. **Meleshko VV** (2003) Selected topics in the history of the two-dimensional biharmonic problem. *Applied Mechanics Reviews* **56**(1), 33–85.
174. **Meleshko VV** (2005) Superposition method in thermal-stress problems for rectangular plates. *International Applied Mechanics* **41**(9), 1043–1058.
175. **Milne-Thomson LM** (1942) Consistency equations for the stresses in isotropic elastic and plastic materials. *Journal of the London Mathematical Society*. S1 **17**(2), 115–128.
176. **Michell JH** (1899) On the direct determination of stress in an elastic solid, with application to the theory of plates. *Proceedings of the London Mathematical Society* **31**(687), 100–124.
177. **Mikhlin SG** (1947) "Fundamental solutions of dynamic equations of the elasticity theory for nonhomogeneous media. *Prikladnaya Matematika i Mekhanica* **11**(4) 423–432 [in Russian].
178. **Mikhlin SG** (1950) *Direct Methods in Mathematical Physics*. Moscow, Leningrad: Gosudarstvennoye Izdatelstvo Tekhnico-Teoreticheskoy Literatury [in Russian].
179. **Mikhlin SG** (1964) *Variational Methods in Mathematical Physics*. New York: Pergamon Press.
180. **Murakami H** (1985) A mixture theory for wave propagation in angle-ply laminates. Part 1: theory. *Journal of Applied Mechanics* **52**, 331–337.
181. **Mishiku M and Teodosiu K** (1967) Solution of an elastic static plane problem for nonhomogeneous isotropic bodies by means of the theory of complex variables. *Journal of Applied Mathematics and Mechanics* **30**(2), 459–468.
182. **Miyamoto Y, Kaysser WA, Rabin BH, Kawasaki A, and Ford RG** (eds) (1999) *Functionally Graded Materials: Design, Processing and Applications*. New York: Springer.
183. **Miyamoto Y, Niino M, and Koizumi M** (1997) FGM research programs in Japan – from structural to functional uses. In Shiota I

and Miyamoto MY (eds), *Functionally Graded Materials 1996.* Amsterdam: Elsevier, pp. 1–8.

184. **Mortensen A and Suresh S** (1995) Functionally graded metals and metal-ceramic composites: part 1 processing. *International Materials Reviews* **40**(6), 239–265.
185. **Mossakovskii VI** (1958) Pressure of a circular die [punch] on an elastic half-space, whose modulus of elasticity is an exponential function of depth. *Journal of Applied Mathematics and Mechanics* **22**(1), 168–171.
186. **Muskhelishvili NI** (1963) *Some Basic Problems of the Mathematical Theory of Elasticity: Fundamental Equations, Plane Theory of Elasticity, Torsion, and Bending*. Groningen: P. Noordhof.
187. **Murakami H and Akiyama A** (1985) A mixture theory for wave propagation in angle-ply laminates. Part 2: application. *Journal of Applied Mechanics* **52**, 338–344.
188. **Muravskii BG** (2001) *Mechanics of Non-Homogeneous and Anisotropic Foundations*. Berlin: Springer.
189. **Murzewski J** (1959) Elastic-plastic stochastically non-homogeneous bodies. In Olszak W (ed.) *Non-Homogeneity in Elasticity and Plasticity.* New York, Pergamon Press pp. 479–489.
190. **Naebe M and Shirvanimoghaddam K** (2016) Functionally graded materials: a review of fabrication and properties. *Applied Materials Today* **5**, 223–245.
191. **Naumov YA and Chistyak VI** (1975) Solving boundary-value problems of elasticity theory for inhomogeneous layers. *Soviet Applied Mechanics* **11**(5), 522–527.
192. **Naumov YA, Shevlyakov YA, and Chistyak VI** (1970) On solving the fundamental problems of the theory of elasticity for a layer with an arbitrary nonhomogeneity along its thickness. *Soviet Applied Mechanics* **6**(7), 706–711.
193. **Nayfeh AH and Nemat-Naser S** (1972) Elastic waves in inhomogeneous elastic media. *Journal of Applied Mechanics Transactions of ASME* **39**, 696–702.
194. **Nielsen LF** (2005) *Composite Materials. Properties as Influenced by Phase Geometry*. Berlin, Heidelberg: Springer.
195. **Noda N** (1991) Thermal stresses in materials with temperature-dependent properties. *Applied Mechanics Reviews* **44**(9), 383–397.
196. **Noda N** (1999) Thermal stresses in functionally graded materials. *Journal of Thermal Stresses* **22**(4–5), 477–512.
197. **Noda N, Hetnarski RB, and Tanigawa Y** (2000) *Thermal Stresses*. Rochester, New York: Lastran Corp.

198. **Nowacki W** (1962) *Thermoelasticity*. Reading: Addison-Wesley Pub. Co.
199. **Nowacki W** (1977) *Thermal Stresses in Anisotropic Bodies*. In Nowacki W and Sneddon IN (eds), *Thermomechanics in Solids*. Wien: Springer, pp. 27–56.
200. **Nowinski JL** (1978) *Theory of Thermoelasticity with Applications*. Alphen Aan Den Rijn: Sijthoff & Noordhoff International Publishers.
201. **Ohde J** (1939) Zur Theorie der Druckverteilung im Baugrund. *Der Bauingenieur* **20**, 451–459.
202. **Olszak W, Rychlewski J, and Urbanowski W** (1962) Plasticity under non-homogeneous conditions. *Advances in Applied Mechanics* **7**, 131–214.
203. **Olszak W** (ed) (1959) *Non-Homogeneity in Elasticity and Plasticity*. New York: Pergamon Press.
204. **Ootao Y and Tanigawa Y** (2000) Three-dimensional transient piezothermoelasticity in functionally graded rectangular plate bonded to a piezoelectric plate. *International Journal of Solids and Structures*, **37**, 4377–4401.
205. **Oral A and Anlas G** (2005) Effect of radially varying moduli on stress distribution of nonhomogeneous anisotropic cylindrical bodies. *International Journal of Solids and Structures* **42**, 5568–5588.
206. **Ostrosablin NI** (1997) Compatibility conditions of small deformations and stress functions. *Journal of Applied Mechanics and Technical Physics* **38**(5), 774–783.
207. **Panferov VM and Leonova ÉA** (1975) A solution of the problems of thermal elasticity with variable moduli. *Strength of Materials* **7**(6), 674–681.
208. **Payton RG** (1966) Elastic wave propagation in a non-homogeneous rod. *The Quarterly Journal of Mechanics and Applied Mathematics* **19**(1), 83–91.
209. **Peng XL and Li XF** (2010) Transient response of temperature and thermal stresses in a functionally graded hollow cylinder. *Journal of Thermal Stresses* **33**(5), 485–500.
210. **Peng XL and Li XL** (2010) Thermoelastic analysis of a cylindrical vessel of functionally graded materials. *International Journal of Pressure Vessels and Piping* **87**(5), 203–210.
211. **Pekeris CL** (1935) The propagation of Rayleigh waves in heterogeneous media. *Physics* **6**, 133–138.
212. **Plevako VP** (1971) On the theory of elasticity of inhomogeneous media. *Journal of Applied Mathematics and Mechanics* **35**(5), 806–813.

213. **Plevako VP** (2002) Influence of the change of material parameters on the stressed state of an inhomogeneous cylinder. *Proceedings of the International Scientific-Technical Conference Problems of Mathematical Modeling of the Modern Technologies PMM-2002*, Khmelnyts'kyy, Ukraine., 11 [in Ukrainian].
214. **Pobedrya BE** (1978) On the problem in stresses. *Soviet Physics Doklady* **23**(5), 351–353.
215. **Pobedrya BE and Gorbachev VI** (1984) Stress and strain concentration in composite materials. *Mechanics of Composite Materials* **20**(2), 141–148.
216. **Podstrigach YS and Osadchuk VA** (1971) Investigation of the stress state of cylindrical shells associated with a given tensor of incompatible strains, and application to the determination of welding stresses. *Materials Science* **4**(4), 292–298.
217. **Podstrigach YS, Lomakin VA, and Kolyano YM** (1984) *Thermoelasticity of Bodies of Nonhomogeneous Structure.* Moscow: Nauka [in Russian].
218. **Pogorzelski W** (1966) *Integral Equations and their Applications*. *Vol 1*. New York: Pergamon Press.
219. **Porter D and Stirling DSG** (1990) *Integral Equations. A Practical Treatment, from Spectral Theory to Applications*. Cambridge: Cambridge University Press.
220. **Popov GI** (1959) On the theory of bending of plates resting upon an elastic nonhomogeneous half-space. *Izvestia Vysshikh Uchebykh Zavedeniy. Stroitelstvo i Architektura* (11–12), 11–19 [in Russian].
221. **Popov GI** (1961) On a method of solution of the axisymmetric contact problem of the theory of elasticity. *Journal of Applied Mathematics and Mechanics* **25**(1), 105–118.
222. **Popov GI** (1962) The contact problem of the theory of elasticity for the case of a circular area of contact. *Journal of Applied Mathematics and Mechanics* **26**(1), 207–225.
223. **Popovich VS and Fedai BN** (1997) The axisymmetric problem of thermoelasticity of a multilayer thermosensitive tube. *Journal of Mathematical Sciences* **86**(2), 2605–2610.
224. **Plevako VP** (1973) Equilibrium of a nonhomogeneous half-plane under the action of forces applied to the boundary. Journal of Applied Mathematics and Mechanics **37**(5), 858–866.
225. **Plevako VP** (1973) The deformation of a nonhomogeneous half-space under the action of a surface load. *International Applied Mechanics* **9**(6), 593–598.

226. **Protsyuk BV and Synyuta VM** (2019) Nonstationary nonaxisymmetric temperature fields of multilayer orthotropic cylinders. *Journal of Mathematical Sciences* **162**(7), 267–287.
227. **Prudnikov AB, Brychkov YA, and Marichev OI** (1992) *Integrals and Series*. New York: CRC Press.
228. **Puro AE** (1973) Application of Hankel transforms to the solution of axisymmetric problems when the modulus of elasticity is a power function of depth. *Journal of Applied Mathematics and Mechanics* **37**(5), 896–900.
229. **Ramirez R, Heyliger PR, and Pan E** (2006) Static analysis of functionally graded elastic anisotropic plates using a discrete layer approach. *Composites Part B: Engineering* **37**(1), 10–20.
230. **Rabin BH and Shiota I** (eds) (1995) *Materials Research Society Bulletin* **20**(1)
231. **Rabin BH and Shiota I** (1995) Functionally gradient materials. *Materials Research Society Bulletin* **20**(1), 14–18.
232. **Reddy JN and Cheng ZQ** (2001) Three-dimensional thermomechanical deformations of functionally graded rectangular plates. *European Journal of Mechanics A Solids* **20**, 841–855.
233. **Rödel J and Neubrand A** (1997) Research program on gradient materials in Germany. In Shiota I and Miyamoto MY (eds), *Functionally Graded Materials 1996*. Amsterdam: Elsevier, pp. 9–14.
234. **Rostovtsev NA** (1961) An integral equation encountered in the problem of a rigid foundation bearing on nonhomogeneous soil. *Journal of Applied Mathematics and Mechanics* **25**, 238–246.
235. **Rostovtsev NA** (1964) On certain solutions of an integral equation of the theory of a linearly deformable foundation. *Journal of Applied Mathematics and Mechanics* **28**, 127–145.
236. **Rostovtsev NA** (1964). On the theory of elasticity of a nonhomogeneous medium. *Journal of Applied Mathematics and Mechanics* **28**(4), 745–757
237 **Rostovtsev NA and Khranevskaia IE** (1971) The solution of the Boussinesq problem for a half-space whose modulus of elasticity is a power function of the depth. *Journal of Applied Mathematics and Mechanics* **35**(6), 1000–1009.
238. **Rushchytsky JJ** (2015) Auxetic linearly elastic isotropic materials: restrictions on elastic moduli. *Archive of Applied Mechanics* **85**(4), 517–522.

239. **Rychahivskyy AV and Tokovyy YV** (2008) Correct analytical solutions to the thermoelasticity problems in a semi-plane. *Journal of Thermal Stresses* **31**(11), 1125–1145.
240. **Sadd MH** (2014) *Elasticity. Theory, Applications, and Numerics*. Amsterdam: Elsevier.
241. **Sadeh WZ** (1967) A note to the general solution of the two-dimensional linear elasticity problem in polar coordinates. *AIAA Journal* **5**(2), 354.
242. **Saiyathibrahim A, Mohamed Nazirudeen SS, and Dhanapal P** (2015) Processing techniques of functionally graded materials – a review. In Ramachandran T, Kokula Krishna Hari K, Thiruvengadam B and James D. (eds), *Proceedings of International Conference on Systems, Science, Control, Communication, Engineering and Technology – ICSSCCET-2015*, 10–11 August 2015, Coimbatore, India . Vol. 1, pp. 98–105.
243. **Sakuraba S** (1935) A contribution to the theory of the Love waves propagating over a semi-infinite solid body of varying elasticity. *Geophysical Magazine* **9**, 211–214.
244. **Samarskii AA and Vabishchevich PN** (2007) *Numerical Methods for Solving Inverse Problems of Mathematical Physics*. Berlin, New York: Walter de Gruyter.
245. **Satô Y** (1959) Numerical integration of the equation of motion for surface waves in a medium with arbitrary variation of material constants. *Bulletin of the Seismological Society of America* **49**(1), 57–77.
246. **Selvadurai APS** (1996) The settlement of a rigid circular foundation resting on a half-space exhibiting a near surface elastic non-homogeneity. *International Journal for Numerical and Analytical Methods in Geomechanics* **20**, 351–364.
247. **Selvadurai APS and Lan Q** (1998) Axisymmetric mixed boundary value problems for an elastic halfspace with a periodic nonhomogeneity. *International Journal of Solids and Structures* **35**(15), 1813–1826.
248. **Sezawa K** (1931) A kind of waves transmitted over a semi-infinite solid body of varying elasticity. *Bulletin of the Earthquake Research Institute University of Tokyo* **9**(3), 310–315.
249. **Shao ZS** (2005) Mechanical and thermal stresses of a functionally graded circular hollow cylinder with finite length. *International Journal of Pressure Vessels and Piping* **82**, 155–163.

250. **Shevlyakov YA, Naumov YA, and Chistyak VI** (1968) On calculating inhomogeneous foundations. *Soviet Applied Mechanics* **4**(9), 42–45.
251. **Shevchuk VA** (2006) Modeling and computation of heat transfer in a system "body – multilayer coating. *Heat Transfer Research* **37**(5), 421–433.
252. **Shevchuk VA, Kalynyak BM, and Tokovyy YV** (2007) An effective approach to determination of thermal stresses in the orthotropic radially inhomogeneous long hollow cylinder. In Chao CK and Lin CY (eds), Proceedings of the Seventh International Congress on Thermal Stresses TS2007, 4–7 June 2007, National Taiwan University of Science and Technology, Taipei, Taiwan, pp. 549–552.
253. **Simons NE and Rodrigues JSN** (1975) Finite element analysis of the surface deformation due to uniform loading on a layer of Gibson soil resting on a smooth rigid base. *Géotechnique* **25**(2), 375–379.
254. **Steele CR** (1969) Asymptotic analysis of stress waves in inhomogeneous elastic solids. *AIAA Journal* **7**(5), 896–902.
255. **Steinberg MA** (1986) Materials for aerospace: U.S. goals for subsonic, supersonic and hypersonic flight and for space exploration call for alloys and composites notable for strength, light weight and resistance to heat. *Scientific American Magazine* **255**(4), 59–64.
256. **Sternberg E and Chakravorty JG** (1959) On the propagation of shock waves in a nonhomogeneous elastic medium. *Journal of Applied Mechanics Transactions of ASME* **24**(4), 528–536.
257. **Sobolev SL** (1989) *Partial Differential Equations of Mathematical Physics*. New York: Dover Pub.
258. **Soldatos KP** (1994) Review of three dimensional dynamic analyses of circular cylinders and cylindrical shells. *Applied Mechanics Reviews* **47**(10), 501–516.
259. **Soldatos KP and Ye JQ** (1994) Three-dimensional static, dynamic, thermoelastic and buckling analysis of homogeneous and laminated composite cylinders. *Composite Structures* **29**(2), 131–143.
260. **Southwell RV** (1936) Castigliano's principle of minimum strain-energy. *Proceedings of the Royal Society of London. Series A, Mathematical and Physical Sciences* **154**(881), 4–21.
261. **Southwell RV** (1940) Castigliano's principle of minimum strain-energy, and the conditions of compatibility for strain. *The London, Edinburgh, and Dublin Philosophical Magazine and Journal of Science* **30**(7), 252–258.

262. **Stippes M** (1966) On stress functions in classical elasticity. *Quarterly of Applied Mathematics* **24**(2), 119–125.
263. **Stoneley R** (1934) The transmission of Rayleigh waves in a heterogeneous medium. *Geophysical Journal International* **3**(6), 222–232.
264. **Sumi N and Ito Y** (1993) The propagation and reflection of thermal stress waves in anisotropic nonhomogeneous hollow cylinders and spheres. *Nuclear Engineering and Design* **140**, 133–145.
265. **Suresh S** (2001) Graded materials for resistance to contact deformation and damage. *Science* **292**(5526), 2447–2451.
266. **Suresh S and Mortensen A** (1997) Functionally graded metals and metal-ceramic composites: part 2 thermomechanical behavior. *International Materials Reviews* **42**(3), 85–116.
267. **Suresh S and Mortensen A** (1998) *Fundamentals of Functionally Graded Materials: Processing and Thermomechanical Behaviour of Graded Metals and Metal-Ceramic Composites*. London, Ashgate Publishing.
268. **Swaminathan K, Naveenkumar DT, Zenkour AM, and Carrera E** (2017) Stress, vibration and buckling analyses of FGM plates – a state-of-the-art review. *Composite Structures* **120**, 10–31.
269. **Swaminathan K and Sangeetha DM** (2017) Thermal analysis of FGM plates – a critical review of various modeling techniques and solution methods. *Composite Structures* **160**, 43–60.
270. **Takahashi T** (1957) The dispersion of Rayleigh waves in heterogeneous media. *Bulletin of the Earthquake Research Institute, University of Tokyo* **35**(2), 297–308.
271. **Tang XF, Zhang LM, Zhang QJ, and Yuan RZ** (1993) Design and structural control of PSZ-MO functionally gradient materials with thermal relaxation. In Holt IB (ed), *Ceramic Transactions: Functionally Gradient Materials*, **34**, pp. 45–463.
272. **Tanigawa Y** (1995) Some basic thermoelastic problems for nonhomogeneous structural materials. Applied Mechanics Reviews **48**(6), 287–300.
273. **Tanigawa Y, Morishita H, and Ogaki S** (1999) Derivation of systems of fundamental equations for a three-dimensional thermoelastic field with nonhomogeneous material properties and its application to a semi-infinite body. Journal of Thermal Stresses **22**(7), 689–711.
274. **Tarn JQ** (2001) Exact solutions for functionally graded anisotropic cylinders subjected to thermal and mechanical loads. *International Journal of Solids and Structures* **38**, 8189–8206.

275. **Tarn JQ and Chang HH** (2005) Extension, torsion, bending, pressuring, and shearing of piezoelectric circular cylinders with radial inhomogeneity. *Journal of Intelligent Material Systems and Structures* **16**, 631–641.
276. **Tarn JQ, Wang YB, and Wang YM** (1996) Three-dimensional asymptotic finite element method for anisotropic inhomogeneous and laminated plates. *International Journal of Solids and Structures* **33**(13), 1939–1960.
277. **Tauchert TR** (1975) A review: quasistatic thermal stresses in anisotropic bodies, with applications to composite materials. *Acta Mechanica* **23**, 113–135.
278. **Teodorescu PP** (2013) *Treatise on Classical Elasticity. Theory and Related Problems*. Dordrecht: Springer.
279. **Thai HT and Kim SE** (2015) A review of theories for the modeling and analysis of functionally graded plates and shells. *Composite Structures* **128**, 70–86.
280**. Tikhonov AN and Arsenin VI** (1977) Solutions of ill-posed problems. Washington, Winston, New York: Halsted Press.
281. **Timoshenko SP** (1953) *History of Strength of Materials: with a Brief Account of the History of Theory of Elasticity and Theory of Structures*. New York: McGraw-Hill.
282. **Timoshenko SP and Goodier JN** (1951) *Theory of Elasticity*. New York: McGraw-Hill Book Company, Inc.
283. **Titchmarsh EC** (1976) *The Theory of Functions*. Oxford: Oxford University Press.
284. **Todhunter I and Pearson K** (1960) *A History of the Theory of Elasticity and of the Strength of Materials: from Galilei to Lord Kelvin. V 1. Galilei to Saint-Venant, 1639 – 1850*. New York, Dover Pub.
285. **Tokova LP and Yasinskyy AV** (2018) Approximate Solution of the One-Dimensional Problem of the Theory of Elasticity for an Inhomogeneous Solid Cylinder. *Journal of Mathematical Sciences* **228**(2), 133–141.
286. **Tokova LP, Yasinskyy AV, and Ma CC** (2017) Effect of the layer inhomogeneity on the distribution of stresses and displacements in an elastic multilayer cylinder. *Acta Mechanica* **228**(8), 2865–2877.
287. **Tokovyy YV** (2014) Direct integration method. In Hetnarski RB (ed). *Encyclopedia of Thermal Stresses* **2.** Dordrecht: Springer, pp. 951-960.
288. **Tokovyy YV** (2019) Plane thermoelasticity of inhomogeneous solids. In Altenbach H and Öchsner A (eds), *Encyclopedia of*

Continuum Mechanics. Berlin, Heidelberg: Springer, https://doi.org/10.1007/978-3-662-53605-6_361-1

289. **Tokovyy YV** (2019) Solutions of axisymmetric problems of elasticity and thermoelasticity for an inhomogeneous space and a half space. *Journal of Mathematical Sciences* **240**(1), 86–97.
290. **Tokovyy YV, Kalynyak BM, and Ma CC** (2014) Nonhomogeneous solids: Integral equations approach. In Hetnarski RB (ed) *Encyclopedia of Thermal Stresses* **7**. Dordrecht: Springer, pp. 3350–3356.
291. **Tokovyy YV, Hung KM, and Ma CC** (2010) Determination of stresses and displacements in a thin annular disk subjected to diametral compression. *Journal of Mathematical Sciences* **165**(3), 342–354.
292. **Tokovyy YV, Huang YH, Yen CY, and Ma CC** (2019) Analytical and experimental evaluation of stresses in elastic annuli subjected to three-point loading on the outer surface. *Applied Mathematical Modelling* **73**, 442–458.
293. **Tokovyy YV and Ma CC** (2007) Analytical determination of residual stresses in a butt-weld of two thin rectangular plates. *Proceedings in Applied Mathematics and Mechanics* **7**(1), 2090013-2090014.
294. **Tokovyy YV and Ma CC** (2008) Analysis of 2D non-axisymmetric elasticity and thermoelasticity problems for radially inhomogeneous hollow cylinders. *Journal of Engineering Mathematics* **61**(2–4), 171–184.
295. **Tokovyy YV and Ma C**C (2008) Thermal stresses in anisotropic and radially inhomogeneous annular domains. *Journal of Thermal Stresses* **31**(9), 892–913
296. **Tokovyy YV and Ma CC** (2009) An explicit-form solution to the plane elasticity and thermoelasticity problems for anisotropic and inhomogeneous solids. *International Journal of Solids and Structures* **46**(21), 3850–3859.
297. **Tokovyy YV and Ma CC** (2009) Analytical solutions to the 2D elasticity and thermoelasticity problems for inhomogeneous planes and half-planes. *Archive of Applied Mechanics* **79**(5), 441–456.
298. **Tokovyy YV and Ma CC** (2009) Analytical solutions to the planar non-axisymmetric elasticity and thermoelasticity problems for homogeneous and inhomogeneous annular domains. *International Journal of Engineering Sciences* **47**(3), 325–486.
299. **Tokovyy YV and Ma CC** (2011) Steady-state heat transfer and thermo-elastic analysis of inhomogeneous semi-infinite solids. In

Vikhrenko VS (ed), *Heat Conduction – Basic Research*. Rijeka: InTech, pp. 249–268.

300. **Tokovyy YV and Ma CC** (2011) Analysis of residual stresses in a long hollow cylinder. *International Journal of Pressure Vessels and Piping* **88**(5–7), 248–255.
301. **Tokovyy YV and Ma CC** (2013) Three-dimensional temperature and thermal stress analysis of an inhomogeneous layer. *Journal of Thermal Stresses* **36**(8), 790–808.
302. **Tokovyy YV and Ma CC** (2015) An analytical solution to the three-dimensional problem on elastic equilibrium of an exponentially-inhomogeneous layer. *Journal of Mechanics* **31**(5), 545–555.
303. **Tokovyy YV and Ma CC** (2015) Analytical solutions to the axisymmetric elasticity and thermoelasticity problems for an arbitrarily inhomogeneous layer. *International Journal of Engineering Science* **92**, 1–17.
304. **Tokovyy YV and Ma CC** (2017) Three-dimensional elastic analysis of transversely-isotropic composites. *Journal of Mechanics* **33**(6), 821–830.
305. **Tranter CJ** (1951) *Integral Transforms in Mathematical Physics*. New York, Wiley.
306. **Tricomi FG** (1957) *Integral Equations*. New York: Interscience Publishers. Inc.
307. **Vainberg DV, Gorodetskii AS, Kirichevskii VV and Sakharov AS** (1972) Finite element method in mechanics of deformable bodies. *Soviet Applied Mechanics* **8**(8), 819 – 840.
308. **Vasil'ev VV and Fedorov LV** (1996) On an elasticity problem posed stresses. Mechanics of Solids **31**(2), 72–80.
309. **Vasilenko AT** (1995) Nonaxisymmetric thermal stressed state of nonhomogeneous anisotropic cylinders. *International Applied Mechanics* **31**(11), 895–899.
310. **Vasiliev VV and Morozov EV** (2007) *Advanced Mechanics of Composite Materials*. Amsterdam: Elsevier.
311. **Verlan AF and Sizikov VS** (1986) *Integral Equations: Methods, Algorithms, Programs*, Kiev: Naukova Dumka [in Russian].
312. **Vigak VM** (1979) *Optimal Control of Nonstationary Temperature Modes*. Kiev: Naukova Dumka [in Russian].
313. **Vigak VM** (1988) *Control of Temperature Stresses and Displacements*. Kiev: Naukova Dumka [in Russian].
314. **Vigak VM** (2004) Correct solutions of plane elastic problems for a half-plane. *International Applied Mechanics* **40**(3), 283–289.

315. **Vigak VM** (1999) Solution of one-dimensional problems of elasticity and thermoelasticity in stresses for a cylinder. *Journal of Mathematical Sciences* **96**(1), 2887–2891.
316. **Vigak VM and Rychagivskii AV** (2000) The method of direct integration of the equations of three-dimensional elastic and thermoelastic problems for space and a halfspace *International Applied Mechanics* **36**(11), 1468–1475.
317. **Vigak VM and Rychagivskii AV** (2002) Solution of a three-dimensional elastic problem for a layer. *International Applied Mechanics* **38**(9), 1094–1102.
318. **Vigak VM and Tokovyi YV** (2002) Construction of elementary solutions to a plane elastic problem for a rectangular domain. *International Applied Mechanics* **38**(7), 829–836.
319. **Vihak VM** (1998) Direct method for integration of plane elasticity and thermoelasticity problems. *Reports of the National Academy of Sciences of Ukraine* 12, 62–67 [in Ukrainian]
320. **Vihak VM** (2000) Continuity equations for a deformable solid. *Journal of Mathematical Sciences* **99**(5), 1655–1661.
321. **Vihak VM, Povstenko YZ, and Rychahivskyy AV** (2001) Integration of elasticity and thermoelasticity equations in terms of stresses. *Strojnĭcky Časopis* **52**(4), 221–234.
322. **Vihak V and Rychahivskyy A** (2001) Bounded solutions of plane elasticity problems in a semi-plane. *Journal of Computational and Applied Mechanics* **2**(2), 263–272.
323. **Vihak VM and Svyryda MI** (1998) Separation of variables in equations of a two-dimensional thermoelasticity problem in terms of stresses for an annular sector. *Reports of the NAS of Ukraine* **2**, 68–74. [in Ukrainian]
324. **Vihak VM, Tsymbalyuk LI, and Shablii OM** (2001) Distribution of residual stresses induced by axially symmetric plastic strains in a layer. *Materials Science* **37,** 19–24.
325. **Vihak VM and Tokovyi YV** (2002) Investigation of the plane stressed state in a rectangular domain. *Materials Science* **38**(2), 230–237.
326. **Vihak VM and Tokovyy YV** (2003) An exact solution of an axisymmetric problem of the elasticity theory in terms of stresses for a cylinder of finite length. *Applied Problems of Mechanics and Mathematics* **1**, 55–60 [in Ukrainian].
327. **Vihak V, Tokovyi YV, and Rychahivskyy A** (2002) Exact solution of the plane problem of elasticity in a rectangular region. *Journal of Computational and Applied Mechanics* **3**(2), 193–206.

328. **Vihak VM and Yershov YG** (2002) Determination of displacements for two-dimensional problems of solid mechanics in polar coordinates. *Mashynoznavstvo* (1), 36–40 [in Ukrainian].
329. **Vihak VM and Yuzvyak MY** (1999) Method of direct integration for plane elasticity and thermoelasticity problems in unbounded domains. *Boundary Value Problems for Differential Equations* **4**, 9−33 [in Ukraininan].
330. **Vihak VM, Yuzvyak MY, and Yasinsky AV** (1998) The solution of the thermoelasticity problem for a rectangular domain. *Journal of Thermal Stresses* **21**(5), 545–561.
331. **Vlasov BF** (1969) Integration of the strain-continuity equations in St. Venant form. *International Applied Mechanics* **5**(12), 1283–1285.
332. **Vlasov BF** (1970) On equations of continuity of deformations. *International Applied Mechanics* **6**(11), 1227–1231.
333. **Vlasov BF** (1971) Equatons for the determination of the Morera and Maxwell stress functions. *Soviet Physics Doklady* **16**(3), 252–254.
334. **Wan YM** (1968) Comment on "A note to the general solution of the two-dimensional linear elasticity problem in polar coordinates. *AIAA Journal* **6**(3), 569.
335. **Wang CD, Tzeng CS, Pan E and Liao JJ** (2003) Displacements and stresses due to a vertical point load in an inhomogeneous transversely isotropic half-space. *International Journal of Rock Mechanics and Mining Sciences* **40**, 667–685.
336. **Watremetz B, Baietto-Dubourg MC, and Lubrecht AA** (2007) 2D thermo-mechanical contact simulations in a functionally graded material: a multigrid-based approach. *Tribology International* **40**(5), 754–762.
337. **Washizu K** (1957) A note on the conditions of compatibility. *Journal of Mathematics and Physics* **36**(4), 306–312.
338. **Watanabe K** (1984) Plane SH-waves in harmonically inhomogeneous elastic media. *Wave Motion* **6**(5), 477–488.
339. **Watanabe Y and Sato H** (2011) Review fabrication of functionally graded materials under a centrifugal force. In Cuppoletti J (ed.) *Nanocomposites with Unique Properties and Applications in Medicine and Industry,* InTech**,** Rijeka, pp. 133–150.
340. **Willis JR** (1981) Variational principles for dynamic problems for inhomogeneous elastic media. *Wave Motion* **3**(1), 1–11.
341. **Wilson JT** (1942) Surface waves in a heterogeneous medium. *Bulletin of the Seismological Society of America* **32**(4), 297–304.
342. **Yang J, Ke LL, and Kitipornchai S** (2009) Thermo-mechanical analysis of an inhomogeneous double-layer coating system under Hertz pressure

and tangential traction. *Mechanics of Advanced Materials and Structures* **16**, 308–318.

343. **Yasinskyy A and Tokova L** (2017) Inverse problem on the identification of temperature and thermal stresses in an FGM hollow cylinder by the surface displacements. *Journal of Thermal Stresses* **40**(12), 1471–1483
344. **Yasinskyy A, Tokovyy Y, and Ierokhova O** (2016) Optimization of two-dimensional nonstationary thermal stresses and displacements in a halfspace through the use of internal heat sources. *Journal of Thermal Stresses* **39**(9), 1084–1097.
345. **Yevtushenko AA, Rozniakowska M and Kuciej M** (2007) Transient temperature processes in composite strip and homogeneous foundation. *International Communications in Heat and Mass Transfer* **34**(9-10), 1108–1118.
346. **Zhang X and Hasebe N** (1999) Elasticity solution for a radially nonhomogeneous hollow circular cylinder. *Journal of Applied Mechanics* **66**, 598–606.
347. **Zhang NH and Wang ML** (2006) A mathematical model of thermoviscoelastic FGM thin plates and Ritz approximate solutions. *Acta Mechanica* **181**(3–4), 153–167.
348. **Zhang HQ and Yang G** (1991) Constructions of the general solution for a system of partial differential equations with variable coefficients. *Applied Mathematics and Mechanics* **12**(2), 149–153.
349. **Zhang J and Li Y** (1997) Numerical simulation of elastic wave propagation in inhomogeneous media. *Wave Motion* **25**(2), 109–125.
350. **Zhuravchak LM and Zabrods'ka NV** (2010) Nonstationary thermal fields in inhomogeneous materials with nonlinear behavior of the components. *Materials Science* **46** (1), 36–46.
351. **Zimmerman RW and Lutz MP** (1999) Thermal stresses and thermal expansion in a uniformly heated functionally graded cylinder. *Journal of Thermal Stresses* **22**, 177–188.